AD-783 752

ROCKET ENGINES ON A COMBINED FUEL

E. B. Volkov, et al

Foreign Technology Division
Wright-Patterson Air Force Base, Ohio

24 June 1974

UNCLASSIFIED
Security Classification

AD-783752

DOCUMENT CONTROL DATA - R & D

(Security classification of title, body of abstract and indexing annotation must be entered when the overall report is classified)

1. ORIGINATING ACTIVITY (Corporate author) Foreign Technology Division Air Force Systems Command U. S. Air Force	2a. REPORT SECURITY CLASSIFICATION UNCLASSIFIED 2b. GROUP

3. REPORT TITLE

ROCKET ENGINES ON A COMBINED FUEL

4. DESCRIPTIVE NOTES (Type of report and inclusive dates)

Translation

5. AUTHOR(S) (First name, middle initial, last name)

Ye. B. Volkov and G. Yu. Mazing

6. REPORT DATE	7a. TOTAL NO. OF PAGES	7b. NO. OF REFS
1973	~~237~~ 256	69

8a. CONTRACT OR GRANT NO. b. PROJECT NO c. d.	9a. ORIGINATOR'S REPORT NUMBER(S) FTD-MT-24-827-74 9b. OTHER REPORT NO(S) (Any other numbers that may be assigned this report)

10. DISTRIBUTION STATEMENT

Approved for public release; distribution unlimited.

11. SUPPLEMENTARY NOTES	12. SPONSORING MILITARY ACTIVITY
	Foreign Technology Division Wright-Patterson AFB, Ohio

13. ABSTRACT

19

DD FORM 1 NOV 68 1473

UNCLASSIFIED
Security Classification

EDITED MACHINE TRANSLATION

FTD-NT-24-827-74 24 June 1974

ROCKET ENGINES ON A COMBINED FUEL

By: Ye. B. Volkov and G. Yu. Mazing

English pages: 237

Source: Raketnyye Dvigateli Na Kombinirovannom Toplive, 1973, pp. 1-184

Country of Origin: USSR
Requester: FTD/PDTA
This document is a SYSTRAN machine aided translation, post-edited for technical accuracy by: Robert D. Hill
Approved for public release; distribution unlimited.

TABLE OF CONTENTS

Volkov, Ye. B., Mazing G. Yu. and Shishkin Yu. N., Rocket engines on combined fuel. M., "Mechanical Engineering", 1973, 184 pages

Examined in the book are problems of the theory of rocket engines which operate on solid-liquid propellant components and rocket engines using a solid propellant with charges of separate equipment.

Different diagrams are given, and the operating principles of such engines are described; data on propellants are given.

Information on the selection of basic parameters of the combustion chambers, heat exchange and fuel combustion in the chambers is presented.

Features of control are noted, and static performances of engines operating on combined fuel are examined.

The book is intended for engineers and scientists of rocket engine design. It will also be useful for students and graduate students of schools of higher education.

There are 18 tables, 74 figures and a bibliography of 69 names.

The introduction and chapter 1 of the book were written by Ye. B. Volkov, chapters 2-4 by G. Yu. Mazing, chapters 5 and 6 by Ye. B. Volkov and Yu. N. Shishkin.

The authors express their gratitude to Doctor of Technical Sciences S. D. Grishin for the valuable remarks made by him during the review of the book and are grateful beforehand to readers for their critical remarks both on the essence of the questions set forth and on the procedure for their presentation. All remarks should be sent to: Moscow, B-78, 1st Basmannyy Street, 3, Publishing House "Mashinostroyeniye."

U. S. BOARD ON GEOGRAPHIC NAMES TRANSLITERATION SYSTEM

Block	Italic	Transliteration	Block	Italic	Transliteration
А а	*А а*	A, a	Р р	*Р р*	R, r
Б б	*Б б*	B, b	С с	*С с*	S, s
В в	*В в*	V, v	Т т	*Т т*	T, t
Г г	*Г г*	G, g	У у	*У у*	U, u
Д д	*Д д*	D, d	Ф ф	*Ф ф*	F, f
Е е	*Е е*	Ye, ye; E, e*	Х х	*Х х*	Kh, kh
Ж ж	*Ж ж*	Zh, zh	Ц ц	*Ц ц*	Ts, ts
З з	*З з*	Z, z	Ч ч	*Ч ч*	Ch, ch
И и	*И и*	I, i	Ш ш	*Ш ш*	Sh, sh
Й й	*Й й*	Y, y	Щ щ	*Щ щ*	Shch, shch
К к	*К к*	K, k	Ъ ъ	*Ъ ъ*	"
Л л	*Л л*	L, l	Ы ы	*Ы ы*	Y, y
М м	*М м*	M, m	Ь ь	*Ь ь*	'
Н н	*Н н*	N, n	Э э	*Э э*	E, e
О о	*О о*	O, o	Ю ю	*Ю ю*	Yu, yu
П п	*П п*	P, p	Я я	*Я я*	Ya, ya

*ye initially, after vowels, and after ъ, ь; e elsewhere. When written as ё in Russian, transliterate as yё or ё. The use of diacritical marks is preferred, but such marks may be omitted when expediency dictates.

* * * * * * * * * *

GRAPHICS DISCLAIMER

All figures, graphics, tables, equations, etc. merged into this translation were extracted from the best quality copy available.

RUSSIAN AND ENGLISH TRIGONOMETRIC FUNCTIONS

Russian	English
sin	sin
cos	cos
tg	tan
ctg	cot
sec	sec
cosec	csc
sh	sinh
ch	cosh
th	tanh
cth	coth
sch	sech
csch	csch
arc sin	$\sin^{-1}$
arc cos	$\cos^{-1}$
arc tg	$\tan^{-1}$
arc ctg	$\cot^{-1}$
arc sec	$\sec^{-1}$
arc cosec	$\csc^{-1}$
arc sh	$\sinh^{-1}$
arc ch	$\cosh^{-1}$
arc th	$\tanh^{-1}$
arc cth	$\coth^{-1}$
arc sch	sech^{-1}
arc csch	csch^{-1}
rot	curl
lg	log

PREFACE

In foreign scientific periodical literature in recent years there has been published a number of data on results of investigations and development of rocket engines using solid-liquid propellants (hybrid rocket engines).

This book is an attempt to generalize and systematize that separate information on the theory of GRD [ГРД - hybrid rocket engines] which has been published up to now and become known to the authors. Considerable attention is given in the book to processes which occur in chambers of the GRD. Since according to features of these processes much in common with the GRD is possessed by the RDTT [РДТТ - solid-propellant rocket engine] with two charges of different composition, then in the book some problems of the theory of RDTT of such type are examined.

The basic content in this book is an account of bases of the theory of the engines; the problems of their calculation, where they are included in the book, are discussed mainly in order to illustrate the use of the theory of engines for needs of practice.

The formulas and numerical values which characterize the engines and their propellants are given in accordance with the SI [СИ - the international system of units]. Parameters and the diagrams of the engines are given on the basis of foreign publications.

INTRODUCTION

All the basic achievements in the development of rocket constructions which were achieved during the recent decades are connected with the considerable progress in the improvement of the performances of engines used in combat and space rockets. Depending on the degree of the perfection of the rocket engine, to a great extent, are the basic features and figures of merit of the rocket or space vehicle on which it is applied. In connection with this, understandable is that considerable attention which is given, in all countries where rockets are built, to the development and perfection of rocket engines.

At present in practice on all (with very rare exception) combat and space rockets and on space vehicles, rocket engines which operate on liquid or solid propellants (ZhRD [ЖРД - liquid-propellant rocket engine] and RDTT) are used.

The use of contemporary ZhRD and RDTT made it possible to create highly perfected rockets and solve a number of most complex technical problems; however, the development of missile construction is continued and will be continued, and in connection with this the perfection of the engines remains as before an important and urgent problem.

Directions of further improvement in the rocket-engine characteristics are determined from an analysis of those basic

requirements for them, which are usually formulated in the theory of rockets and according to which it is necessary that:

a) the engine have the largest possible specific impulse;

b) the engine with the given thrust force or with this fuel reserve have as less inherent mass as possible;

c) the engine in all possible operating conditions provide with the assigned limits the required operational mode - thrust, time of the action, control of the parameters, the necessary number of switching on and off, etc.;

d) the engine possess a reliability not less than that assigned;

e) the operation of the engine be simple and safe for the personnel;

f) the cost of engine be as low as possible.

Depending on the type of rocket (flight vehicle) on which the engine is used, the relative degree of importance of one requirement or the other, of course, is changed. Thus, the requirements for an increase in the specific impulse and reduction in the specific mass are all the more important, the greater the flying range of the rocket (and therefore are most important for space rockets); the requirements of the simplicity of operation and low cost, on the contrary, for space rockets are less important than those for rockets of mass use.

Furthermore, there are requirements which are characteristic for engines of rockets of only one form. Thus, for instance, only for engines of combat rockets, as a rule, is there formulated the requirement that the engine for a long time (years) be stored

in a state of readiness for launching and would be started very rapidly (in seconds); for engines of space vehicles there appear their specific requirements for a launch possibility under conditions of weightlessness and vacuum, etc.

A large part of the engine performances and, consequently, the possibility of accomplishing the corresponding requirements for the engines depend on the form and quality of the propellant used in the engine. In connection with this, the question of the selection of the propellant acquires exceptionally great importance. Let us explain this by some examples.

The temperature and composition of combustion products in the chamber of rocket engine are determined mainly by properties of the propellant and, therefore, determined by these properties is the specific impulse of the engine, since it is proportional to $\sqrt{RT_к}$, where R and $T_к$ are, respectively, the gas constant and temperature of the combustion products.

It is very obvious that depending on the properties of the propellant (for example, on its density) are the masses of the tanks of the liquid propellant, devices for its feed into the chamber of the ZhRD, the mass of the chamber of the RDTT and a number of other engine components. The greater the density of the propellant, the less the required volumes of the tank and chamber, and the less, therefore, the mass of the entire rocket.

The control of thrust of the engine, the repeated turning off and turning on of it are accomplished mainly by a change in the quantity of propellant ignited per unit time in the engine chamber. Since for the different forms of propellant this change can be carried out with greater or less work, then the form of the propellant has an extremely important effect on such qualities of engines as the possibility of their control and repeated starting.

The cost of the rocket launching depends to a great degree on the form of propellant - in terms of the cost of the propellant itself, in terms of the cost of the materials used in the engine, and in terms of the composition and cost of the units of the complex, which are changed depending on the form of the propellant.

The effect of properties of the propellant on the feature of operation of the engine, on the possibility of the storage of it for a prolonged time in the state of readiness for launching, etc. does not require a special explanation.

In connection with the noted, the engines which operate on liquid and solid propellants have considerable distinctions. Each of the engines of these types possess their advantages and disadvantages.

The advantages of the ZhRD are:

a) the possibility of the achievement of a high specific impulse.

This advantage of the liquid-propellant rocket engine is connected with the fact that as separately stored propellant components for an engine of this type it is possible to have substances which with mixing and burning give very high energy output;

b) the relatively low intrinsic mass of the engine - especially for the prolonged operating engines with high thrust;

c) the possibility of the repeated turning on and off of the engine and the control of its thrust, which is provided by relatively simple control of the feed of each of the propellant components in the chamber;

d) the possibility of relatively prolonged engine operation.

In practice for the liquid-propellant rocket engine, the operating time is limited only to the reserve of the propellant. The heat resistance of the chamber is provided for during this time by the cooling of its construction by the propellant components;

e) the low cost of the propellant itself, especially in the case of the use as its components of substances whose production is well assimilated by industry and has a wide raw-material base.

The basic shortcomings of a liquid-propellant rocket engine are connected, first of all, with the fact that as a result of the need for having aboard the liquid-propellant rocket various tanks and devices for feeding the fuel into the chamber, its construction, production and operation become complicated, and also the possibilities of prolonged storage of the rocket with the loaded fuel and achievements of high reliability are reduced. Many of these shortcomings are reflected not only on the rocket itself, but also on the entire rocket complex. Furthermore, by virtue the specific features of the scheme and operating conditions of the liquid-propellant rocket engine, the final development of these engines, especially engines with high parameters and very powerful thrust, is made difficult and can require high expenditures of means and time.

And finally a shortcoming of the liquid-propellant rocket engine is the relatively low density of the propellants used in these engines, especially in the case of the use of liquid hydrogen as the fuel. The low density of propellant leads to an increase in the overall dimensions of the rocket.

The advantages of RDTT [РДТТ - engines operating on solid propellants] are the following:

a) the simplicity of the device and operation; the possibility of simplification (in comparison with a liquid-propellant rocket engine) of the complex used for the application of the rocket;

b) the high density of the propellants;

c) the possibility of prolonged storage of the engines in a state of readiness for launching and of rapid starting the engine.

Furthermore, according to the results achieved abroad in the field of final development of the RDTT, it is possible to assume that the advantages of the RDTT should include the possibility of obtaining very high values of thrust in one unit.

Along with the noted merits, the RDTT possesses noticeable shortcomings, which include the following:

a) the relatively low value of specific impulse.

This shortcoming of the RDTT is explained by the fact that propellant components, which could give high specific impulse, in one solid substance are not very compatible;

b) in RDTT it is extremely difficult to carry out control of thrust in magnitude and the repeated turning on and off of the engine. Design complications of the engine, which are necessary in this case, are so great that in the overwhelming majority of the cases the control of thrust and the repeated turning on of the RDTT are considered to be unsuitable;

c) the considerable cost of many solid fuels;

d) the considerable difficulties connected with the transportation of the charged engines of high thrust, or the need for

the complication of the complex and operation of the rocket in the case of their loading at the site of the application;

e) the sensitivity of the RDTT to external conditions; defects of the charge in them (cracks) can lead to emergencies and disruption of the rocket launching, but it is difficult to detect the defects.

Thus, both liquid-propellant engines, and engines which operate on solid fuel, along with the advantages, possess definite shortcomings. The engines of both examined types are continuously improved, and some of their qualities can be improved. However, at the same time, many of the shortcomings noted above in these engines cannot be eliminated completely, and they are connected with the use in engines of only liquid or only solid components of the propellant.

In connection with this, the interest which has been exhibited in recent years in engines whose propellant consists of substances of a different aggregate state (liquid and solid) is understandable. Such engines are conventionally designated as *hybrid rocket engines* (GRD's).

The hybrid rocket engines are investigated considerably less fully than the liquid-propellant engines and engines which operate on solid fuel. However, an analysis of the design and features of engines of this type makes it possible with great confidence to conclude that:

a) the propellant of hybrid rocket engines makes is possible to achieve values of specific impulse which exceed its values for the RDTT and approach values of specific impulse for best liquid-propellant rocket engine; in this case the density of the propellants of the GRD considerably exceeds the density of the propellants which consist only of liquid components, and the

cost of the propellants of the GRD can be very low;

b) the presence in the propellant of the GRD of a liquid component is allowed considerably more than in the RDTT, the possibility of the working out of the control of the thrust, the repeated turning on and off of the engine and also the coolings of its chamber;

c) the characteristic of GRD with respect to the mass will not be inferior with the corresponding development of these engines to characteristics with respect to the mass of engines using liquid or solid propellants;

d) although the operating characteristics of rockets or other flight vehicles with the GRD will be inferior to the appropriate characteristics of rockets with RDTT, they will be better than those in the case of the use on these rockets and apparatuses of engines which operate only on liquid propellants.

All these qualities of the GRD make it possible to use them on rockets and flight vehicles of different classes and purposes, including combat and space rockets.

Besides the engines which operate on solid-liquid propellant components (GRD's), as a possible new type of rocket engine based on chemical energy sources there can be examined engines with two separate solid-propellant charges, one of which contains an excess of oxidizer and the other, an excess of fuel. This engine is called an RDTT of separate equipment (RDTT of RS) [РС - rocket missile] or an RDTT with the *separate propellant components*.

The RDTT of separate charge and hybrid rocket engines are united into the class of KRD [КРД - *combined rocket engines*] or *rocket engines which use a combined propellant*.

CHAPTER 1

GENERAL INFORMATION ABOUT COMBINED ROCKET ENGINES

1.1. OPERATING CONDITIONS OF THE COMBINED ROCKET ENGINE

1.1.1. Operating Conditions of a GRD

One of the possible designs of a GRD [ГРД - an engine which operates on solid and liquid-propellant components] is given in figure 1.1. The engine includes a chamber 1 with charge 2 of solid-propellant components and injection head 3; tank 5 with a liquid-propellant component; cylinder 8 with compressed gas; valves 4 and 7; and pressure reducer 6. Elements 4-8 form the system of storage and feed of the liquid component.

Figure 1.1. Schematic diagram of a GRD: 1 - chamber; 2 - charge of solid component; 3 - injection head; 4, 7 - valves; 5 - tank with liquid component; 6 - reducer; 8 - cylinder with gas pressure.

The solid and liquid-propellant components are selected so that one of them contains an excess of the combustible elements (carbon, hydrogen, etc.) and the other - the oxidizing elements (oxygen, fluorine and chlorine). These components are called the fuel and oxidizer, respectively.

The charge of the solid component can have a different form. Figure 1.1 shows the charge prepared in the form of a single-channel cylindrical grain.

At the moment of turning on the GRD, valve 7 is open, and the compressed gas through reducer 6 under a definite pressure enters into the tank. After the opening of valve 4, the liquid component, being displaced from the tank by the gas, passes to the injection head 3 of the chamber. By means of the injectors the liquid component is divided into jets and drops and is guided into the channel of the charge of solid component. The solid component is ignited; the gases which are formed on its surface are mixed in the channel of the charge with a liquid component. The mixture of the fuel and oxidizer burns, the combustion products proceed to the nozzle and escape through it. In the stationary operational mode the consumption of propellant G_Σ (total flow rate of liquid and solid components - $G_ж$ and $G_т$) is equal to the flow rate of the gases through the nozzle, and in the chamber a definite pressure $p_к$ is maintained.

As is evident from a description of the principle of operation of the GRD, the operating process and design of this engine have some general features with the operating processes and designs of both the ZhRD and RDTT. With the ZhRD the hybrid engine is brought together by the presence of the feed system of the liquid propellant component (including injectors) and the operating process of this system; the engine which operates on solid fuel is brought together by the use of the chamber which contains the charge of the solid component.

The specific impulse of the hybrid rocket engine, just as the specific impulse (specific thrust) of a rocket engine of other types which operate on chemical energy sources, depends mainly on the propellant composition (content of energy in the propellant) and on the parameters of the operating process in the chamber.

The propellant composition of the GRD, in turn, is determined by the composition of components and the relationship of their consumption in the engine operation. Consequently, at these propellant components, the assigned geometry (dimensions of the nozzle) of the chamber and the invariable external pressure,

$$I = I\left(K = \frac{G_{\text{ж}}}{G_{\text{т}}},\ p_{\text{к}}\right);$$

the pressure in the chamber and the thrust of the engine depend on the consumption of the propellant G_{Σ}:

$$p_{\text{к}} \sim G_{\Sigma};\quad P = IG_{\Sigma}.$$

Thus, the fundamental characteristics of the GRD in its operation are determined by the propellant component flow. By changing the feed of liquid component into the chamber (for example, by a change in the cross section of the throttle installed in the main line which connects the chamber with the tank), it is possible to affect all the engine characteristics. This provides the possibility of the control of the GRD. By cutting off the feed of the liquid component (shutting off the main line), it is possible to discontinue the operating process, i.e., turn off the engine; if necessary the engine can be started and stopped repeatedly.

1.1.2. Features of Fuel Combustion in a GRD

Laws governing the burning of fuel in the GRD are very important for determining the many features of engines of this type. In the estimate and calculation of characteristics of the hydrojet, just as the characteristics of engines which operate on solid fuel, it is necessary to know the dependences which determine the linear rate of combustion of the solid-propellant component. These dependences differ from those which are usually used for the calculation of the rate of combustion of solid fuels in RDTT, which is associated with distinctions in the organization of the process of burning and in the composition of these propellants. As is known, the solid fuel of the RDTT contains in its composition a combustible and oxidizing substances, as a result of which reaction the interactions of the fuel and oxidizer already begin in the solid phase and conclude in the layer of gas which directly adjoins the surface of the fuel. In the GRD the solid part of the fuel most frequently consists only of fuel or only of oxidizer, and therefore for the fuel of engines of this type the presence of the reactions occurring in the solid phase is not characteristic.

The solid component is heated thoroughly by the heat which enters from the combustion zone. Upon reaching on the surface of the solid component of a definite temperature its gasification begins. Depending on the composition of the solid component, the process of gasification can occur differently. This process can be melting with the subsequent evaporation of the liquid phase, sublimation (the transfer of a substance from a solid state into a gaseous state without intermediate conversion into a liquid) or pyrolysis (chemical decomposition with the formation of gaseous substances). The products of gasification enter into the channel of the charge and, being mixed here with another component, form the mixture in which the exothermic reactions of oxidation occur.

If we understand (as is understood, for example, in the ZhRD) the process of fuel combustion as being the entire totality of processes in the chamber which leads to the formation of gaseous products which escape from the nozzle of the chamber, then one should, first of all, note that the process of burning in the GRD is extremely complex.

In order to compile the process of burning in the GRD, one should consider additionally the fact that the liquid component enters into the oxidation processes also in the gaseous form, i.e., having been preliminarily vaporized. Figure 1.2 gives the diagram of the burning of the hybrid propellant in a GRD.

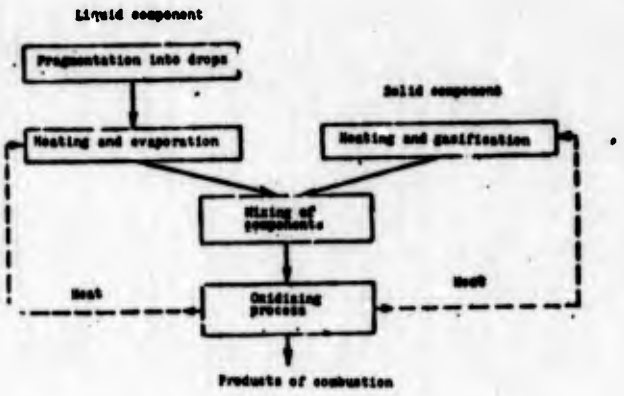

Figure 1.2. Diagram of the burning of a solid-liquid propellant.

Since the very reactions of oxidation occur in the gas phase, which has sufficiently high temperature, these reactions occur very rapidly, and determining for the time of the course of burning are processes of the preparation of the combustible mixture. This burning was called diffusion.

Just as in the ZhRD, the quantity of heat which is released as a result of the fuel combustion and, therefore, the efficiency

of the use of the energy acquired in the fuel depend in a GRD on the relationship of the consumption of the components with their combustion. In connection with this, it is extremely important to carry out fuel combustion with the assigned relationship of its components. The basic condition for this is the provision for good carburetion in the chamber, which is reached by the appropriate operation of the devices which spray the liquid component and determine the nature of motion of the mixture in the channel of the charge. The smaller the atomization of the liquid propellant is, and the more intense its mixing with products of gasification of the solid component will begin to be realized, the better the process of burning in the chamber will occur, and the fuller the combustion of the fuel will be.

From that said above about the nature of the burning of hybrid propellants, it may be concluded, first of all, that in application to the solid component it is more correct to use not the terms "burning" and "rate of burning", but the terms "gasification" and "rate of gasification"[1]. Furthermore, it may be concluded that the determining factors for the rate of gasification should be the factors which affect the intensity of the heat feed to the surface of the solid component and also the thermophysical characteristics of the most solid component.

Heat from the combustion zone is transferred to the surface of the solid component by means of convection and radiation. The process of heat transfer is extremely complex; however, it is possible with sufficient confidence to name those factors which affect the heat-transfer intensity more greatly than others. Such factors should include the rate of the washing of the solid

---

[1]In foreign sources the term "regression" (regression - reverse motion) is frequently used.

component by the flow of gas, the composition, the density and gas pressure, and also the temperature in the combustion zone.

The first factor affects only the intensity of the heat transfer by convection, and the others, furthermore, affect the intensity of the radiation heat exchange. The account of all noted factors, just as the composition of the solid component, finds reflection in empirical relations, for the rate of gasification of the solid component, which most frequently in general are written in the following manner:

$$u=\bar{u}_1 p_к^{\nu}(\rho v)^{\beta} A^{\alpha},$$

where $\bar{u}_1$ - the empirical coefficient which considers the properties of the propellant components; $p_к$, ρ, v - pressure, density and rate of flow of the gases, respectively; A - the discharge coefficient, which considers the properties of the combustion products; ν, β, α - empirical coefficients.

From the continuity equation of the gas flow which moves in a channel with transverse cross section F and with per-second flow rate G, we will obtain

$$\rho v = G/F$$

and, therefore,

$$u \sim \left(\frac{G}{F}\right)^{\beta}.$$

But the per-second flow rate of the gases through the cross section of the channel increases over its length as a result of the entrance of an additional mass as a result of the gasification of a solid component. Therefore, in the case of applying a charge with a cylindrical channel (F=const), the rate of gasification will increase along the length of the channel, which will

lead to the distortion of its initial form, and by a greater degree, the more the flow rate along the length of the charge is changed.

One of the shortcomings of engines which operate on solid fuel, as was noted above, is their sensitivity to the defects of the charge (to cracks, cavities, etc.). The appearance of a crack in a charge of propellant of an RDTT leads to a sharp increase in the burning surface (since the propellant burns in cracks), an appropriate increase in the gas formation in the chamber, and concludes in certain cases even with the destruction of the engine. In engines which operate on liquid-solid propellants, the appearance of cracks in the charge are not as dangerous.

As follows from the examined diagram of burning in the GRD, the necessary condition of the gasification of a solid component is the intense entrance of heat from the combustion zone, i.e., from the flow of the gas which moves along the channel of the charge. Since the heat from this flow will enter less intensely into the cracks than the main surface, the rate of gasification here is lowered, which decreases the effect of the appearance of cracks on the gas formation of the charge.

1.1.3. Propellant Ignition in the GRD

The condition of the maintaining of the steady state of burning of a hybrid propellant in the GRD is the continuous head feed from the combustion zone to the surface of gasification of the solid component. At the moment of starting of the engine, the combustion zone, naturally, does not exist, and for gasification any other special heat source should be used. In connection with this, the question concerning the system of ignition of the propellant for the GRD is no less important than that for rocket engines of other types.

In the literature different methods and ignition systems of the propellant in the GRD are mentioned. It is indicated that if the solid component is capable of independent burning, then it is possible to use a pyrotechnic igniter of the same type as is used in the RDTT. In this case the process of gasification (burning) begins owing to the thermal effect of products of combustion of the igniter on the grain surface.

In the GRD, where the oxidizer is hydrogen peroxide, it is convenient to carry out decomposition of the peroxide at the entry into the chamber. Then into the channel of the charge there will enter the gas heated to more than 700°C, the gasification of the solid component is initiated under the action of heat which comes from products of the decomposition of peroxide, and an additional device for the propellant ignition is not required.

Demonstrated was a small GRD (see [46]), in the propellant of which the oxidizer was oxygen and which was started by means of the injection of a small quantity of propane, which was ignited in the oxygen by means of a starting spark plug. However, it was noted that this system of ignition complicates the engine and is suitable only for a hydrojet with low thrust.

As a method of ignition of the hybrid propellant, which to the greatest degree satisfies the requirements for the simplicity and reliability of the starting of the engine, the ignition with the use of the self-igniting substances is examined. In the theory of the ZhRD this method of ignition is called sometimes "chemical."

There are solid-liquid fuel pairs, with the contact of components of which the exothermic reactions, which lead to the propellant ignition begin. If from these pairs we form the fuel of the GRD, then the problem concerning the starting of the engine is simply solved. Any number of shut-down and starting of the engine is realized by a simple cessation and renewal of the feed of the liquid component.

But if the basic propellant components of the GRD upon contact are not self-ignited, then any third starting component, which is capable of spontaneous combustion upon contact with one of the basic propellant components can be selected. In the case where the starting component is a solid substance and is intended for self-ignition upon contact with the basic liquid component of the propellant, it can be applied to the channel surface of the charge of the solid component. In this case only one starting of the engine is possible. If the starting component, the liquid, self-ignites upon contact with the solid part of the propellant, then it is injected into the chamber at the moment of starting directly before the feed of the basic liquid component. By the complication of the design of the engine, it is possible to insure the repeated injection into the chamber of the starting component and thereby the repeated inclusion of the chamber into operation.

The ignition can be carried out by the creation of a porous solid component and the filling of the pores by the liquid self-igniting upon contact with another component. The gasification surface should upon ignition of the engine have a sufficient quantity of open pores in order to provide ignition; however, the pores should, at the same time, be so small that the liquid does not escape from them.

One also considers it possible to insure ignition by means of the inclusion into the solid component of particles capable of reactions with heat liberation upon contact with the liquid component.

1.1.4. Diagram and Operating Process of the RDTT with Divided Propellant Components (RDTT RS)

The possible schematic diagram of the RDTT with separate propellant components is given in figure 1.3. The engine includes two chambers 1 and 2 with solid-propellant grains connected with

each other by the channel in which the gas flow regulator 3 is installed. Chamber 2 (gas generator) has the igniter 4.

Figure 1.3. Schematic diagram of an RDTT with separate propellant components: 1 - thrust chamber; 2 - gas generator; 3 - gas flow regulator; 4 - igniter.

The propellant of chamber 2 should be capable of independent burning. At the moment of starting, the engine actuates the igniter, and the propellant in chamber 2 burns, and the combustion products formed enter into the channel of the charge of chamber 1 and pass through it in the direction toward the nozzle, heating the surface of the propellant in chamber 1.

Depending on the composition of the solid component in chamber 1, there begins one process of the other of its gasification (burning, sublimation, etc.). The products of gasification enter into the channel, are mixed with the gases which were formed in chamber 2, and enter with them into the reaction of the interaction, formed as a result of which are the combustion products which escape through the engine nozzle.

It is obvious that the processes in chamber 1, to a considerable degree, are similar to processes in the chamber of the GRD, which also gives grounds to refer to one group of engines as hybrid engines (GRD's) and RDTT with separate propellant components.

Since the thrust of the RDTT RS is determined by the parameters of the operating process (pressure) in chamber 1, and chamber 2 serves only for obtaining one of the propellant components in a gaseous form, subsequently chamber 1 will be called *thrust* and chamber 2 - *gas generator*.

The examined design of the RDTT with the separate propellant components is more complex than the design of the standard RDTT, and this is its shortcoming. However, unlike the "classical" design of the engine which operates on solid fuel, the design of the RDTT with the separate components makes it possible:

a) to select the propellant components (placed in separate chambers) in the wider range of their characteristics than prerequisites are created for an improvement in the energy parameters of the engine;

b) by regulating the gas feed from the gas generator into the thrust chamber, to change the total flow rate of the propellant into engine and thereby regulate its thrust.

1.2. CLASSIFICATION OF THE KRD

Engines which operate on hybrid propellants and RDTT with separate propellant components can be greatly distinguished in design and features of the organization of the operating process. There is no universally recognized classification of the KRD as yet.

In table 1.1 a possible version of the classification of rocket engines is proposed.

Let us examine some features of the designs and operating processes of KRD of different types.

Table 1.1

Criterion according to which the classification is carried out	KRD	
	GRD	RDTT RS
Form of propellant components		
Arrangement of the propellant components	a) in the chamber - fuel, in the tank - oxidizer (direct design); b) in the chamber - oxidizer, in the tank - fuel (reverse design); c) mixed direct design; d) mixed reverse design	a) in the thrust chamber - component with an excess of fuel, in the gas generator - component with an excess of oxidizer (mixed direct design); b) in the thrust chamber - component with an excess of oxidizer, in the gas generator - component with an excess of fuel (mixed reverse design)
Possibility of control of the engine in operation	a) controlled; b) uncontrolled	a) controlled b) uncontrolled
Adjustment of the engine up to operation	a) adjusted; b) unadjusted	a) adjusted; b) unadjusted
Number of possible startings	a) single starts; b) repeated starts	a) adjusted; b) unadjusted
Place at the input of the component into the chamber	a) only through the head; b) only at the nozzle; c) both through the head and nozzle	a) only through the head; b) only at the nozzle; c) both through the head and nozzle
Number of propellant components	a) on two components; b) on three components	
Type of feed system of liquid component	a) with pressure feed system; b) with pump feed system	

In such a case when in the chamber of the GRD there is placed fuel and in the tank of the GRD - the oxidizer, it is accepted to call the design of the engine *direct*, in the opposite case - *reverse*[1]. Sometimes as the propellant components of the GRD it is more preferable to use not "pure" oxidizer and fuel but mixed substances, for example, the mixture of a solid oxidizer and fuel, i.e., a solid fuel of the type of fuel used in an RDTT of standard design. Let us call the design of the GRD with this fuel, respectively, the "mixed direct", or "mixed reverse," depending on which component is stored in the tank.

The majority of the GRD developed and investigated at present belongs to the number of engines of direct design. This is connected with the fact that the use of a *liquid oxidizer* and a *solid fuel* gives greater possibilities for creating an engine with high energy characteristics than does the use of a solid oxidizer and liquid fuel.

In a gas generator of the RDTT RS there must be the component which consists of a mixture of the fuel and oxidizer. In the thrust chamber, unlike the gas generator, the arrangement of a "pure" component (only fuel or only oxidizer) is possible.

Above it has already been noted that in hybrid engines and RDTT with separate propellant components, it is possible to change, in the process of their operation, the feed of the external component into the chamber. In this way the control of engines is realized. The purpose of the control can be the change in the different parameters of the KRD - the thrust, the relationship of flow rates of the components, etc. Depending on whether the

---

[1]The names "direct" and "reverse" for design of the GRD are not connected with features of design and operating processes of these engines and are random. However, these names have already been accepted in literature and for convenience will be used by us.

parameters of the engine with its operation are controlled or not controlled, the GRD and RDTT RS are divided into controlled and uncontrolled.

As was noted above, the rate of the gasification of the solid component depends on the flow rate of the gases along the surface of gasification (it is proportional to value $G_{ж}^{\beta}$). Hence it follows that by changing the flow rate of the liquid component into the chamber for the purpose of the control of the engine, we exert an effect also on the flow rate of the solid component of fuel, whereupon in a design with the feed of the liquid component only into the head of the chamber (see figure 1.1) this effect cannot be "controlled" - it is unambiguously determined by the value of coefficient β. In connection with this, in engines of such design the control of the thrust is accompanied by a change in the relationship of flows of the fuel component, i.e., the flow rate of solid component is changed with a change in the flow rate of the liquid component not in the same degree. This is a shortcoming of the GRD of this design, since the relationship of the flow rates of the components is selected at the optimum, and any deviation from it makes the engine characteristics worse.

One can avoid a change in the relationship of flow rates of components if passing through the channel of the charge of the solid component will be not the entire liquid component fed into the chamber, and if the portion of the flow rate of the liquid component directed into the channel of the charge, with the control of the engine, is controlled in the appropriate manner.

For realization of this system of control of the GRD, its chamber should be made according to the diagram depicted on figure 1.4. Unlike the previously examined diagrams of a chamber with the introduction of the liquid component only into the head, in this case the liquid component is inserted in two places: besides its feed through the injectors installed on the head, it is fed

partially into the volume of the chamber located between the charge of the solid component and the nozzle. The process of fuel combustion in this type of chamber is divided according to the feed of the liquid component into two zones; therefore, the pre-nozzle volume where burning is concluded is occasionally referred to as the *afterburner*. A similar design of gas feed from the gas into the thrust chamber can appear in an RDTT of separate loading, in connection with which for this engine type, just as for the GRD, the classification according to the place of the introduction of components into the chamber is introduced.

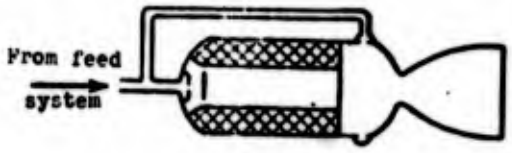

Figure 1.4. Diagram of a GRD with feed of the liquid component into the head and pre-nozzle volume of the chamber.

As rocket engines of any other type, the KRD are subjected to the effect of external conditions (for example, ambient temperatures), as a result of which of their characteristics can be changed in different cases of application. The insuring of the maintaining of the engine characteristics within the assigned limits under any possible conditions of its use is possible with the introduction of an adjustment. For the GRD the adjustment can be realized by covering the throttle installed in the line of feed of the liquid component, and for an RDTT with separate propellant components - by covering the throttle in the pipeline which connects the gas generator and thrust combustion chamber. Adjustments of the KRD cannot be made, and, in accordance with this, the combined engines are divied into *adjustable* and *non-adjustable*.

The propellant of hybrid rocket engines can include not only two but three components[1]. Thus, for instance, examined as

[1]Engines which operate on the hybrid propellant, which includes three components, are occasionally referred to as *tribrid*.

a possible design is the design of a GRD in which, besides the liquid oxidizer and solid fuel, the use of hydrogen is provided. It is assumed that hydrogen is fed in a liquid state into the pre-nozzle part of the chamber for the purpose of decreasing the molecular mass of the gases which escape through the nozzle (for an increase in the specific impulse) with the simultaneous cooling of the gases and the facilitation thereby of the operating conditions of the nozzle. The use of three propellant components in the RDTT with separate components does not make sense, and therefore the classification according to the number of propellant components is provided only for the engines which operate on liquid-solid propellants.

The hybrid rocket engines can be greatly distinguished also by features of the system of feed of the liquid component. The two basic groups of the feed systems of the liquid component distinguished above in the classification of the GRD (pressurization and pump), in turn, are distinguished by a number of criteria. Diagrams of feed systems of the components will be examined in more detail subsequently.

Classification of the KRD according to the number of possible inclusions (startings), apparently, does not need an explanation.

We have examined only those criteria for the classification of the KRD which are connected with the features of their designs and operating conditions. Besides this, the combined rocket engines, of course, can be classified also according to others - general for all rocket engines - criteria, for example, according to the thrust force magnitude (low thrust, high thrust, etc.), according to purpose (KRD of carrier rockets, KRD of space vehicles, etc.) and so on.

1.3. PROPELLANTS FOR THE KRD

1.3.1. Classification of the Propellant

The propellants for combined rocket engines are divided:

by the quantity of the components into a) two-component and b) three-component;

by the form of the components into

a) propellants which contain a liquid oxidizer and solid fuel (propellant of the GRD of direct design);

b) propellants which consist of a solid oxidizer and liquid fuel (propellant of a GRD of reverse design);

c) propellants in which the solid component is not a "pure" oxidizer or "pure" fuel but a mixture of an oxidizer and fuel (propellant of a GRD of mixed design);

d) propellants in which the fuel and oxidizer are solid (propellant of an RDTT of separate loading).

The general requirements for the propellants of a KRD coincide with general requirements for propellants of rocket engines of other types:

a) the propellant should provide as large a specific impulse of the engine as possible, i.e., possess as large a reserve of the energy as possible, which is liberated in the burning process. In this case it is desirable that the combustion temperature be low, and the increase in the specific impulse was provided by the presence of as large a value as possible of the gas constant of the combustion products (as small a molecular mass of them as possible);

b) the density (mass per unit volume) of the propellant should be as large as possible;

c) the propellant components should be stable with storage, and the boiling and freezing points of the liquid component should be such that the operation of engine under the assigned conditions would be possible;

d) the propellants should be convenient and safe in operation, and as far as possible, nonagressive and nontoxic;

e) properties of the propellants should provide a stable engine operation in the assigned range of the modes; the liquid component should possess the properties which make it possible to use it for the cooling of the engine chamber;

f) the propellant components should have sufficient raw-material and production bases and have an accessible cost.

Besides these general requirements, for the propellant components of the KRD under certain conditions which depend on the type and purpose of the engine for which the propellant is intended, there can be presented other, special, requirements, for example:

a) definite requirements for the law of the rate of gasification of the solid component, which result from conditions of components of the engine and its control;

b) requirements for the relationship of the solid-liquid components (larger portion of one component or the other), which ensures the obtaining of the desirable parameters of the entire engine;

c) the requirement for the spontaneous combustibility of the propellant components and others;

It is usually impossible to satisfy all the requirements for the propellants in an equally high measure, and it is necessary (depending on the specific conditions of the use of the propellant) to determine the relative importance of the different requirements, giving then primary attention to the execution of precisely those which are considered the most important.

1.3.2. Oxidizers of Propellants for the KRD

As *liquid oxidizers* of propellants for hybrid rocket engines in practice there can be used all the oxidizers which are applied or are considered as being possible for use in propellants of liquid-propellant rocket engines. The properties of some liquid oxidizers are given in table 1.2.

Table 1.2

Oxidizer	Formula	Density* kg/m³	Melting point, °C	Boiling point, °C	% of free oxidizer (oxygen, fluorine, chlorine) throughout mass	Other characteristic problems
Oxygen	O_2	1140	−218	−183	100	—
Hydrogen peroxide	H_2O_2	1460	−1	150	47	Unstable
Nitric acid	HNO_3	1520	−41,2	86	64	Aggressive; toxic
Nitrogen tetroxide	N_2O_4	1450	−11	21	70	—
Tetranitro-methane	$C(NO_2)_4$	1620	13,6	127	49	—
Fluorine	F_2	1510	−218	−188	100	Aggressive; toxic
Fluorine oxide	F_2O	1520	−223	−144	100	Aggressive; toxic
Chlorine trifluoride	ClF_3	1825	−82,6	+12,1	100	Toxic

*The density for liquified gases is given at a temperature close to boiling point.

Besides the oxidizers enumerated in this Table, some of their mixtures can be used. Thus the mixture of nitric acid and nitrogen tetroxide with their definite proportion is the oxidizer which exceeds according to the number of the indices the initial products (for example, $t_{пл}$ can be lower than that of HNO_3; the density is higher than the density of both initial components; the aggressiveness is decreased with respect to the structural materials; the efficiency of the use of this oxidizer with a number of fuels) increases. The mixtures of oxygen and fluorine are considered promising.

From the oxidizers and their mixtures given in table 1.2, the greatest interest at present is in the following:

a) oxygen, fluorine and their mixture are oxidizers of high energy efficiency, but they are inconvenient in inversion as a result of the low boiling point (under the usual conditions these substances are gases), and fluorine, furthermore, due to its aggressiveness and toxicity;

b) hydrogen peroxide is a sufficiently effective oxidizer convenient for use in the GRD as a result of its capability for rapid decomposition on catalysts with the formation of hot gas, which then can be effectively used in the chamber of a GRD. The shortcoming of H_2O_2 is the difficulty of providing its stability with prolonged storage in tanks of the engine;

c) mixtures of nitric acid and nitrogen tetroxide are oxidizers of prolonged storage and relatively simple in inversion, although possessing a comparatively low energy efficiency.

All the oxidizers (with the exception of fluorine) given in the table 1.2 have the raw-material and production bases developed in many countries and relatively low cost.

The contemporary *solid oxidizers* contain oxygen and, furthermore, sometimes a certain quantity of chlorine as the basic oxidizing element. The solid compounds of fluorine exist; however, the quantity of free fluorine in them is insignificant, and therefore the compounds of fluorine as solid oxidizers are not used.

The majority of the oxygen solid oxidizers are either nitrates or perchlorates of elements (sodium, potassium, lithium) or groups (ammonium, hydrazine, nitronium, etc.). More effective oxidizers are the perchlorates. The use of oxidizers in which used are perchlorates with an addition of other oxidizing substances is possible.

Some properties of a number of solid oxidizers are given in table 1.3.

Table 1.3

Oxidizer	Formula	Density kg/m^3	% of free oxygen	Temperature of start of decomposition °C
Ammonium nitrate	NH_4NO_3	1720	20	170
Ammonium perchlorate	NH_4ClO_4	1950	34	150
Potassium perchlorate	$KClO_4$	2520	46	400
Nitronium perchlorate	NO_2ClO_4	2250	66	100
Lithium perchlorate	$LiClO_4$	2430	60	400
Ammonium perchlorate+hydrazine nitrate	70% NH_4ClO_4+30% $N_2H_4HNO_3$	1850	26	150
Nitrosyl perchlorate	$NOClO_4$	2170	61.7	-

The decomposition of solid oxidizers begins from the formation of intermediate products - oxides of nitrogen, ammonia, perchloric acid, and others. At higher temperatures the nitrogen oxides are decomposed into nitrogen and free oxygen. Lithium perchlorate is decomposed in a liquid state ($t_{пл}$=236°C) and nitronium and ammonium perchlorates are decomposed into gaseous products in the solid phase.

Some of the solid oxidizers at increased pressures are capable of independent burning. Ammonium perchlorate, for example, burns without any additions at pressures higher than $22 \cdot 10^5$ Pa. Under certain conditions (a pressure increase, the presence of impurities) the burning of solid oxidizers can turn into an explosion. Nitronium and lithium perchlorates are sensitive to the mechanical and thermal effect more than others.

A positive quality of all the examined solid oxidizers is their considerable density.

Some oxidizers are hygroscopic, which impedes their use in engines. The very hygroscopic ones are, in particular, nitronium and potassium perchlorates.

All the solid oxidizers are crystal powders. The preparation of grains which possess high mechanical qualities from "pure" oxidizers is made difficult, in connection with which it can prove to be advisable to add to the oxidizer a certain quantity of fuel-binding substances - natural rubber, resin, etc. In foreign literature (see [53]) reports have been presented on the conducting of successful tests of a GRD in which the grain of the oxidizer was prepared from a composition containing 90% of ammonium perchlorate with additions.

Ammonium perchlorate possesses a number of very favorable properties for use as a solid oxidizer in the KRD - it has a low

temperature of decomposition, is decomposed only into gaseous products (since it does not contain metals), possesses low hygroscopicity, and is accessible and cheap. However, ammonium perchlorate, as is evident from the table 1.3, is the oxidizer which contains a relatively small quantity of free oxygen.

The most effective oxidizers - perchlorates of nitronium, nitrosyl and lithium - possess a number of negative qualities, which although they do not make their use impossible, they impede it to a great degree. Furthermore, these substances are high in cost.

1.3.2. Combustible Propellants for KRD

From the elements, on the basis of which are created the combustible propellants for KRD hydrogen and carbon are more common than others and will be used, and the hydrogen, as a result of its low molecular mass, provides the achievement of very high values of specific impulse.

The high thermal effect of the reactions is reached with the oxidation of a number of metals (lithium, beryllium, boron, and aluminum). However, the oxides of these metals possess a high boiling point (for Be - 2900°C, for Al - 2980°C, for B - 3250°C, and for Li - 1700°C), which makes the presence of the condensed phase in products of the combustion of fuels which contain these elements. Furthermore, the oxides of some of the enumerated elements have a very high molecular mass (Al_2O_3 - 101.94, B_0O_3 - 69-64 etc.), which does not make it possible to obtain a high specific impulse if in the products of combustion these oxides will be great.

The use of metals therefore is effective only in such cases when, besides them, the fuel has other combustible elements, especially hydrogen. In this case it is possible to obtain a

high thermal effect of the reactions of burning with a relatively low molecular mass of products of combustion and, as a result, insure the conditions for obtaining a high specific impulse. It is inconvenient to insert metals into the liquid propellant component; and therefore usually they are a composite part of the solid component.

As *liquid combustible* propellants for the GRD virtually all, both cryogenic and high-boiling, combustible propellants of liquid-propellant rocket engines can be used.

The properties of some most commonly used or promising of these fuels are given in table 1.4.

Table 1.4.

Fuel	Formula	Density kg/m^3	Melting point	Boiling point	Other characteristic properties
Hydrogen	H_2	71	-259.4	-252.1	-
Hydrazine	N_2H_4	1010	2	113.7	Toxic
Unsymmetric dimethyl hydrazine	$N_2H_2(CH_3)_2$	790	-58	63.1	Toxic; hygroscopic
Kerosene	$C_{7.21}H_{13.29}$	830	-60	180	-
Pentaborane	B_5H_9	633	-46.6	58.2	Stable only with storage in a hermetically sealed tank; toxic

The operating characteristics of the first four fuels given in table 1.4 are well-known. As regards pentaborane, this fuel, as a result of its high toxicity and capability for spontaneous combustion in air, is inconvenient for use. However, at the present there are additives which sharply raise (by more than 100°C) the spontaneous combustion temperature and thereby making

it possible to simplify the conditions of the use of propellants which include pentaborane.

Different substances can be used as *solid-combustible* propellants for the KRD. The range of solid fuels is very wide; it can include substances of different classes: polymeric compounds, hydrides of metals, and others.

Table 1.5 gives the properties of some substances which can be used as the fuel in propellants for the KRD.

Mixtures of different fuels can be used. Thus, for instance, a report was given (see [26]) on tests of the GRD, the combustible in the propellant of which was lithium aluminum hydride with an addition of polyethylene. It was established that good mechanical properties of a charge of this mixture and the high specific impulse were reached upon the inclusion into the mixture of 95% $LiAlH_4$ and 5% $(C_2H_4)_x$.

Table 1.5

Fuel	Formula	Density kg/m^3
Polyethylene	$(C_2H_4)_x$	920
Polyethylenamin	$(C_2H_5)_x$	1100
Natural rubber	85% SKDN+9.6% Al+3.4% S	1000
Lithium hydride	LiH	800
Aluminum hydride	AlH_3	1500
Lithium aluminum hydride	$LiAlH_4$	920
Beryllium hydride	BeH_2	1600
Dihydrazine acetylene	$C_2H_6N_4$	1130

Table 1.5 gives pure metals (Be, Al, Li), although they could theoretically be considered as the possible fuels for a GRD.

Above some negative qualities of metalliferous fuels were already noted. Furthermore, the use of pure metals as fuels is extremely inconvenient for a whole number of reasons. Thus lithium is very easily melted ($t_{пл}$=186°C), beryllium has high thermal conductivity, and because of this it is difficult to raise the temperature of its surface to the ignition point, and so on. Therefore, it is considered that it is better to use not pure metals but their compounds, mainly hydrides, as fuels.

When evaluating the properties of fuels on the basis of berillium, it is necessary to keep in mind the high toxicity of the products of their combustion. The conducting in open air of firing tests of the RDTT with a propellant which contains Be causes great poisoning of the atmosphere (see [9]), the development of devices which make it possible to clean the combustion products from the berillium compounds is extremely expensive and complicates the engine test stands. Furthermore, beryllium is still expensive; for example, in the USA it costs 110-220 dollars per 1 kg.

1.3.4. Propellants for KRD (Fuel Pairs)

On the basis of the fuels and oxidizers enumerated above, it is possible to create different fuel pairs.

Table 1.6 gives the thermodynamic properties of fuels. Values of specific impulse are calculated with pressure differentials of $p_к/p_а$=40/1 and 70/1 for the case of engine operation on the ground; the specific impulse with $p_к/p_а$=70/0.05 is determined with $p_Н$=0. Values of the specific impulses are given with $K=K_{опт}$, i.e., with the relationships of flow rates of components which ensure the maximum value of the specific impulse.

The fuels 1-13 consist of a liquid oxidizer and solid fuel, i.e., they are the propellants of the GRD of direct design.

Table 1.6

No.	Oxidizer	Fuel	$K_{ст} = G_{ок}/G_{гор}$	Density, kg/m³	$p_к/p_а$	$T_к$ in K	Specific impulse, (kg/s)
1	H_2O_2 (98%)	Polyethylene	6,55	1350	40/1	2957	2580
					70/1	2995	2720
2	H_2O_2 (98%)	Natural rubber+18% Mg	5,56	1440	40/1	3029	2600
					70/1	3075	2750
3	H_2O_2 (98%)	Natural rubber+18% Al	5,64	1500	40/1	3058	2610
					70/1	3101	2760
4	H_2O_2 (98%)	AlH_3	1,02	1470	40/1	3764	2910
					70/1	3844	3100
					70/0,05	3844	4000
5	H_2O_2 (98%)	$LiAlH_3$	1,08	1130	40/1	3068	2770
					70/1	3101	2930
6	H_2O_2 (98%)	BeH_2	1,23	1510	40/1	—	3310
					70/1	3164	3520
7	N_2O_4	$C_2H_6N_4$+10% natural rubber	1,5	1300	40/1	3580	2750
8	70% HNO_3 30% N_2O_4	80% $C_2H_6N_4$+20% natural rubber	2,13	1380	40/1	3320	2610
9	HNO_3	Natural rubber+Al	3,72	1370	40/1	3229	2490
					70/1	3278	2620
10	N_2O_4	BeH_2	1,67	1500	40/1	3620	3060
					70/1	3673	3260
					70/0,05	—	4260
11	ClF_3	LiH	5,82	1550	40/1	4190	2810
					70/1	4267	2960
12	O_2	Natural rubber	2,38	1090	40/1	3618	2810
					70/1	3637	2960
13	F_2	LiH	4,3	1290	40/1	4762	3390
					70/1	4893	3600
14	O_2	80% BeH_2+20% H_2	1,17	1210	40/1	3507	3900
					70/1	3566	4160
					70/0,05	—	5340
15	F_2	85% LiH+15% H_2	6,2	1300	40/1	4744	3530
					70/1	4879	3730
					70/0,05	—	4520
16	NO_2ClO_4	NDMG	2,4	1470	40/1	3466	2680
					70/1	3535	2830
17	NO_2ClO_4	B_5H_9	3,40	1420	40/1	3950	2770
18	NO_2ClO_4	$LiAlH_4$	0,94	1290	40/1	3342	2680
					70/1	3390	3600
19	NO_2ClO_4	AlH_3	0,90	1790	40/1	3847	2710
					70/1	3936	2880
					70/0,05	—	3690
20	NO_2ClO_4	BeH_2	1,62	1950	40/1	3696	3040
					70/1	3760	3240

The number of these propellants includes both propellants on the basis of oxidizers with a high boiling point and propellants the oxidizer in which cryogenic substances serve.

The higher values of specific impulse in the GRD, just as in the liquid-propellant rocket engine, are obtained in the case of the use of liquid oxygen and fluorine, which are oxidizers which possess higher energy efficiency than the high-boiling H_2O_2, N_2O_4 and HNO_3.

Examined as one of the most probable liquid oxidizers for GRD abroad is the highly concentrated hydrogen peroxide. The composition of combustion products of the propellant, which includes this oxidizer and the metalliferous fuel, possesses the characteristic features which can be examined in the example of the composition of products (in %) obtained in the case of the combustion of H_2O_2 (98%) and BeH_2 with $p_к = 70 \cdot 10^5$ Pa:

H	0.48
H_2	14.67
Be	1.21
BeH	0.35
H_2O	0.003
BeO	83.287

Attention is drawn to the fact that almost the entire oxygen is connected by metal, as a result of which the combustion products contain much free hydrogen, and this is a favorable fact which determines the high value of the theoretical value of the specific impulse.

At the same time, with the high concentration of the condensate (mainly BeO), the acceleration of the combustion products in the nozzle is accompanied by an intense consolidation of the particles,

and even at very small dimensions in the chamber ($\sim$1 μm) in the region of the throat their average diameter increases to dozens of micrometers (see [2]). In this case losses of the specific impulse can exceed 10%.

Propellants 14 and 15 are three-component compositions. These propellants, besides the solid fuel, include liquid fuel - hydrogen. Specifically, these propellants provide the achievement of the highest values of the specific impulse. The presence of metals in propellants of this type makes it possible to obtain the temperature in the chamber higher (by approximately 100-200°) than in the case of using similar basic components without the additions of metals (O_2+H_2 or F_2+H_2). At the same time, the concentration in the propellant of a large quantity of hydrogen provides a low molecular mass of the combustion products. As a final result the product $RT_к$, on which the specific impulse depends, is larger.

From the bipropellants of this group, according to magnitude of the specific impulse, the propellants the fuel in which is berillium hydride are distinguished.

Propellants 16 and 17 contain a solid oxidizer and liquid fuel and are examples of propellants of a hydrojet of reverse design.

When using these propellants, as is evident from table 1.6, it is possible to obtain sufficiently high values of specific impulse; however, used as an oxidizer in these propellants is nitronium perchlorate, which, as was already mentioned, is thus far insufficiently assimilated. The use of this type of well assimilated and widely used ammonium perchlorate as an oxidizer in the propellants would lead to a certain decrease in the specific impulse.

The propellants 18, 19 and 20 include only solid components,

i.e., they refer to propellants of the RDTT with separate components. The highest value of the specific impulse can be obtained with these propellants in the case of the use of berillium hydride as a combustible.

Table 1.6 gives values of the specific impulse calculated from the mass flow rate of the propellant. Since, besides the requirement for high energy efficiency, the propellants have the requirement for high density and to evaluate the propellants it is convenient to use the volumetric specific impulse $I_{об}=I_{\rho_т}$, i.e., the thrust which is necessary for the flow rate of the propellant at 1 l/s (here $\rho_т$ is the density of the propellant in kg/l).

Figure 1.5 gives data which makes it possible to compare between each other the solid, liquid and hybrid propellants according to values of the mass and volumetric specific impulses. Theoretical values of the specific impulse are determined for the expansion ratio of gases in the nozzle $p_к/p_а=70/1$.

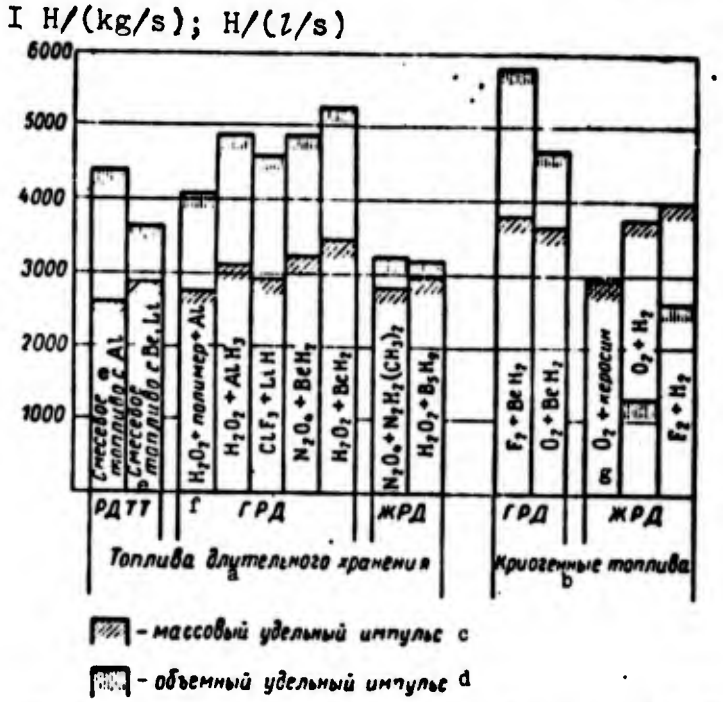

Figure 1.5. Comparison of the propellants of different rocket engines according to specific impulses.
Key: (a) Long-term storable propellants; (b) Cryogenic propellants; (c) Mass specific impulse; (d) Volumetric specific impulse; (e) Mixture fuel with; (f) polymer; (g) kerosene.

The data given in figure 1.5 indicate the great energy possibilities of engines which operate on hybrid propellants. According to the magnitude of the volumetric specific impulse, the GRD's when using a number of fuel compositions, substantially exceed other types of rocket engines which operate on chemical energy sources.

1.4. FEATURES OF A SYSTEM OF CHAMBERS AND FEED SYSTEMS OF THE LIQUID PROPELLANT COMPONENT IN A GRD

1.4.1. Chambers of Hybrid Rocket Engines

The design of the simplest chamber of the GRD (feed of liquid component only through the head; components are self-igniting; nozzle is not cooled) differs from the design of the chamber of the RDTT only by the presence of the injectors and the absence of igniters.

The charge of the solid component should have a form which provides the necessary change in the surface of gasification during the entire operating time of the engine. In foreign GRD's charges with channels whose cross section is not changed along the length of the charge or changed along the sections were tested and are used. Some of the forms of cross sections of the channels, which were mentioned in foreign literature, are given in figure 1.6.

Figure 1.6. Forms of the charges of solid component.

To evaluate the possibility of the selection of one form or the other of the charge in the GRD, it is necessary to keep in

mind that the rate of gasification of many solid propellant components is small and is 1-5 mm/s. This means that the charges of the GRD should have little thickness of the burning arch and a very developed surface of gasification. The relationships of the dimensions of charges of the simplest forms prove to be (especially for large engines) unfavorable. If, for example, the gas formation of the charge should be 25 kg/s at a rate of gasification of 2.5 mm/s and ρ_T=2000 kg/m^3, then the burning surface S should be equal to

$$S=\frac{G}{u\rho_T}=\frac{25}{2{,}5\cdot 10^{-3}\cdot 2000}=5\ м^2.$$

If, furthermore, the operating time of the engine is 50 s, and the diameter of the internal channel is equal to 0.1 m, then the external diameter of the grain should be equal to $D=0.1+2\cdot 50\cdot 2.5\cdot\cdot 10^{-3}=0.35$ m, and its length $L=S/\pi D=5/n\cdot 0.1\sim 16$ m. It is completely obvious that this relationship of the dimensions of the grain (length of 16 m with a diameter of 35 cm) is unacceptable. The way out can be found by using either a multichamber design (for example, eight chambers each 2 m in length) or multichannel charges. True, both versions have their shortcomings: the use of several chambers complicates the structure and makes it heavier, but the use of a multichannel charge impedes the final development of the controls of injection of the liquid component. In connection with this, it is desirable that the rate of gasification of the solid component be more than its magnitude reached at the present for many fuel pairs.

In foreign press reports are given about attempts to develope GRD's which have chambers made from designs which differ from the examined simplest designs.

French scientists (see [59]) have tested a GRD the design of the chamber which is given in figure 1.7. Placed in chamber casing 1 is the charge 2, which is a cylindrical channel-free grain

installed on stops 3. The liquid component is fed through injector 4 into the pre-nozzle space. The charge is gasified on the end. If the grain were fixed in the chamber, then in the process of the engine operation the surface of gasification would be moved relative to the injectors, which would change the conditions of burning. In order to avoid this, cavity A of the chamber is connected with the pipeline of the feed of the liquid component, as a result of which the pressure in this cavity with engine operation will be higher than the pressure in the chamber. Under a pressure differential the charge of the solid component is moved with the gasification downward, being pressed the whole time against the stops 3.

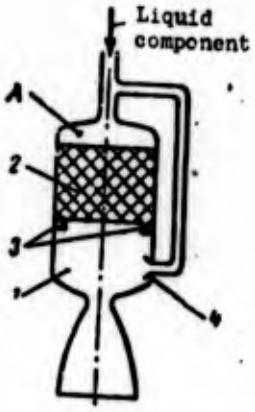

Figure 1.7. Diagram of a GRD with a moving charge: 1 - chamber; 2 - moving charge; 3 - stops; 4 - injector; A - cavity of chamber.

This design, apparently, can be used only in such a case when it is possible to insure a reliable seal on the surface of contact of the charge with the chamber wall. In the described experiments the charge was prepared from polybutadiene, and the airtightness was provided by the elastic properties of the fuel itself. The high combustion efficiency and performance stability (combustion period reached 34 s) are noted.

It is indicated that the similar chambers can appear suitable for a GRD with little thrust and prolonged operating time. Apparently, the chambers of this design are more suitable for a GRD with non-self-igniting propellant components, otherwise there

additionally appears the problem of the insulation of the solid component from the liquid component over the surface receiving the pressure.

Figure 1.8 gives a design of the chamber of a GRD with a sectional charge. Installed between the sections of the charge 2 are throttle washers 3, prepared just as the sections of charge, from the solid propellant component. The presence of throttle disks causes intense agitation of the flow of gases in channels of the sections, owing to which the mixing of the components is improved, and the completeness of their combustion is raised.

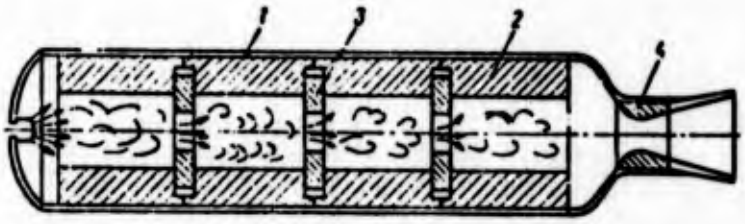

Figure 1.8. Chamber of a GRD with a sectional charge: 1 - housing; 2 - charge of solid component; 3 - throttle disk; 4 - nozzle.

Examined as a possible design of the chamber of the GRD is the design of the chamber in which a charge from a porous solid component is installed. The liquid component is fed the external part of the charge and, passing through the pores, enters into the channel of the charge evenly over its entire surface.

The operation of the injection head has for the GRD a very large value, not less than for a liquid-propellant rocket engine, where, as is known, the final working out of controls of the fuel injection is always given considerable attention. The injectors of the chamber of the GRD determine the conditions of the entry of the liquid propellant component into the channel of the charge, and, thereby, the factors which affect the intensity of the heat exchange and burning in the channel are determined.

In certain cases, as has already been indicated earlier, the liquid component is gasified before the channel inlet, which improves the conditions of carburetion.

Figure 1.9 shows a design of the chamber of a GRD, the oxidizer of the fuel in which is hydrogen peroxide. Before entering into the chamber, the peroxide passes through a catalyst where it is decomposed.

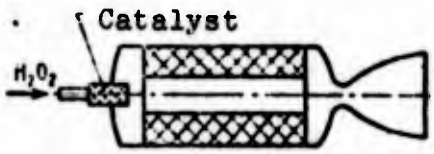

Figure 1.9. Chamber of a GRD with feed of H_2O_2 into the head.

Data on the tests of a GRD with different types of injectors for the feed of the liquid component are published. Some of these data are given in figure 1.10. Used as the oxidizer in an experimental engine was a mixture of fluorine and oxygen, as the fuel polyethylene was used. The line shows the calculated curve of the dependence of the specific impulse on the relationship of the flow rate of the components, the dots - experimental data for the different types of injectors, circles - for jet injectors, squares - for jet injectors with the intersection of the jets, and rhombs - for injectors with the turbulence of the liquid.

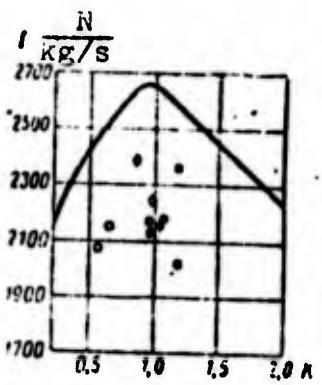

Figure 1.10. Dependence of specific impulse on the relationship of the flow rate of components for the propellant "polyethylene+FLOX".

As follows from figure 1.10, the type of injectors has a very considerable effect on the combustion efficiency of the propellant. The fullest combustion in this case was provided by injectors with swirling. This means that the agitation of the flow of the liquid component at the channel inlet of the charge favorably affects the fuel combustion.

The type of injector also affects the rate of gasification of the solid component. Thus, for instance, according to data of a Swedish firm the use in a GRD, the oxidizer of the fuel in which is white smoking nitric acid, of centrifugal injectors instead of jet injectors considerably increases the rate of the gasification on the initial section of the charge. The effect of the type of injector on the rate of gasification was traced approximately to 2/3 of the length of the grain.

Figure 1.11 gives the shape of the burnout of the charge made from $LiAlH_4$ in an engine where the oxidizer consisted of products of the decomposition hydrogen peroxide. The zone of the increased rate of gasification is clearly visible. The authors of works on the study of these engines explain this local increase in the rate of gasification by the effect of products decomposition H_2O_2, which is connected with the operation of the injectors.

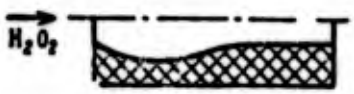

Figure 1.11. Shape of burnout of a charge.

As is known from the theory of the liquid-propellant rocket engine, in order that the liquid propellant burns completely, a definite volume of the chamber is necessary - for a liquid-propellant rocket engine operating on high-boiling propellant components, for example, the volume of approximately 1 l for the fuel consumption of 1 kg/s is required.

A definite volume is necessary for a fuel combustion in hybrid rocket engines. This volume is formed by the volume of the channel of the charge and by the volume of the pre-nozzle part of the chamber (the volume of the chamber of the liquid-propellant rocket engine is usually connected to the volume before the critical throat area of the nozzle). In the pre-nozzle part of the chamber, escaping from the channel of the charge are gases in which there are not completely mixed and not completely reacted propellant components.

In order to insure the afterburning of the components, a definite length of the free volume of the chamber is required. This was confirmed experimentally - the lengthening of the chamber beyond the charge lead to an increase in the combustion efficiency. However, as in liquid-propellant rocket engines, the lengthening of the chamber in the GRD is useful only up to a certain value, since with the lengthening of the chamber thermal losses grow. Furthermore, naturally, an increase in the free volume of the chamber leads to a deterioration in its characteristics with respect to the mass and the dimensional characteristics.

The experiments also established that it is possible to intensify the afterburning of the components in the cavity beyond the charge and without a noticeable increase in its volume. For this it is necessary to create turbulence of the flow of the combustion products by installation in the cavity beyond the charge of the diaphragm with openings. Figure 1.12 shows the diagram of an experimental chamber of a GRD with this diaphragm turbulence ring.[1]

---

[1]The authors of the article, in which this design is given, call the diaphragm a "mixing disk."

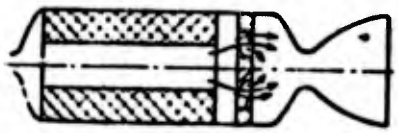

Figure 1.12. Chamber of a GRD with a diaphragm turbulence ring.

According to the results of tests of chambers of the GRD, it can be concluded that in such cases when there actually occurs the incompleteness of combustion in the zone before the turbulence ring, its introduction noticeably increases the efficiency of the engine operation. Thus, for instance, tests of the GRD with nonmetalized solid fuels showed that the turbulence ring sometimes gave an increase in the combustion efficiency by 10-15%.

However, in experiments with an engine where used as the fuel was $LiAlH_4$, the setting of the turbulence ring in front of the nozzle barely had an effect on the combustion efficiency, and from this the conclusion was made that in this engine the reason for the incompleteness of combustion was not the absence of an effective mixing and small volume of the burning, but the insufficiently high temperature in the chamber with which the reactions with the participation of metals were not completed.

In all the works devoted to the studies of chambers with turbulence ring, one notes the great difficulty of providing their stability - even when using the most thermoresistant materials. In foreign literature (see [65]) it is also indicated that the combustion efficiency of the propellant in the GRD can be improved by the setting of turbulence ring at the channel inlet of the charge.

Nozzles of chambers of the majority of the GRD which were mentioned in the foreign press were not made cooled. An increase in the heat resistance of the nozzle in this case is provided by the same methods which are applied in the RDTT, i.e., the use of graphite inserts, coatings of heat-resistant materials, and so on.

However, one should focus attention to the fact that the temperature of the products of combustion of many propellants for GRD is higher than the temperature of products of combustion of solid propellants, and therefore providing the stability of the nozzle of the GRD in certain cases is more difficult than it is in the RDTT. Furthermore, it is noted that for inserts of graphite the contact with the oxidizer is extremely dangerous, and in connection with this it is required to insure complete combustion of the propellant before that cross section of the nozzle where graphite materials are applied.

But, on the other hand, unlike the RDTT, in a hybrid rocket engine there is the possibility of flow-through cooling of the chamber by a liquid component. Since the cylindrical part of the chamber is reliably shielded from the heating by a charge of solid component, and the head is located usually in the zone of low temperatures, then virtually it is necessary to cool only the nozzle. Not all the liquid propellant components of the GRD are equally convenient for the cooling of the nozzle; however, many of them can be used when needed for this purpose.

As an example of the chamber of the GRD let us examine the chamber (figure 1.13) of an experimental engine designed for producing a thrust of ~400 N at a pressure in the chamber of about $15 \cdot 10^5$ Pa and operating time of 18 s. The engine is made in the direct design; the fuel has the base of toluidine, and the oxidizer - nitric acid. The liquid component is fed only into the head of the chamber through a centrifugal injector. The charge of solid component is made in the form of a single-channel grain. In the upper part of the channel a layer of the substance which self-ignites upon contact with the oxidizer is applied. Located below the charge of the solid component is the graphite insert, which fulfils several functions. The transverse disc of the insert with openings serves as the turbulence ring; after the turbulence ring the insert forms the chamber where afterburning of fuel mixture

occurs. With the tests a combustion efficiency equal to 0.95 is obtained. The nozzle of the chamber is cooled by the oxidizer.

GRAPHIC NOT REPRODUCIBLE

Figure 1.13. Chamber of an experimental GRD.

1.4.2. Feed Systems of the Liquid Propellant Component in the GRD

It has already been noted that the feed systems of the liquid propellant components in the GRD can be divided into two groups - pressure and pump.

The basic one in the operation of pressure feed systems of the liquid component is its displacement from the tank into the chamber by compressed gas.

In the liquid-propellant rocket engine, for the creation of tank pressure when using a pressure feed system, gas, powder and liquid high-pressure containers (also called gas generators) are used. In the first case the gas for the creation of tank pressure is fed from the cylinder where it was stored previously; in the second case the gas is formed during the combustion of the solid fuel; and in the third case the gas is formed during the burning of the propellant components of the jet engine.

Similar systems can be used also for hybrid rocket engines.

The pump feed system of a liquid component assumes to be the installation of the pump in the main line which connects the tank with the chamber. In this case the tank pressure can be considerably less than the pressure in the chamber.

Just as in the liquid-propellant rocket engine, for the feed system of the liquid propellant component in a GRD as a pump drive it is most convenient to use a gas turbine. Unlike the turbopump unit of the liquid-propellant rocket engine, the turbopump unit of a hybrid engine will include only one fuel pump in the chamber.

As gas generators for the turbine different devices can be used. If, for example, the oxidizer in the propellant is hydrogen peroxide, then it is most rational to use the peroxide gas generator whose design and construction are well developed in the liquid-propellant rocket engine.

From a similar design there can also be made the system of the feed of the liquid component in all those cases where just as for hydrogen peroxide, it is possible to insure its decomposition into gaseous products with heat liberation. If we use a solid propellant, with the combustion of which gases which possess the parameters necessary for the turbine and the composition (corresponding temperature, the absence in gases of solid particles and resinous products) are obtained, then it is possible to realize a design with a gas generator which operates on a solid propellant.

And finally it is possible to obtain gas for a turbine by the combustion of a hybrid propellant, including the propellant used in the engine. This design can be realized in two versions. In the first case in the design the GRD connects a special gas generator with the charge of the solid component. The liquid component is fed by the main pump not only into the chamber, but also into the gas generator. Here there occurs with the necessary

(ensuring the required gas parameters) relationship of flow rates of the components, the fuel combustion, as a result of which the gas which feeds the turbine is formed.

Another version is based on the gas bleed from the main chamber, with the subsequent cooling by its liquid component, which performs the role of a refrigerant and is fed in this quantity in order to bring the parameters of the gas directed into the turbine to the necessary values.

For the contemporary liquid-propellant rocket engine with a pump propellant feed system, two possible circuits are examined - with the afterburning of the gas generator (closed or covered circuit) and without the afterburning of the generator gas (broken or open circuit). For the GRD it is also possible to use both these circuits.

In the theory of the liquid-propellant rocket engine it is shown that the engines made according to the circuit with the afterburning of the generator gas have (especially at high pressures in the chamber) a larger specific impulse than do engines with the ejection of the working medium of the turbine into the atmosphere. This is correct with respect to the GRD, and therefore in these engines the use of the closed circuits at high pressures in the chamber can prove to be more preferable than the use of the open circuits.

However, it is necessary to keep in mind that since the pressure optimum in relation to characteristics with respect to mass in the chamber of the GRD should be lower than that in the liquid-propellant rocket engine (as a result of the fact that the chamber of the GRD is considerably more in terms of dimensions), then the gain in the specific impulse upon the transition from the open circuit to the closed one for engines of this type will be less considerable than that for the liquid-propellant rocket engine.

A comparison of the pressure and pump propellant feed systems is carried out usually in terms of their characteristics with respect to mass. It is known that the greater the pressure in the engine chamber, its thrust and operating time, the more the pressure propellant feed system in the liquid-propellant rocket engine with respect to mass loses to the pump feed system.

The criterion for determining the need for the transfer in the liquid-propellant rocket engine from the pressure feed system to the pump system is sometimes accepted as the definite value of the thrust impulse $I_\tau = \int_0^{\tau_д} P d\tau$, where $\tau_д$ is the operating time of the engine. In accordance with this, the pressure system is used at low values of I_τ, and the pump is used at high values. This approach is legitimate for a GRD. But since in the GRD the mass of the tank of the liquid component is a smaller part in the total passive mass of the engine than in the jet engine (namely, the mass of tanks most greatly depends on the type of the feed system), then it is possible to expect that the range of values of the parameters, in which it is advantageous to use the pressure feed system, in the GRD will be wider than in the liquid-propellant rocket engine.

1.5. STATE OF THE DEVELOPMENT OF THE KRD ABROAD

The first information about tests of hybrid rocket engines appeared in foreign literature in 1956, when American data on study of the GRD operating on hydrogen peroxide and polyethylene were published. In the subsequent period, interest in the GRD and the quantity of published data on its development has rapidly increased. Investigations of the GRD were carried out by many leading firms of the USA, and also specialized organizations in France, Sweden and West Germany. In 1964 in France were conducted

the first flight tests of a rocket with a GRD[1].

In spite of the apparent simplicity of the design and operating conditions of the hybrid rocket engines, their first investigations showed that without the solution to a whole number of scientific problems (mainly from the region of the burning of hybrid propellants) it is not possible to create hybrid engines capable of competing with other types of rocket engines.

In particular, it was established that the burning of hybrid propellants occurs, if we do not take any special measures, with very low combustion efficiency. The losses to the incompleteness of combustion in the GRD were estimated at tens of percent, whereas in the liquid-propellant rocket engine and RDTT they consist of a total of several percent.

There was a revealing of the nonuniformity of the burnout of charges along the length of the channel, which, as was found, is the consequence of the dependence of the intensity of gasification of solid components on conditions of the flow of gases in the channel. It was explained that in the process of control of the GRD, the relationship of the propellant component flow can be substantially changed, as a result of which the energy engine characteristics are decreased, and the nonsimultaneous burnout of the components can occur.

In connection with these shortcomings, it was generally possible to place in doubt the advisability and possibility of the development of a GRD whose characteristics would be comparable with characteristics of rocket engines of other types. Therefore, primary attention in the studies of hybrid rocket engines was given

---

[1]In the Soviet Union the rocket whose engine operated on liquid oxygen and hardened (gelatinous) gasoline, i.e., in fact was made from the design of the GRD, was launched in 1933 (see [2]).

to the study of intrachamber processes. Results of these investigations as a whole can be estimated as encouraging.

The combustion efficiency by sampling of the propellant properties, rational shaping of the charges, selection of the appropriate type and parameters of controls of the injection of the liquid component, and the use of devices which create turbulent flows in the chamber was raised very substantially, and at present the combustion efficiency can reach values of 0.95 and more (see [58]).

Means are established for the compensation of an undesirable change in the relationship of the propellant component flows with the control of the engine by the selection of fuel pairs which ensure the defined law of the gasification of the solid component, by the use of special designs of the engine chambers, and so on.

Simultaneously with the investigation of these, most important, questions concerning the burning of hybrid propellants and the control of the GRD, the positive qualities expected from engines of this type - high stability of operation, insensitivity to defects of the charge, the possibility of repeated starting, etc. - were confirmed.

According to results of investigations of the GRD carried out abroad, it can be concluded that the development of engines of this type with characteristics close to those calculated, became real. This means that it is possible to develop rocket engines which possess such qualities which under certain conditions make the use of the GRD more preferable than the use of rocket engines of other types.

From the data given in the foreign press, it follows that the use of hybrid rocket engines of two groups is indicated: 1) those operating on relatively low-efficiency propellants but possessing

other important qualities (simplicity, reliability, cheapness, etc.) and 2) those operating on highly efficient propellants but differing by the increased complexity of the design and operation.

The GRD of the first group includes, for example, engines of direct design in which used as the oxidizers are the high-boiling substances (nitrogen tetroxide, hydrogen peroxide, etc.). The specific impulse of such GRD's is 2600-3000 N/(kg/s). The engines of this group have a simple design, are cheap and relatively simple in their final development and operation, and allow prolonged storage. In view of the high density of the propellant components these GRD's have a high volumetric specific impulse and are very compact.

The GRD of the second group can include engines with oxidizers with high-boiling oxidizers (mixture of oxygen and fluorine), and especially GRD's with the addition in the fuel of a third component. As was noted above, GRD of such type can insure a specific impulse not lower than the specific impulse of the most effective liquid-propellant rocket engine, but, at the same time, the use in these engines of liquified gases complicates their design, impedes the provision for high reliability and complicates the operation. The volumetric specific impulse of such GRD's is higher than the specific volumetric impulse of the best liquid-propellant rocket engines, which makes it possible, other conditions being equal, to create a flight vehicle with a GRD which is more compact than in a flight vehicle with the liquid-propellant rocket engine.

The GRD's of the first group are of interest, first of all, for their use in systems intended for military purposes. The GRD's of the second group approach more for the solution of problems in space research. However, in certain cases a shift in these fields of the rational use is possible; for example, the use of GRD's which operate on propellants with oxidizers with

a high boiling point and in space systems can prove to be advisable.

An example of the GRD of the first group can be the engine (see [56]) used on the flying target "Sandpiper A", which is in the armament of the navy of the USA (figure 1.14). The target is intended for weapons tests and the training of aircrews. Flight tests of target with a GRD were carried out in 1967. It is assumed that the target can accomplish flights at a velocity which corresponds to M=3-4, at heights of up to 27,000 m, and with completion of the maneuver.

The engine of the target is made from the direct design of the GRD with a gas pressure chamber and includes chamber 5 with solid fuel, tank 3 with an oxidizer, tank 2 with compressed nitrogen and automation which ensures the functioning of the engine in the assigned system. Placed in the pipeline which connects tank 3 with chamber 5 is the regulator (valve) 7 of the oxidizer feed.

Used as the fuel is acrylic plastic with an addition of magnesium, and are used liquid nitrogen oxides as the oxidizer. The diameter of the chamber is 254 mm, and the critical throat diameter of the nozzle is 100 mm. The force intensity of the thrust can be previously assigned within limits of 270-2270 N (according to other data within limits of 270-1370 N), for which before the rocket launching the disk for regulating the oxidizer feed is turned manually.

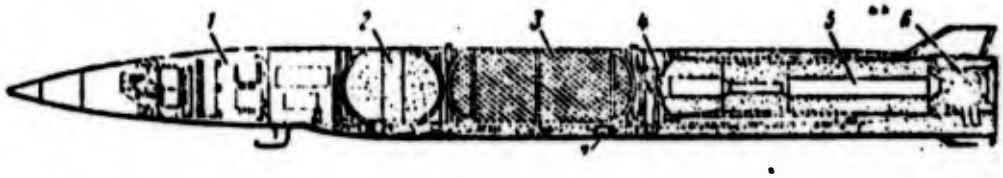

Figure 1.14. Diagram of the flying target "Sandpiper A" with a GRD of the firm UTC: 1 - control equipment; 2 - tank for nitrogen; 3 - tank for liquid oxidizer; 4 - igniter; 5 - combustion chamber with solid-propellant charge; 6 - nozzle; 7 - valve for feed control of the oxidizer.

Thus, on this GRD before the starting an adjustment on the line of the oxidizer feed is realized. Subsequently, it is assumed to implement control of the regulator on instructions from the earth or according to a program, i.e., to introduce control of the engine. It is noted that a similar GRD, as a result of the possibility of the control of its thrust, is convenient for installation on a rocket of the class "air to surface" of increased range with maneuvering in the flight process toward the target.

The final development of the GRD for the target "Sandpiper A" was realized very rapidly and required low expenditures. It is reported that before the beginning of flight tests of the target, a total of 21 firing bench tests of the engine was conducted, and the execution of the planned flight test program proved to be possible to interrupt before the termination of the tests - in view of the rapid confirmation of the efficiency of all elements of the target, including the GRD.

In foreign literature it is noted that GRD's can be used for stabilization of the flight of carrier rockets. The GRD's in this case can operate on a fuel with an oxidizer with a high boiling point, should develop little thrust (sometimes less than 10 N) during prolonged time and allow repeated starting and stopping. It is indicated also that the engines which operate on a hybrid propellant are especially attractive for purposes of space research and, in particular, for flights which require prolonged inertial motion with periodic ignition of the engines, since these engines possess high stability to the effect of space conditions, the simplicity of starting and stopping, a precise value of impulse, and the possibility of thrust control.

The United Technological Center (USA), on contract with NASA, in the beginning of 1970 completed the first test series of an experimental GRD using a high-energy propellant for the upper stages of carrier rockets (see [61]).

Used as the fuel in propellant of this engine is polybutadiene with additives of lithium and lithium hydride, while used as the oxidizer is a mixture of liquid fluorine and liquid oxygen. A diagram of the GRD is given in figure 1.15. The engine is made by the design with a pressure propellant feed system and includes a chamber 4, made of fiberglass, with a charge of solid component 3, oxidizer tank 1, cylinder with helium 2 placed for the packing of the layout in the oxidizer tank, and automation. The diameter of the chamber is somewhat more than one meter, and the length of the engine is ~3.7 m.

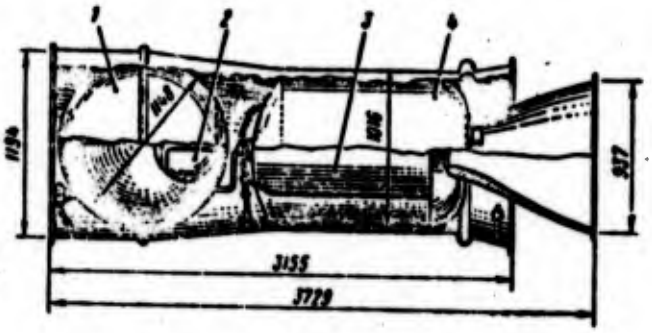

Figure 1.15. GRD's with a pressure feed system: 1 - oxidizer tank; 2 - cylinder with helium; 3 - solid-propellant charge; 4 - chamber.

In the process of the tests the engine developed a thrust of up to $5 \cdot 10^4$ N with the time of tests of up to 50 s. The flight model which is the one to be developed should have approximately two times higher thrust and an operating time of up to 80 s.

Investigated abroad are GRD's based on three-component propellants (with the introduction of hydrogen into the chamber). It is indicated that the use of such GRD's on the last stages of the space rockets will make it possible to increase substantially their useful load. However, in foreign sources it is noted that the future of similar engines is problematic, since for them it is necessary to compete with rocket engines of such promising type as the nuclear engines.

There is great interest in the studying of the possibility of the designing of GRD's with high thrust intended for the use on starting stages of space rockets. It is reported that the characteristics of this GRD with a thrust of $1400 \cdot 10^4$ N are defined (see [61]). The length of the engine should be 47 m, the diameter - 4.6 m, and the mass - about $70 \cdot 10^4$ kg. The oxidizer is assumed to be nitrogen tetroxide, and the other component is the fuel, which is used in the large American RDTT (mixture of fuel-binding substance and aluminum). The control of the thrust force vector is designated to be realized by means of liquid injection (oxidizer) in the supercritical part of the nozzle. The engine housing is assumed to be manufactured from steel. By way of preparation for the creation of this large GRD, engine testing with a thrust at $18 \cdot 10^4$ H is conducted; the following stage should be the final development of the engine with a thrust of $113 \cdot 10^4$ N.

In the example of the GRD with a thrust of $1400 \cdot 10^4$ N, it is possible to examine the relationships of the cost of engines of different types. The cost of the rocket engine is determined by expenditures during its final development, production, operation and cost of materials and propellant. American specialists consider that in the case where we are speaking about engines with a thrust of $1400 \cdot 10^4$ N, the cost of the engine which operates on a hybrid propellant will be the lowest of the costs of rocket engines of all possible types. It is indicated that by the moment of the creation of the GRD its cost will be 3.7 million dollars, i.e., 5.3 dollars per 1 kg of mass, and, subsequently, it will be lowered to 3.6 dollars per 1 kg of mass. Similar data for most promising large RDTT are estimated at 6.6 and 4.85 dollars per 1 kg of mass. The cost of liquid-propellant rocket engines is substantially higher even in comparison with the cost of the RDTT.

Thus in the case where it is required to create an engine with an intrinsic mass (including the propellant) on the order of thousands of tons, the savings on the cost of the engine when

using a GRD can (according to foreign data) are millions of dollars for one rocket. Let us also note the fact that the greatest difference in cost is obtained with a comparison of the GRD and liquid-propellant rocket engine, i.e., those engines which are similar to each other in other characteristics.

The design of large GRD's can be different. If there is developed a propellant with a high speed of gasification of the solid component, then the creation of a GRD with one chamber will become possible. If the velocity of gasification is low, it is necessary to use packets of chambers.

Figure 1.16a and b gives two packet designs of the GRD. Both engines have pressure feed systems of the liquid component; in both designs the tank of this component is common for all chambers. From the figure it is evident how simple and compact the large GRD's can be even in the case of the use of a packet of chambers.

The magnitude of the relationship of flow rates of the propellant component K can determine the relationship of the overall dimensions of the GRD. At the low value of K the optimum ratio of the length of the engine installation to its diameter will be more (see figure 16a) than that at a large value of K (see figure 1.16b). Moreover, in the first case a change in the thrust is reached by a relatively small change in the flow rate of the liquid propellant component. Control of the force thrust vector of the engine is easily realized by an injection of the liquid component into the supercritical part of the nozzle (see figure 1.16b); it is indicated, furthermore, that this control can be produced by the redistribution of the liquid component between the chambers (change in the modulus of thrust of various chambers) (see figure 1.16a).

In contrast to the GRD, whose developments are conducted quite intensely, the investigations of the RDTT with separate propellant components have received relatively little attention

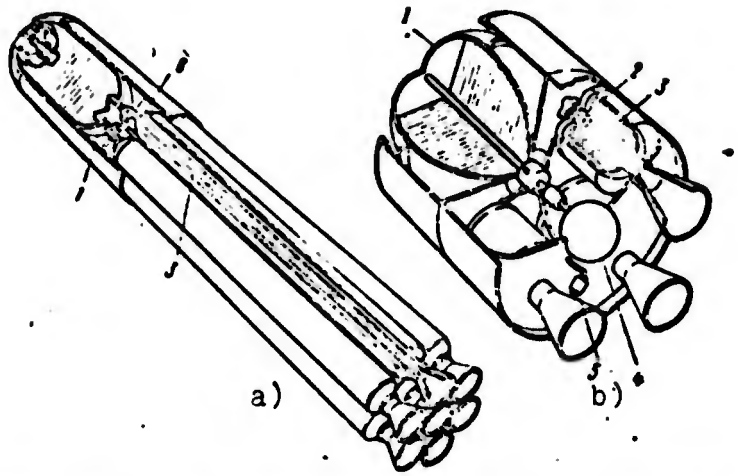

Figure 1.16. GRD's of the packet design: 1 - oxidizer tank; 2 - injector; 3 - solid-propellant charge; 4 - pressurized system; 5 - injector for injection of the liquid component into the supercritical part of the nozzle; 6 - ignition system.

abroad. This is connected, apparently, with the fact that in the creation of an engine with two propellant components, each of which is solid, many more difficulties are encountered than during the final development of an engine which operates on a solid-liquid propellant. In the presence of two solid components it is more difficult to obtain high-energy engine characteristics; it is extremely complicated to create and use highly efficient solid oxidizers; is difficult to insure control; the solution to the problem concerning the engine cutoff will be complex and so on.

However, various reports about works abroad on RDTT with separate propellant components all the same have appeared (for example, see work [53]). Thus there was a report on the conducting in the beginning of the 1960's by one of the American rocket firms of tests of RDTT of the spearate loading in which the thrust chamber contained a charge of a solid component enriched by an oxidizer (90% of ammonium perchlorate), and there was a gas generator with the grain enriched by fuel and capable of independent burning, with gas generation at a temperature of 870°C. The tests have been evaluated as being successful. In the process of the tests the efficiency of the system, the possiblity of the control and

cutoff of the engine, and the obtaining of its characteristics close to those calculated were confirmed.

In conclusion of the first chapter devoted to the presentation of general information about the KRD, let us note the basic advantages and shortcomings of engines which operate on hybrid propellants, in comparison with other types of rocket engines based on chemical energy sources. In connection with the inadequacy of the development of the GRD, some evaluations of their qualities are, naturally, approximate.

According to the mass specific impulse GRD's exceed the engines which operate on solid fuel and approach liquid-propellant rocket engines. According to the volumetric specific jet engines using solid-length propellant components exceed and liquid-propellant rocket engines. The basic problems in development and creation of the GRD's from the viewpoint of an increase in their energy characteristics are the search and the assimilation of fuel pairs high in energy and the provision for a sufficiently full combustion of the propellant.

The GRD's are simpler in design than the liquid-propellant engines; however, they are more complex than the engines which operate on solid fuel. It is possible to expect that approximately these three engine models with respect to operational simplicity will also be correlated with each other.

With respect to cost the final development and manufacture, the engines using hybrid propellants, apparently, at least will not be worse than the liquid-propellant and solid-propellant engines. In such cases when it is necessary to create engines with very high thrust, the GRD's, possibly, will prove to be cheapest.

With respect to the stability of the operating conditions and the nonsusceptibility to the action of external factors, the

GRD's cannot be inferior to other engines and in certain cases can exceed them.

As for the possibility of adjustment and control, engines on hybrid propellants unconditionally exceed engines on solid fuel and approach the liquid-propellant engines.

In relation to the possibility of providing for a prolonged operation (from conditions of heat resistance of the nozzle) and the multiplicity of starting and stopping, the GRD's exceed the RDTT and approach the liquid-propellant rocket engine.

Thus on the basis of the results of investigations and development of the GRD published recently in foreign press, it is possible to expect that these engines will exceed the liquid-propellant rocket engine in the magnitude of the volumetric specific impulse, in the simplicity of design and operation, and also in cost, and they will be inferior to them with respect to the mass specific impulse and convenience of control.

The GRD's will exceed the RDTT with respect to energy characteristics (both in mass and volumetric specific impulses), where possible in control, in less sensitivity to the defects of the charge, where possible in repeated starting and prolonged operation, and will be inferior to RDTT in the simplicity of design and operation.

Unfortunately, in foreign press are absent data relative to characteristics of the GRD with respect to mass; however, it is possible with great confidence to expect that according to these characteristics the GRD will occupy the intermediate position between the liquid-propellant rocket engine and the RDTT and that, therefore, according to characteristics with respect to mass the engines using hybrid propellants will not substantially be inferior to the liquid-propellant engines.

CHAPTER 2

HEAT EXCHANGE IN THE COMBUSTION CHAMBER OF COMBINED ROCKET ENGINES

The heat exchange between hot gas, which is a mixture of the fed component with the fuel combustion products, and the surface of the solid component is an important link of the operating conditions of the KRD [КРД - combined rocket engine] which determines the flow rate of the solid component and, thereby, the output engine characteristics. The dependences from which determined is the value of the heat flux from the gas to the solid surface are part of the formulas for the calculation of the rate of gasification of the solid component given in chapter 3.

The determining forms of heat exchange in the KRD are the forced convection and radiation. Relationship of convective and radiation heat fluxes depends on the gas-dynamic parameters of the flow in the chamber and the composition of the combustion products. For fuel pairs on the basis of hydrocarbon fuels, the decisive role in heat exchange is played by convection. The intensity of radiation in this case is determined by the content in the gas mixture of CO_2 and H_2O and, by analogy with the ZhRD [ЖРД - liquid-propellant rocket engine] it is estimated at 30-50% of the value of the convective heat flux. For fuel compositions on the basis of metal-containing fuel, the role of radiation substantially increases.

In the examination of convective heat exchange under conditions of the KRD, it is possible to distinguish the following characteristic cases:

1) the motion of homogeneous gas flow along the long channels of constant cross section;

2) the motion of homogeneous gas flow on the channel of the charge divided into various sections by the throttling elements (turbulence ring, combustible throttle washers);

3) the motion of two-phase flow along the long channel of constant cross section.

For all the indicated cases in the derivation of relations for convective heat exchange, the walls of the channel are assumed to be impenetrable. The effect of the feed of the substance into the boundary layer on the magnitude of heat heat flux to the surface in calculations of the rate of gasification is considered to be the corrective function of blowing-in.

2.1. CONVECTIVE HEAT EXCHANGE IN CHANNELS OF A CHARGE OF CONSTANT CROSS SECTION WITH THE MOTION OF THE HOMOGENEOUS GAS FLOW

For the majority of the models of the KRD known at the present time, the gas-dynamic channel of the combustion chamber on the section of the charge is a channel with constant cross section along the length. The intensity of the heat exchange in this channel increases with an increase in the mass flow rate of the gases along the charge in direction toward the engine nozzle.

Local values of the coefficient of convective thermal conductivity from the gas to the smooth impenetrable wall in this case, with an accuracy acceptable for engineering calculations, can be determined from the criterial empirical relations obtained for

the convective heat exchange with gradient-free flow in the tube or along the surface of the plate and having the form

$$Nu = c\,Re^{n}Pr^{m},$$

where $Nu=\frac{\alpha l}{\lambda}$ - Nusselt number;

$Re=\frac{vl}{\nu}$ - Reynolds number;

$Pr=\frac{\nu c_p \rho}{\lambda}$ - Prandtl number;

c, n, m - constant dimensionless numbers;

l - determining dimension;

α - heat-transfer coefficient;

λ, ν - the coefficients of thermal conductivity and kinematic viscosity of the gas respectively;

c_p, ρ - specific heat capacity and density of the gas respectively

Table 2.1 gives a summary of the basic relations of such type known from literature.

In the formulas given in table 2.1,

T_{00} - stagnation temperature of the gas flow;

T_s - surface temperature.

Subscript "d" with numbers Nu and Re indicates that accepted as the determining dimension in this relation is the diameter of the channel; subscript "z" means that the determining dimension is the distance from the beginning of the channel to the examined cross section.

Although relations (2.1)-(2.3) were obtained from experiments in circular tubes, they are extensively used during calculations of heat transfer in channels of noncircular transverse cross section. In this case the transfer from circular tubes to cross

sections of complex profile (under conditions of the KRD - ring, segment, star, etc) is provided by introduction into the calculated relations of the equivalent hydraulic diameter:

$$d = \frac{4F_к}{\Pi_г},$$

where $F_к$ is the area of the free cross section of the chamber;

$\Pi_г$ is the perimeter of burning (gasification).

Table 2.1.

Number of formula	Authors	Formula	Remarks	Source
(2.1)	G. Kraussol'd, M. A. Mikheyev	$Nu_d = 0{,}023\,Re_d^{0.8} Pr^{0.4}$	–	[23]
(2.2)	A. A. Gukhman, N. V. Ilyukhin	$Nu_d = 0{,}0162 Re_d^{0.82} Pr^{0.82} (T_\infty/T_s)^{0.005}$		[10]
(2.3)	B. S. Petukhov, V. V. Kirillov	$Nu_d = 0{,}044\,\varepsilon\, Re_d^{0.75} Pr^{0.43} [\tau(\bar{T})]^{0.33}$; $\varepsilon = 1{,}3\,(z/d)^{-0.12}$ with $z/d < 10$; $\varepsilon = 1$ with $z/d \geq 10$	$\tau(\lambda)$ – gas-dynamic function	[27]
(2.4)	The same	$Nu_z = 0{,}034\, Re_z^{0.77} Pr^{0.43} [\tau(\lambda)]^{0.33} \times (z/d)^{0.05}$	–	[27]
(2.5)	E. R. Ekkert	$Nu_z = 0{,}036\, Re_z^{0.8} Pr^{0.33}$	Obtained for a flat plate	[45]
(2.6)	T. Davey	$Nu_d = 0{,}036\, Re_d^{0.8} Pr^{0.4} (z/d)^{-0.2} \times (T_\infty/T_s)^{0.18}$	–	[51]

As follows from relations (2.1)-(2.6) given in table 2.1, the intensity of the convective heat exchange in the long pipelines is determined mainly by the value of the Re number, which for conditions of the GRD [ГРД - hybrid rocket engine] is advantageous to present in the form

$$Re = \frac{Gz}{g\mu F_к} = \frac{\bar{G}z}{\mu}, \qquad (2.7)$$

where $\bar{G}=G/gF_к$ - mass flow rate of the gases;

μ - coefficient of dynamic viscosity;

z - distance to the given cross section from the end of the charge turned toward the leading base.

Together with the Nusselt number, in the theory of heat-mass transfer the Stanton number is also applied:

$$St=\frac{\alpha}{c_p\rho w}.$$

The connection between the different numbers is established by the relation

$$St=\frac{Nu}{Re\cdot Pr}, \qquad (2.8)$$

which allows on formulas (2.1)-(2.6) to turn to a new one which contains instead of Nu the St number.

2.2. CONVECTIVE HEAT EXCHANGE IN THE CHANNEL OF THE SECTIONAL CHARGE OF THE KRD

The layout of the combustion chamber of the KRD, with the channel divided by throttling devices into separate sections (cavities), is shown in figure 1.8. Each of the sections is a flowing volume into which from the narrow channel of the throttle at high velocity there enters the gas, which creates within the section a powerful circulation motion (figure 2.1).

Although within each section the gas flow has a complex three-dimensional structure, knowledge of this structure is not necessary for determining the average parameters of heat exchange. In determining these parameters we will proceed from a simplified scheme assuming that the entire volume filled by the vortices possesses with respect to the turbulence the property of isotropy, i.e., that the statistical properties of turbulence in this case

do not depend on the selection of the direction. This makes it possible to use the relations for isotropic turbulence.

As a fundamental characteristic of the eddy motion of gas it is advantageous to use the function of the dissipation of mechanical energy, or specific dissipation D, equal to the dissipation of energy per unit time per unit volume. In the examined case it is possible to consider that the processes of dissipation occur evenly over the entire volume of the section.

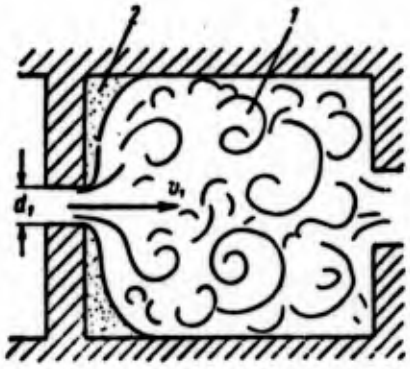

Figure 2.1. Diagram of motion of the gas within sections of the charge: 1 - region of isotropic turbulence; 2 - stagnation zone.

With a considerable distinction in the diameters of the throttling device and channel of the charge, the kinetic energy, calculated from the average rate of the axial flow of gas, is negligible in comparison with the kinetic energy of the gas flowing into the section. Thus, for instance, with the ratio of diameters 2:5, which occurred with the testing of one of the model engines made from this design (see [67]), the kinetic energy of the averaged axial flow is less than 3% of the kinetic energy of the inflowing jet.

The kinetic energy of the inflowing jet converts into the energy of turbulent motion, which then, in the process of dissipation, is converted into heat. Consequently, in the first approximation, it is possible to accept that

$$D=\dot{G}\bar{A}\frac{1}{W}. \qquad (2.9)$$

where G is the per-second mass consumption of the gas through the channel of the throttle; $\bar{A}$ - the kinetic energy of a unit of mass of the entering gas; W - the volume of the sectional cavity.

According to the conventional spectral structure of the isotropic turbulent motion, which obtained substantiation in the works of A. N. Kolmogorov, G. Taylor and other researchers, the process of the dissipation of mechanical energy precedes the decay of large-scale pulsations on smaller vortices. The process of the size reduction of the scale of pulsations occurs up to a certain scale of motion l_0 called the internal scale of turbulence, beginning from which the flow of gas acquires a viscous nature.

The turbulent pulsations of the scale $l \approx l_0$ can no longer fall into smaller ones: they gradually disappear due to viscosity effect, and the kinetic energy which they possess is converted into heat. According to the theory of isotropic turbulence, such small-scale vortices are the basic source of the dissipation of mechanical energy of turbulent motion. The internal scale of turbulence for the isotropic turbulent motion is connected with the specific dissipation by relation (see [14; 39])

$$l_0=\left(\frac{\mu^3}{\rho^2 D}\right)^{1/4}. \qquad (2.10)$$

where μ - the coefficient of dynamic viscosity;
ρ - the density of the gas.

In the layer of gas adjacent to the charge's surface, viscosity forces will predominate. In this region a decisive role is acquired by heat transfer by molecular thermal conductivity, in consequence of which heat flux to the surface is expressed by the relation

$$q=\frac{\lambda_r}{l_0}(T_r-T_s),$$

where $l_в$ - the thickness of the viscous layer;

T_e - temperature on the external boundary of this layer.

By assuming the value T_e to be close to the average temperature in the nucleus of the gas volume, the coefficient of convective heat transfer to the surface can be presented as

$$\alpha = \frac{\lambda_г}{l_в}. \tag{2.11}$$

The thickness of the viscous layer can be taken as being proportional to the internal scale of turbulence:

$$l_в = \text{const} \cdot l_0. \tag{2.12}$$

Then from relations (2.9), (2.10), (2.11) and (2.12), with $Pr \approx 1$ we obtain the formula for determining the average heat-transfer coefficient in the given volume:

$$\alpha_{ср} = \text{const} \cdot \lambda_г \left(\frac{\rho^2 G \bar{\lambda}}{\mu^3 W} \right)^{1/4}. \tag{2.13}$$

After expressing the flow rate of gas and its kinetic energy by parameters at the entry into the given volume, we will obtain

$$\alpha_{ср} = \text{const} \cdot \lambda_г \left(\frac{\rho^3 v_1^3}{\mu^3} \frac{\pi d_1^2}{8W} \right)^{1/4}, \tag{2.14}$$

where d_1 - the diameter of the channel of the throttle device;

v_1 - gas velocity in the output cross section of this channel.

Relation (2.14) can be converted to the dimensionless form, having accepted for the characteristic dimension the diameter of the channel of the throttle device d_1, which determines in the first approximation, the dimension of the large turbulent vortices:

$$Nu_d = c\, Re_d^{3/4} \left(\frac{d^3}{W} \right)^{1/4}. \tag{2.15}$$

where Re_d is the Reynolds number calculated for the parameters of the output cross section of the channel of the throttle; c - experimental constant.

Relations (2.14) and (2.15) can be used for the calculation of the heat exchange over the surface of separate sections, with the exception of the narrow stagnation zone on the rear surface of the throttle washer (see figure 2.1).

It must be noted that the role of the circulation flow of gas as the determining factor of convective heat exchange is not limited to a sectional charge. To a considerable extent it is also exhibited in the charge with an unthrottled channel on the initial section of flow, causing an increased rate of gasification of the solid component on this section.

2.3. CALCULATION OF THE COEFFICIENT OF CONVECTIVE HEAT TRANSFER FOR TWO-PHASE FLOW IN A CHANNEL WITH IMPENETRABLE WALLS

The presence of a large quantity of solid particles in the products of combustion of hybrid propellants with metallized fuels affects both the nature of the heat exchange between the gases and surface of the engine and the quantitative indices of this process. Especially high concentrations of the condensed phase in the flow occur in gas generators on metallized fuel in the RDTT [РДТТ - solid-propellant rocket engine) RS [РС - rocket missile].

The presence in the turbulent flow of solid particles substantially affects the velocity distribution in the transverse cross section of flow and, consequently, the temperature profile and the coefficient of convective heat transfer.

The distinction in profiles of homogeneous and two-phase turbulent flows is conditioned by the fact that in the two-phase

flow there appear additional losses of the kinetic energy with the aerodynamic interaction of particles with the carrying medium.

Interaction of the small particles with turbulent pulsations proves to be different depending on the dimension of the turbulent vortices. In the interaction of the particles with the large vortices, a full increase in the particles by the vortex occurs. In this case the particles with their surrounding layers of gas are transferred as one whole. In the interaction of the particles with the small vortices, a full increase in the particles does not occur, and the relative motion between the particle and the medium appears. The consequence of this is the additional dissipation of energy of the turbulent pulsations.

The aerodynamic resistance of the medium to the motion of the spherical particle is expressed by the formula

$$F=\psi\frac{\pi d_T^2}{4}\frac{\rho u^2}{2}, \qquad (2.16)$$

where d_T - the diameter of the particle;

$u=V_T-V_g$ - the difference in the absolute velocities of the particle and medium;

ψ - the drag coefficient, which is a function of

$$Re_{T\,u}=\frac{d_T u}{\nu},$$

where ν is the kinematic viscosity coefficient;

$$\psi=\frac{a}{Re_{T\,u}}.$$

Here a is a certain constant value, which is selected depending on the range $Re_{T\,u}$.

For small values of $Re_{T\,u}$ ($Re_{T\,u}\approx 1$) the drag coefficient is equal to $\psi=24/Re_{T\,u}$ and relation (2.16) becomes Stokes' law:

$$F = 3\pi\mu d_T u.$$

The equation of motion of the particle streamlined by the vortex takes the form

$$\rho_T W_T \frac{dV_T}{dt} = F - \rho_g W_T \frac{dV_g}{dt}, \tag{2.17}$$

where W_T is the volume of the particle; ρ_T, ρ_g - densities of the particle and gas, respectively.

Since the turbulent pulsations bear a quasi-periodic nature, it is possible to accept that

$$V_g = V_{gm} \sin \omega t, \tag{2.18}$$

where V_{gm} is the amplitude of the turbulent pulsations of velocity;

ω - angular velocity.

The solution to equation (2.17) in the substitution of expressions (2.16) and (2.18) gives the value of the relative particle speed:

$$u = \frac{\left(1 - \frac{\rho_g}{\rho_T}\right) V_{gm}}{\sqrt{1 + \frac{1}{\omega^2 \tau_p^2}}} \sin(\omega t - \theta_u), \tag{2.19}$$

where

$$\tau_p = \frac{4\rho_T d_T^2}{3a\mu}; \quad \theta_u = \operatorname{arc\,tg}(\omega\tau_p).$$

Let us call the value τ_p which has the dimensionality of time the relaxation time of the oscillating particle. The work of the resisting forces which act on a separate particle is determined as follows:

$$A_F = \int_0^x F dx.$$

Since dx=udt, the work of the resisting forces for the period T will be

$$A_F = \int_0^T \frac{a}{8} \pi \psi d_ч \mu^2 dt.$$

The work of the resisting forces performed per unit time per unit volume of the gas suspension is equal to

$$D_ч = \sum^n \frac{1}{T} \int_0^T \frac{a}{8} \pi \psi d_ч \mu^2 dt,$$

where n is the number of particles per unit volume of the gas suspension.

Strictly speaking, since the majority of the two-phase systems possesses considerable polydispersion, calculation of the integral should be produced separately for particles of different dimensions, and then the sum of their values should be calculated by taking into account the distribution of particle sizes in the dispersed phase. In our derivations we will proceed from the average for the given disperse system of the diameter of particles defined on the basis of the known distribution of their dimensions as the ratio of the cube of the mean volumetric diameter of particles to the square of their diameter averaged over the surface (diameter of Sotter). The same must be noted relative to values V_{gm} and ω.

In turbulent flow it is necessary to deal with the spectrum of turbulent pulsations which are distinguished by amplitude and angular velocity. For the sake of simplicity of the relations, it is advantageous to turn to a certain effective value of V_{gm}. As such value it is expedient to use the frictional velocity (velocity of friction) V_τ, which is the standard of turbulence of this flow and which has an identical order of magnitude with the average quadratic velocity of turbulent pulsations:

$$V_{gm} = k_в V_\tau.$$

Let us note that as the analysis carried out by us shows, for characteristic conditions $\omega^2\tau_p^2 \approx 10^2 - 10^4$, and, therefore, it is possible to accept that $1+(1/\omega^2\tau_p^2)\approx 1$.

Since the density of the material of the particle usually exceeds the density of the carrying medium by more than a hundred times, it is possible to accept that

$$1-(\rho_g/\rho_\tau)\approx 1.$$

Let us express the number of particles n by the mass concentration η, which is the mass ratio of the solid phase which is contained in a unit of volume to the mass of the gas medium in this same volume:

$$n=\frac{6\eta\rho_g}{\pi d_\tau^3\rho_\tau}. \qquad (2.21)$$

By substituting equations (2.19) and (2.21) into (2.20) and integrating the obtained expression, taking the accepted corrections and assumptions into account, we find

$$D_\tau=\frac{k_n^2 V_\tau^2\rho_g\eta}{\tau_p}.$$

We convert it to a form more convenient for the calculations:

$$D_\tau=k_D\frac{V_\tau^2\rho_g\eta}{t_p}, \qquad (2.22)$$

where $t_p=\frac{\rho_\tau d_\tau^2}{18\mu}$; $k_D=\frac{k_n^2 a}{24}$.

Let us formulate the equation of energy of turbulent motion for a two-phase flow. In this case we will proceed from the following assumptions:

1) the two-phase flow on the examined section is hydrodynamically

completely developed, and the Re number is sufficiently high;

2) the concentration of the condensed phase is constant over the entire cross section of the flow;

3) the local values averaged in time of the axial velocities of the condensed and gas phases are equal;

4) the tangential stress τ is constant according to thickness of the boundary layer.

In this case the equation of the energy of turbulent motion assumes the form

$$\rho_g \frac{V_*^2}{\varkappa x} = \tau \frac{d\bar{u}}{dx} + k_D \frac{\tau \rho_g V_*^2}{t_p}, \qquad (2.23)$$

where x - the distance from the wall;
$\bar{u}$ - the local value of the average axial velocity;
κ - the universal constant of turbulence (κ=0.4).

The left side of the equality is expressed as the kinetic energy of the turbulent pulsations which enter per unit volume per unit time. On the right side the first term is expressed as the work produced by forces of turbulent viscosity per unit volume per unit time, and the second term - the specific dissipation of energy with the flow about the solid particles.

Hence

$$\frac{d\bar{u}}{dx} = \frac{V_*}{\varkappa} \frac{1}{x} - k_D \frac{\eta}{t_p}.$$

Integrating, we obtain

$$\bar{u} = \frac{V_*}{\varkappa} \ln x - k_D \frac{\eta}{t_p} x + C.$$

or

$$\frac{\bar{u}}{V_*}=\frac{1}{\varkappa}\ln x-k_D\frac{\eta}{t_pV_*}x+C. \qquad (2.24)$$

Since the right side of equality (2.24) is the dimensionless value which does not depend on the selection of the measuring system, the constant of integration should include the logarithm of length. With considerable particle sizes $\left(\mathrm{Re}_{\tau\tau}=\frac{d_\tau V_*}{\nu}\gg 1\right)$ it is possible to accept that

$$C=C_2-\frac{1}{\varkappa}\ln d_\tau.$$

At small values of $\mathrm{Re}_{\tau\tau}$

$$C=C_1-\frac{1}{\varkappa}\ln\frac{\nu}{V_*}.$$

In this case

$$\frac{u}{V_*}=\frac{1}{\varkappa}\ln\frac{x}{d_\tau}-k_D\frac{\eta}{t_pV_*}x+C_2,\ (\mathrm{Re}_{\tau\tau}\gg 1); \qquad (2.25)$$

$$\frac{u}{V_*}=\frac{1}{\varkappa}\ln\frac{V_*}{\nu}x-k_D\frac{\eta}{t_pV_*}x+C_1,\ (\mathrm{Re}_{\tau\tau}\approx 1). \qquad (2.26)$$

Since the constants κ, C_1 and C_2 in a homogeneous flow do not depend on the flow rate and properties of the gas, it is possible to assume that for a two-phase flow their values will remain the same as for the homogeneous flow equal to 0.4, 5.5 and 8.5, respectively. Under this condition relations (2.25) and (2.26) with $\eta=0$ automatically convert into the well-known formulas of the universal velocity distribution for a homogeneous flow.

By knowing the velocity profiles, it is possible to determine the rate of flow u_a average over the cross section.

$$u_a=\frac{1}{\pi R^2}\int_{x_a}^{R}2\pi(R-x)\bar{u}dx, \qquad (2.27)$$

where R is the radius of the channel; $x_л$ - the thickness of the laminar sublayer.

Substituting into expression (2.27) the equation of the velocity profile and omitting with integration the terms which include $x_л$ (in view of the smallness of $x_л$ in comparison with R), by solving the obtained equation relative to V_τ, we find

$$V_\tau = \frac{u_a + \frac{k_D V_\tau R}{3 t_p}}{\frac{1}{\varkappa} \ln \frac{R}{d_\tau} + C_2 - \frac{3}{2\varkappa}}. \qquad (2.28)$$

Since $V_\tau = \sqrt{\frac{c_f}{2}}\, u_a$, we obtain the following expression for determining the coefficient of friction c_f:

$$\sqrt{\frac{c_f}{2}} = \frac{1 + \frac{k_D V_\tau R}{3 t_p u_a}}{\frac{1}{\varkappa} \ln \frac{R}{d_\tau} + C_2 - \frac{3}{2\varkappa}}. \qquad (2.29)$$

With $\eta=0$ the relation (2.29) becomes the well-known formula according to which the coefficient of friction for completely rough tubes is determined. After substituting the value of t_p, the expression (2.29) can be rewriten in the form

$$\sqrt{\frac{c_f}{2}} = \frac{1 + 6 k_D \eta \frac{R}{d_\tau} \cdot \frac{Q_f}{Q_\tau} \frac{1}{\mathrm{Re}_\tau}}{\frac{1}{\varkappa} \ln \frac{R}{d_\tau} + C_2 - \frac{3}{2\varkappa}}. \qquad (2.30)$$

Thus in dependence for c_f obtained by us analytically, the coefficient of friction is expressed in the form of a function of the following parameters:

$$c_f = f\left(\eta, \frac{R}{d_\tau}, \frac{Q_f}{Q_\tau}, \mathrm{Re}_\tau = \frac{d_\tau u_a}{\nu}\right).$$

As was shown by the comparison carried out by us of results of the calculation according to formula (2.30) with experimental data known from literature, the obtained relation provides good convergence of the calculation with the experiment.

Let us turn to the calculation of the coefficient of convective heat transfer for a two-phase flow.

The role of the solid particles in the process of heat transfer from the nucleus of the two-phase flow to channel surface is reduced to the following:

1) the presence in the flow of solid particles increases its turbulence, changes the structure of the boundary layer, amplifying the heat transfer by turbulent pulsations to the wall;

2) in the turbulent zone the solid particles perform the role of the heat-absorbing elements, thereby changing the effective heat capacity of the medium;

3) the particles which are located on the boundary of the turbulent zone and small laminar sublayer with high thermal resistance, possessing substantially higher heat transfer in comparison with the gas medium, play the role of heat-conducting bridges.

The evaluation of the role of solid particles as heat-conducting bridges in the field of the laminar sublayer shows that at values n=1-10 the relative increase in the heat flux to the wall due to the effect of this factor does not exceed 2-3%, and in engineering calculations it is possible not to consider it.

With the equality of the local average rates of the solid and gas phases, it is possible to proceed from the assumption about the thermal equilibrium of the phases. In this case the effective value of the specific heat capacity of a unit of mass of a two-phase substance will be

$$c_{pf} = \frac{c_{pg} + \eta c_T}{1 + \eta}, \qquad (2.31)$$

where c_{pg} and c_T are the specific heat capacities of the gas and solid substance, respectively.

The determining of the coefficient of convective heat transfer for a two-phase flow carried out by us is based on the analogy between the heat transfer and momentum, i.e., on the so-called Reynolds analogy expressed in dimensionless form:

$$St=\frac{c_f}{2s}, \qquad (2.32)$$

where s is the coefficient of Reynolds analogy.

According to L. Krokko, with sufficient practical accuracy it is possible to accept that

$$s=Pr^{2/3}.$$

After substituting into expression (2.32) the value $St=\frac{\alpha}{\varrho_g c_{pf} u_g}$ and equation (2.30), we obtain

$$\alpha=\varrho c_{pf}\frac{u_g}{Pr^{2/3}}\left[\frac{1+6k_D\eta\frac{R}{d_T}\frac{\varrho_g}{\varrho_T}\frac{1}{Re_T}}{\frac{1}{\varkappa}\ln\frac{R}{d_T}+C_2-\frac{3}{2\varkappa}}\right]^2. \qquad (2.33)$$

The obtained relations can be expressed by the number Nu, after multiplying both sides of the equality by $2R/\lambda$, where λ is the thermal conductivity of the gas

$$Nu=Re\,Pr^{2/3}\frac{1+\gamma_1\frac{c_T}{c_{pg}}}{1+\eta}\left[\frac{1+6k_D\eta\frac{R}{d_T}\frac{\varrho_g}{\varrho_T}\frac{1}{Re_T}}{\frac{1}{\varkappa}\ln\frac{R}{d_T}+C_2-\frac{3}{2\varkappa}}\right]^2. \qquad (2.34)$$

Figure 2.2 depicts results of calculations of Nu according to formula (2.34) and experimental data of L. Farbar and K. Depew (see [35]), obtained for a monodisperse two-phase flow. Used as the solid phase were glass balls d_T=30 μm in diameter. The airflow with different concentrations of the solid particles was regulated in order to insure the constancy of the Reynolds number from the airstream parameters.

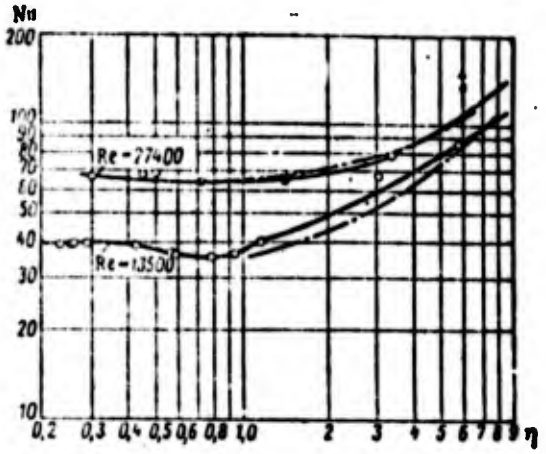

Figure 2.2. Dependence of the Nusselt number on the mass concentration of the solid particles: -·-·- – calculated curve; ——— – experiment.

The calculations were performed in connection with the conditions of the experiment. In the calculations it was accepted that $k_D=1$. As is evident from the curve, relation (2.34) provides good convegence of the calculated data with the experiment.

The effect of the condensed phase for particles of the given dimension at the assigned values of Re begins to appear with $\eta>1$ and leads to a sharp increase in the heat-transfer coefficient with $\eta>1.5$-2.0.

CHAPTER 3

HETEROGENEOUS BURNING IN THE COMBINED ROCKET ENGINE

Fuel combustion in the KRD [КРД - combined rocket engine] includes the atomization and evaporation of the liquid component, the heating and gasification of the solid component, the chemical interaction of the components (the burning proper), and the equalizing of the composition and parameters of the combustion products. Heterogeneous burning, which comprises a specific feature of the KRD, is the most complex and responsible of all the processes which form the operating conditions of the combustion chamber of the engine in the complex. This forces one to distinguish it as an independent object of study in the examination of operating conditins of the KRD.

A number of experimental works devoted to the study of heterogeneous burning in the KRD is known. A brief summary of these works is given table 3.1.

The basic question in the theoretical research on heterogeneous burning in the KRD is the establishment of the structure and parameters of the boundary layer with the feed of the mass and burning. The works published at present in this field with fundamental differences in the model of the phenomenon taken in them are enumerated in table 3.2.

Table 3.1.

Researcher	Fuel	Oxidizer
Smith (1938-1941)	Carbon	O_2
G. Bartel and V. Rene' (1946)	Carbon	Air
D. Dembrov and M. Pompa (1952)	Petroleum	$KClO_4$; NH_4NO_3; NH_4ClO_4
G. Moore and K. Bermann (1956)	Polyethylene	H_2O_2
D. Ordahl (1959)	Pressed metal	Compounds of halogens
A. Mute and M. Barrére (1960)	Organic plastic	HNO_3
B. Adelman (1961)	Rubber and aluminum	N_2O_4
K. Brunetti (1961)	Rubber	N_2O_4
K. Mettsler et al.	PMM, polyethylene, aluminum	O_2
G. Maksmen and M. Gilbert (1963)	Plexiglass	O_2
T. Hauser and M. Peck (1963)	PMM, polystyrene	O_2
L. Smut and S. Price (1965)	Butyl rubber, PBAK[1]	O_2+F_2
L. Smut and S. Price (1963)	Hydride of lithium-butyl rubber	O_2+F_2
R. Osmon	Lithium	H_2O_2

[1]Copolymer of polybutadience and acrylic acid.

Table 3.2.

Researcher	Model of flow	Flow pattern	Relationship between the oxidizer and fuel in the flame	Effect of mass exchange on conditions in the boundary layer
G. Bartel and V. Rens (1946	Cylindrical channel	Turbulent	Stoichiometric	Not examined
S. Penner (1960, 1962)	The same	Laminar	Variable	Not examined
A. Mute and M. Barrére (1961)	Flat plate	Laminar	Stoichiometric	Not examined
S. Faynmen (1962)	Cylindrical channel	Laminar and turbulent	Stoichiometric	Not examined; examined partially
G. Maksmen and M. Gilbert (1963)	Flat plate	Turbulent	Excess of fuel	Examined partially

Below by us are set forth relations for the calculation of the basic parameters of the burning of hybrid propellants which are similar to the relations of G. Maksmen and M. Gilbert, but they were obtained by another means and differ from them by the expression for the parameter of blowing-in B.

3.1. PROCESSES WHICH OCCUR IN THE GAS PHASE. POSITION OF THE FRONT OF BURNING

As schlieren and shoadow photographs show, burning in a GRD occurs in the relatively thin zone of the flame within the boundary layer above the surface of gasification of the solid component. Therefore, for the construction of relations which determine the parameters of burning in the KRD, it is necessary, first of all, to examine the processes of energy and mass exchange in a turbulent boundary layer above the surface of gasification of the solid component.

Processes of the transfer of the momentum, substance and energy in the laminar sublayer are described by the following equations:

$$\frac{\partial}{\partial z}(\rho u)+\frac{\partial}{\partial x}(\rho v)=0; \tag{3.1}$$

$$\rho u\frac{\partial u}{\partial z}+\rho v\frac{\partial v}{\partial x}=\frac{\partial}{\partial x}\left(\mu\frac{\partial u}{\partial x}\right)-\frac{\partial p}{\partial z}; \tag{3.2}$$

$$\rho u\frac{\partial C_i}{\partial z}+\rho v\frac{\partial C_i}{\partial x}=\frac{\partial}{\partial x}\left(\rho D_i\frac{\partial C_i}{\partial x}\right)+W_i; \tag{3.3}$$

$$\rho u\frac{\partial I}{\partial z}+\rho v\frac{\partial I}{\partial x}=\frac{\partial}{\partial x}\left[\lambda\frac{\partial T}{\partial x}+\sum\rho D_i I_i\frac{\partial C_i}{\partial x}+\mu\frac{\partial}{\partial x}\left(\frac{u^2}{2}\right)\right]. \tag{3.4}$$

where x is the coordinate normal to the surface of the charge;

z - the coordinate which coincides with the direction of the gas flow above the surface of the charge;

v, u - components of velocity along directions of the x and z coordinates, respectively;

μ, λ, D - coefficients of dynamic viscosity, thermal conductivity and diffusion, respectively;

C_i - local concentration of the i-th component;

T - local temperature;

I_i - full thermodynamic enthalpy of the

The system of equations (3.1)-(3.4) coincides in form with the appropriate system of equations with turbulent flow. In the latter case one should only replace coefficients μ, λ and D with the appropriate characteristics of turbulent transfer. The methods used in the solution to both systems (for a turbulent zone and for a laminar sublayer) are formally identical, in view of which there is no need to examine each of these solutions separately.

Equations (3.1) and (3.2) are, respectively, equations of continuity and momentum written in standard form. Let us discuss equations (3.3) and (3.4) in more detail.

Equation (3.3) describes the process of transfer of the i-th component. The expression in parentheses on the right side of the equation is the mass specific flow of the i-th component through the area perpendicular to the x axis. The value of this specific flow caused by molecular diffusion is determined by Fick's law. In the problem examined by us, the diffusion flow along the z coordinate can be disregarded; therefore the term in equation (3.3) corresponding to this flow is absent. When deriving equation (3.3) for our case, it appears possible also to disregard flows which appear as a result of the presence of gradients of pressure and temperature (pressure diffusion, thermal diffusion). The second term on the right side of equation (3.3) is the mass rate of formation of the i-th component with chemical reactions (per unit time per unit volume).

Equation (3.4) is the law of the conservation of energy with the thermal, chemical and mechanical processes which occur in the boundary layer. When deriving equation (3.4), the concept of the full thermodynamic enthalpy of the i-th component is used, and it is the sum of the enthalpy of this component at the given temperature and heat of its formation from the elements:

$$I_i = \int_0^T c_{pi}\,dT + I_i^0.$$

The full enthalpy of the mixture is equal to

$$I = \sum^{i} C_i I_i + \frac{u^2}{2}.$$

The first term in the bracket of equation (3.4) expresses the heat flux caused by the molecular thermal conductivity. The second term is the quantity of heat transferred together with the diffusing components of the mixture. In this case the heat absorbed or isolated with the chemical reactions occurring in the volume is included in the full enthalpy I_i, which with the chemical

reactions is not changed. The last term in the bracket considers the transfer of the mechanical energy due to the presence of viscosity forces.

Equations (3.3) and (3.4) can be simplified by utilizing the following dimensionless criteria:

$\mathrm{Pr}=\frac{\mu c_p}{\lambda}$ - Prandtl number;

$\mathrm{Le}_i=\frac{\varrho c_p D_i}{\lambda}$ - Lewis-Semenov number;

$\mathrm{Sc}_i=\frac{\mu}{\varrho D_i}$ - Schmidt number (Prandtl diffusion number).

In this case equations (3.3) and (3.4) take the following form:

$$\varrho u\frac{\partial I}{\partial x}+\varrho v\frac{\partial I}{\partial x}=\frac{\partial}{\partial x}\left[\frac{\mu}{\mathrm{Pr}}\left(\frac{\partial I}{\partial x}\right)+\mu\left(1-\frac{1}{\mathrm{Pr}}\right)\frac{\partial}{\partial x}\left(\frac{u}{2}\right)^2+\right.$$

$$\left.+\sum\varrho D_i\left(1-\frac{1}{\mathrm{Le}}\right)I_i\frac{\partial C_i}{\partial x}\right]; \qquad (3.5)$$

$$\varrho u\frac{\partial C_i}{\partial x}+\varrho v\frac{\partial C_i}{\partial x}=\frac{\partial}{\partial x}\left(\frac{\mu}{\mathrm{Sc}_i}\frac{\partial C_i}{\partial x}\right)+W_i. \qquad (3.6)$$

Equations (3.5) and (3.6) are considerably simplified if we accept Pr=1; Le=1; and Sc=1. This simplification is based on the fact that for gas and gas mixtures whose components have an identical number of atoms in the molecules, the coefficients of viscosity ν, molecular diffusion D and thermal diffusivity $a=\lambda/\varrho c_p$ in accordance with the kinetic theory of the gas have similar values.

Under this assumption dependences (3.5) and (3.6) take the following form:

$$\varrho u\frac{\partial I}{\partial x}+\varrho v\frac{\partial I}{\partial x}=\frac{\partial}{\partial x}\left(\mu\frac{\partial I}{\partial x}\right); \qquad (3.7)$$

$$\varrho u\frac{\partial C_i}{\partial x}+\varrho v\frac{\partial C_i}{\partial x}=\frac{\partial}{\partial x}\left(\mu\frac{\partial C_i}{\partial x}\right)+W_i. \qquad (3.8)$$

If in equation (3.2) we disregard the value of the second term on the right side, i.e., consider the flow in the channel of the GRD in the first approximation as being gradient-free, we will obtain

$$\rho u \frac{\partial u}{\partial x} + \rho v \frac{\partial v}{\partial x} = \frac{\partial}{\partial x}\left(\mu \frac{\partial u}{\partial x}\right). \qquad (3.9)$$

By comparing equations (3.9) and (3.7), it is not difficult to establish that equation (3.7) has the particular integral

$$I = a_1 u + b_1, \qquad (3.10)$$

where a_1 and b_1 are the arbitrary constants determined from the boundary conditions.

By examining as boundaries of the investigated region the surface of gasification, $u_s=0$ and $I=I_s$, and the front of burning in the gas phase, $u=u_f$ and $I=I_f$ we find:

$$b_1 = I_s;\ a_1 = \frac{I_f - I_s}{u_f}$$

and, therefore,

$$I = \frac{u^2}{2} + \frac{I_f - I_s}{u_f} u + I_s. \qquad (3.11)$$

Similarly, from the comparison of equations (3.9) and (3.8) it follows that with $W_1=0$ (frozen chemical reaction) there is a particular integral of the form

$$C_i = a_2 u + b_2, \qquad (3.12)$$

where constants a_2 and b_2 are determined from the boundary conditions.

Hence it follows that the profile of full enthalpy linearly depends on the rate and does not depend on the occurrence of the chemical reactions, and also that the concentration of this component linearly depends on rate outside the zone of reaction.

In the solution to this problem the boundary layer is divided into two regions: region I - between the surface of gasification and the front of the burning; region II - between the front of the burning and the external boundary of the boundary layer.

The mass rate of the generation of the i-th component at the front of the chemical reaction referred to a unit of area is defined as the difference in the mass flows of the i-th component which enter into the zone of reaction on the right and emerge from it on the left:

$$-\tilde{m}_i=\left[\rho D_i\left(\frac{\partial C_i}{\partial x}\right)_f\right]_{np}-\left[\rho D_i\left(\frac{\partial C_i}{\partial x}\right)_f\right]_{a}. \qquad (3.13)$$

With the adopted assumption Pr=Le=1, $\rho D=\mu$. By replacing $\partial C_i/\partial x$ by the product $(\partial C_i/\partial u)\,(\partial u/\partial x)$, we will obtain

$$-\tilde{m}_i=\tau_f\left[\left(\frac{\partial C_i}{\partial u}\right)_{np}-\left(\frac{\partial C_i}{\partial u}\right)_{a}\right]. \qquad (3.14)$$

Here and throughout the subscript "f" denotes the front of the chemical reaction (burning); τ_f - the tangential stress on the reaction front. Hence

$$\left(\frac{\partial C_i}{\partial u}\right)_{np}=\left(\frac{\partial C_i}{\partial u}\right)_{a}-\frac{\tilde{m}_i}{\tau_f}. \qquad (3.15)$$

In view of the linear dependence of C_i on u, for region II it is possible to write

$$\left(\frac{\partial C_i}{\partial u}\right)_{f_{np}}=\frac{C_{ie}-C_i}{u_e-u_f}. \qquad (3.16)$$

By equating the right sides of equations (3.16) and (3.15), we obtain

$$\left(\frac{\partial C_i}{\partial u}\right)_{f_a}=\left[C_{ie}-C_{if}+\frac{\tilde{m}_i}{\tau_f}(u_e-u_f)\right]\frac{1}{u_e-u_f}. \qquad (3.17)$$

Relations (3.12) and (3.17) are geometrically represented on

figure 3.1. From this figure it follows that the sum of the first and third terms in the bracket of equation (3.17) can be considered as a certain fictitious concentration on the external boundary of the boundary layer, which corresponds to the linear dependence of C on u for region I. Consequently, with the retention of this sum relations (3.17) remains valid for any point of region I, if with retention of the indicated sum in it, instead of C_{1f} and u_f we substitute values of C and u for this point.

For the surface of gasification we will obtain

$$\left(\frac{\partial C_1}{\partial u}\right)_s = \left[C_{1s} - C_{1s} + \frac{\tilde{m}_1}{\tau_f}(u_e - u_f)\right]\frac{1}{u_e}. \qquad (3.18)$$

In this case

$$\left(\frac{\partial C_1}{\partial x}\right)_s = \frac{1}{u_e}\left(\frac{\partial u}{\partial x}\right)\left[C_{1s} - C_{1s} + \frac{\tilde{m}_1}{\tau_f}(u_e - u_f)\right]. \qquad (3.19)$$

The boundary condition for the surface of gasification, in connection with the components which are formed on this surface, takes the following form:

$$(1 - C_{gs})(\rho v)_s = -\rho_s D_g \left(\frac{\partial C_{gs}}{\partial x}\right)_s = -\mu_s \left(\frac{\partial C_g}{\partial x}\right)_s. \qquad (3.20)$$

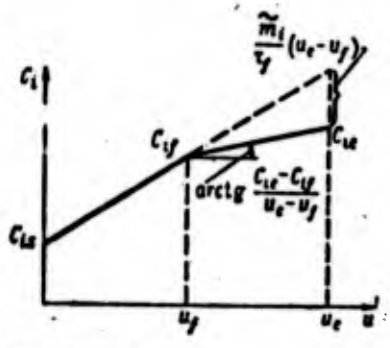

Figure 3.1

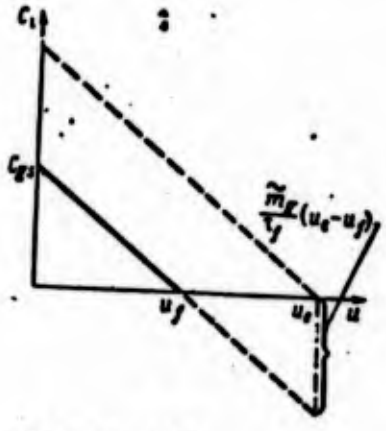

Figure 3.2

By utilizing the modified parameter of blowing-in[1]

$$B=\frac{(\rho v)_s}{\rho_e u_e St}=\frac{2(\rho v)_s}{C_f \rho_e u_e}=\frac{(\rho v)_s u_e}{\tau_s},$$

from equations (3.19) and (3.20) we will obtain

$$C_{gs}=\frac{B}{B+1}\left[1+\frac{C_{Ke}}{B}+\frac{\tilde{m}_f}{\tau_f B}(u_e-u_f)\right]. \tag{3.21}$$

Equation (3.21) can be rewritten in the form

$$C_{gs}=\frac{B}{B+1}\left(1+\frac{C_{Ke}}{B}-\lambda_f\frac{1-\bar{u}_f}{\bar{\tau}_f}\right), \tag{3.22}$$

where $\bar{\tau}_f=\frac{\tau_f}{\tau_s}$; $\bar{u}_f=\frac{u_f}{u_e}$; and $\lambda_f=\frac{\tilde{m}_f}{(\rho v)_s}$ are portions of the sublimate absorbed in the plane of reaction.

Relations for the concentration on the surface of the section of two phases for other components are similarly derived. The distinction consists of the boundary condition on the surface, which for these components is written in the form

$$C_{is}(\rho v)_s=-\rho_s\left(\frac{\partial C_i}{\partial x}\right)_s. \tag{3.20a}$$

If one considers that the relationship of the components which participate in the reaction on the front of burning is determined by the equation of reaction

$$n_g M_g+n_R M_R\rightarrow n_p M_p, \tag{3.23}$$

where M_g, M_R and M_p are molecular masses of the components, then for the surface S we will obtain

---

[1]The parameter of blowing-in B is called modified, unlike the parameter of blowing-in

$$B_0=\frac{(\rho v)_s}{\rho_e u_e St_0}.$$

$$C_{Rs}=\frac{1}{B+1}\left[C_{Re}-\frac{n_R}{n_g}\frac{M_R}{M_g}B\lambda_f\frac{1-\bar{u}_f}{\bar{\tau}_f}\right]. \qquad (3.24)$$

Assuming that all the products of gasification of the solid component (entire sublimate) are oxidized on the front of burning, i.e., that $C_{gf}=0$, then, by utilizing the prerequisite of graphing on figure 3.1, for the present case we will obtain the geometric diagram presented in figure 3.2. From it there follows

$$\frac{C_{gs}+\frac{\bar{m}_g}{\bar{\tau}_f}(u_e-u_f)}{u_e}=\frac{C_{gs}}{u_f}, \qquad (3.25)$$

whence we obtain the additional expression for C_{gs}:

$$C_{gs}=\frac{B\bar{u}_f}{\bar{\tau}_f}. \qquad (3.26)$$

By equating the right sides of equations (3.26) and (3.22), and after assuming in the latter that $C_{ge}=0$, we obtain

$$\bar{\tau}_f=1+B\bar{u}_f. \qquad (3.27)$$

The profiles of concentrations in the coordinate system $C-\bar{u}$ with the diffusion of burning can be two types, which are represented in figure 3.3a and b.

Case 1 (see figure 3.3a), with the occurrence of the reaction of burning on the surface of gasification, is possible when the rate of gasification is lower than the level necessary to provide for the stoichiometric relationship of the reacting components on this surface.

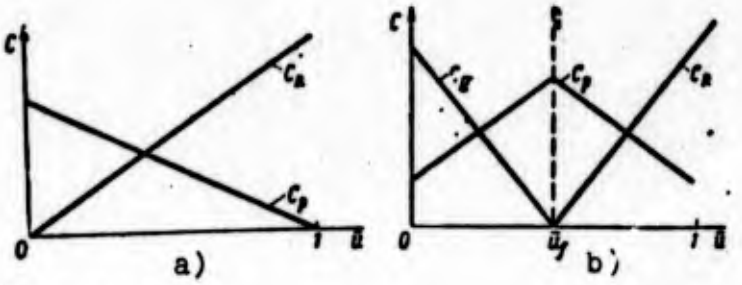

Figure 3.3

By utilizing the derived relationships, it is possible to estimate the minimum rate of gasification, lower than which the reaction of burning will occur directly on the boundary surface of the phases. If in relation (3.24) we assume that $C_{Rs}=0$; $\bar{u}_f=0$; $\bar{\tau}_f=1$; and $\lambda_f=1$, we obtain the parameter of blowing-in corresponding to this rate:

$$B_{min}=\frac{M_g n_g}{M_R n_R} C_{Re}. \tag{3.28}$$

The solution for case 1 is of practical interest for the calculation of the removal of material of heatproof coatings and nozzle liners.

For the solid components utilized in fuel compositions of the KRD, case 2 is more characteristic, when the ratio of the specific flow rate of the combustible material from the charge's surface to the flow rate of the oxidizing component which reaches this surface is considerably higher than the stoichiometric. In this case the plane of the reaction of burning is remote from the surface (see Fig. 3.3b).

If in equation (3.24) we assume that $C_{Rs}=0$, assuming that the entire oxidizing component transferred from the nucleus of flow to the surface of gasification is wholly expended at the front of burning, then from equations (3.24) and (3.27) there follows the relation which determines the position of the front of burning:

$$\bar{u}_f=\frac{\frac{M_R n_R}{M_g n_g}-\frac{C_{Re}}{B}}{\frac{M_R n_R}{M_g n_g}+C_{Re}}. \tag{3.29}$$

This relation, taking expression (3.28) into account, can be rewritten in the form

$$\bar{u}_f=\frac{1-\frac{B_{min}}{B}}{1+B_{min}}. \tag{3.29a}$$

The maximum position of the front of burning with $B \to \infty$ will be determined by formula

$$\bar{u}_{f\,\max} = \frac{1}{1 + B_{v.in}}.$$

A small quantity of works on determining the position of the flame with burning in GRD is known. Work [21] gives Schlieren photographs obtained for the plexiglass "oxygen-system." The flame in the photograph takes the form of a glowing band whose removal from the surface of gasification depends on the degree of dilution of the oxidizer in the incoming flow. If the flow of the oxidizer is not diluted ($C_{OH}=1.0$), the flame is located at a distance of $x_f/\delta=0.1$ from the surface of gasification, which corresponds to the value $\bar{u}_f=0.55$. (Here δ is the boundary layer thickness). With dilution of the oxidizer the flame is receded from the surface of the charge as follows from relation (3.29). Thus with a degree of dilution of 50% ($C_{OH}=0.5$) the position of the flame is determined by the ratio $x_f/\delta=0.2$, which corresponds to $\bar{u}_f=0.65$. The calculation according to equation (3.29) for these cases gives the following values: $\bar{u}_f=0.52$ (with $C_{OH}=1$) and $\bar{u}_f=0.68$ (with $C_{OH}=0.5$).

The high temperatures on the flame front and in the flow core of the KRD, in conjunction with the chemical agressiveness of the medium, impede the studies of the structure of the boundary layer. The knowledge of the relations which express the parameters of the flame at different dilution of the component fed into the chamber by an inert substance allows the results of measurements with high dilution of the component (i.e., at low temperatures) to be extrapolated into the high-temperature range.

In work [21], this method was used for determining the temperature of the products of combustion of the "polymethylmetacrylate-oxygen" system. The measurement of temperatures in the flow was conducted by means of tungsten and tungsten-coated thermocouples. The thermocouples were placed in the flow of oxygen with a different

degree of dilution of it by nitrogen (from 50 to 25%). Then the obtained results were extrapolated up to a 100% oxygen content (figure 3.4).

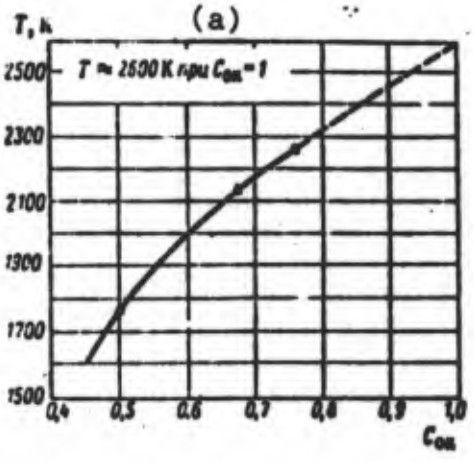

Figure 3.4. Combustion temperature of the "polymethylmetacrylate-oxygen" system depending on the degree of dilution of the oxidizer.
Key: (a) With.

A similar method can also be used for determining other parameters of burning.

3.2. CALCULATION OF THE RATE OF GASIFICATION OF A SOLID COMPONENT

The heat flux to the surface of gasification of the solid component in general is the sum of the convective and radiation flows:

$$q_0 = q_{к.0} + q_р.$$

For hybrid systems with weak radiation of the combustion products, which include the majority of systems with a nonmetallized fuel, the heat flux to the surface of gasification can be presented in the form

$$q_0 = q_{к.0}\varphi_0 \qquad (3.30)$$

where $\varphi_0 = 1 + \frac{q_р}{q_{к.0}} \approx 1 + \frac{q_р}{q_к}$ is the correcting coefficient which considers the effect of radiation.

The convective heat flux to the surface is equal to

$$q_{w\,s}=-\lambda_s\left(\frac{\partial T}{\partial x}\right)_s-\rho D\sum I_i\left(\frac{\partial C_i}{\partial x}\right)_s. \qquad (3.31)$$

Since

$$dI=\sum C_i dI_i+\sum I_i dC_i=\bar{c}_p dT+\sum I_i dC_i,$$

where

$$\bar{c}_p=\sum C_i c_{pi},$$

equation (3.31) can be presented in the form

$$q_{w\,s}=-\frac{\lambda}{\bar{c}_p}\left(\frac{\partial I}{\partial x}-\sum I_i\frac{\partial C_i}{\partial x}+\frac{\rho D\bar{c}_p}{\lambda}\sum I_i\frac{\partial C_i}{\partial x}\right). \qquad (3.32)$$

Having used the simplifying assumption $\mathrm{Le}=\frac{\rho D\bar{c}_p}{\lambda}=1$, we will obtain

$$q_{w\,s}=-\frac{\lambda}{\bar{c}_p}\left(\frac{\partial I}{\partial x}\right)_s.$$

Since

$$\left(\frac{\partial I}{\partial x}\right)_s=\left(\frac{\partial I}{\partial u}\right)_s\left(\frac{\partial u}{\partial x}\right)_s=\frac{\tau_s}{\mu_s}\left(\frac{\partial I}{\partial u}\right)_s,$$

we obtain

$$q_{w\,s}=\varphi_q\frac{\lambda_s\tau_s}{\mu_s\bar{c}_p}\left(\frac{\partial I}{\partial u}\right)_s.$$

By using equation (3.11) and taking into account that $\left(\frac{\lambda}{\mu\bar{c}_p}\right)_s=\frac{1}{\mathrm{Pr}_s}$, we find

$$q_s=\varphi_q\frac{\tau_s}{\mathrm{Pr}_s}\frac{I_f-I_s}{u_f}. \qquad (3.33)$$

With the steady state of the gasification ($\dot{m}_s$=const, see section 3.3)

$$q_s=\dot{m}_s c_\tau(T_s-T_s').$$

After expressing $\dot{m}_s$ by the modified parameter of blowing-in, the last equality can be presented in the form

$$q_s = \frac{\tau_s B}{u_e} c_\tau (T_s - T_s'). \qquad (3.34)$$

By equating the right sides of equations (3.33) and (3.34), and after accepting $Pr_s = 1$, we will obtain

$$B = \frac{\varphi_q}{\bar{u}_f} \frac{I_f - I_s}{c_\tau (T_s - T_s')}. \qquad (3.35)$$

After substituting the expression for $\bar{u}_f$ from (3.29a) into equation (3.25) we will obtain

$$B = \frac{I_f - I_s}{c_\tau (T_s - T_s')} \varphi_q (1 + B_{min}) + B_{min}. \qquad (3.36)$$

Mass rate of gasification determined in terms of parameter B is equal to

$$\dot{m}_s = B \rho_e u_e \mathrm{St}.$$

After dividing and multiplying the right side of this equality by St_0, we obtain

$$\dot{m}_s = B \rho_e u_e (\mathrm{St}/\mathrm{St}_0) \mathrm{St}_0. \qquad (3.37)$$

Ratio St/St_0 is the so-called *function of blowing-in*, which considers the obstructing thermal effect, i.e., a decrease in the heat feed to the surface with the blowing of gases through it in the boundary layer. As the majority of the investigations shows, ratio St/St_0 can, in the first approximation, be considered as the function of one variable - parameter B or B_0.

Assuming that under these conditions the analogy of Reynolds remains valid, i.e., that the ratio of the Stanton numbers is equal to the ratio of the coefficient of surface friction c_j/c_{j0} with the blowing-in of the gases and without it, G. Maksmen (see [21]) obtained the following theoretical relations:

$$\frac{\mathrm{St}}{\mathrm{St}_0} = \left[\frac{\ln(1+B)}{B}\right]^{4/5} \left[\frac{1 + \frac{13B}{10} + \frac{4B^2}{11}}{(1+B)[1+(B/2)]^2}\right]^{1/5} \qquad (3.38)$$

Figure 3.5 gives the graph of this function. From an analysis of the graph it follows that in the range $5<B<100$, which covers all the possible cases of the operation of the GRD [ГРД - hybrid rocket engine] relation (3.38) with a sufficient degree of accuracy can be approximated by the formula

$$St/St_0 = 1{,}2B^{-0{,}77}. \qquad (3.39)$$

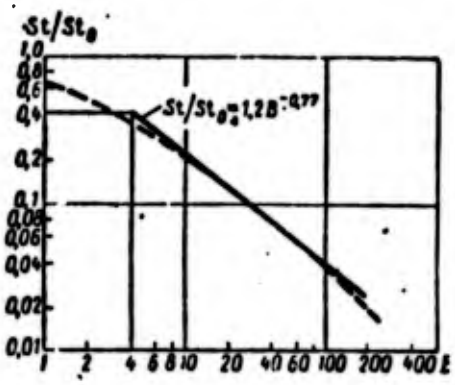

Figure 3.5. Effect of the feed of the mass into the boundary layer on value St/St_0: – – – – precise calculation according to equation (3.38); ——— – approximation according to equation (3.39).

Having substituted expressions (2.1) (2.8) and (3.39) into equation (3.39), after elementary transforms, assuming that Pr=1, we will obtain

$$\dot{m}_s = 0{,}0276\bar{G}\left(\frac{\bar{G}d}{\mu}\right)^{-0{,}2} B^{0{,}23}. \qquad (3.40)$$

Relations for cases of the flow in the channel with throttle washers and of the flow of a two-phase flow are similarly derived. In this case the appropriate indicated cases of formula (2.15) and (2.34) are substituted into equation (3.37) instead of (2.1).

Results of calculations according to formulas (3.40) and (3.36) for the "polymethylmetacrylate-oxygen" system and experimental data for this system taken from work [21] are given in figure 3.6.

In the calculations the following was accepted:

$$q_0=1;\ T_f=2600\ \text{K};\ T_s=600\ \text{K};\ Q_s=1590\ \text{кДж/(кг·К)};\ \bar{c}_p=1{,}68\ \text{кДж/(кг·К)};\ B_{min}=0{,}521;\ \mu=5{,}4\cdot10^{-5}\ \text{кг/(м·с)};\ d=2{,}54\ \text{см}.$$

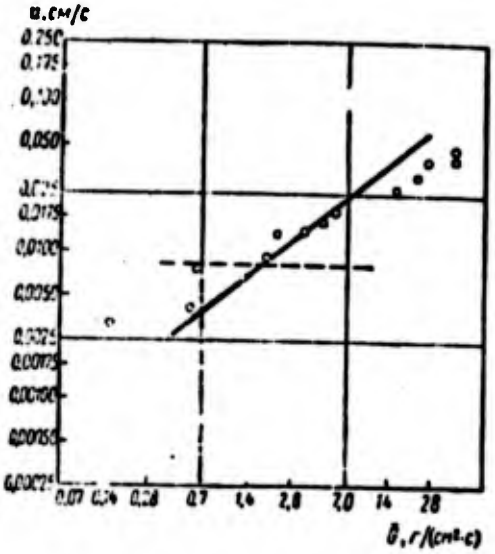

Figure 3.6. Dependence of the rate of gasification of polymethylmetacrylate on the specific oxidizer flow rate ("polymethylmetacrylate-oxygen") system): O - experiment; d_0=2.54 cm L/d_0=10; □ - experiment; d_0=1.27 cm, L/d_0=10; —— - theoretical data from equation (3.40); - - - - boundry of the formation of the liquid layer. (Initial diameter of the channel d_0=2.54 cm).

Abbreviation: см/с=cm/s; $см^2 \cdot с = cm^2 \cdot s$.

In the case of the applying of equation (3.40) to the hybrid systems for which the heat exchange by radiation plays a secondary role, the coefficient ϕ_q can be calculated from the approximate formula:

$$\varphi_q \approx 1 + (q_p/q_{к0}) \approx 1 + (a_p/a_{к0}).$$

This approach is justified for the majority of the hybrid compositions with nonmetallized fuel. Thus, for instance, according to data of work [21] with the burning of the "plexiglass-oxygen" system the radiant heat flux measured with by a pyrometer is approximately 5 to 10% of the convective flow.

In cases when the radiant heat flux plays a significant role in the heat exchange with the charge's surface, in the formula the value ϕ_q should be replaced by the real value of convective heat flux to the surface, which is changed depending on the parameter of blowing-in which, in turn, is connected with ϕ_q. There appears the sequence of relations for which it is difficult to obtain the solution in an explicit form it.

To obtain the solution it is possible to use the following scheme:

1) being assigned the arbitrary values ϕ_q, from formula (3.36) calculate values of parameter of blowing-in corresponding to them;

2) calculate the ratio of the rate of gasification at this value ϕ_q to the rate of gasification at $\phi_q=1$. As follows from formula (3.40),

$$\bar{u}=\frac{\dot{m}_{s(\varphi)}}{\dot{m}_{s(\varphi=1)}}=\left[\frac{B_{(\varphi)}}{B_{(\varphi=1)}}\right]^{0.23};$$

3) determine the relative decrease in the convective heat flux to the charge's surface caused by the blowing-in of products of gasification,

$$\bar{q}_к=\frac{St}{St_0};$$

4) find the ratio of the heat fluxes

$$\frac{q_p}{q_{к0}}=(\varphi_q-1)\bar{q}_к;$$

5) present the obtained results as a function of ratio $q_p/q_{к0}$, where $q_{к0}$ is the convective heat flux determined for the assigned gas-dynamic conditions with respect to the relation for the flow in tubes with impenetrable walls.

Results of the calculations carried out for the "plexiglass-oxygen" system by the indicated scheme are given in figure 3.7. The thermodynamic characteristics of this system were borrowed from work [21].

By utilizing a similar graph according to the assigned $q_p/q_{к0}$ (or in terms of their calculated values for the assigned parameters of the gas flow it is possible to find value $\bar{u}$, and having determined the rate of gasification by formula (3.40) with $\phi_q=1$, it is possible then to recalculate it for the assigned ratio $q_p/q_{к0}$.

The obtained curve makes it possible to trace the effect of the radiation heat exchange on the rate of gasification of the solid component. At the fixed value of $q_{н0}$ the intensification of the heat exchange by the radiation, accompanied by an increase in the rate of gasification, leads to the weakening of the convective heat flux which reaches the charge's surfaces. Therefore, an increase in the rate of gasification, with an increase in the radiant heat flux, is retarded. Simultaneously relative role of $q_{н\,s}$ and q_p is sharply changed. Thus with q_p and $q_{н0}$, as follows from the graph, the rate of gasification is 65% higher than the value obtained with $q_p=0$, although the value of the initial heat flux $q_{s0}=q_{н0}$ was doubled.

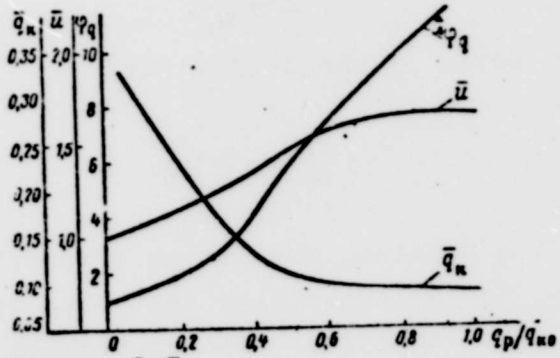

Figure 3.7

3.3. PROCESSES WHICH OCCUR IN A SURFACE LAYER OF THE SOLID COMPONENT WITH BURNING

With the steady state of burning in the GRD the surface of gasification of the solid component is moved deep into the material at a constant linear rate u. In this case the temperature on the surface of gasification is maintained constant equal to T_s.

The distribution of temperature in the unit of the solid component before the front of gasification at u=const can be obtained from the standard equation of thermal conductivity, which for the moving coordinate system which is moved deep into the material at the rate of u is converted to the following form:

$$a\frac{d^2T}{dx^2}=-u\frac{dT}{dx}. \qquad (3.41)$$

3.3.1. Case of the Gasification of the Material Without Transfer Through the Liquid State (Figure 3.8)

The integration constants of equation (3.41) are determined from the conditions:

when $x=\infty$; $T=T_н$;

when $x=0$, $T=T_s$.

The equation of the temperature field acquires the following force:

$$T=T_н+(T_s-T_н)e^{-\frac{ux}{a}}. \qquad (3.42)$$

The distance from the surface of gasification to the layer with temperature T is determined by the dependence

$$x=\frac{a}{u}\ln\frac{T_s-T_н}{T-T_н}.$$

If as the conditional boundary of heating we accept the isotherm which corresponds to the condition

$$\frac{T-T_н}{T_s-T_н}=0{,}05,$$

then the depth of heating determined of this condition will be

$$x_{пр}\approx\frac{3a}{u}.$$

The temperature gradient at the surface of gasification

$$\left(\frac{\partial T}{\partial x}\right)_s=-(T_s-T_н)\frac{u}{a}. \qquad (3.43)$$

The value of the flow of heat removed from the surface of deep into the solid component will be equal to

$$q_т = -\lambda\left(\frac{\partial T}{\partial x}\right)_s = \rho c_т u (T_s - T_н).$$

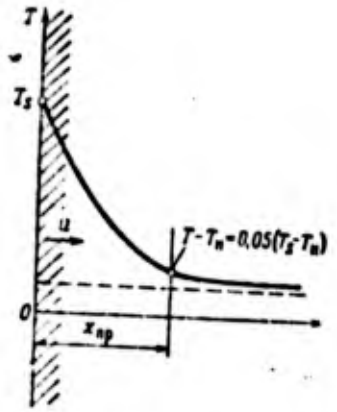

Figure 3.8. Temperature profile in the charge of the solid component with the steady-state process of gasification.

The difference in the heat fluxes (fed to the surface of gasification from the gas phase and diverted deep into the solid material) will be

$$q_г - q_т = \rho u Q_s,$$

where Q_s is the quantity of heat absorbed with gasification per 1 kg of material.

The quantity of heat accummulated in the heated layer, in the calculation of per unit of surface area of gasification, taking into account equation (3.42), will be equal to

$$Q_т = \int_0^{\infty} \rho c_т (T - T_н)\, dx = \frac{\lambda (T_s - T_н)}{u}. \qquad (3.44)$$

Let us introduce the following notation:

$$T_s' = T_н - \frac{Q_s}{c_т}.$$

The value T_s' is the conditional temperature which would be established on the surface of the material as a result of heat absorption with gasification but in the absence of heat feed outside.

From the equation of thermal balance for the surface of gasification it follows that

$$q_г = c_г \dot{m}_s (T_s - T_s'). \qquad (3.45)$$

3.3.2. Case of the Gasification of the Material with the Formation of a Liquid Layer (figure 3.9)

In this case the rates of displacement of the front of melting and front of gasification, changing with time in the beginning of the process, are very rapidly equalized. After this the thickness of the liquid layer included between these fronts is maintained constant in time.

The temperature distribution in the solid material before the front of melting is determined by system of equations:

$$\left.\begin{aligned} a_т \frac{d^2T}{dx^2} &= -u\frac{dT}{dx}; \\ -\lambda_ж \left|\frac{dT}{dx}\right|_ж &= -\lambda_т \left|\frac{dT}{dx}\right|_т + \rho_т \mu Q_{пл}; \\ T_{(x=-\infty)} &= T_н. \end{aligned}\right\} \qquad (3.46)$$

The first term on the right side of equation (3.46) is the flow of heat removed from the front of melting deep into the material. With the steady-state process it is equal to

$$-\lambda_т \frac{dT}{dx} = \rho_т \mu c_т (T_{пл} - T_н).$$

Let us denote

$$T'_{пл} = T_н - \frac{Q_{пл}}{c_т}.$$

Then equation (3.46) will take the following form:

$$-\lambda_ж \left|\frac{dT}{dx}\right|_ж = \rho_т \mu c_т (T_{пл} - T'_{пл}). \qquad (3.47)$$

The temperature distribution in the liquid layer with the constancy of thermophysical characteristics along the thickness of this layer is determined by the equation of thermal conductivity:

$$a_ж \frac{d^2T}{dx^2} = -u\frac{dT}{dx}.$$

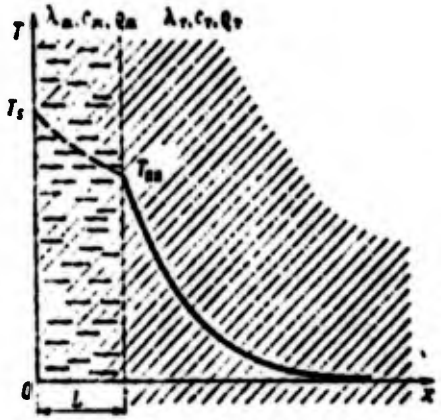

Figure 3.9. Temperature configuration in the charge of the solid component with the formation of a liquid layer.

By integrating it twice, we obtain

$$T = -\frac{1}{b} C_1 e^{-bx} + C_2,$$

where

$$b = \frac{a}{a_ж}.$$

After the substitution of integration constants, the equation of the temperature field of the liquid layer takes the following form:

$$T = T_s - \frac{c_т Q_т}{c_ж Q_ж} (T_{ж.з} - T'_{н.з}) e^{bL} (1 - e^{-bx}). \qquad (3.48)$$

Assuming that x=L and $T=T_{пл}$, equation (3.48) relative to the thickness of the liquid layer is solved:

$$L = \frac{a_ж}{a} \ln \left[1 + \frac{c_ж Q_ж}{c_т Q_т} \frac{T_s - T_{ж.з}}{T_{ж.з} - T'_{н.з}} \right]. \qquad (3.49)$$

The excessive increase in the thickness of the liquid layer at the low rate of gasification can adversely affect the process of the fuel combustion. On the surface of the film, under some conditions there appears a ripple, from crests of which into the gas flow drops ("drop removal") are separated. In this case the model of burning examined above in the boundary layer becomes not applicable, and the rate of combustion can no longer be calculated from relations (3.36)-(3.40). For the operating conditions of the engine, as a whole the "drop removal" of the solid component is undesirable, since the large drops do not manage to burn in the zone of the flame, and the combustion efficiency falls. Furthermore, this process is characterized by the lesser stability of the flow rate of the solid component.

The possibility of this phenomenon should be considered when selecting the material used as the solid component. For example,

the liquid layer obtains considerable development when using polyethylene (see [20]), which for this reason for the organization of the process of burning in the engine is less desirable than polymethylmetacrylate (PMM) [ПММ]. However, the emergence of the liquid layer under specific conditions of heating is possible for many materials, including for the PMM.

Let us determine the lower boundary of the temperature mode (mode of heating) of the solid unit with which the phenomenon of the "drop removal" begins.

By analogy of this phenomenon with the stability of the liquid film with the cooling of the ZhRD [ЖРД - liquid-propellent rocket engine], it is possible to confirm that the thickness of the stable film should not exceed the thickness of the laminar sublayer $x_л$ in the boundary layer of external flow. As is known from the universal law of the velocity distribution in the boundary layer, this thickness is equal to

$$x_л = \frac{x^* \nu_ж}{V_\tau}, \qquad (3.50)$$

where V_τ is the frictional rate: $V_\tau = \sqrt{\tau_s / \rho_ж}$;

τ_s - the stress of friction on the interface "gas-liquid";

$\rho_ж$, $\nu_ж$ - the density and viscosity of the liquid respectively;

x^* - the dimensionless thickness of the laminar sublayer ($x^*=11.6$).

Equating the right sides of expressions (3.50) and (3.49), we find the threshold rate of gasification $u_{кр}$, below which the "drop removal" of substance from the surface begins to have an effect

$$u_{кр} = \frac{a_ж V_\tau}{\nu_ж x^*} \ln\left[1 + \frac{c_ж \rho_ж}{c_г \rho_г} \frac{T_s - T_{s1}}{T_{s1} - T'_{ж1}}\right]. \qquad (3.51)$$

By virtue of the adopted assumptions, equation (3.51) can be

used only for a rough evaluation of the threshold rate.

On the graph given above of the rate of gasification of the PMM (see figure 3.6), according to the experimental data of work [21] the region of the "drop removal" of the solid component is located below the value of $u_{кр}$=0.008 cm/s. Boundary of the region of the "drop removal" is shown in figure by 3.6 by a dashed line.

3.4. Processes Which Occur on the Surface of Gasification of Solid Component

In the derivation of the formula for determining the rate of gasification, the processes which occur on the very surface of gasification were not examined as such by us: they were a reflection in the boundary condition of the problem of the heat-mass transfer in the form of finite energy characteristics. In view of the important role of these processes in the general process of fuel combustion, they deserve special examination.

The entrance of the solid component into the gas medium can be caused by different phenomena: charge in the state of aggregation (sublimation, melting with subsequent evaporation); chemical transformations caused by the heating of the material; the dispersion of the condensed particles of high-boiling additions.

The materials which can be used as a solid component of the GRD, in accordance with features of their thermal properties, can be divided into the following groups:

1) solid fuels of the hydrocarbon type;
2) solid oxidizers;
3) metallized fuels;
4) solid fuels with an excess of the combustible;

Table 3.3

Material	PMM	Nylon	Poly-ethyl-ene	Poly-sty-rene	Lithium aluminum hydride
Formula of monomer	$C_5H_8O_2$	$C_6H_{11}NO$	C_2H_4	C_8H_8	$LiAlH_4$
Molecular mass of monomer	100	113	28	104	38
Density in kg/m^3	1119-1210	1100	920	1025	920
Specific heat capacity c in kJ/(kg·K)	1.46	1.87	2.30	1.92	2.01
Coefficient of thermal conductivity λ in W/(m·C)	0.184	0.242	0.352	0.252	–
Diffusivity a in m^2/s	$0.95 \cdot 10^{-7}$ – $1.29 \cdot 10^{-7}$	$1.32 \cdot 10^{-7}$	$1.29 \cdot 10^{-7}$	$1.29 \cdot 10^{-7}$	–
Temperature of gasification in C[1]	665	675	675	640	398-408
Heat of combustion in kJ/kg	26,150	35,600	43,300	39,400	40,000

[1]Temperature at which noticeable decomposition of this substance begins.

3.4.1. Solid Fuels of the Hydrocarbon Type

As an analysis of materials of this type potentially suitable for use in the GRD shows, the greatest practical interest is in polymers; of these first of all there are the polyethylene, polystyrene, nylon and polymethylmetacrylate (PMM [ПММ] or plexiglass). Characteristic properties of these fuels are given in table 3.3 compiled according to works [4, 18, 26, 32].

The gasification of the indicated compounds with heating is the consequence of their chemical decomposition - pyrolysis.

In the GRD the pyrolysis of polymers occurs in the mode of rapid heating of the substance (mode of thermal shock). The temperature gradient in the material near the surface according to equation (3.43) will be equal to

$$\frac{dT}{dx}=(T_s-T_н)\frac{u}{a}.$$

The effective time of heating of the material to the temperature of surface in the first approximation will be defined as

$$t_{пр}\approx\frac{x_{пр}}{u}=\frac{3a}{u^2}. \qquad (3.52)$$

For the PMM at the rate of gasification of $\sim$1.0-1.5 mm/s, accepting according to work [38] the effective thermal diffusivity factor to be equal to $1\cdot10^{-7}$ m^2/s, we obtain $\tau_s\approx10^{-1}$ s.

At such high heating rates the so-called linear pyrolysis of the substance is realized when the reaction front of the chemical decomposition is propagated in the substance at a constant rate and one-dimensionally.

As the experiment shows, the pyrolysis of the majority of the polymers is a first-order reaction with respect to the initial

substance. In this case the mass rate of gasification is connected with characteristics of the kinetics of the pyrolysis and with the surface temperature T_s by the relation

$$\dot{m}_s = \rho u = K_{ms} e^{-E/RT_s}, \qquad (3.53)$$

where E is the activation energy for determining the decomposition reaction;

R - the universal gas constant;

K_{ms} - the pre-exponential factor.

Values E and K_{ms} can be determined by experimental data:

$$E = 2R \frac{\ln u_1 - \ln u_2}{(1/T_{s2}) - (1/T_{s1})};$$
$$\ln K_{ms} = \ln u_1 + \frac{E}{2RT_{s1}} + \ln \rho_r,$$

where u_1 and u_2 are the linear rates of pyrolysis (gasification) which correspond to temperatures of the surface of gasification T_{s1} and T_{s2}.

The basic difficulty of the experiment consists of the precise determining of the surface temperature T_s. One of the possible methods of the determining of T_s is the use of microthermocouples sealed into the material. In the process of heating the thermocouples first record a change in the temperature of the solid material, and then, after the passage of the junction of the thermocouple through the surface of gasification, the temperature of the gas medium. The sharp bend on the temperature curve, caused by the transfer of the thermocouple from the condensed phase to the gas phase, makes it possible to establish the temperature of the surface of gasification. This method was used in work [38].

The registration of T_s can be realized also with the aid of optical methods.

For determining the kinetic characteristics of the linear pyrolysis the method of the hot plate has recently received considerable widespread use. The essence of this method lies in the fact that the fact that the specimen of the tested substance is pressed with a constant force against a metallic plate heated to the assigned temperature, which is maintained constant. During the experiment the surface temperature of the plate and the rate of the displacement of the specimen are recorded (see [34, 36, 44, 50]).

As the investigations show, the linear pyrolysis in its kinetic characteristics significantly differs from the thermal destruction of the same material with slow heating. Meanwhile, until recently for the study of the thermal destruction of polymers, methods were applied which were based on slow heating (the order of several degrees per minute) of the substance with which throughout the entire mass of the tested specimen an identical temperature (isothermal conditions of process was established).

These isothermal methods (weight, volumetric, calorimetric) traditional for chemical laboratory practice, cannot be used for the investigation of the kinetics of pyrolysis in a GRD which occurs under completely different conditions. For this reason the use of kinetic characteristics of pyrolysis determined for polymers by isothermal methods and for the calculation of the rate of gasification of these materials in a GRD is inadmissible.

Table 3.4 gives experimental values of the rate of the gasification of the PMM obtained on experimental GRD given in work [38] and also the temperatures of the surface of gasification corresponding to these velocities measured by means of chromel-alumel thermocouples 15-25 μm in diameter. In the other two columns calculated values of the velocity of gasification are given. Data of column (1) were calculated by T. Hauser and M. Peck according to the kinetic characteristics of PMM obtained by S. Madorskiy (see [18]) with isothermal heating under conditions

of a vacuum. The activation energy obtained under these conditions is 155.000 kJ/mole.

Table 3.4.

T_s, K	$u \cdot 10^3$ cm/s			T_s, K	$u \cdot 10^3$ cm/s		
	Experiment	Calculation (1)	Calculation (2)		Experiment	Calculation (1)	Calculation (2)
660	7.7	0.11	4.12	675	7.3	0.27	4.96
705	9.0	0.65	7.02	710	7.5	0.94	7.41
705	7.5	0.77	7.02	655	8.5	0.094	3.87
670	8.0	0.18	4.67				

The calculated values of u differ from the experimental values by one whole order. Given in column (2) are values of u calculated by us according to kinetic characteristics of the linear pyrolysis of PMM obtained by the method of the hot plate by R. Chaiken (see [50]). Although the great scattering of values of T_s, as a result of the inadequancy of the experiment recognized by the very authors of work [38], impedes the objective comparison of data of the calculation and experiment, as is evident from the table, the calculation gives values of u close to the experimental values.

As investigations of the linear pyrolysis of some polymers show, with high heating rates and the nonisothermal nature of the process the redistribution of rates of various stages of pyrolysis occurs. In this case the kinetic characteristics of the process are changed. Thus, according to data of works [36] and [50], at low rates of the decomposition of polystyrene ($u<3 \cdot 10^2$ cm/s) the activation energy is $(17\text{-}21) \times 10^4$ kJ/mole, approaching the value obtained by the classical isothermal methods at high rates for the same material [$E=(5\text{-}6) \cdot 10^4$ kJ/mole], which proves to be close to the latent heat of vaporization of the monomer ($\sim 4 \cdot 10^4$ kJ/mole).

Similar to this for the PMM, according to R. Chaiken's data, $E=146\cdot10^3$ kJ/mole at low rates of decomposition, and $E=46\cdot10^3$ kJ/mole at high rates.

These values approach respectively to the value of E measured by S. Madorskiy (see [18]) by the isothermal method and to the latent heat of vaporization of the monomer.

In connection with this the assumption was expressed about the fact that at high rates of decomposition the determining link is the evaporation of the monomer from the surface, while at low rates the continually determining link is the reaction of the formation of the monomer, which diffuses then through the mass of the polymer to the surface.

The basic energy characteristic of the process of gasification is the total heat of gasification, i.e., the quantity of heat expended for the warming up and decomposition of 1 kg of the substance:

$$Q_s=Q_s+c_v(T_s-T_0),$$

where Q_s is strictly the heat of the chemical transformations which occur on the surface of the material.

With the calorimetric methods used at present, determined in the experiment is value Q_Σ from which only approximately is it possible to separate the value Q_s. In view of a distinction in the temperature conditions of the experiment and the procedures for conducting it, the obtained characteristics are substantially separated. Thus, for instance, for PMM in work [21] for the calculation of the rate of gasification $Q_\Sigma=1300$ kJ/kg is taken, and in work [34] $Q_\Sigma=1590$ kJ/kg is obtained.

The effective heat of gasification can be considered as the difference in the enthalpies of the polymer at the initial temperature of the charge and vapors of the monomer (basic product of

gasification) at the surface temperature. This approach open/ discloses the possibility of calculated determination of Q_{Σ}.

Since Q_{Σ} is the function of state and does not depend on the means of transformation of the system from the initial state to the final one, for the calculation it is possible to take any sequence of chemical transformations, having selected it such that it would include reliable characteristics.

Since the thermodynamic properties of monomers at high temperatures are well-known, in the majority of the cases for the calculations the following conditional scheme of the process is advisable. The polymer is decomposed to the monomeric liquid state at the initial temperature $T_{н}$ with the latent heat of depolymerization $Q_{деп}$. Then the monomer at this temperature is vaporized with the absorption of the latent heat of vaporization $Q_{исп}$. Further the vapors of the monomer are heated from the initial temperature $T_{н}$ to the surface temperature T_{s}.

In this scheme the effective heat of gasification is calculated as follows:

$$Q_{э}=Q_{деп}+Q_{исп}+I_{м.s}-I_{м.н},$$

where $I_{м\ s}$ is the enthalpy of vapors of the monomer at the surface temperature; $I_{м.н}$ - the enthalpy of vapors of the monomer at the initial temperature of the charge.

3.4.2. Solid Oxidizers

The chemical compounds which can be used as solid oxidizers in the KRD were examined in section 1.3. The majority of them is used as oxidizers of solid rocket propellants. The kinetics of the chemical decomposition of these substances is quite well studied at present.

As regards the solid oxidizers, which from conditions of

chemical incompatibility did not obtain use in the RDTT [PATT - solid-propellant rocket engine], then, unfortunately, in view of the absence of literature data, here it is not possible to examine their kinetic characteristics.

The basic thermophysical characteristics of some solid oxidizers utilized in solid rocket propellants are shown in table 3.5 borrowed from work [25].

In comparison with hydrocarbon fuels, the solid oxidizers are characterized by higher thermal conductivity.

The rate of decomposition of the solid oxidizers over a wide range of temperatures, according to numerous experimental studies, follows the Arrhenius law. Experimental values of pre-exponential factors and activation energy are given in table 3.5.

Table 3.5

Ozidizer	ρ kg/m^3	c $\frac{kJ}{kg \cdot K}$	λ $\frac{kJ}{kg \cdot K}$	a m^2/s	Q_s $\frac{kJ}{kg}$	K_{ms} m/s	E/2R K
Ammonium perchlorate	1950	1.26	0.46	$1.86 \cdot 10^{-7}$	1050	46	10,000
Ammonium nitrate	1720	1.09	0.67	$2.72 \cdot 10^{-7}$	810	120	3,550

Unlike the polymers, the decomposition of solid oxidizers is accompanied by heat liberation.

It is considered that the most probable decomposition reactions of ammonium nitrate are:

$$NH_4NO_3 \rightarrow 2H_2O + N_2O + 75{,}5 \text{ kJ/mole};$$
$$2NH_4NO_3 \rightarrow 4H_2O + N_2 + 2NO + 58{,}6 \text{ kJ/mole}.$$

The value Q_s obtained from experiment given in the table 3.5 is the average of the thermal effects of both reactions.

The typical value of the surface temperature of the gasification of ammonium nitrate is ∿600K.

The process of the gasification of ammonium perchlorate proves to be more complex. Its basic stages are considered as:

1) the endothermic process of decomposition with the formation of NH_3 and $HClO_4$;

2) the exothermic reactions in the solid phase connected with changes in the crystal structure at high temperatures;

3) the exothermic reactions of the interaction of products of gasification with the solid product.

As a whole the process of the gasification of ammonium perchlorate is exothermic. The value of the surface temperature under conditions in the RDTT is ∿1100 K.

3.4.3. Metallized Fuel

The conditions of the organization of the burning of metals, which include, first of all, their heating to the melting point and ignition and also the feed (dispersion) of metallic particles into the gas phase and into the zone or reaction, cause the need for the introduction into the composition of the solid component of the gasifying ingredients. These are usually the hydrocarbon fuels - the binder and mineral oxidizer. Unlike the solid rocket propellants, where these components are basic, in the metallized fuel of the GRD they play an auxiliary role.

When evaluating the necessary content of the gasifying ingredients in the metallized fuel, usually we proceed from the

assumption that the initial stage of the process of burning is the decomposition of the oxidizer and binder and their interaction with the neutral position of the metal, which plays at this stage the role of the heat storage element (thermal flow).

The heating temperature, conditioned by reactions of the interaction of the gasifying components, usually designated by the symbol T*, is used as an estimated criterion of the burning of this fuel composition.

The temperature T*, obtained as a result of the nonequilibrium thermochemical calculation of the system, should not be identified with the surface temperature of the metallized fuel.

In the opinion of a number of researchers (see [17]) in propellants of such type, as a result of the high concentration of metal, there is the tendency toward the formation on the surface of the charge of a continuous film of molten metal. As studies of the burning of some solid rocket propellants show, even with the mass content of aluminum up to 20% the layer of the molten metal almost completely convers the burning surface. This is more probable for compositions with a higher concentration of the metal.

When using hydrides of metals as a solid component, the need to introduce auxiliary gasifying ingredients is eliminated. As a result of the thermal decomposition of hydrides of metals, the hydrogen which ensures the dispersion of the metal is isolated.

Thus, for instance, the thermal decomposition of lithium aluminum hydride occurs without the melting of the initial substance in the temperature range of 125-135°C. The reaction has two stages:

$$1)\ LiAlH_4 \rightarrow LiAlH_2 + H_2;$$
$$2)\ LiAlH_2 \rightarrow LiH + Al + 0{,}5H_2.$$

The second of them is slower. Since the mass concentration of aluminum in the examined case is 67.5%, being isolated as a result of the second reaction, it forms a continuous liquid film on the surface of the charge. The aluminum film is periodically blown away by the hydrogen being formed during decomposition. The periodic feed of aluminum - the basic combustible ingredient - into the combustion zone is supposedly the reason for the low-frequency periodic fluctuations of pressure which were observed in the GRD on the fuel pair $LiAlH_4+H_2O_2$ (see [26]). Fluctuations at a frequency of 9 Hz had an amplitude of +14--7% with respect to the medium pressure in the chamber.

Thus for metallized fuels in the majority of cases the surface of the charge with burning is the fusion of the metal whose temperature in one case proves to be close to T*, and in another case (for hydrides of metals) it is determined by the thermal effect of decomposition reactions.

3.5. Dependence of the Rate of Gasification of the Solid Component on Different Factors

From literature sources several experimental data on the rate of the gasification of solid components of a hybrid rocket propellant (GRT) [ГРТ] obtained by different researchers are known. In a number of cases the experiments pursued a limited purpose: the obtaining of the law of gasification for a definite fuel pair in the narrow range of the operating conditions, which is of practical interest for this engine installation. However, also known are studies of the process of gasifications carried out in a wide plan for the purpose of determining the different factors which affect the rate of gasification with a change in the operating conditions in great range.

G. Maksmen, K. Wooldridge and F. Mazzi (see [21]), for the testing of the model of burning in a turbulent boundary layer proposed by them, conducted experiments on the determination of

parameters of the burning hybrid system "oxygen-polymethylmetacrylate (PMM)." The gaseous oxygen was fed into the combustion chamber from high-pressure cylinders through a controlling valve and flow meter. In the working part of the combustion chamber, after the honeycomb and diffuser, a gas flow with a low turbulence level was provided.

In installation flat specimens of PMM, fastened to the support above the boundary layer which is formed on the lower wall of the tube, were tested. The interruption of the process of gasification was provided by the cessation of the oxygen feed with the subsequent purging of the entire system by nitrogen.

To investigate the processes of combustion which occur in the gas phase, the Schlieren method of photography was used. The average rate of gasification of PMM was calculated by the loss of mass determined by the weighing of the assembly of the plate of PMM with the holder before and after the experiment. The experiments were carried out at atmospheric pressure in the combustion chamber. In experiments in essence the effect of one parameter - mass flow rate G=pv was investigated. A series of the experiments was conducted with a 50% dilution of oxygen by nitrogen.

These researchers conducted the determining of the average rates of gasification of PMM on single-channel cylindrical charges. The rates of gasification were determined from the difference in masses of the specimen before and after the experiment, the average area of the internal surface of the cylinder and the combustion period. All the experiments were carried out at atmospheric pressure. In the investigations the following were varied: the combustion period, the ratio of the length of specimen L to the diameter of channel d and the absolute dimensions of the specimen with the fixed ratio of the length of the specimen to the diameter of the channel.

Results of the experiments are represented on the graph given in figure 3.6.

Results of experiments confirm the dependence of the rate of gasification on the mass flow rate to the power of 0.8. The rate of gasification somewhat decreases with an increase in ratio L/d, which corresponds to its dependence on the Re number calculated along the length of the charge to the power of -0.2.

The certain dependence of the average rate of gasification on the combustion period and absolute dimensions of the specimen is explained by the inadequacy of the experiment. With short times to a great degree the warm-up period of the material (activation time) is affected, and this leads to a reduction in u_{cp}. The charge with the less initial diameter of the channel is characterized by a larger percentage change in the area of the channel, which leads to a reduction in u determined from the average parameters for specimen with less diameter.

T. Hauser and M. Peck (see [38]) were also engaged in the study of the system "oxygen-plexiglass." On cylindrical charges of PMM they determined the rates of the gasification of the material at different distance from the initial cross section at different moments of time. Unlike the foregoing investigations, T. Hauser and M. Peck, in determining the rate of gasification, proceeded by way of differentiation of the experimental dependence in the diameter of the channel on the time obtained with a change in the time of interruption of the process.

Dependence of the radius of channel on time was represented in the form of the polynomial:

$$r = A + Bt^{0.8} + Ct^{0.3},$$

where A, B and C are constants, and the instantaneous values of the rate of gasification were defined as

$$u = \frac{0,8B}{t^{0.2}} + \frac{0,3C}{t^{0.7}}.$$

Furthermore, they took measurements of the surface temperature

of gasification, making it possible to establish the relation of the rate of gasification with the kinetics of the pyrolysis of the PMM.

The obtained data are given in table 3.4. L. Smut and S. Price (see [30]) conducted studies of the dependence of the rate of gasification of nonmetallized solid components of hybrid propellants on the composition of fuel, composition and oxidizer consumption and also on the combustion-chamber pressure.

The combustion-chamber pressure varied from $1.37 \cdot 10^5$ to $12 \cdot 10^5$ Pa. The measured consumption of the gaseous oxidizer fed from the high-pressure cylinders varied from 0.98 g/(cm^2·s) to 11.9 g/(cm^2·s). Specimens of solid fuel took the form of plates. The rate of gasification was determined from the combustion period and data of measurements of specimens by a micrometer before and after the experiment. Rates of combustion were determined for five cross sections of the specimen and were averaged over its length. The total consumption was averaged along the length of the specimen and with respect to time.

Butyl rubber, PBAK (copolymer polybutadiene and acrylic acid) and polyurethane were tested as a solid fuel. It was shown that with the same composition of the oxidizer, the rates of the gasification of all the fuels are virtually identical.

The mixture of fluorine with oxygen was used as an oxidizer. The experiments carried out with a fuel of one composition (100% butyl rubber) and with a different composition of the oxidizer showed that a decrease in the concentration of fluorine in the oxidizer leads to an almost exponential decrease in the rate of gasification (figure 3.10).

With any composition of the oxidizer in the region of its low consumption a change in the rate of gasification with a change in the mass flow rate follows dependence with a power of 0.8.

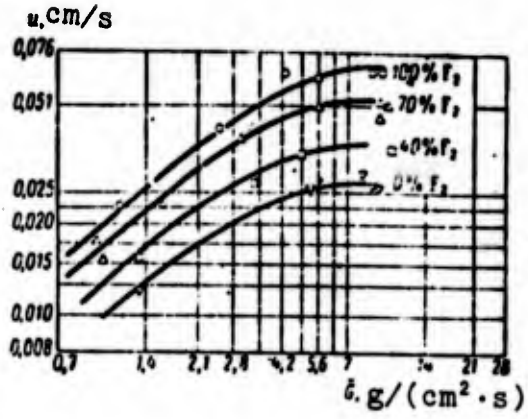

Figure 3.10. Effect of the total mass flow rate and composition of the oxidizer on the rate of gasification of butyl rubber when using a mixture of fluorine and oxygen as the oxidizer. (Nominal pressure is equal to $4.12 \cdot 10^5$ Pa).

The most important moment of the investigations of L. Smut and S. Price is the evaluation of the joint effect of pressure and mass flow rate on the rate of gasification (figure 3.11 and 3.12).

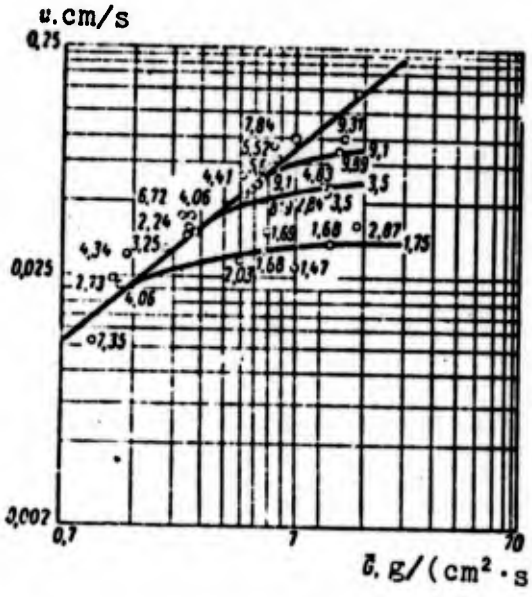

Figure 3.11. Effect of the total mass flow rate and pressure on the rate of gasification of specimens of butyl rubber when using as 100% fluorine as the oxidizer. (Near each experimental point the pressure in $Pa \cdot 10^{-5}$ is shown): □ - data of bench tests of the engine at a combustion-chamber pressure equal to $69 \cdot 10^5$ Pa.

In the region of low values $\overline{G}$ at all pressures, the rate of gasification varies in proportion to the mass flow rate to the power of 0.8. At high values of the mass flow rate the rate of gasification ceases to depend on it. This state more rapidly begins at low pressures in the chamber. At a constant value of $\overline{G}$ the rate of gasification with an increase in the pressure will be increased until the level which corresponds to the dependence of the rate of gasification on $\overline{G}$ to the power of 0.8 is achieved.

With a further increase in pressure it has a very weak effect on the change in the rate of gasification or does not affect it al all.

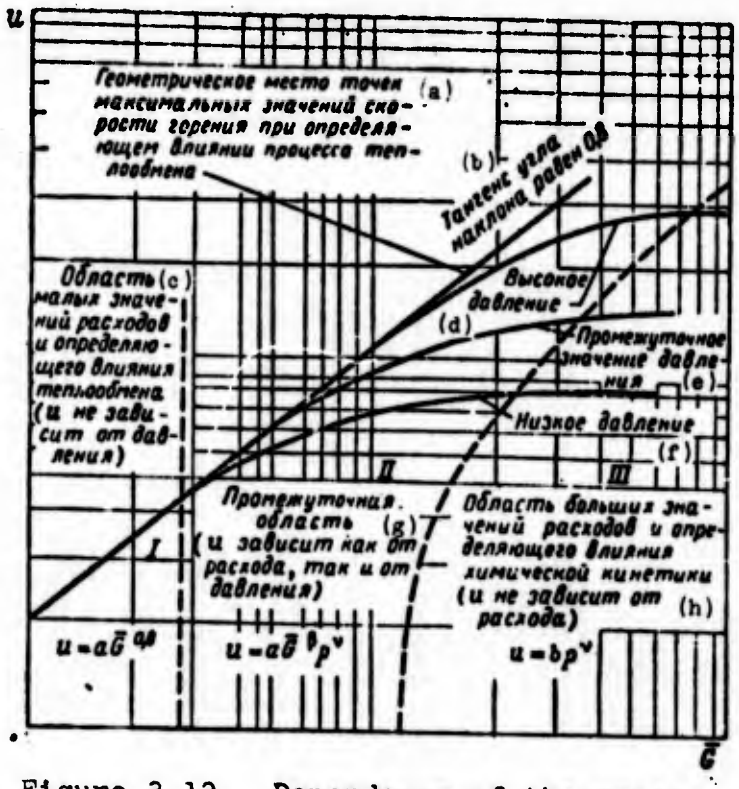

Figure 3.12. Dependence of the rates of gasification of standard nonmetallized hybrid systems on pressure and flow rate. Key: (a) Geometric locus of points of maximum values of the rate of combustion in determining the effect of the process of heat exchange; (b) Slope tangent angle is equal to 0.8; (c) Region of small values of flow rate and determining effect of the heat exchange (and it does not depend on pressure); (d) High pressure; (e) Intermediate pressure value; (f) Low pressure; (g) Intermediate region (and it depends both on the flow rate and pressure); (h) Region of high values of flow rate and the determining effect of chemical kinetics (and it does not depend on flow rate).

Additionally given on figure 3.11 are two values of the rate of gasification obtained during firing tests of an engine operating

on fuel which is 100% butyl rubber at a high combustion chamber pressure ($69 \cdot 10^5$ Pa).

L. Smut and S. Price also conducted studies of the burning of hybrid propellants with a metal-bearing fuel. Used as the fuel were compositions from butyl rubber and lithium hydride with the content of the latter from zero to 90% (see [29]). A mixture of fluorine with oxygen was used as an oxidizer.

During the experiments the effect of different factors on the rate of gasification was studied. It was shown that for the metallized fuels as a whole the law established earlier for carbonic compounds is retained. In the region of low oxidizer flow rates experimental values of the rate of gasification do not depend on pressure and increase iwth an increase in the oxidizer flow rate according to power dependence with the exponent 0.8. In the region of large oxidizer flow rates the rate of gasification does not depend on the flow rate but depends substantially on the pressure (figure 3.13). An increase in the percentage content of the hydride of lithium increases the rate of gasification and decreases its pressure dependence (figure 3.14).

From compositions with the metal-bearing fuel, the fuel pair H_2O_2+$LiAlH_4$ is also well studied. Work [26] gives results of tests carried out on 90% hydrogen peroxide and lithium aluminum hydride with an addition of 5% polyethylene. The solid-propellant charges in the form of cylindrical grains whose diameter is 70 mm and length is 508 mm were manufactured with pressmolding. Gasification of the fuel occurred on the surface of the axial channel.

Tests were carried out on a model engine at a constant oxidizer flow rate and pressures of $7.9 \cdot 10^5$ to $21.5 \cdot 10^5$ Pa. The average rate of the gasification of lithium aluminum hydride was determined from results of the weighing of the charge before and after each testing. In the calculation of rate of combustion, it was assumed that the charge's surface in the process of gasification retains a cylindrical form.

Figure 3.13. Effect of the total specific oxidizer flow rate $\bar{G}$ and pressure on the rate of the burnout of a charge with a composition of 50% butyl rubber +50% LiH (composition of the oxidizer: 30% O_2+70% F_2). (Near each experimental point the pressure in Pa·10^{-5} is shown).
Key: (a) Slope tangent angle of the power dependence is equal to 0.8.

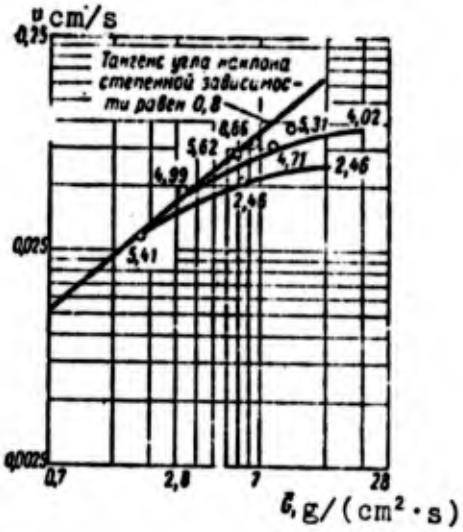

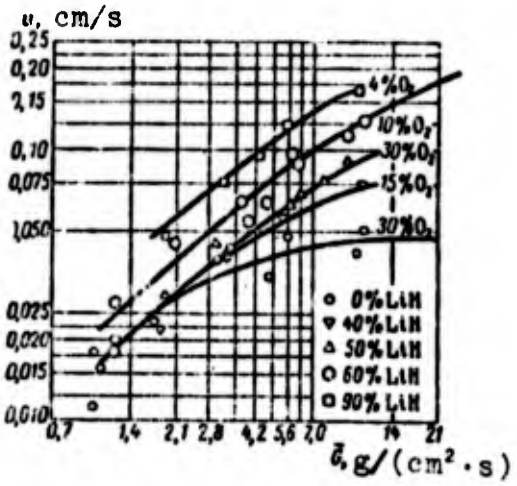

Figure 3.14. Effect of the percentage content of LiH in solid fuel on the rate of its gasification. (Oxidizer is oxygen + fluorine. The oxidizer contains such a quantity of oxygen which is necessary for the oxidation of carbon in the composition of the fuel in CO. All the data are reduced to the pressure of $4.12 \cdot 10^5$ Pa).

The thus obtained law of gasification for this fuel pair takes the following form:

$$u = 33{,}4 \cdot 10^{-4} p_к^{0{,}4} \bar{G}_ж^{0{,}4}.$$

With substitution into this relation of $\bar{G}_ж$ in g/(cm^2·s) and $p_к$ in Pa, the rate of gasification is obtained in mm/s.

The dependence of the rate of gasification of pressure for this fuel pair is considered to be its advantage, since this is desirable for providing the possibility of the control of thrust.

As was noted earlier, an essential shortcoming in contemporary fuel pairs of the GRD is the low rate of gasification of the solid component, involving a number of design difficulties during the designing. Therefore, an increase in the rate of gasification is considered to be one of the urgent problems of the development of the GRD. Let us examine the basic trends in the solution to this problem.

1. *An increase in the heat-transfer coefficient from the gas flow to charge's surface by means of the agitation of the flow.* An example of this solution is a diagram of the engine presented in figure 1.8. In this engine the charge is divided into sections between which throttle washers made of a combustible material are furnished. They can be manufactured from the same material as that of the basic charge. To provide for a simultaneity of the burnout of the material of charge and washers, on the ends of the sections annular grooves are provided. Tests of the model engine made in this design, with the diameter of charge of 70 mm, showed also the possibility of an increase in the combustion efficiency of the propellant: the specific impulse increase from 1970 (standard design) to 2536 N/(kg/s).

2. *The use of porous (grain) charges with the feed of the liquid component through the pores.* The use of porous charges in the opinion of some researchers (see [19] will make it possible to increase the frontal rate of gasification by almost 100 times because of the considerable development of the contact surface of the material.

3. *The use of materials with a low heat of gasification or those which possess an exothermic effect of gasification.*

3.6. Heating of Solid Component With Ignition

For materials the rate of decomposition of which follows the Arrhenius dependence, it is advantageous to examine the process of

heating in the moving coordinate system, the origin of which is connected with the surface of the charge.

The temperature field of the charge is found as a result of the integration of the system of equations

$$a_т \frac{\partial^2 T}{\partial x^2} = \frac{\partial T}{\partial t} - u \frac{\partial T}{\partial x}; \qquad (3.54)$$

$$\varrho u = K_{m_s} \exp(-E/2RT_s);$$

With x=0,
$$-\lambda_т \left(\frac{\partial T_т}{\partial x}\right)_s = -\lambda_т \left(\frac{\partial T_т}{\partial x}\right)_s - \varrho_т u Q_s; \qquad (3.55)$$

with x=∞,
$$T(\infty, t) = T_н;$$

with t=0,
$$T(x, 0) = T_н.$$

Here the first equation of system (3.54) is the equation of the nonstationary thermal conductivity in the moving coordinate system. Equation (3.55) expresses the condition of thermal balance of the charge's surface. The left side of equation (3.55), which is heat flux to the charge's surface q_s, can be expressed also by the effective heat-transfer coefficient α_f:

$$-\lambda_т \left(\frac{\partial T_т}{\partial x}\right)_s = \alpha_f (T_{0г} - T_s),$$

where $T_{0г}$ is the temperature in the flow core of the hot gas.

Figure 3.15 gives a graph of the change in time of the temperature of the surface T_s and rate of gasification with nonstationary heating of the PMM obtained as a result of the numerical integration of the system of equations given above for conditions α_f=2.1 W/(m^2·K); $T_{0г}$=2000K.

As is shown by an analysis of results of the numerical integration of system of equations (3.54)-(3.55) carried out for different materials and conditions of heating, the temperature profile in the material with nonstationary heating is approximated with acceptable accuracy by the exponential

$$T - T_н = (T_s - T_н) e^{-kx}, \qquad (3.56)$$

where h is the coefficient of approximation determined for each moment of time from the boundary condition (3.55) according to formula

$$h = \frac{q_s - \rho u Q_s}{\lambda_T (T_s - T_n)}. \qquad (3.57)$$

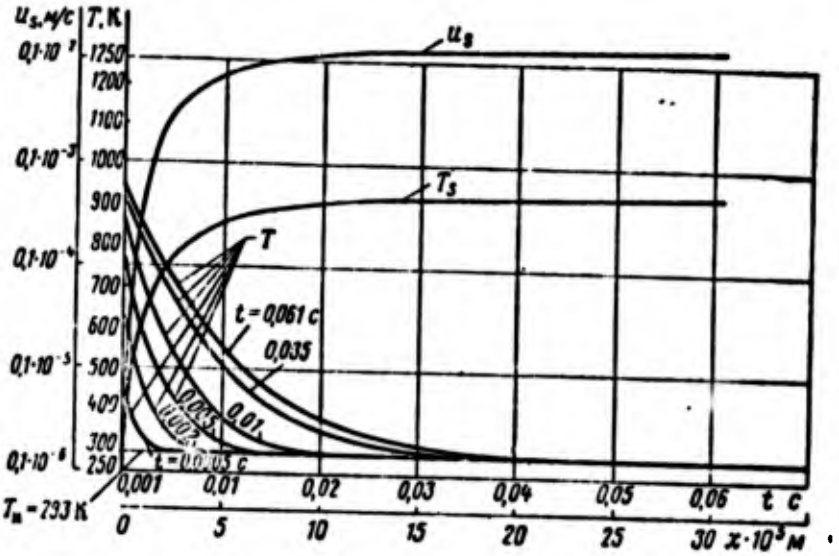

Figure 3.15. Change in temperature and rate of the removal of the solid component (rate of gasification) with heating.
Appreviation: м/с=m/s; м=m

For a comparison figure 3.16 gives two temperature profiles in the PMM calculated for the same moment of time ($t=1\cdot10^{-4}$ s) correspondingly by the integration of the system of equations (3.54) (configuration I) and by formula (3.56) (configuration II) with the starting data indicated in the caption to figure 3.16. The error of the approximation does not exceed 10%.

The solution based on the joint integration of equations (3.53), (3.54) and (3.55) is bulky and laborious.

Let us examine the possibilities of obtaining the approximate solution which allows with minimum expenditures at least estimating tentatively the time of the nonstationary heating of the charge and its relation with the determining parameters of the process.

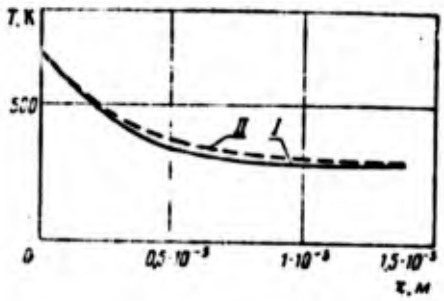

Figure 3.16. Temperature configuration in the charge of the solid component with nonstationary heating $T_н$=293 K; T_s=683.9 K; $T_{0г}$=2000 K; $\alpha_г$=2.1 W/(m²·K); t=0.0001 s): ——— - precise calculation; ---- approximation according to equation (3.56).

For the initial most prolonged stage of the period of ignition, in view of the low temperature of the charge's surface, the limiting "narrow" place of the process is the kinetics of the pyrolysis of the solid component. The rate of gasification remains low until the temperature of the surface achieves a certain value of T_s^*, which corresponds to the beginning of the steep segment of the Arrhenius curve (figure 3.17). Temperature T_s^* in the first approximation is defined as the point of intersection with the horizontal axis tangent to the Arrhenius curve at the point of its bend. In accordance with this, the temperature is defined from relations (3.53) at T_s^*=E/8R.

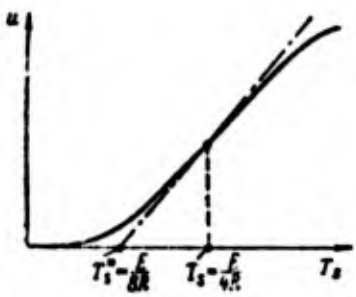

Figure 3.17

At the low rates of gasification the temperature field of the charge can be calculated from the standard relations of the nonstationary thermal conductivity for a semi-infinite body.

In the simplest case, with constant heat flux to the surface q_s, the distribution of temperature in the charge for an arbitrary moment of time t is expressed by the formula

$$T=T_н+\frac{2q_s}{\lambda_з}\sqrt{a_з t}\,\mathrm{ierfc}\left(\frac{x}{2\sqrt{a_з t}}\right), \qquad (3.58)$$

where ierfc is the integral of the function of Gauss errors with the argument

$$\left(\frac{x}{2\sqrt{a_з t}}\right).$$

In the first rough approximation the time necessary for establishing the steady state of the gasification can be taken equal to the time of heating of the inert material (without gasification) up to the establishment on its surface of temperature T_s^*.

According to relation (3.58) with x=0 this time is equal to

$$t = \frac{(T_s^* - T_n)^2 \lambda_T c_T \rho_T}{1{,}227 q_s^2}.$$

CHAPTER 4

SELECTION OF THE BASIC PARAMETERS OF COMBUSTION CHAMBER OF A COMBINED ROCKET ENGINE

Examined in this chapter in a general setting is the selection of the basic working parameters of the combustion chamber of the KRD [КРД - combined rocket engine] in the stage of the ballistic design when in the first approximation the mass and overall characteristics of the flight vehicle with this engine are determined.

The basis of the solution to this problem consists of:

a) relations for the rate of gasification of the solid component;

b) relations which connect the pressure in the chamber with the parameters of loading and conditions of the feed of the second component;

c) geometric characteristics of the charge.

As a result of the solution the basic dimensions of the chamber and charge should be determined, and these provide:

a) the arrangement in the chamber of the assigned reserve of the solid component;

b) the necessary surface of gasification which determines the

assigned consumption of the fuel and, consequently, the thrust of the engine;

c) the necessary operating time of the engine determined by the full time of gasification of the solid component.

As a basic type of the combustion chamber of the KRD is accepted the chamber with the surface of gasification of the solid component placed along the continuous axial gas channel. This type of the chamber includes both versions with the fastened charges - with gasification over the surface of the internal channels and the freely insertable charges - and with gasification also over the external surface.

In view of the fact that the rate of gasification with diffusion burning in a GRD [ГРД - hybrid rocket engine] increases in the direction of motion of the gas flow, in a number of cases it can appear advisable to make a charge with the thickness of the arch variable over its length in order to avoid the formation during gasification of degressive residues. The required profile of the channel in such cases can be established in the stage of the final working out of the charge.

In the stage of the ballistic design in all cases in determining the basic dimensions of the charge and parameters of the combustion chamber, it is possible to assume that the area of the free cross section of the chamber is constant over the entire length of the charge. Based on this assumption are the relations given below.

4.1. THE RATE OF GASIFICATION AVERAGE OVER LENGTH OF THE CHARGE AND FLOW RATE OF THE SOLID COMPONENT

The rate of the gasification of the solid component is an important characteristic of operating conditions of the KRD which

determines the parameters of interior ballistics and the output engine characteristics, which conditions the selection of the dimensions of the charge, and consequently, the masses and overall dimensions of the product.

The rate of gasification is changed along the length of the charge, increasing along the direction toward the engine nozzle. In the first stage of the ballistic design, in the determining of the basic dimensions of the charge and combustion chamber it is advantageous to use the rate of gasification averaged along the length of the charge L:

$$u_{cp}=\frac{1}{L}\int_0^L u dl.$$

Let us derive the relation for determining u_{cp}. Let us isolate, along the length of the channel of the charge, the elementary section with length dl, which is remote from the initial end of the charge at distance l (figure 4.1).

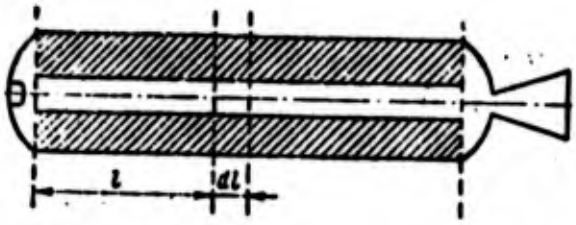

Figure 4.1

The arrival of gases in this section will be

$$dG=\rho_T \Pi_l u dl, \qquad (4.1)$$

where Π_l is the perimeter of gasification.

Let us use the simplified expression for the rate of gasification:

$$u=u_1\left(\frac{G}{F_{kr}}\right)^{\nu} p_k^{n}, \qquad (4.2)$$

where G is the local value of the flow rate of gases; $p_н$ - the pressure in the chamber taken constant along the length of the charge; $F_н$ - the cross-sectional area of the channel of the charge, assumed to be constant along the length of the charge.

Having substituted equation (4.2) into (4.1), after the separation of variables and integration, we obtain

$$L\Pi_т\varrho_т u_1 p_к^{\nu} F_к^{-\beta} = \frac{1}{1-\beta}\left(G_Σ^{1-\beta} - G_{ж.г}^{1-\beta}\right). \qquad (4.3)$$

Integration is realized within these limits: according to variable l - from zero to L, according to the variable G - from $G_{ж.г}$ (flow rate of the liquid component fed into the head part of the chamber) to $G_Σ$ (total flow rate of gases at the end of the charge).

From equation (4.3) we find the per-second flow rate of the solid component:

$$G_т = \left[(1-\zeta)u_1\varrho_т \frac{\Pi_г}{F_к^{\beta}} L p_к^{\nu} + G_{ж.г}^{1-\beta}\right]^{\frac{1}{1-\beta}} - G_{ж.г}. \qquad (4.4)$$

For a channel of cylindrical form with a diameter d, this relation takes the following form:

$$G_т = \left[4^{\beta}\pi^{1-\beta}(1-\zeta)u_1\varrho_т L d^{1-2\beta} p_к^{\nu} + G_{ж.г}^{1-\beta}\right]^{\frac{1}{1-\beta}} - G_{ж.г} \qquad (4.5)$$

Equation (4.3) can be rewritten in the form

$$\Pi_т\varrho_т u_1 p_к^{\nu} L\left(\frac{G_{ж.г}}{F_к}\right)^{\beta} = \frac{G_{ж.г}}{1-\beta}\left[\left(\frac{G_Σ}{G_{ж.г}}\right)^{1-\beta} - 1\right]. \qquad (4.6)$$

By applying for the relationship of the flow rates of the components the following notations:

$$\phi = \frac{G_т}{G_Σ};\quad K = \frac{G_ж}{G_т} = \frac{1-\psi}{\psi},$$

we obtain

$$G_{ж}=\frac{1-\psi}{\psi}G_{г};\quad \frac{G_{г}}{G_{ж}}=\frac{1}{1-\psi}.$$

Let us denote

$$\bar{u}_{ж}=u_{1}p^{*}\left(\frac{G_{ж.г}}{F_{к}}\right)^{\beta}. \qquad (4.7)$$

Obviously $\bar{u}_{ж}$ is the rate of the gasification of solid component determined according to the flow rate of the liquid component fed into the head part of the chamber.

By introducing (4.7) into equation (4.6), and after expressing the flow rate of the solid component by the rate of its gasification averaged along the length of the charge $G_{т}=\rho_{т}\Pi_{т}Lu_{ср}$, we obtain the expression for determining $u_{ср}$:

$$u_{ср}=\bar{u}_{ж}\frac{\psi}{1-\psi}(1-\beta)\frac{1}{\left(\frac{1}{1-\psi}\right)^{1-\beta}-1}. \qquad (4.8)$$

Let us present the obtained relation in the form

$$u_{ср}=\bar{u}_{ж}K(\beta,\ \psi), \qquad (4.9)$$

where $K(\beta,\ \psi)$ is the function determined only by the relationship of the flow rates of the components and by index β:

$$K(\beta,\ \psi)=\frac{\psi}{1-\psi}(1-\beta)\times \\ \times\frac{1}{\left(\frac{1}{1-\psi}\right)^{1-\beta}-1}. \qquad (4.10)$$

Numerical values of function $K(\beta,\ \psi)$ are represented in the form of families of curves in figure 4.2. As follows from these curves, at small values of ψ ($\psi<0.2$-0.3), characteristic for the fuel pairs of a GRD of direct design, the value of this function

proves to be very close to unity. In this case with sufficient practical accuracy, it is possible to take $u_{ср}=\bar{u}_{ж}$. In the remaining cases one should use the correcting factor $K(\beta, \psi)$.

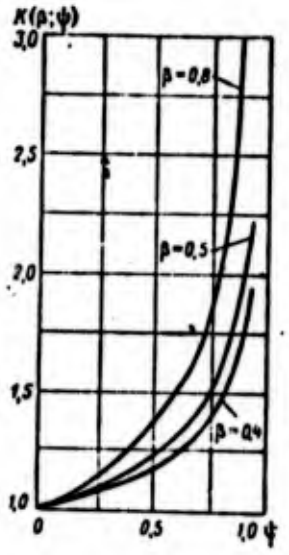

Fig. 4.2

As will be shown further, instead of $u_{ср}$ the use of value $\bar{u}_{ж}$ or $\bar{u}_{ж}K(\beta, \psi)$ virtually equal to it substantially simplifies the solution to the problems of ballistic design.

4.2. RELATION OF THE WORKING AND CALCULATED COMBUSTION-CHAMBER PRESSURES OF THE KRD WITH PARAMETERS OF LOADING

In the connecting of the basic design characteristics of the KRD with its thrust parameters in the stage of ballistic design, we proceed from the medium working combustion-chamber pressure of the engine $p_к$ assumed to be constant in volume of the chamber.

The value $p_к$ in the steady-state engine operating conditions is determined by the flow rate of gases through the nozzle G_Σ, the nozzle throat area $F_{кр}$ and the characteristics of combustion products of the fuel, i.e., R, T_0, and k.

The flow rate of gases through the nozzles is equal to

$$G_г = A p_к F_к, \qquad (4.11)$$

where the discharge coefficient A is determined from the expression

$$A = \frac{\varphi_c}{\sqrt{RT_0}} \left(\frac{2}{k+1}\right)^{\frac{1}{k-1}} \sqrt{\frac{2k}{k+1}}.$$

The total mass flow rate of the gases can be represented also in the form

$$G_г = G_ж + G_т = G_ж + \varrho_т \Pi_т L u_{ср}. \qquad (4.12)$$

By equating the right sides of equations (4.11) and (4.12) and using relation (4.9), we obtain the following expression for the coefficient ψ:

$$\psi = \frac{G_т}{G_г} = \frac{u_1 p_к^n \left(\frac{\varphi G_ж}{F_к}\right)^{\beta} A^{-\alpha} \Pi_т L \varrho_т}{A p_к F_{кр}}, \qquad (4.13)$$

where $\phi = G_{ж.п}/G_ж$ is the coefficient which considers the feed of the liquid component into the pre-nozzle volume behind the charge. If double admission is not applied, $\phi = 1$.

Let us introduce the following notations:

$$\frac{F_к}{F_{кр}} = K_c; \quad \frac{\Pi_т L}{F_к} = \varkappa.$$

By using these notations, and also taking into account that $G_ж = G_Σ(1-\psi)$, we obtain

$$p_к = \left[\frac{\psi}{(1-\psi)^{\beta} \varphi^{\beta}} \frac{A^{1+\alpha-\beta}}{u_1 \varrho_т \varkappa K_c^{1-\beta}}\right]^{\frac{1}{n+\beta-1}}. \qquad (4.14)$$

The obtained equation expresses the interconnection between the working pressure, the relationship of flow rates of the components and the geometric parameters of the engine at the assigned propellant properties.

In actuality, the pressure along the length of the chamber is variable: its highest value is observed in the front part of the engine. The pressure differential along the length of the charge will be greater, the higher the rate of the gas flow in the final cross section of the charge. This fact should be considered in determining the calculated pressure, according to which the required wall thickness of the chamber is calculated, and also in the calculation of the charge for strength.

In order to determine the maximum combustion chamber pressure in its front base, let us examine the change in the gas-dynamic flow parameters along the charge in the section limited by its end cross sections "г" (head part) and "с."

For the channel of constant cross section the full momentum of the gas flow is constant:

$$Gv+pF=\text{const.}$$

This equality can be presented in the form

$$Gv+pF=\frac{pF}{r(\lambda)}=\text{const,} \qquad (4.15)$$

where $r(\lambda)=\frac{1-\frac{k-1}{k+1}\lambda^2}{1+\lambda^2}$ is tabular gas-dynamic function; $\lambda=\frac{v}{a_{кр}}$ - the dimensionless rate;

$$a_{кр}=\sqrt{\frac{2k}{k+1}RT_0};$$

k - adiabatic index; R - gas constant; T_0 - stagnation temperature of the gas flow in the examined cross section.

By utilizing the transform of B. M. Kiselev, the equality of the full momentum of flow for the two extreme cross sections of the charge can be written in the form

$$G_{ж.г}\frac{k_г+1}{2k_г}a_{кр.г}z(\lambda_г)=G_c\frac{k_c+1}{2k_c}a_{кр.c}z(\lambda_c),$$

where

$$z(\lambda)=\lambda+\frac{1}{\lambda}.$$

Having divided both sides of the equality by the complex with $z(\lambda_г)$, after elementary transforms we will obtain

$$z(\lambda_г)=\sqrt{\frac{k_c+1}{k_c}\frac{k_г}{k_г+1}\frac{R_c}{R_г}}\frac{G_c}{G_{ж.г}}\sqrt{\frac{T_{0c}}{T_{0г}}}z(\lambda_c). \qquad (4.16)$$

The complex of the thermodynamic characteristics with $z(\lambda_c)$ in the solution to the gas-dynamic problem is assumed to be known, since these characteristics are the result of the thermodynamic calculation of the engine.

It is necessary to add to the examined relation the flow equation for the finite cross section of the charge presented in the form

$$G_c=\sqrt{k_c\left(\frac{2}{k_c+1}\right)^{\frac{k+1}{k-1}}\frac{1}{RT_{0c}}}y(\lambda_c)p_cF_ж, \qquad (4.17)$$

where $y(\lambda_c)=\left(\frac{k+1}{2}\right)^{\frac{1}{k-1}}\frac{\lambda_c}{\sqrt{1-\frac{k-1}{k+1}\lambda_c^2}}$ is the tabular gas-dynamic function.

The calculation of pressure in the front part of the engine with the use of the relation given above is produced in the following order:

1. By taking the pressure in pre-nozzle volume and in the finite cross section of the charge equal to the assigned working pressure $p_н$, from equation (4.17) for the assigned magnitude of flow rate G_c and the taken area of channel $F_н$, we find the value of the gas-dynamic function $y(\lambda_c)$, and then from tables of this function we determine the value of argument λ_c corresponding to it.

2. From equation (4.16), with the known thermodynamic characteristics of the fuel combustion products and products of gasification of the liquid component, in terms of the found value of $z(\lambda_c)$ we calculate the value of $z(\lambda_г)$, and then according to it we determine the value of $\lambda_г$ and $r(\lambda_г)$.

3. From equation (4.15), we find the pressure in the front part of the engine equal to

$$p_г = p_к \frac{r(\lambda_г)}{r(\lambda_c)}. \qquad (4.18)$$

The calculation is greatly simplified when using tables of gas-dynamic functions [12].

The change in the dimensionless rate λ in the cylindrical channel of the charge described by relation (4.16) is the result of two forms of the effect: thermal, expressed by the ratio of temperatures $T_{0c}/T_{0г}$, and flow, expressed by the ratio of flow rate $G_c/G_г$, which with the one-way feed of the liquid component is equal to $1/(1-\psi)$.

Figure 4.3 depicts the dependence of the relative pressure differential along the length of the charge at a fixed value of λ_c calculated for three fuel pairs.

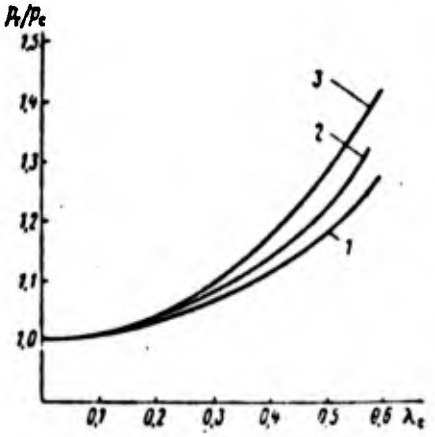

Figure 4.3. Dependence of the relative pressure differential along the length of the combustion chamber of GRD on the dimensionless rate in the finite cross section of the charge: 1 - $(C_2H_4)_x+H_2O_2$; 2 - Li Al $H_4+H_2O_2$; 3 - Li Al $H_4+NO_2Cl\ O_4$.

The fuel pair 1 characterizes the fuel compositions of a GRD of direct design with a small content of the solid component. In this case virtually only the temperature effect is exhibited, and the relative change in pressure does not exceed 25-28% of its value in pre-nozzle volume.

The fuel pair 3 characterizes the fuel compositions of a GRD of reverse design. In this case the temperature effect is supplemented by high flow-rate effect on the flow, in consequence of which the pressure differentials in the examined range λ_c increase to 42%.

The curves for the fuel pair 2, which characterizes the fuel compositions of the GRD of direct design with a high value of ψ, occupy an intermediate position on the graph.

With the simplest approach to the determining of the strength of the chamber casing, the calculated pressure is determined as follows:

$$p_{расч} = \varphi_p p_к$$

where ϕ_p is the safety factor.

4.3. BASIC FORMS OF CHARGES FOR THE KRD AND THEIR CHARACTERISTIC OF PROGRESSIVENESS

A charge of the solid component should have a form which ensures the necessary change in the gas inflow during engine operation in order to obtain the law of the change in thrust required by the assigned flight conditions of the flight vehicle.

When selecting the form of the charge in the GRD, it is necessary to keep in mind that the rate of gasification of the majority of the solid-propellant components is small and comprises,

under conditions common for the GRD, 1-5 mm/s. Because of this the charges of the GRD have little thickness of the burning arch and the extended surface of gasification.

Amother important fact which must be considered when selecting the form of the charge is the need for thermal protection of walls of the combustion chamber, which is reached most simply by the use of charges fastened to the chamber casing. In this case gasification of the sclid component occurs only over the surface of internal channels of the charge.

It is necessary also that the shape of the charge would exclude the formation of the degressive residues remaining after the gasification of the basic mass of the charge, i.e., after the burn-up of the arch thickness e_1, which is the shortest distance from the internal to tne external surface of the charge.

Let us note that in the GRD the effect of the geometry of the charge on the operating engine characteristics proves to be more complex than that in the RDTT [РДТТ - solid-propellant rocket engine), where in essence it is reduced to a change in the burning surface of the solid fuel.

In the RDTT the characteristic of progressiveness of the shape of charge is $\sigma=S/S_0$ - the ratio of the current value of burning area to the initial value. This ratio, irrespective of the propellant properties, determines the progressiveness of burning of the charge.

According to the relation (4.14), the nature of the pressure change in the chamber of the GRD and the relationship of flow rates of the components ψ during the operation is determined by the geometric complex

$$\varkappa K_c^{1-\beta}=\frac{\pi_1 L}{F_{\kappa}^{\beta}F_{\kappa p}^{1-\beta}}.$$

The relative change in this complex with time when $F_{кр}$=const is expressed by the characteristic

$$\Gamma = \frac{\bar{\Pi}_г}{\bar{F}_к^{\beta}}, \qquad (4.19)$$

where

$$\bar{\Pi}_г = \frac{\Pi_г}{\Pi_{г0}}; \quad \bar{F}_к = \frac{F_к}{F_{к0}};$$

$\Pi_{г0}$ and $F_{к0}$ are values of parameters which correspond to the beginning of burning.

The characteristic Γ is considered to be the effect of the relative change with time of both the surface of gasification and the flow passage cross-sectional area, which affects by the specific mass flow rate the rate of gasification.

Consequently, in the GRD the characteristic of progressiveness, together with the geometric parameters of the charge, includes the exponent β which reflects the properties of the fuel and features of the process of burning.

If the value Γ increases according to the operating time of the engine, then this means that under conditions of constant pressure or constant flow rate of the liquid component the relationship of the flow rates of components, which is realized in the burning process, is displaced (in the absence of double admission) to the side of an increase in the flow rate of the solid component.

In the examination of characteristics of progressiveness of the charge, it is advantageous to take the value $z=e/e_1$ as the conditional time scale, where e is the thickness of the layer which is subjected to gasification by this moment in time; e_1 - arch thickness, i.e., the minimum dimensions of the charge which determines the time of gasification of the basic mass of the solid component.

Thus the functional dependence of the value of Γ on z is the most important criterion when selecting the shape of the charge for the GRD.

Charges of the second chamber of the RDTT of separate loading (RDTT RS [PC - rocket missile]) have the same requirements as do charges for the GRD. This eliminates the need for examining the shape of such charges separately. As regards the charges of the first chamber of the RDTT RS, in shape they correspond to charges of the RDTT whose characteristics are very thoroughly discussed in literature on engines of this type.

Examined below are properties of some shape of charges which are of interest for the KRD.

4.3.1. Charge With an Axial Cylindrical Channel

The basic advantages of this charge should be the simplicity of its final working out and manufacture, the full protection of the chamber walls from heating during the entire operating time of the engine, and also the minimum quantity of degressive residues.

Let us examine the characteristic Γ for this charge. For it

$$\Pi_r = \Pi d;\ F_k = \frac{\pi d^2}{4};\ \Gamma = \bar{d}^{1-2\theta},$$

where $\bar{d}=d/d_0$.

Since $d=d_0+2e$, $e_1=(D-d)/2$, we obtain the following relation which connects $\bar{d}$ with z:

$$\bar{d} = 1 + \frac{2z}{(1/\bar{e}_1)-2}, \qquad (4.20)$$

where D is the external diameter of the charge;

$$\bar{e}_1 = e_1/D.$$

For this charge under the conditions of constant pressure with $\beta=0.5$ and $\Gamma=1$, ratio ψ is maintained constant; with $\beta<0.5$ in proportion to the height of the channel Γ is increased, and the relative flow rate of the solid component is increased. With $\beta<0.5$ the value of Γ is decreased, and ψ is decreased.

Results of the calculations for $\beta=0.4$ and 0.8 are represented in figure 4.4. As follows from these curves, the examined shape of the charge provides a relatively small change in Γ with $\bar{e}_1<0.2$ in the interval of the examined values β. For $\beta=0.4$ an increase in Γ in the process of gasification of the charge does not exceed 11%. When $\beta=0.8$ with $\bar{e}_1=0.2$ the maximum reduction of Γ is 27%.

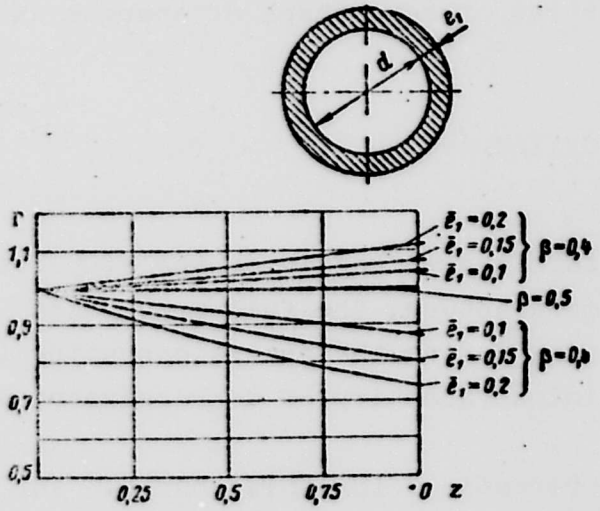

Figure 4.4. The change in Γ depending on z for a charge with an axial cylindrical channel.

A considerable shortcoming in this charge is the relatively small surface of gasification, which causes, in turn, the low removal of thrust from the midsection of the engine.

4.3.2. Cylindrical Two-Channel Charge (Figure 4.5)

This shape of the charge is obtained with separation of the axial cylindrical channel by the diametric cross connection with

a thickness of $2e_1$. By retaining the basic advantages of the charge with the cylindrical channel, this charge possesses a considerably larger surface of gasification (see [47]).

Let us give the basic relation for the calculation of the geometric characteristics of this charge.

The perimeter of the surface of gasification is equal to

$$\Pi_r = 4D\left[0{,}5-\bar{e}_1(1-z)\right]\left[0{,}0175\arccos\frac{\bar{e}_1(1-z)}{0{,}5-\bar{e}_1(1-z)}+\right.$$
$$\left.+\frac{\sqrt{0{,}25-\bar{e}_1(1-z)}}{0{,}5-\bar{e}_1(1-z)}\right], \qquad (4.21)$$

where the arc cos must be taken in degrees.

The flow passage cross-sectional area of the channels is equal to

$$F_к = D^2\left[0{,}5-\bar{e}_1(1-z)\right]^2\left[0{,}01745\arccos\frac{\bar{e}_1(1-z)}{0{,}5-\bar{e}_1(1-z)}-\right.$$
$$\left.-\frac{2\bar{e}_1(1-z)\sqrt{0{,}25-\bar{e}_1(1-z)}}{\left[0{,}5-\bar{e}_1(1-z)\right]^2}\right]. \qquad (4.22)$$

The calculated values of the characteristic Γ for this charge at different values of $\bar{e}_1$ and β are given in figure 4.5.

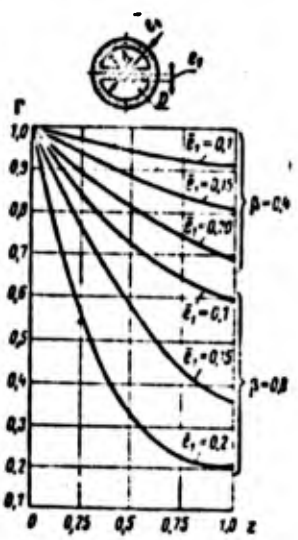

Figure 4.5. Change in Γ depending on z for a cylindrical two-channel charge.

4.3.3. Cylindrical Four-Channel Charge
(Figure 4.6 of Work [68])

Let us give the basic relation for the calculation of the geometric characteristics of this charge.

The perimeter of the surface of gasification is equal to

$$\Pi_r = 4D\left\{0{,}01745\,[0{,}5-\bar{e}_1(1-z)]\left[90^\circ-2\arcsin\frac{\bar{e}_1(1-z)}{0{,}5-\bar{e}_1(1-z)}\right]+\right.$$
$$\left.+2\left[\sqrt{0{,}25-\bar{e}_1(1-z)}-\bar{e}_1(1-z)\right]\right\}. \qquad (4.23)$$

Flow passage cross-sectional area of the channels is equal to

$$F_k = 4D^2\left\{0{,}00873\,[0{,}5-\bar{e}_1(1-z)]^2\left[90^\circ-2\arcsin\frac{\bar{e}_1(1-z)}{0{,}5-\bar{e}_1(1-z)}\right]-\right.$$
$$\left.-\bar{e}_1(1-z)\left[\sqrt{0{,}25-\bar{e}_1(1-z)}-\bar{e}_1(1-z)\right]\right\}, \qquad (4.24)$$

where z varies within limits of zero to one.

The calculated values of the characteristic Γ for this charge at different values of $\bar{e}_1$ and β are given in figure 4.6.

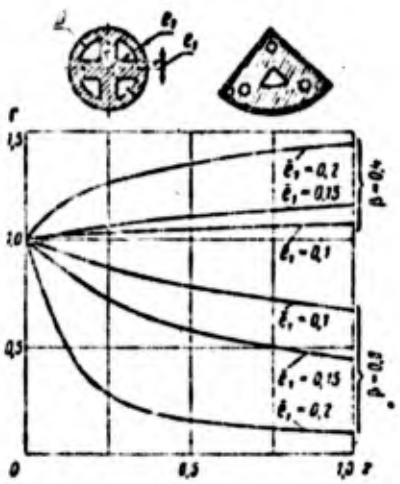

Figure 4.6. Change in Γ depending on z for a cylindrical four-channel charge.

Shortcomings in the charges of the last two shapes should include the formation of degressive residues due to rounding in

the process of gasification of acute angles of the contour. The mass of degressive residues can be reduced to a minimum by the fulfilment of supplementary channels with the optimum selection of their diameters and arrangement on the cross section of the charge.

Figure 4.6 shows one of the separately manufactured sectors of a four-channel charge, having three supplementary channels of larger diameter and two channels of smaller diameter.

4.4. SELECTION OF DIMENSIONS AND PARAMETERS OF LOADING OF THE COMBUSTION CHAMBER OF A GRD

The selection of dimensions and parameters of loading of the combustion chamber of a GRD is conducted on the basis of the assigned: operating time of the engine τ, its thrust P or thrust-to-weight ratio η and mass of the charge of the solid component ω_τ. Together with the provision for the assigned values of these parameters, in the design one attempts to obtain the minimum mass of the design of the combustion chamber.

The basic relation considered below can be used both for the fastened charges which are gasified over the surface of the internal channels and for the freely insertable elements which are gasified over the external surface.

The total operating time of the engine τ is defined as the time necessary for the complete burnout of the solid component under the assigned law of a change in the feed of the liquid-propellant component.

As a fundamental characteristic of loading it is possible to use the loading factor of the cross section of the chamber with the charge used in the design of the RDTT (see [42]):

$$\varepsilon = S_\tau / F_{\text{н.с.}} \qquad (4.25)$$

where $S_т$ is the current value of the cross-sectional area of the charge; $F_{к.с}$ - the cross-sectional area of the chamber.

The mass of the charge of the solid component is defined as

$$m_т = \rho_т F_{к.с} \varepsilon_0 L n. \tag{4.26}$$

The selection of the initial value of the parameter $\varepsilon_0 = S_{т0}/F_{к.с}$, the diameter of the chamber $D_{к.с}$, the number of the chambers n and the length of the large L with its taken shape comprise the content of the stated problem.

Let us examine the relation between the parameters of loading ε_0 and the total operating time of the engine τ with the assigned diameter of the combustion chamber $D_{к.с}$. To establish this relation we use the elementary relation

$$-F_{к.с} d\varepsilon = \Pi(\varepsilon) u dt, \tag{4.27}$$

where $\Pi(\varepsilon)$ is the current value of the perimeter of burning examined for the charge of the taken shape as the single-valued function of the current value ε; u - the current value of the rate of gasification.

Hence the total operating time will be determined as follows:

$$\tau = -\int_{\varepsilon_0}^{0} \frac{F_{к.с} d\varepsilon}{\Pi(\varepsilon) u}. \tag{4.28}$$

In the solution to this problem we use the rate of gasification averaged along the length of the charge, determined by relation (4.9), which can be presented in the form

$$u = u_1 \left[\frac{G_{к.г}}{F_{к.с}(1-\varepsilon)}\right]^{\nu} p_к^{\nu} K(\vartheta, \psi). \tag{4.29}$$

By substituting equation (4.29) into (4.28), we obtain

$$\tau = -\frac{F_{к.с}^{1+\beta}}{u_1} \int_{\varepsilon_0}^{0} \frac{(1-\varepsilon)^{\beta} d\varepsilon}{\Pi(\varepsilon) G_{ж.г}^{\beta} p_к^{n} K(\beta, \psi)}. \qquad (4.30)$$

The values $G_{ж.г}$ and $p_к$ entering into the integrand in general should be considered as time variables connected with the change ε. The dependence $\Pi(\varepsilon)$ is determined by the shape of the charge.

In the simplest case for a charge with a cylindrical channel which burns from within, $\Pi=\pi d$. Since for this charge

$$\varepsilon = \frac{D_{к.с}^2 - d^2}{D_{к.с}^2}, \qquad (4.31)$$

then

$$d = D_{к.с}\sqrt{1-\varepsilon};$$
$$\Pi(\varepsilon) = \pi D_{к.с}\sqrt{1-\varepsilon}, \qquad (4.32)$$

where d is the current diameter of the channel.

Consequently, for a charge with a cylindrical channel

$$\tau = -\frac{F_{к.с}^{1+\beta}}{u_1 \pi D_{к.с}} \int_{\varepsilon_0}^{0} \frac{(1-\varepsilon)^{\beta-0.5} d\varepsilon}{G_{ж.г}^{\beta} p_к^{n} K(\beta, \psi)}. \qquad (4.33)$$

Let us examine the basic cases of the calculation of this charge, which correspond to the standard operational modes of the GRD.

Case I. *Engine operation with a constant flow rate of the liquid component* ($G_{ж}$=const) *fed only through the injection head, with* ν=0 *(pure diffusion burning).*

Assuming that for the process $K(\beta, \psi) \approx$ const, from equation (4.33) we obtain

$$\tau = \frac{1}{\beta + 0.5} \frac{F_{к.с}^{1+\beta}}{\pi D_{к.с} u_1 G_{ж}^{\beta}} \frac{1-(1-\varepsilon_0)^{\beta+0.5}}{K(\beta, \psi)}. \qquad (4.34)$$

Since $u_1=\frac{G_{\text{т}}^{\beta}K(\beta,\psi)}{F_{\text{к.с}}^{\beta}}=u_{\text{к}}$ is the rate of the gasification of the solid component, which corresponds to the end of the engine operation, equation (4.34) can be given the following form:

$$\tau=\frac{1}{\beta+0,5}\frac{D_{\text{к.с}}}{4u_{\text{к}}}\left[1-(1-\varepsilon_0)^{\beta+0,5}\right]. \qquad (4.34a)$$

With $\beta=0.5$ $\tau=\frac{D_{\text{к.с}}\varepsilon_0}{4u_{\text{к}}}$. (4.34b)

According to equation (4.29), the rates of gasification of the solid component at the beginning and end of the engine operations are connected by the relation

$$\frac{u_0}{u_{\text{к}}}=\frac{1}{(1-\varepsilon_0)^{\beta}}, \qquad (4.35)$$

and for the intermediate value ε

$$\frac{u_0}{u}=\left(\frac{1-\varepsilon}{1-\varepsilon_0}\right)^{\beta}. \qquad (4.36)$$

The relative change in the flow rate of the solid component in the process of the engine operation is determined as follows:

$$\frac{G_{\text{т}}}{G_{\text{т}0}}=\frac{ud}{u_0d_0}=\left(\frac{1-\varepsilon_0}{1-\varepsilon}\right)^{\beta-0,5}. \qquad (4.37)$$

The maximum deviation of the flow rate of the solid component from its initial value, occurring at the end of the engine operation, will be

$$\frac{G_{\text{т.к}}}{G_{\text{т}0}}=(1-\varepsilon_0)^{\beta-0,5}. \qquad (4.38)$$

For fuel pairs which have the exponent in the law of burning $\beta>0.5$, the flow rate of the solid component in the process of burning is decreased (figure 4.7), the result of which is a change in the combustion temperature and pressure in the engine, which in turn leads to a change in the specific impulse.

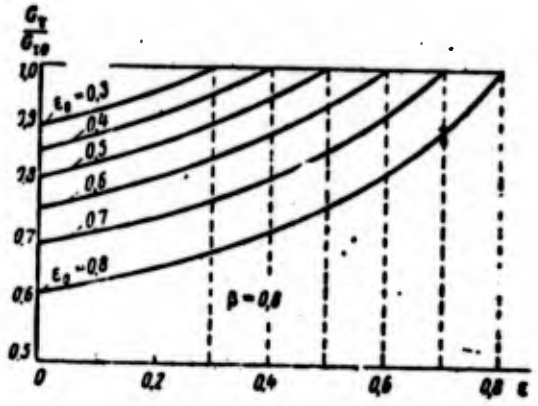

Figure 4.7

The maximum relative change in parameter ψ, which characterizes the relationship of flow rates of the liquid and solid components, will be

$$\frac{\psi_0}{\psi_к} = \frac{1-\psi_0+\psi_0(1-\varepsilon_0)^{\beta-0,5}}{(1-\varepsilon_0)^{\beta-0,5}}. \qquad (4.39)$$

From relation (4.13) for determining the operating pressure with $\nu=0$ and $\alpha=0$, taking expressions (4.32) and (4.39) into account, we will obtain

$$\frac{p_к}{p_0} = \frac{A_0}{A_к}\,\frac{K(\beta,\psi_к)}{K(\beta,\psi_0)}\,[1-\psi_0+\psi_0(1-\varepsilon_0)^{\beta-0,5}].$$

Thus the pressure drop with $G_ж$=const in the process of the engine operation is defined by both the reduction in the total flow rate of the fuel and the decrease in burning temperature (discharge coefficient A) as a result of a change in ψ.

The GRD which operates under the conditions of $G_ж$=const can be used in objects for which the required flight is provided under the thrust of an engine which varies within the limited limits.

In the solution to the problem concerning the expediency of the use of the mode $G_ж$=const, in an engine to be designed it

is necessary, on the one hand, to be guided by the considerations of the simplicity of design of the engine and the functioning of the system of fuel feed in this mode and, on the other hand, to consider the loss from the reduction of I_1 caused by the deviation ψ from the optimum value and by the pressure drop in the engine.

Let us convert the relation (4.31) into the form convenient for calculations in the ballistic design of products with GRD.

Let us express the flow rate of the liquid component thus:

$$G_{ж} = \frac{\omega_{ж}}{n\tau} = \frac{(1-\bar{\psi})\mu_{ж} Q_0}{n\tau}, \qquad (4.40)$$

where Q_0 is the starting mass of the product; $\mu_{н}$ - relative fuel reserve; ψ - average value ψ for the operating time of the engine, which determines the relationship of the components in the airborne reserve of fuel; n - number of combustion chambers in the package.

As was noted earlier, the linear rate of the gasification of the majority of the solid components used at present in the KRD was low. Therefore, for the disposition of the assigned quantity of the solid component with a small arch thickness, which ensures the assigned operating time, there appears the need for the use of a package design of the engine (see figure 1.16).

With such a layout of the engine installation it is necessary that the ratio of the external diameter of the separate combustion chamber to the gauge of the product would be equal to value D corresponding to the dense packing of the chambers into the package with the assigned n. The value of D is determined from the elementary geometric relationships and depends only on the number of chambers in the package n. Values of D for different n are given in table 4.1.

Table 4.1

n	3	4	5	7	12	14	19
$\tilde{D}$	0,464	0,414	0,370	0,333	0,244	0,220	0,200
$n\tilde{D}^2$	0,645	0,686	0,685	0,776	0,715	0,675	0,760

The cross-sectional area of one chamber of the package is connected with the area of the midsection $F_м$ by the relation

$$F_{к.с}=F_м\tilde{D}^2B_к^2.$$

With further transforms the notation $Q_0/F_м=П_0$ - the initial transverse load is used.

By substituting the obtained relations into equality (4.34) and solving it relative to the diameter of the chamber $D_{к.с}$, we obtain

$$D_{к.с}=4(\beta+0{,}5)\bar{\tau}^{1-\beta}\mu_1\left[\frac{(1-\bar{\psi})\mu_к П_0}{n\tilde{D}^2B_к^2}\right]^{\beta}\frac{K(\beta,\psi)}{1-(1-\varepsilon_0)^{\beta+0.5}}. \qquad (4.41)$$

Let us examine the limitations which can be placed on selection ε_0. At a high value of ε_0 and at a considerable length of the charge, there appear great pressure differentials along the length of the chamber. This affects the value of the calculated pressure, i.e., leads to an increase in the mass of the structure. At large pressure differentials there appears the threat of the strength of the charge. At a very high value of ε_0, the rate of the gas flow at the end of the charge can approach the speed of sound, which in the limit will lead to the appearance of the second critical cross section, and this is inadmissible for normal engine operation.

Let us introduce the limiting condition:

$$\lambda_c\leqslant\lambda_{доп}.$$

The flow rate of gases in the finite cross section of the charge at the initial moment of time will be determined as follows:

$$G_c = AF_{\text{к.с}}(1-\varepsilon_0)q(\lambda_c)p_{c0}. \tag{4.42}$$

where p_{c0} - is the full pressure in the gas flow in this cross section; $g(\lambda_c)$ - gas-dynamic function.

Since $nG_{c0}=G_{\Sigma 0}$, we can express G_{c0} thus:

$$G_{c0} = \frac{P_0}{I_{10}n}, \tag{4.43}$$

where P_0 is the initial thrust of the engine; I_{10} - the specific impulse at the relationship of the flow rate of the components ψ_0 and the operating pressure in the engine $p_{к0}$.

After writing from formulas (4.42) and (4.43) the expression for the cross-sectional area of the chamber, and after substituting this expression into the formula for the mass of the charge (4.26), we obtain

$$\omega_т = \frac{\varrho_т P_0 L}{I_{10}Aq(\lambda_c)p_{к0}} \frac{\varepsilon_0}{1-\varepsilon_0}. \tag{4.44}$$

In the design of engines and flight vehicles of different purpose, usually assigned as the starting parameters are initial thrust-to-weight ratio $n_0=P_0/Q_0$ and relative fuel reserve $\mu_к=\omega/Q_0$. In order to introduce them into equation (4.44), let us divide both its sides into the starting mass of the flight vehicle Q_0. In this case we will obtain

$$\bar{\omega}_{т_к} = \frac{\varrho_т n_0}{I_{10}Aq(\lambda_c)p_{c0}} \frac{L\varepsilon_0}{1-\varepsilon_0}. \tag{4.45}$$

Let us introduce the following notations:

$$\tau_f = \frac{I_{10}\mu_к}{n_0}; \quad u_f = \frac{Aq(\lambda_c)p_{c0}}{\varrho_т}.$$

The first of the complexes (τ_j) is the given operating time of the engine calculated from values I_{10} and η_0. The second complex (u_j) is a certain characteristic velocity.

By solving equation (4.45) relative to ε_0, with the use of the introduced notations, we obtain

$$\varepsilon_0 = \frac{\bar{\psi} u_j \tau_j}{\bar{\psi} u_j \tau_j + L}. \tag{4.46}$$

The complex $\bar{\psi} u_j \tau_j$ is a certain characteristic length L_j. Let us note that in the design of the charge of the RDTT with the assigned combustion period (arch thickness) and Pobedonostsev's parameter κ, the formula for determining ε_0 takes the following form (see [42]):

$$\varepsilon_0 = \frac{\varkappa e_1}{\varkappa e_1 + L}. \tag{4.47}$$

It is easy to note that in structure formula (4.46) is similar to formula (4.47), with the only difference being that in the latter the role of the characteristic length is played by complex κe_1 (or $\kappa u_{cp} \tau$).

We use further the relation which determines the possibility of the disposition of the required reserve of the solid propellant component at the taken length of the charge L in a flight vehicle of definite gauge:

$$\bar{\psi} \omega_2 = F_{\text{к.с}} n \varepsilon_0 \rho_\tau L. \tag{4.48}$$

After dividing both sides of equality (4.48) by Q_0 and after substituting into it the value L from formula (4.46), we obtain

$$\varepsilon_0 = 1 - \frac{\tau_0 \Pi_0}{B_a^2 \rho_\tau L_j I_{10} \eta \bar{L}^2}. \tag{4.49}$$

Formulas (4.41), (4.44) and (4.49) form the system of equations for the solution of the stated problem. The sequence of

solution is represented as follows:

1) after calculating preliminarily

$$L_f = \bar{\psi} \frac{Aq(\lambda_c)\, p_{c0} f_{10} \mu_n}{Q_1 \eta_0}$$

and after determining, by the taken value of n, the value nD^2 corresponding to it (see Table 4.1), according to formula (4.49) we determine ε_0;

2) according to formula (4.41), by substituting into it the obtained value ε_0, we find $D_{н.с}$;

3) we find the length of the charge L:

$$L = L_f \frac{1-\omega_0}{\omega_0};$$

4) we find the masses of the separate elements of the combustion chamber;

5) we find the total mass of the solid component $\omega_т = n\omega_{т1}$ and then the mass of the liquid component:

$$\omega_ж = \frac{1-\bar{\psi}}{\bar{\psi}} \omega_т;$$

6) with respect to the mass of the liquid component, we define the mass of the fuel tank, system of fuel feed and accessories;

7) we define starting mass of the flight vehicle Q_0 as the sum of the masses of its basic elements;

8) we check whether or not the obtaining of values $\mu_н$, $П_0$

and η_0 assigned for the design is provided. With the noncoincidence of the obtained values with the assigned, we first repeat the calculation, being assigned another value of n. From the variants which ensure the satisfactory convergence from the indicated parameters, we select that which provides the smallest starting mass of the flight vehicle.

Case II. *Engine operation at constant pressure* (p=const) *and constant relationship of the flow rate of components* (ψ=const) *with double intake into the combustion chamber of the liquid component* (see figure 1.4).

With an invariable critical cross section of the nozzle the pressure constancy and coefficient ψ requires that in process of the engine operation both the total flow rate of the fuel and the flow rate of each of the two components individually remain constant.

The condition of constancy of the flow rate of the solid component is expressed by the equality

$$ud = \text{const},$$

which can be written in the form

$$ud = u_{\text{н}} D_{\text{н.с}}. \tag{4.50}$$

After substituting expression (4.50) into (4.28), after integration we obtain

$$\tau = \frac{D_{\text{н.с}} \varphi}{4 u_{\text{г}}}.$$

Let us examine two variants of the solution to this problem: a) with $\beta > 0.5$ and b) with $\beta < 0.5$.

a) With $\beta > 0.5$ for the observance of equality (4.50) it is required that the flow rate of the liquid component in the channel

$G_{ж.г}$ increase, providing the necessary increase in the rate of gasification of solid component.

Let us designate the ratio of the flow rate of the liquid component fed into the channel of the charge to the total flow rate of this component by symbol ϕ:

$$\varphi=\frac{G_{ж.г}}{G_{ж}}.$$

It is obvious that when $\beta>0.5$ the coefficient ϕ in the process of the engine operation should increase, reaching a value close to unity at the end of the operation. For the simplicity of the calculations let us take $\phi_{ж}=1$. From condition ud=const it follows that

$$\frac{G_{ж.г}^{\beta}}{(1-\varepsilon)^{\beta-0.5}}=\text{const}=G_{ж}^{\beta}, \qquad (4.51)$$

since for the end of the operation with $\varepsilon=0$, $G_{ж.г}=G_{ж}$.

Hence we obtain

$$\varphi=(1-\varepsilon)^{\frac{\beta-0.5}{\beta}}.$$

For the beginning of the operation ($\varepsilon=\varepsilon_0$)

$$\varphi_0=(1-\varepsilon_0)^{\frac{\beta-0.5}{\beta}}.$$

The flow rate of the gases in the finite cross section of the charge at the initial moment of time will be determined as follows:

$$G_{г0}=\bar{\lambda}F_{к.с}(1-\varepsilon_0)q(\lambda_c)p_{ст} \qquad (4.42a)$$

Here the notations are the same as those in equation (4.42). The exception is the coefficient A, which is calculated for the composition of gases in the cross section "c", which differs from the composition of the final combustion products in front of the nozzle.

$$G_{c0}=G_т+\varphi_0 G_к=G_{\Sigma 0}\psi\left(1+\varphi_0\frac{1-\psi}{\psi}\right). \tag{4.52}$$

Since $G_{\Sigma 0}=P_0/I_{10}^n$, from relations (4.26), (4.42a) and (4.52) we obtain

$$\omega_т=\frac{Q_т P_0 L}{I_{10}\tilde{\lambda}q(\lambda_c)p_{c0}}\frac{\varepsilon_0}{1-\varepsilon_0}\psi\left(1+\varphi_0\frac{1-\psi}{\psi}\right). \tag{4.53}$$

By analogy with the derivation of relation (4.46), we find

$$\varepsilon_0=\frac{L_{f\varphi}}{L_{f\varphi}+L}, \tag{4.54}$$

where

$$L_{f\varphi}=\frac{\tilde{\lambda}q(\lambda_c)p_{c0}I_{10}\mu_к}{Q_т\varphi_0}\frac{1}{1+\varphi_0\frac{1-\psi}{\psi}}. \tag{4.55}$$

The relation for ε_0 is obtained in the same way as in the preceding case [see equation (4.46)].

The sequence of the solution to the problem remains the same as that in the preceding case.

The distinction in the calculation of the basic parameters is determined by the distinction in the formulas for determining $D_{к.с}$ and the characteristic lengths - L_f and $L_{f\phi}$.

Working relation for determining $D_{к.с}$ is obtained from equations (4.30) and (4.50) by means of the transforms examined in the preceding case:

$$D_{к.с}=\frac{4\tau^{1-\beta}u_1}{\varepsilon_0}\left[\frac{(1-\bar{\psi})\rho_к\Pi_0}{n\bar{D}^2B_м^2}\right]^{\beta}K(\beta,\psi). \qquad (4.56)$$

b) With $\beta<0.5$ for the observance of equality (4.50) it is required that, with an increase in the diameter of the channel of the charge, the flow rate of the liquid component in the channel decrease, i.e., coefficient ϕ should decrease from unity in the beginning of the operation up to its minimum value $\phi_н$ at the end. From condition ud=const it follows that:

$$\frac{G_ж^{\beta}}{(1-\varepsilon_0)^{\beta-0.5}}=G_{ж.г}^{\beta},$$

since with $\varepsilon=\varepsilon_0$, $G_{ж.г}=G_ж$; with $\varepsilon=0$, $G_{ж.г}=G_{ж.г.к}$; hence

$$\varphi_к=(1-\varepsilon_0)^{-\frac{\beta-0.5}{\beta}}.$$

The flow rate of the gases in the finite cross section of the charge at the initial moment of time will be equal to

$$G_{г0}=G_{т0}+G_{ж.г}=G_г,$$

i.e., the same as that in case I.

Consequently, relations (4.42), (4.44) and (4.49) for case I prove to be suitable also for the calculation of this variant. In this case length L_f and coefficient A should be defined in the same way as in case I.

The working formula for determining the diameter of the chamber $D_{к.с}$ is derived from relation (4.29), substituted into which is the value $u_к$ equal to

$$u_к=u_1\left(\frac{G_ж\varphi_к}{F_{к.с}}\right)^{\beta}=u_1\frac{G_ж^{\beta}}{F_{к.с}^{\beta}}(1-\varepsilon_0)^{0.5-\beta}.$$

By carrying out the transforms similar to those which were used for case I, we obtain

$$D_{к.с} = 4\tau^{1-\beta}\mu_1\left[\frac{(1-\bar{\psi})\mu_в\Pi_0}{\pi\bar{D}^2B_к^2}\right]^\beta K(\dot{\beta},\dot{\psi})\frac{(1-\varepsilon_0)^{0.5-\beta}}{\varepsilon_0}. \qquad (4.57)$$

Case III. *Engine operation at variable pressure* ($p_к$=var) *adjustable according to the defined program and with the constant relationship of the flow rate of the components* (ψ=const) *with double intake into the combustion chamber of the liquid component.*

In the design of the GRD different laws of the change in pressure and thrust can be selected in accordance with the assigned program of flight of the flight vehicle.

With any variant of the programmed pressure control, if ψ=const, the direct ratio between the pressure and flow rate of the combustion products and, consequently, between the pressure and flow rate of separate propellant components is retained. The change in the combustion efficiency and temperature of the gases, depending on the pressure change in the ballistic design in the first approximation, can be disregarded. Consequently,

$$G_\Sigma = G_{\Sigma 0}\frac{p_к}{p_{к0}};\quad G_т = G_{т0}\frac{p_к}{p_{к0}}.$$

The second equation can be rewritten in the form

$$\frac{G_т}{G_{т0}} = \frac{\Pi(\varepsilon)a}{\Pi(\varepsilon_0)a_0} = \frac{p_к}{p_{к0}}. \qquad (4.58)$$

By substituting equation (4.58) into (4.28), we obtain

$$\tau = -\frac{F_{к.с}^{1+\beta}}{\pi D_{к.с}(1-\varepsilon_0)^{0.5}\mu_1 G_{т_0}^\beta}\int_{\varepsilon_0}^{0}\frac{d\varepsilon}{(p_к(\varepsilon)/p_{к0})}. \qquad (4.59)$$

Here $p_к(\varepsilon)$ is the pressure in the engine assigned as a function of the current value ε. This relation can take a different form in

conformity with the required program of motion of the flight vehicle. The curve of the change $p_к(\varepsilon)$ can be stepped or monotonic with a decrease or increase in pressure in the process of the engine operation.

We will be limited to an examination of the case of the monotonic decrease in pressure (and, consequently, thrust). Such a law of the pressure control is of interest, for example, for the cruising flight of a flight vehicle with climb when the magnitude of thrust force required for the compensation of drag of the flight vehicle in the process of flight decreases.

Let us examine the linear law of the decrease in pressure:

$$p_к/p_{к0}=(p_{кт}/p_{к0})+\frac{\varepsilon}{\varepsilon_0}\left(1-\frac{p_{кт}}{p_{к0}}\right), \qquad (4.60)$$

where $p_{к0}$ is the initial pressure in the engine; $p_{кт}$ - the pressure at the end of the engine operation.

By substituting equation (4.60) into (4.59), we obtain

$$\tau=\frac{p_{к.с}^{1+\beta}\varepsilon_0}{\pi D_{к.с}(1-\varepsilon_0)^{0,5}u_1 G_{к0}^{\beta}}\frac{p_{к0}}{p_{к0}-p_{кт}}\ln(p_{к0}/p_{кт}).$$

CHAPTER 5

STATIC CHARACTERISITICS OF COMBINED ROCKET ENGINES

5.1. GENERAL INFORMATION

The static characteristics of rocket-engines can be called the relations which connect their parameters in steady-state operating condition.

The static characteristics are used in the solution of a whole number of problems:

a) in the analysis of the effect of external factors and design characteristics of components of the engine on its basic parameters (thrust, specific impulse, operating time);

b) in conducting the adjustment of the engine;

c) for obtaining the data necessary in the calculation of the control system of the engine, etc.

The static characteristics are considered the interconnections and mutual effect of all components of the engine in the process of its operation.

The static characteristics can be found either analytically or graphically.

The use of the analytical method assumes the compilation and solution of the system of equations which describe the operation of separate elements of the KRD [НРД - combined rocket engine]. Many equations of the engine components are nonlinear; and therefore the system of equations is complex, and its solution is difficult to arrive at even on calculators. The linearization of the equations makes it possible to simplify the solution. This approach gives the necessary accuracy only in the study of engine characteristics in the vicinity of the nominal system; however, this proves to be sufficient for the solution of many problems, and therefore the determining of static characteristics on the basis of the system of linearized equations of the engine components is utilized rather widely in the theory of rocket engines of different types.

The graphic method, the basis of which is the construction of graphs which characterize the interconnection of the parameters of the engine, gives relatively low accuracy, is inconvenient and bulky in the study of engines of the complex designs, and therefore it is applied mainly only for a qualitative analysis of the interconnection of characteristics and processes of separate engine components.

Taking that above said into account we will conduct and analysis of the static characteristics of the KRD analytically with the use of systems of linearized equations of units of the KRD.

5.2. EQUATIONS OF UNITS OF A HYBRID ROCKET ENGINE

5.2.1. Equation of the Chamber of a Hybrid Rocket Engine

Let us examine engine chamber (figure 5.1) with the introduction of the liquid component not only through the head into the channel of the charge ($G_{ж.г}$), but also into afterburner ($G_{ж.д}$). The charge is grain with a cylindrical channel.

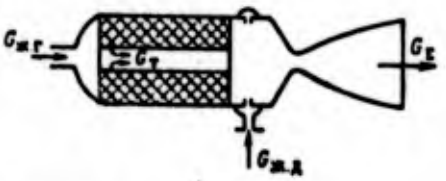

Figure 5.1. Diagram of the chamber of a hybrid rocket engine with afterburning.

Let us assume as a basic assumption that parameters of the operating conditions in the chamber (pressure, temperature, gas constant, etc.) are the concentrated values (in the region of the nozzle entry).

The operating conditions in the chamber in steady-state conditions are described by the following system of equations:

the equation of mass conservation

$$G_{ж.г}+G_{ж.к}+G_т=G_с; \tag{5.1}$$

the equation of gasflow through the nozzle

$$G_с=\frac{\varphi_с b p_к F_{кр}}{\sqrt{RT_к}}, \tag{5.2}$$

where $b=\left(\frac{2}{n+1}\right)^{\frac{n+1}{2(n-1)}}\sqrt{n}$, and n is the polytropic exponent;

the equation of the gas formation of the solid component

$$G_т=\left[4^{\vartheta}\pi^{1-\vartheta}(1-\vartheta)u_1\varrho_т L d^{1-2\vartheta}p_к^{\vartheta}+G_{ж.г}^{1-\vartheta}\right]^{\frac{1}{1-\vartheta}}-G_{ж.г}; \tag{5.3}$$

the equation of the relationship of the propellant component flow

$$K=\alpha K_{стех}=\frac{G_ж}{G_т}, \tag{5.4}$$

where α is the coefficient of excess of the liquid component; $K_{стех}$ - the stoichiometric relationship of the flow rate of the components;

the equation of the dependence of the efficiency of combustion products in the chamber on temperatures of the propellant components ($T_т$ - solid, T - liquid) and on the coefficient of excess of the liquid component α

$$RT_к = RT_к(a, T_т, T_ж); \tag{5.5}$$

the equation of the dependence of the coefficient of the rate of gasification of the solid component on its temperature

$$u_1 = u_1(T_т); \tag{5.6}$$

the equation of the distribution of the liquid component between its introductions into the head and afterburner

$$\varphi = \frac{G_{ж.г}}{G_ж}. \tag{5.7}$$

Solving together equations (5.2), (5.4) and (5.5), which are linearized in vicinities of the nominal system, we obtain the equation of the chamber of the GRD [ГРД - hybrid rocket engine] in small relative deviations:

$$a^{p_к}_{к.с}\delta p_к + a^{G_ж}_{к.с}\delta G_ж + a^{G_т}_{к.с}\delta G_т + b^{F_{кр}}_{к.с}\delta F_{кр} + b^{\varphi}_{к.с}\delta\varphi_с + \\ + c^{T_ж}_{к.с}\delta T_ж + c^{T_т}_{к.с}\delta T_т = 0, \tag{5.8}$$

where $\delta p_к$, $\delta G_ж$,..., $\delta T_т$ are the relative deviations of the corresponding parameters from their nominal values $\bar{p}_к$, $\bar{G}_ж$,... $\bar{T}_т$:

$$\delta p_к = \frac{\bar{p}_к - p_к}{\bar{p}_к} = \frac{\Delta p_к}{\bar{p}_к};$$

$$\delta G_ж = \frac{\bar{G}_ж - G_ж}{\bar{G}_ж} = \frac{\Delta G_ж}{\bar{G}_ж};\ \ldots;\ \delta T_т = \frac{\bar{T}_т - T_т}{\bar{T}_т} = \frac{\Delta T_т}{\bar{T}_т}.$$

The dimensionless coefficients[1]

$$a^{p_к}_{к.с} = b^{F_{кр}}_{к.с} = b^{\varphi}_{к.с} = -1; \quad a^{G_т}_{к.с} = \frac{\bar{k}}{1+\bar{k}} - \frac{1}{2}\frac{\bar{a}}{R\bar{T}_к}\frac{\partial RT_к}{\partial a};$$

---

[1]Notations a are accepted for coefficients with deviations of the working parameters and characteristics of the process; notations b - for coefficients with deviations of the design dimensions and characteristics; notations c - for coefficients with deviations of external factors which affect the process.

$$a^{G_т}_{к.с} = \frac{1}{1+\bar{K}} + \frac{1}{2}\,\frac{\bar{\alpha}}{R\bar{T}_к}\,\frac{\partial RT_к}{\partial \alpha};\quad c^{T_к}_{к.с} = \frac{1}{2}\,\frac{\bar{T}_ж}{R\bar{T}_к}\,\frac{\partial RT_к}{\partial T_ж};$$

$$c^{T_т}_{к.с} = \frac{1}{2}\,\frac{\bar{T}_т}{R\bar{T}_к}\,\frac{\partial RT_к}{\partial T_т}.$$

By linearizing equation (5.3) and taking equation (5.6) into account, we obtain the equation of the gas formation of a unit of solid component in the small relative deviations:

$$a^{G_т}_{б.з}\delta G_т + a^{G_{ж.т}}_{б.з}\delta G_{ж.т} + a^{p_к}_{б.з}\delta p_к + b^{u_1}_{б.з}\delta u_1 + b^{\rho_т}_{б.з}\delta \rho_т + \\ + b^{L}_{б.з}\delta L + b^{d}_{б.з}\delta d + c^{T_т}_{б.з}\delta T_т = 0, \qquad (5.9)$$

where the coefficients

$$a^{G_т}_{б.з} = -1;\ a^{G_{ж.т}}_{б.з} = 1 - f(\bar{\varphi}, \bar{K});\ a^{p_к}_{б.з} = \frac{\nu}{1-\beta} f(\bar{\varphi}, \bar{K});$$

$$b^{L}_{б.з} = b^{\rho_т}_{б.з} = b^{u_1}_{б.з} = \frac{1}{1-\beta} f(\bar{\varphi}, \bar{K});\quad b^{d}_{б.з} = -\frac{2\beta - 1}{1-\beta} f(\bar{\varphi}, \bar{K});$$

$$c^{T_т}_{б.з} = \frac{\bar{T}_т}{\bar{u}_1}\,\frac{\partial u_1}{\partial T_т}\,\frac{1}{1-\beta} f(\bar{\varphi}, \bar{K}).$$

Here
$$f(\bar{\varphi}, \bar{K}) = (1+\bar{\varphi}\bar{K})\left[1 - \left(\frac{\bar{\varphi}\bar{K}}{1+\bar{\varphi}\bar{K}}\right)^{1-\beta}\right]. \qquad (5.10)$$

Let us note that easily obtained from equations (5.8) and (5.9) are equations of the engine chamber of solid fuel known in the theory of the RDTT [РДТТ - solid-propellant rocket engine]. After assuming $\bar{K}=0$, $\bar{\alpha}=0$, $\beta=0$, and after introducing values of the coefficients, we find

$$\left.\begin{aligned} &\delta p_к - \delta G_т + \delta F_{кр} + \delta \varphi_c - \frac{1}{2}\,\frac{\bar{T}_т}{R\bar{T}_к}\,\frac{\partial RT_к}{\partial T_т}\,\delta T_т = 0; \\ &\delta p_к - \delta G_т + \delta u_1 + \delta \rho_т + \delta d + \delta L + \frac{\bar{T}_т}{\bar{u}_1}\,\frac{\partial u_1}{\partial T_т}\,\delta T_т = 0. \end{aligned}\right\} \qquad (5.11)$$

5.2.2. Equation of the Main Fuel Line

The pressure differential in the main line is determined in

general by the sum of the losses of pressure for the overcoming of local resistances and losses to friction. Losses in elements of the main line in the majority of the cases are proportional to the square of the rate of the motion of the liquid, i.e., to the square of its flow rate through the main line. After designating the pressure differential in the main line by $\Delta p_м$, flow rate by $G_м$ and density of the liquid by $\rho_ж$, we can write

$$\Delta p_м = \xi_м \frac{G_м^2}{2\rho_ж}, \qquad (5.12)$$

where $\xi_м$ is the generalized drag coefficient of main line which considers all the resistances along its length.

By linearizing this expression, we will obtain the equation of hydraulic main line in small relative deviations:

$$a_м^{G_м} z G_м + a_м^{\Delta p_м} z \Delta p_м + b_м^{\xi_м} z \xi_м + c_м^{\rho_ж} z \rho_ж = 0, \qquad (5.13)$$

where $a_м^{G_м} = 2;\ a_м^{\Delta p_м} = -b_м^{\xi_м} = c_м^{\rho_ж} = -1.$

5.2.3. Equation of the Slow-Burning Charge

If the PAD [ПАД - show-burning charge] operates in the supercritical system of the outflow of gases into the tank, its equations coincide with equations of the chamber of the solid-propellant engine, i.e., with equations (5.11).

5.2.4. Equations of the Centrifugal Pump

The operation of the pump in the feed system of the liquid propellant component of the GRD is described by equations of pressure and power.

The equation of pressure, which determines the pressure increase in the pump written in analytical form, usually gives

low accuracy, and the pressure characteristics are assigned, as a rule, in the form of curves, including in coordinates $Q_н/n$-H/n^2, where $Q_н$ is the volumetric per-second fluid flow rate through the pump ($Q_н=G_н/\rho_ж$); H - pressure ($H=\Delta p_н/p_ж$); n - rotation frequency in r/min.

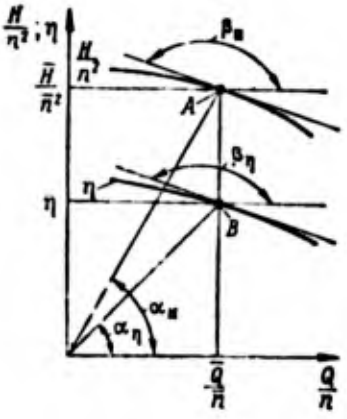

Figure 5.2. Pressure pump performance.

Figure 5.2 shows this curve. Here the curve of the dependence of the efficiency of the pump η on $Q_н/n$ is given. Points A (on the pressure characteristic) and B (on the efficiency line) correspond to the nominal system. Deviations of the parameters from the nominal values are connected with the steepness of the characteristics at points of the nominal system (angles β and β) and the location of these points (angles α and α).

The equation of the pump pressure head in low deviations takes the following form:

$$a_н^{\Delta p_н}\delta\Delta p_н + a_н^{G_н}\delta G_н + a_н^{n}\delta n + b_н^{H_0}\delta H_0 + c_н^{Q_ж}\delta Q_ж = 0, \qquad (5.14)$$

where the coefficients

$$a_н^{\Delta p_н} = -b_н^{H_0} = -1; \quad a_н^{G_н} = -\frac{\operatorname{tg}\beta_н}{\operatorname{tg}\alpha_н}; \quad a_н^{n} = 2-\frac{\operatorname{tg}\beta_н}{\operatorname{tg}\alpha_н};$$

$$c_н^{Q_ж} = 1-\frac{\operatorname{tg}\beta_н}{\operatorname{tg}\alpha_н};$$

δH_0 - the error of the manufacture of the pump according to the value of pressure, i.e., a distinction of the pump pressure from the calculated at nominal values of n and $Q_н$; value δH_0 is determined by the experiment;

$G_н=Q_{нρж}$ - the mass pump capacity.

The equation of the pump power takes the form

$$N_н = \frac{G_н \Delta p_н}{\rho_н \eta_н}.$$

By linearizing this equation and taking into account the error of manufacture of the pump according to the efficiency ($\delta\eta_{НО}$), with nominal values of $Q_н$ and n we obtain, when using equation (5.14), the equation of the pump power in small deviations:

$$a^{N}_{N_н}\delta N_н + a^{G}_{N_н}\delta G_н + a^{n}_{N_н}\delta n + b^{H_0}_{N_н}\delta H_0 + b^{\eta_0}_{N_н}\delta\eta_{н0} + c^{\rho_0}_{N_н}\delta\rho_{0н} = 0, \qquad (5.15)$$

where

$$a^{N}_{N_н} = b^{\eta_0}_{N_н} = -b^{H_0}_{N_н} = -1;\quad a^{G}_{N_н} = 1 + \frac{\operatorname{tg}\beta_н}{\operatorname{tg}\alpha_н} - \frac{\operatorname{tg}\beta_т}{\operatorname{tg}\alpha_т};$$

$$a^{n}_{N_н} = 2 + \frac{\operatorname{tg}\beta_т}{\operatorname{tg}\alpha_т} - \frac{\operatorname{tg}\beta_н}{\operatorname{tg}\alpha_н};\quad c^{\rho_0}_{N_н} = \frac{\operatorname{tg}\beta_т}{\operatorname{tg}\alpha_т} - \frac{\operatorname{tg}\beta_н}{\operatorname{tg}\alpha_н}.$$

It is logical to consider that in the nominal system the pump has an efficiency close to the maximum. In this case tg β=0, and the expressions for coefficients in equation (5.15) are simplified.

5.2.5. Equations of Turbine

The fundamental equation of the turbine, which enters usually into the system of equations of the engine, is the equation which determines the effective power of the turbine:

$$N_e = G_{тг}\, h_0 \eta_e. \qquad (5.16)$$

where $G_{тг}$ is the flow rate of the working medium through the turbine; h_0 - the available heat drop (work of adiabatic expansion of 1 kg of gas); η_e - effective efficiency of the turbine.

By linearlizing equation (5.16), we obtain

$$\delta N_e = \delta G_{тг} + \delta h_0 + \delta\eta_e. \qquad (5.17)$$

The available heat drop

$$h_0 = \frac{n_a}{n_a - 1} RT_r \left[1 - \left(\frac{1}{\pi_T} \right)^{\frac{n_a - 1}{n_a}} \right],$$

where $\pi_T = p_\Gamma / p_T$ is the expansion ratio of the gas in the nozzle ring (ratio of gas pressures p_Γ - before the nozzles and p_T - after the nozzles); n_a is the polytropic exponent (n_a=const).

The effective efficiency of the turbine

$$\eta_e = \eta_u \eta_{T.B} \eta_M,$$

where η_u is the circular efficiency of the turbine; $\eta_{T.B}$ - the coefficient which considers losses to friction, ventilation and gas overflow through the blades; η_M - mechanical efficiency.

The components of efficiency complexly depend on the mode parameters and design features of the turbine (see [5]). By omitting the transforms necessary for determining the increases δh_0 and $\delta \eta_c$, let us give the equation of the active turbine in final form:

$$a_T^{N_e} \delta N_e + a_T^{G_{\Gamma\Gamma}} \delta G_{\Gamma\Gamma} + a_T^n \delta n + a_T^{RT_r} \delta (RT_r) + b_T^{F_{кр.г}} \delta F_{кр.г} + b_T^{F_{а.г}} \delta F_{а.г} + b_T^{\eta_e} \delta \eta_e' = 0, \qquad (5.18)$$

where the coefficients

$$a_T^{G_{\Gamma\Gamma}} = -a_T^{N_e} = b_T^{\eta_e'} = 1; \quad a_T^n = A_T; \quad a_T^{RT_r} = 1 - \frac{A_T}{2};$$

$$a_T^{a_r} = \frac{n_a - 1}{n_a} \frac{1}{\pi_T^{\frac{n_a - 1}{n_a}} - 1};$$

$$b_T^{F_{кр.г}} = -b_T^{F_{а.г}} = -\frac{2(n_a - 1)}{2\pi_T^{\frac{n_a - 1}{n_a}} - n_a - 1}.$$

In equation (5.18) and in expressions for the coefficients:

$F_{кр.г}$ is the nozzle throat area of the turbine;

$F_{a\,r}$ - the total nozzle exit area;

n - the frequency of rotation of the turbine rotor in r/min;

$\delta\eta_e'$ - the deviation of efficiency from its calculated value due to the errors in the manufacture of the turbine;

$$A_T = 1 - \mu_T \bar{x}\,\frac{\mu_T + \frac{\psi_T \cos\beta_2}{B_T}\left(\varphi_T\sqrt{1-\rho_T}\cos\alpha_1 - \mu_T^2\bar{x}\right)}{\varphi_T\sqrt{1-\rho_T}\cos\alpha_1 - \mu_T^2\bar{x} + \mu_T\psi_T\cos\beta_2 B_T};$$

$$B_T = \sqrt{\varphi_T^2 - 2\bar{x}\varphi_T\cos\alpha_1 + \bar{x}^2};$$

$\bar{x} = \frac{u}{c_{ad}}$ - the ratio of the circular velocity on blades to the adiabatic velocity ($c_{ad} = \sqrt{2gh_0}$);

α_1 - the nozzle cant angle;

β_2 - the exit angle of the blade;

ρ_T - the degree of the reactivity of the turbine;

φ_T, ψ_T - the loss factors of velocity in the nozzles and on the blades, respectively;

μ_T - the ratio of diameters of the inlet and outlet of the rotor.

5.2.6. Equations of the Generator of the Working Medium of the Turbine (Gas Generator)

A. <u>The generator is one-component and the propellant is solid.</u> The gas generator in this case can be considered as a solid-propellant engine, and equations of the gas generator take the form of (5.11).

B. <u>The generator operations on a hybrid propellant</u>. The gas generator can be considered as a GRD, and its equations take the form of (5.8) and (5.9).

C. <u>The generator is based on hydrogen peroxide</u>. In this case an increase in the flow rate o gas in the turbine is equal to an increase in the feed of hydrogen peroxide into the generator:

$$\delta G_{\text{гг}} = \delta G_{H_2O_2}.$$

The change in the efficiency of the gas can be caused by changes in the concentration of hydrogen peroxide $K_{H_2O_2}$ and its temperature $T_{H_2O_2}$:

$$\delta(RT_{\text{г}}) = f(\delta K_{H_2O_2}, \delta T_{H_2O_2}).$$

5.3. ACCURACY OF OPERATION OF THE GRD

The parameters of the hybrid rocket engine in the process of its work will not be equal to their expected (assigned) values. The reason for the deviations of the parameters of each GRD from the assigned is the action of the external and internal disturbances (factors), which does not entirely succeed in considering and compensating for.

The number of external disturbances includes deviations in temperature of the propellant components produced by changes in the ambient temperature. With a certain approximation let us include in these disturbances the deviations (from nominal values) of the density and chemical composition of the liquid component.

The internal disturbances can be very diverse; they include errors in the manufacture and adjustment of all the units and assemblies making up the engine and also deviations in the characteristics of the charge of the solid-propellant component.

Thus, for instance, the internal disturbances which can appear and act in the combustion chamber include: deviations in the dimensions of the charge (δL, δd); deviations in the critical cross section of the nozzle ($\delta F_{\text{кр}}$); deviations in the discharge coefficient ($\delta \phi_c$); deviations in the coefficient of the rate of gasification (δu_1); and deviations in the density of solid component ($\delta \rho_т$), and so on.

All these deviations are, in particular, the consequence of errors permitted in the manufacture of the propellant and chamber, and these errors can be placed in the assigned limits (allowances), and therefore each error itself is estimated as being permissible.

Besides the inaccuracies in the manufacture, there can be other reasons for the appearance of some internal disturbances. Thus, for instance, in the process of the operation of the GRD, heat erosion of the critical cross section of its nozzle (uncooled) can occur.

According to data given in foreign literature (see [64]), in the operation of the GRD on a propellant which includes an oxidizer FLOX (70% F_2+30% O_2) and a solid fuel based on lithium, lithium hydride and polybutadiene, the heat erosion of the nozzle insert manufactured from pyrolytic graphite reaches 4% for 63 seconds.

In a way similar to that which was done for the chamber, it is possible to establish the possible internal disturbances for other engine components.

For the hydraulic main line such a basic disturbance will be the deviation in the coefficient of hydraulic friction $\delta\xi$; for a pump - deviations in pressure and efficiency of the pump; for a turbine - deviations in efficiency of the turbine, and so on.

Let us note that in the relation to the hydraulic main line, pump and turbine we showed the generalized internal disturbances. It would be possible, instead of each of them, to introduce several particular disturbances causing the combined appearance of the introduced generalized disturbances. Thus, for instance, instead of the deviation in the coefficient of hydraulic friction of the main line, it would be possible to introduce the totality of deviations in the form and dimensions of separate elements of this main line (sections of the pipelines, valves, throttles, injectors, etc.), which determines value $\delta\xi$ as a final result. Instead of

deviations in the pump pressure, it would be possible to introduce deviations in those dimensions and form of its elements on which depend the deviations in pressure (deviations in dimensions of the wheel of the pump, in the form of blades, etc).

However, the introduction of such particular disturbances into systems of equations of the GRD would make the accuracy of the final result of the solution worse as a result of errors in models of the operation of each element and, furthermore, would complicate the very decision process.

The use of generalized disturbances ($\delta\xi$, δH_0, $\delta\eta_e$ etc.) makes it possible to simplify the systems of equations and their solution and also raise the accuracy of final results of the calculation, since the values of these disturbances are determined reliably by experiment.

An analysis of the accuracy of operation of a GRD, or as it is sometimes stated, an analysis of the effect on the operation of GRD of external and internal disturbing effects (factors), is carried out in the quasi-steady system in this sequence:

a) according to the design of the GRD and taking into account the features of the device of its separate units, formulate the system of static equations of engine components in small deviations; in this case all the disturbances whose action must be considered in the analysis are introduced into the system;

b) solve the system of equations relative to the parameters whose change under the action of the disturbances must be determined;

c) are introduce into the solution the assigned values of the disturbances and find the deviations of the corresponding parameters. The maximum scatter of the parameters is usually determined under the assumption that all the possible internal and external

disturbances are of random nature and obey the law of normal distribution:

$$\delta X_{np.z} = \pm \sqrt{\sum_{k=1}^{n} (a_x^{i_k} \delta i_k)^2 + \sum_{p=1}^{m} (a_x^{j_p} \delta j_p)^2 + 2 \sum_{p<l} a_x^{j_p} a_x^{j_l} \delta j_p \delta j_l k_{p.l} + 2 \sum_{k<q} a_x^{i_k} a_x^{i_q} \delta i_k \delta i_q k_{k.q}}.$$

where δi_k, δj_p are values of internal and external disturbances; $a_x^{i_k}$, $a_x^{j_p}$ - coefficients of the effect of disturbances on parameter X; $k_{p.l}$, $k_{q.k}$ - correlation coefficients.

If the system of equations is too complex for obtaining the general solution, then calculations of the effect of the disturbances are carried out on a computer. The purpose of the calculations is for determining the coefficients of effect, i.e., the numbers which show the amount of deviation of the parameter of the engine caused by a single disturbance.

Let us examine two examples of the evaluation of the effect of external and internal disturbances on parameters of the work of a GRD. As a first object let us examine the uncontrolled GRD with a pressure feed system of the liquid-propellant component, and as the second - the GRD (also without control) with a pump feed system.

5.3.1. Hybrid Rocket Engines With a Pressure Feed System of the Liquid-Propellant Component

A diagram of the engine is given in figure 5.3. Point 1 is the place of separation of the main line which feeds the liquid component.

Operation of the given GRD is described by the following system of equations:

$$
\left.
\begin{aligned}
&1)\ a^{p_к}_{к.с}\delta p_к + a^{G_ж}_{к.с}\delta G_ж + a^{G_т}_{к.с}\delta G_т + b^{F_{кр}}_{к.с}\delta F_{кр} + b^{\tau_с}_{к.с}\delta\tau_с = 0;\\
&2)\ a^{G_т}_{б.з}\delta G_т + a^{G_{ж.г}}_{б.з}\delta G_{ж.г} + a^{p_к}_{б.з}\delta p_к + b^{L}_{б.з}\delta L + b^{m_1}_{б.з}\delta m_1 +\\
&\qquad + b^{Q_т}_{б.з}\delta Q_т + b^{d}_{б.з}\delta d = 0;\\
&3)\ a^{G_ж}_{G_ж}\delta G_ж + a^{G_{ж.г}}_{G_ж}\delta G_{ж.г} + a^{G_{ж.д}}_{G_ж}\delta G_{ж.д} = 0;\\
&4)\ a^{G_ж}_{м}\delta G_ж + a^{\Delta p_{б-1}}_{м}\delta\Delta p_{б-1} + b^{\xi_{б-1}}_{м}\delta\xi_{б-1} + c^{Q_ж}_{м}\delta Q_ж = 0;\\
&5)\ a^{G_{ж.г}}_{м}\delta G_{ж.г} + a^{\Delta p_{1-к.с}}_{м}\delta\Delta p_{1-к.с} + b^{\xi_{1-к.с}}_{м}\delta\xi_{1-к.с} +\\
&\qquad + c^{Q_ж}_{м}\delta Q_ж = 0;\\
&6)\ a^{G_{ж.д}}_{м}\delta G_{ж.д} + a^{\Delta p_{1-к.д}}_{м}\delta\Delta p_{1-к.д} + b^{\xi_{1-к.д}}_{м}\delta\xi_{1-к.д} +\\
&\qquad + c^{Q_ж}_{м}\delta Q_ж = 0;\\
&7)\ a^{\Delta p_{б-1}}_{б-1}\delta\Delta p_{б-1} + a^{p_1}_{б-1}\delta p_1 + b^{p_б}_{б-1}\delta p_б = 0;\\
&8)\ a^{\Delta p_{1-к.с}}_{1-к.с}\delta\Delta p_{1-к.с} + a^{p_1}_{1-к.с}\delta p_1 + a^{p_к}_{1-к.с}\delta p_к = 0;\\
&9)\ a^{\Delta p_{1-к.д}}_{1-к.д}\delta\Delta p_{1-к.д} + a^{p_1}_{1-к.д}\delta p_1 + a^{p_к}_{1-к.д}\delta p_к = 0.
\end{aligned}
\right\} \qquad (5.19)
$$

In the system of equations (5.19):

equations (1) and (2) are equations of the chamber written, respectively, in the form of (5.8) and (5.9);

equation (3) is the equation of the balance of flow rate of the liquid component obtained from equation $G_ж = G_{ж.г} + G_{ж.д}$; in equation (3)

$$a^{G_ж}_{G_ж} = -1;\quad a^{G_{ж.г}}_{G_ж} = \bar{\gamma};\quad a^{G_{ж.д}}_{G_ж} = 1 - \bar{\gamma};$$

equations (4)-(6) are equations of sections of the main lines written in the form of (5.13); the first of them is for the section "tank-point 1"; the second is for the section "point 1-head of the chamber"; and the third is for the section "point 1-afterburner";

equations (7)-(9) are equations of the balance of pressure on these three sections of the main line; in these equations p_1 is the pressure at point 1; $\Delta p_{б-1} = p_б - p_1$; $\Delta p_{1-к.с} = \Delta p_{1-к.д} - p_1 - p_{к.с}$.

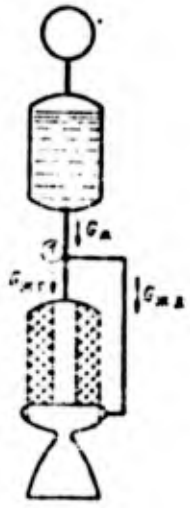

Figure 5.3. Diagram of a GRD with a pressure feed system of the liquid-propellant component (with after-burner): 1 - place of separation of the main line which feeds the liquid component.

Coefficients of equations (7)-(9):

$$a^{\Delta p_6}_{6-1} = a^{\Delta p_{1-к.с}}_{1-к.с} = a^{\Delta p_{1-к.з}}_{1-к.з} = -1;$$

$$b^{p_6}_{6-1} = \frac{\bar{p}_6}{\Delta \bar{p}_{6-1}}; \quad a^{p_1}_{6-1} = -\frac{\bar{p}_1}{\Delta \bar{p}_{6-1}};$$

$$a^{p_1}_{1-к.с} = \frac{\bar{p}_1}{\Delta \bar{p}_{1-к.с}}; \quad a^{p_к}_{1-к.с} = -\frac{\bar{p}_к}{\Delta \bar{p}_{1-к.с}};$$

$$a^{p_1}_{1-к.з} = \frac{\bar{p}_1}{\Delta \bar{p}_{1-к.з}}; \quad a^{p_к}_{1-к.з} = -\frac{\bar{p}_к}{\Delta \bar{p}_{1-к.з}}.$$

The scattering of parameters of the pressure-feed system is considered in the system of equations (5.19) by deviations in the tank pressure $\delta p_б$. If there is a need for a more detailed account of features of the operation of the system of the pressure feed of the tank, it is necessary to introduce equations of the pressure accumulator into the system of equations.

System (5.19) is a closed system of equations. The unknowns in it are:

$$\delta p_к;\ \delta Q_м;\ \delta J_т;\ \delta Q_{к.с};\ \delta Q_{м.з};\ \delta \Delta p_{б-1};\ \delta \Delta p_{1-к.с};\ \delta \Delta p_{1-к.з};\ \delta p_1.$$

The external and internal disturbances are exhibited in the form:

$$\delta F_{кр};\ \delta\bar{\tau};\ \delta L;\ \delta d;\ \delta Q_{т};\ \delta u_{1};\ \delta Q_{ж};\ \delta\rho_{б};\ \delta\bar{\xi}_{б-1};\ \delta\bar{\xi}_{1-к.с};\ \delta\bar{\xi}_{1-к.з}.$$

The disturbances which are exhibited in the deviation of pressure of the propellant component at the output from the tank ($\delta p_б$) usually include a change in the axial acceleration n_x, a change in the height of the liquid column in the tank in proportion to the production of the component $h_ж$, and deviations in the pressure feed of the gas cushion of the tank $p_п$:

$$\delta p_б = \frac{\bar{p}_ж}{\bar{p}_б}(\delta h_ж + \delta n_x) + \frac{\bar{p}_п}{\bar{p}_б}\delta p_п,$$

where $p_ж = \rho_ж h_ж n_x$ is the pressure of the liquid column.

The axial acceleration

$$n_x = \frac{j_x + g_h \sin\theta}{g},$$

where j_x is the path acceleration, g_h - the gravity acceleration at height H, and θ is the pitch angle.

The values of coefficients in equations of system (5.19) are completely determined by values of the independent dimensionless coefficients, exponents and relations:

$$\bar{K} = \frac{\bar{G}_ж}{\bar{G}_т};\quad \nu;\ \beta;\ \bar{\tau} = \frac{\bar{G}_{ж\,т}}{\bar{G}_ж};\quad \frac{\bar{p}_к}{\Delta\bar{p}_i}\left(\Delta\bar{p}_i = \Delta\bar{p}_{б-1};\ \Delta\bar{p}_{1-к.с};\ \Delta\bar{p}_{1-к\,з}\right).$$

After determining for the specific engine by these magnitudes the values of coefficients of the system of equations (5.19), and after assigning external and internal disturbances, it is possible from system (5.19) to determine all the deviations of the parameters from the nominal ones, and, therefore, the real values of these parameters and their possible scattering.

As an example the calculations for GRD with these initial characteristics are conducted:

$p_к = 40 \cdot 10^5$ Pa; $K = 5$; $\beta = 0{,}65$; $\nu = 0$; $\bar{\varphi} = 0{,}8$;
$\Delta\bar{p}_{б-1} = 3 \cdot 10^5$ Pa; $\Delta\bar{p}_{1-кс} = \Delta\bar{p}_{1-кд} = 10 \cdot 10^5$ Pa.

Obtained as a result of the calculations are the coefficients of the effect of internal and external disturbances on the basic parameters of the engine: $p_к$, $G_т$, $G_ж$, $\bar{K}(\delta K = \delta G_ж - \delta G_т$. Values of these coefficients are given in table 5.1.

Table 5.1

No.	Disturbance	Deviations of parameters per unit of the deviation of the disturbing factor.			
		$\delta p_к$	$\delta G_ж$	$\delta G_т$	δK
1	$\delta F_{кр}$	−0,410	+0,630	+0,394	+0,236
2	$\delta\varphi_c$	−0,410	+0,630	+0,394	+0,236
3	$\delta\alpha_1$	+0,073	−0,113	+1,000	−1,113
4	$\delta Q_т$	+0,073	−0,113	+1,000	−1,113
5	δL	+0,073	−0,113	+1,000	−1,113
6	δd	−0,022	+0,034	−0,300	+0,334
7	$\delta\xi_{б-1}$	−0,044	−0,048	−0,030	−0,018
8	$\delta\xi_{1-кд}$	−0,025	−0,038	+0,039	−0,077
9	$\delta\xi_{1-кс}$	−0,122	−0,119	−0,137	+0,018
10	$\delta Q_ж$	+0,192	+0,205	+0,128	+0,077
11	$\delta p_б$	+0,782	+0,835	+0,522	+0,313

Figure 5.4 gives a graph of the dependence of δp on the action of different disturbances.

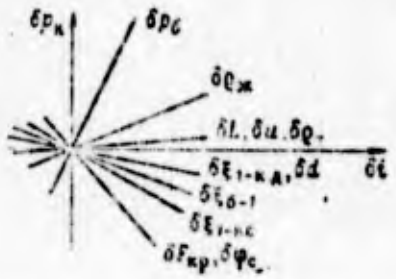

Figure 5.4. Dependence of $\delta p_к$ on the action of different disturbances.

Although for the calculation the conditional engine was selected, some qualitative conclusions according to the results of the calculation can be made.

1. The effect of $\delta F_{кр}$ on pressure in the chamber of the GRD is less than that for the RDTT, where, as is known, $\delta p_к = \frac{1}{1-\nu}\delta F_{кр}$ (and under our conditions,

i.e., with $\nu=0$, $\delta p_к/\delta F_{кр}=1$ should have been).

Physically this is explained by a decrease in the flow rate of the liquid component with an increase in $p_к$, i.e., by the presence of an additional factor which counteracts the pressure change in the chamber.

2. The effect of tank pressure on the parameters of the GRD is rather substantial. An increase in $p_б$ produces an increase in the feed of the liquid component and then (because of this) an increase in the gas formation of the charge and pressure in the chamber.

3. An increase in the length of the charge, density of the propellant and rate of gasification (coefficient u_1) produces a considerable increase in the gasification of the solid component, increase in pressure in the chamber and, as a result, a reduction in the fluid flow rate. Such changes in flow rates of the components cause the most considerable change in the coefficient of their relationship.

4. By a change in the hydraulic friction on the lines of the feed of the liquid component it is possible to change differently not only the flow rate of the liquid component, but also the gas formation of the solid and thereby the relationship of the propellant component flow rate. This fact can be used for the adjustment and control of an engine of a similar design.

5. An increase in the density of the liquid component produces an increase in its feed into the chamber and, as a result, an increase in the gas formation of the solid charge and pressure in the chamber.

In connection with the latter fact, let us focus attention on the fact that with a change in the temperature of the liquid

component the maximum operating time of the engine will be changed.[1] If we designate by symbols $\omega_т$ and $\omega_ж$, respectively, the masses of the solid and liquid components in the engine (mass servicing of the liquid and mass of charge of the solid components), then the times of the burnout of both components will be

$$\tau_т = \omega_т / G_т; \quad \tau_ж = \omega_ж / G_ж.$$

Deviations of the times of burnout will correspondingly be equal to

$$\delta\tau_т = \delta\omega_т - \delta G_т; \quad \delta\tau_ж = \delta\omega_ж - \delta G_ж.$$

Masses of the propellant with a change in the ambient temperature are not changed. Therefore,

$$\delta\tau_т = -\delta G_т; \quad \delta\tau_ж = -\delta G_ж.$$

Thus, in the examined case with a change of 1% of the density of the liquid component the following changes: the time of its burnout by 0.2% and the time of the burnout of the solid charge by 0.13%. The greater the temperature of the liquid component (the lesser the density) will be, the slower the components will be expended. The time of the expenditure of the propellant components increases with an increase in the temperature, but the rate of this increase in the components will be different (figure 5.5).

If the engine is designed for operation with $t=t_{ном}$, and in this case the condition of the simultaneous burnout of the components is provided, then with $t>t_{ном}$ the solid component will

---

[1] The temperature effect of the surrounding medium on the rate of the gasification of the solid component (in terms of coefficient u_1) is not considered by us as a result of the absence of experimental data on this question.

burn faster than will the liquid. In this case the time which limits the operating time of the entire engine will be the time of the burnout of this (solid) component. With $t<t_{ном}$ the liquid component will burn faster, and the operating time of the engine cannot be more than the time of the burnout of this (now already liquid) component.

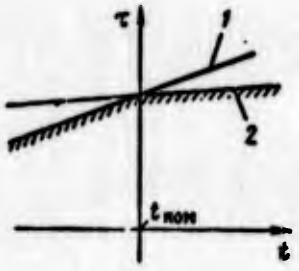

Figure 5.5. Dependence of the time of the consumption of propellant components on temperature: 1 - liquid component; 2 - solid component.

In certain cases (for example, when oxidizer is hydrogen peroxide, or when the unit of the solid component is capable of gasification without the feed of the liquid component), the engine can operate also after the burnout of one of the propellant components; however, the efficiency of its operation sharply falls, and with many fuel pairs the operation on one component generally is impossible. Therefore, the presence of the examined phenomenon should be considered in the calculations of the GRD.

5.3.2. Hybrid Rocket Engines With a Pump Feed System of the Liquid-Propellant Components

Let us examine the engine (figure 5.6) with a pump feed of the liquid component and with the gas generator based on hybrid propellant. Used as a liquid propellant component of the gas generator is the liquid-propellant component of the engine.

At point 2 part of the liquid component ($G_{жгг}$) is diverted into the gas generator. The remaining flow rate $G_{ж}$ at point 1 is divided into components $G_{ж.г}$ and $G_{ж.д}$ directed correspondingly into the head of the combustion chamber and into the afterburner.

The system of equations of this engine includes:

a) two equations of the engine chamber;

b) two equations of the balance of the fluid flow rate (distribution of total flow rate on $G_{ЖГГ}$ and $G_{Ж}$ and the distribution of $G_{Ж}$ on $G_{Ж.Г}$ and $G_{Ж.Д}$);

c) six equations of the hydraulic main lines (from the tank to the pump; from the pump to point 2; from point 2 to the gas generator; from point 2 to point 1; from point 1 to the head of the chamber; from point 1 to the afterburner);

d) six equations of the balance of pressures in these main lines;

e) two equations of the gas generator;

f) two equations of the pump;

g) the equation of the turbine;

h) the equation of the balance of powers of the turbine unit.

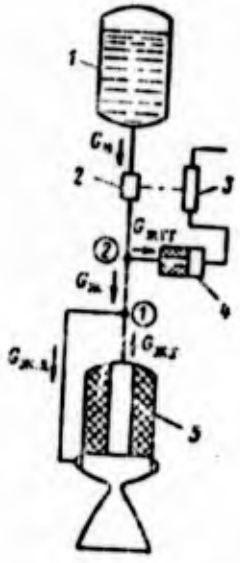

Figure 5.6. Diagram of a GRD with a pump feed system of the liquid component: 1 - tank; 2 - pump; 3 - turbine; 4 - gas generator; 5 - chamber.

Thus the system of equations comprise in this case 22 equations. The unknowns which can be found from this system are the deviations of pressures in the chamber, gas generator, and other characteristic points of the design of the engine; deviations of all components of the flow rate of the liquid component and gas formation of the charge; deviations of power, frequency of rotation of the TNA [THA - turbopump unit], and so on.

Accepted as the external and internal disturbances (factors) are the same factors as in the foregoing example and also deviations of the design parameters of the pump, turbine and gas generator.

The values of coefficients in equations which describe the operation of the GRD of the examined design are completely determined by values of the following independent dimensionless coefficients, exponents and relations:

$$K;\ \bar{\zeta};\ \nu;\ \bar{\varphi};\ \operatorname{tg}\beta_{\text{н}}/\operatorname{tg}\alpha_{\text{н}};\ \operatorname{tg}\beta_{\text{т}}/\operatorname{tg}\alpha_{\text{т}};\ \bar{A}_{\text{т}};\ n_{\text{т}};\ \pi_{\text{т}};$$
$$\alpha_{\text{к.с}}=G_{\text{ж}}/G_{\text{в}};\ K_{\text{гг}};\ \bar{\zeta};\ \bar{p}_{\text{к}}/\Delta\bar{p}_{i};\ \Delta\bar{p}_{\text{т}}/\Delta\bar{p}_{j}.$$

where Δp_i and Δp_j are the pressure differentials on characteristic sections of the main lines.

Table 5.2 shows the coefficients of the effect for a GRD with the following initial characteristics:

$$\bar{p}_{\text{к}}=100\cdot10^{5}\ \text{Pa};\ \nu=0;\ \bar{\varphi}=0{,}8;\ \bar{A}_{\text{т}}=0{,}75;\ \operatorname{tg}\beta_{\text{н}}/\operatorname{tg}\alpha_{\text{н}}=-0{,}25;$$
$$\bar{\beta}=0{,}65;\ \operatorname{tg}\beta_{\text{т}}/\operatorname{tg}\alpha_{\text{т}}=0;\ \bar{K}_{\text{гг}}=40;\ \bar{\alpha}_{\text{к.с}}=0{,}97;\ \bar{p}_{\text{б}}=5{,}5\cdot10^{5}\ \text{Pa};$$
$$\Delta\bar{p}_{\text{б}-\text{н}}=0{,}5\cdot10^{5}\ \text{Pa};\ \Delta\bar{p}_{\text{н}-2}=2\cdot10^{5}\ \text{Pa};\ \bar{p}_{\text{г}}=70\cdot10^{5}\ \text{Pa};\ \Delta\bar{p}_{1-\text{к.а}}=$$
$$=\Delta\bar{p}_{1-\text{к.с}}=10\cdot10^{5}\ \text{Pa};\ \bar{K}=5.$$

According to results of the calculations given in table 5.2, it is possible, in particular, to conclude that for this engine:

a) the flow rate of the liquid component is most greatly affected by the characteristics of the pump and turbine and also the density of the liquid component; noticeable also is the effect

of the coefficient of hydraulic friction of the main line of the feed of the liquid-propellant component in the gas generator, which can be used for the adjustment and regulation of the engine;

Table 5.2

No	Disturbance	Deviations of parameters per unit of deviation of the disturbance factor			
		$\delta p_к$	$\delta G_ж$	$\delta G_т$	δK
1	$\delta F_{кр}$	−1,000	−0,018	0	−0,018
2	$\delta_{\bar{г}с}$	−1,000	−0,018	0	−0,018
3	δL	+0,178	+0,003	+1,066	−1,063
4	δu_1	+0,178	+0,003	+1,066	−1,063
5	$\delta Q_т$	+0,178	+0,003	+1,066	−1,063
6	δd	−0,053	−0,001	−0,321	+0,320
7	$\delta F_{кр.т}$	+0,100	+0,118	+0,067	+0,041
8	$\delta F_{ст}$	+0,307	+0,325	+0,205	+0,120
9	$\delta F_{с.т}$	+0,100	+0,118	+0,068	+0,050
10	$\delta L_т$	+0,016	+0,017	+0,011	+0,006
11	$\delta u_{1т}$	+0,016	+0,017	+0,011	+0,006
12	$\delta Q_{т.с}$	+0,016	+0,017	+0,011	+0,006
13	$\delta d_т$	−0,005	−0,005	−0,003	−0,002
14	δH_0	−0,341	−0,363	−0,227	−0,136
15	$\delta \eta_ж$	+1,023	+1,084	+0,685	+0,409
16	$\delta \eta_т$	+1,023	+1,084	+0,685	+0,409
17	$\delta f_б$	+0,030	+0,032	+0,020	+0,012
18	$\delta_{б-ж}$	−0,030	−0,003	−0,002	−0,001
19	$\delta_{ж-2}$	−0,012	−0,012	−0,008	−0,004
20	δ_{2-1}	0	+0,002	+0,001	+0,001
21	$\delta_{1-к.с}$	−0,010	+0,001	−0,062	+0,062
22	$\delta_{1-к.з}$	+0,002	0	+0,012	−0,012
23	$\delta_{с-гг}$	−0,115	−0,155	−0,097	−0,058
24	$\delta_{2ж}$	+0,974	+1,011	+0,650	+0,390

b) the flow rate of the solid component is most perceptible to deviations of the charge, rate of gasification and density of the component. The effect of these deviations on $G_т$ in the GRD with the pump fuel feed is more considerable than it is in a GRD with the pressure feed of the liquid component (compare tables 5.2 and 5.1). This is explained by the fact that in this case the flow rate of the liquid component is less perceptible to a pressure change in the chamber, and therefore its change cannot, in the same degree as in the GRD with a pressure feed system, compensate for a change in the gas formation of the charge;

c) the flow rate of the solid component (just as for the liquid) is perceptible to changes in the pump and turbine performance, which is connected with the effect of the flow rate of the liquid component on the gas formation of the charge;

d) under certain conditions (the presence of δu_1; $\delta \rho_т$; δL; $\delta \eta_н$; $\delta \eta_т$, etc.) considerable change in the correlation coefficient of the propellant component flow occurs;

e) deviations of flow rates of the liquid and solid components depend differently on the density (and, therefore, on temperature) of the liquid component, which, as in the case of the GRD with a pressure feed system, can cause the nonsimultaneous burnout of the propellant components.

5.4. ADJUSTMENT OF THE HYBRID ROCKET ENGINE

The scattering of parameters of the engine worsens its characteristics, which, naturally, are always selected at the optimum for the calculated system. In connection with this for the ZhRD [ЖРД - liquid-propellant rocket engine] and RDTT the methods of a reduction in the scattering of their parameters (methods of adjustment) are developed.

For an engine which operates on solid fuel, the adjustment, as is known, is carried out by a change in the nozzle throat area before the beginning of the engine operation, and for a liquid-propellant rocket engine - by a change in the hydraulic friction in main lines of the fuel feed. For the GRD both methods of adjustment are possible; however, in design considerations an adjustment by a change in the cross section of the nozzle is very inconvenient, and as a basic method of the adjustment, just as for the ZhRD, it is advantageous to accept the adjustment by a friction change in main lines of the feed of the liquid component.

Since understood by adjustment is the totality of the operations the purpose of which is the reduction to a minimum of the scattering of any one (or several) parameter of the engine, then depending on the stated purpose there can be the following forms of adjustment:

a) adjustment for the purpose of the minimization of scattering of pressure in the chamber $p_к$;

b) adjustment for the purpose of the minimization of scattering of thrust of the engine P;

c) adjustment for the purpose of the minimization of scattering of flow rates of components (or any component - $G_т$ or $G_н$);

d) adjustment for the purpose of the minimization of spreading of the relationship of flow rates of components K and so on.

The methods of adjustment and its results to a great degree depend on the specific features of the design and even on units of the rocket engine. In connection with this, let us examine only the most general positions with respect to the adjustment of the GRD, i.e., those which remain identical for a sufficiently wide class of these engines.

The possibilities of adjustment of the GRD are set according to the system of equations of the following form:

$$\Delta p_к = \sum_{i=1}^{n} b'_{p_к} \Delta i + \sum_{j=1}^{m} c'_{p_к} \Delta j; \tag{5.20}$$

$$\Delta G_н = \sum_{i=1}^{n} b'_{G_н} \Delta i + \sum_{j=1}^{m} c b_{G_н} \Delta j; \tag{5.21}$$

$$\Delta G_т = \sum_{i=1}^{n} b'_{G_т} \Delta i + \sum_{j=1}^{m} c b_{G_т} \Delta j; \tag{5.22}$$

$$\Delta K = \sum_{i=1}^{n} b'_K \Delta i + \sum_{j=1}^{m} c'_K \Delta j. \tag{5.23}$$

where n is the number of internal disturbances m - the number of external disturbances; δi - internal disturbance; δj - external disturbance; b_i, c_i - coefficients of the effect of the internal or external disturbance on the appropriate parameter respectively.

Equations (5.20)-(5.23) are obtained from the system of static equations of the engine components in small deviations [for example, from the system of equations (5.19) for a GRD with a pressure feed system of the liquid component]. In this case the system can be simplified by means of the elimination from it of those disturbances which with adjustment it is not proposed (or is impossible) to consider. Since with adjustment only some (basic measured) disturbances can be considered the number of terms in equations of the system can be reduced very substantially.

5.4.1. Adjustment of the Hybrid Rocket Engine With the Pressure Feed System of the Liquid Component (See Figure 5.3)

5.4.1.1. Adjustment for the Purpose of Minimization of the Spreading of Pressure in the Chamber

The adjustment can be produced by a change in the hydraulic friction of any of the main lines of the engine. It is most convenient (since this causes less deviation in K) to produce a change in the hydraulic friction either on the section "tank-point 1" (see figure 5.3) or on the section "point 1-head of the combustion chamber", i.e., with a change in $\delta\xi_{б-1}$ and $\delta\xi_{1-к.с}$. Let us suppose that an adjustment according to the first version is selected. Then, assuming that $\delta p_к = 0$, from equation (5.20) we find the condition of the adjustment:

$$\delta\xi_{б-1} = -\frac{1}{b^{\xi_{б-1}}_{p_к}}\left(\sum_{i=1}^{s} b^{i}_{p_к}\delta i' + \sum_{j=1}^{t} c^{j}_{p_к}\delta j'\right), \qquad (5.24)$$

where s and t are the quantities of the internal and external

disturbances which are considered in the adjustment; $\delta i'$ and $\delta j'$ are the disturbances considered.

By introducing the measured values of the considered disturbances $\delta i'$ and $\delta j'$ into equation (5.24), we determine the value $\delta\xi_{б-1}$ required for the compensation of these disturbances. Since the nominal value of hydraulic friction $\bar{\xi}_{б-1}$ is known, from $\delta\xi_{б-1}=(\bar{\xi}_{б-1}-\xi_{б-1})/\bar{\xi}_{б-1}$ we find that value of the friction $\xi_{б-1}=\bar{\xi}_{б-1}(1+\delta\xi_{б-1})$ which should be had by the hydraulic main line in order that the pressure in the chamber would be maintained at the necessary level. The required friction of the main line is provided, for example, by the installation in it of a throttle of definite dimension.

Although condition (5.24) is obtained on the assumption that $\delta p_к$ in equation (5.20) is equal to zero, in actuality the adjustment cannot insure the full elimination of the spreading of pressure in the chamber. This is explained by the fact that equation (5.20) does not consider all the disturbances which affect $p_к$; it is extremely difficult to consider (measure) part of them, and some (for example, $\delta\phi_с$) are virtually impossible. Furthermore, all the measurements of the disturbances are implemented with errors, which makes unavoidable the retention of the effect on $p_к$ of those disturbances which with adjustment are considered (true, to a lesser degree, than without adjustment, since the errors of measurement are less than the measured values).

If we designate the errors of measurement of the considered disturbances by symbols $\delta i''$ and $\delta j''$, then the maximum spreading of pressure in the chamber, under the assumption of the independence of the action of the disturbances, will be

$$\delta p_{к\ пред}=\pm\sqrt{\sum_{i=1}^{n-k}(b'_{p_к}\delta i)^2+\sum_{i=1}^{k}(c'_{p_к}\delta i'')^2+\sum_{j=1}^{m-l}(c'_{p_к}\delta j)^2+\sum_{j=1}^{l}(c'_{p_к}\delta j'')^2}. \qquad (5.25)$$

The scattering of the remaining parameters ($G_н$, $G_т$, K) can

be determined by relations whose form we show in the example of relation for the spreading of the flow rate of the liquid component:

$$\delta G_{\text{ж.прел}} = \left| \sum_{i=1}^{n} \left(b^{i}_{G_{\text{ж}}} - \frac{b^{i_{б-1}}_{G_{\text{ж}}}}{b^{i_{б-1}}_{p_{\text{ж}}}} b^{i}_{p_{\text{ж}}} \right) \delta i'' + \right.$$

$$\left. + \sum_{j=1}^{l} \left(c^{j}_{G_{\text{ж}}} - \frac{c^{i_{б-1}}_{G_{\text{ж}}}}{c^{i_{б-1}}_{p_{\text{ж}}}} c^{j}_{p_{\text{ж}}} \right) \delta j'' \right| +$$

$$+ \left| \sqrt{\sum_{i=1}^{n-1} (b^{i}_{G_{\text{ж}}} \delta i \beta + \sum_{i=1}^{n} (b^{i}_{G_{\text{ж}}} \delta i'' \beta + \sum_{j=1}^{m-1} (c^{j}_{G_{\text{ж}}} \delta j \beta + \sum_{j=1}^{l} (c^{j}_{G_{\text{ж}}} \delta j'' \beta} \right|. \qquad (5.26)$$

5.4.1.2. Adjustment for the Purpose of Minimization of the Spreading of Pressure in the Chamber and the Spreading of the Relationship of flow rates of the Components

With the adjustment of the engine from two parameters, it is necessary to have two controlling effects. Virtually they can be any two of the three hydraulic resistances ($\xi_{б-1}$, $\xi_{1-к.д}$, $\xi_{1-к.с}$) available in the engine. Let us suppose that as adjusting elements $\xi_{б-1}$ and $\xi_{1-к.д}$ are selected. Assuming that in equations (5.20) and (5.23) $\delta p_{к}=0$ and $\delta K=0$ respectively, we find the conditions of adjustment in the form of the equations

$$\left.\begin{aligned} \sum_{i=1}^{n} b^{i}_{p_{\text{ж}}} \delta i + \sum_{j=1}^{m} c^{j}_{p_{\text{ж}}} \delta j = 0; \\ \sum_{i=1}^{n} b^{i}_{K} \delta i + \sum_{j=1}^{m} c^{j}_{K} \delta j = 0. \end{aligned}\right\} \qquad (5.27)$$

By solving the system of equations (5.27) relative to $\delta\xi_{б-1}$ and $\delta\xi_{1-к.д}$, we find the required values of deviations of the hydraulic friction:

$$\delta\xi_{б-1} =$$

$$= \frac{b^{i_{1-к.д}}_{K} \sum_{i=1}^{n} b^{i}_{p_{\text{ж}}} \delta i' - b^{i_{1-к.д}}_{p_{\text{ж}}} \sum_{i=1}^{n} b^{i}_{K} \delta i' + b^{i_{1-к.д}}_{K} \sum_{j=1}^{l} c^{j}_{p_{\text{ж}}} \delta j' - b^{i_{1-к.д}}_{p_{\text{ж}}} \sum_{i=1}^{l} c^{j}_{p_{\text{ж}}} \delta j'}{b^{i_{1-к.д}}_{p_{\text{ж}}} b^{i_{б-1}}_{K} - b^{i_{б-1}}_{p_{\text{ж}}} b^{i_{1-к.д}}_{K}}; \qquad (5.28)$$

$$\delta\xi_{1-\kappa.1} = \frac{b_{p_\kappa}^{i_0-1}\sum_{i=1}^{n} b_K^i \delta i' - b_K^{i_0-1}\sum_{i=1}^{n} b_{p_\kappa}^i \delta i' + b_{p_\kappa}^{i_0-1}\sum_{j=1}^{l} c_{p_\kappa}^j \delta j' - b_K^{i_0-1}\sum_{j=1}^{l} c_{p_\kappa}^j \delta j'}{b_{p_\kappa}^{i_1-\kappa.1} b_K^{i_0-1} - b_{p_\kappa}^{i_0-1} b_K^{i_1-\kappa.1}}. \quad (5.29)$$

Values of the maximum spreading of pressure and the relationship of the propellant component flow are found by relations of form (5.25).

5.4.2. Adjustment of the GRD With a Pump Feed System

The approach to the solution of the problem of adjustment of the GRD and the calculation of the maximum scattering of the parameters after the adjustment remains the same as that for a GRD with a pressure feed system of the liquid component. As a controlling effect it is possible to select a change in any of the hydraulic frictions of main lines of the engine.

In the engine where the gas generator operation on a propellant which includes a liquid component, it is most advantageous to carry out adjustment by a change in the hydraulic friction of the main line of the feed of this component into the gas generator, since the coefficient of the effect of this disturbance ($\delta\xi_{2-гг}$) on the parameters of the engine (see table 5.2) is considerably more than the coefficients characteristic for the friction of other sections.

5.5. STATIC CHARACTERISTICS OF THE RDTT OF SEPARATE LOADING

The system of equations which describe the operation of the RDTT of separate loading with a bypass of part of the gas from the first chamber in the pre-nozzle space of the second chamber (figure 5.7) includes equations of two chambers and equations of the propellant component flow through the pipelines and nozzle.

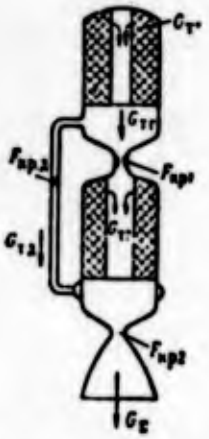

Figure 5.7. Diagram of an RDTT of separate loading (RDTT RS [PC - rocket missile]).

In this case the equation of the gas generator corresponds to the equation of the standard RDTT, and the equation of the thrust chamber - to the equation of the chamber of the hybrid rocket engine. The system of equations includes the following:

equation of gas inflow in the gas generator

$$G_{т1}=u_1 p_{к1}^{n_1} s_1 \varrho_1; \qquad (5.30)$$

equation of the nozzle flow of the gas generator

$$G_{т.г}=\frac{\varphi_{c1} b_1 p_{к1} F_{кр1}}{\sqrt{RT_{к1}}}; \qquad (5.31)$$

equation of the flow through the gas conductor of the bypass

$$G_{т.п}=\frac{\varphi_{с.п} b_1 p_{к1} F_{кр т}}{\sqrt{RT_{к1}}}; \qquad (5.32)$$

equation of the balance of flow rates from the gas generator

$$G_{т1}=G_{т.г}+G_{т.п}; \qquad (5.33)$$

equation of the gas inflow in the thrust chamber

$$G_{т2}=\left[4^{\beta}\pi^{1-\beta}(1-\beta)\,u_2^{\beta}\varrho_{т2}L_2 d_2^{1-2\beta} p_{к2}^{n_2\beta}+G_{т.г}^{1-\beta}\right]^{\frac{1}{1-\beta}}-G_{т.г}; \qquad (5.34)$$

equation of flow through the nozzle of the thrust chamber

$$G_{с}=\frac{\varphi_{с2} b_2 p_{к2} F_{кр2}}{\sqrt{RT_{к2}}}; \qquad (5.35)$$

equation of the balance of flow rates of components from the thrust chamber

$$G_{\Sigma} = G_{\tau 1} + G_{\tau 2}; \tag{5.36}$$

correlation coefficient of flow rates of components in the thrust chamber

$$K = \frac{G_{\tau 2}}{G_{\tau 1}}; \tag{5.37}$$

coefficient of bypass

$$\varphi = \frac{G_{\tau.r}}{G_{\tau 1}}. \tag{5.38}$$

In the case of the subcritical outflow of combustion products from the gas generator into the thrust chamber, equation (5.31) takes the form

$$G_{\tau.r} = \frac{\varphi_{c1} p_{\kappa 1} F_{c1}}{\sqrt{RT_{\kappa 1}}} \sqrt{\frac{2n}{n-1}\left[\left(\frac{1}{\pi_{c1}}\right)^{2/n} - \left(\frac{1}{\pi_{c1}}\right)^{\frac{n+1}{n}}\right]},$$

where $\pi_{c1} = p_{\kappa 1}/p_{\kappa 2}$.

For the RDTT RS, which has the gas conductor of the bypass, the system of equations will consist of equations (5.30)-(5.37).

In linearlized form equations (5.30)-(5.36) will be written as follows:

$$a^{G_{\tau 1}}_{\delta.11} \delta G_{\tau 1} + a^{p_{\kappa 1}}_{\delta.11} \delta p_{\kappa 1} + b^{s_1}_{\delta.11} \delta s_1 + b^{\pi_1}_{\delta.11} \delta \pi_1 + b^{\varphi_{\tau 1}}_{\delta.11} \delta \varphi_{\tau 1} = 0, \tag{5.39}$$

where $a^{G_{\tau 1}}_{\delta.11} = -1;\ a^{p_{\kappa 1}}_{\delta.11} = \nu_1;\ b^{\pi_1}_{\delta.11} = b^{s_1}_{\delta.11} = b^{\varphi_{\tau 1}}_{\delta.11} = 1.$

For the supercritical outflow

$$a^{G_{\text{т.г}}}_{\text{к.с1}}\delta G_{\text{т.г}}+a^{p_{\text{к1}}}_{\text{к.с1}}\delta p_{\text{к1}}+b^{\bar{\tau}_{\text{с1}}}_{\text{к.с1}}\delta\bar{\tau}_{\text{с1}}+b^{F_{\text{кр1}}}_{\text{к.с1}}\delta F_{\text{кр1}}=0, \tag{5.40}$$

where $a^{G_{\text{т.г}}}_{\text{к.с1}}=-1;\ a^{p_{\text{к1}}}_{\text{к.с1}}=b^{\bar{\tau}_{\text{с1}}}_{\text{к.с1}}=b^{F_{\text{кр1}}}_{\text{к.с1}}=1.$

For the subcritical outflow

$$a^{G_{\text{т.г}}}_{\text{к.с1}}\delta G_{\text{т.г}}+a^{p_{\text{к1}}}_{\text{к.с1}}\delta p_{\text{к1}}+a^{p_{\text{к2}}}_{\text{к.с1}}\delta p_{\text{к2}}+b^{\bar{\tau}_{\text{с1}}}_{\text{к.с1}}\delta\bar{\tau}_{\text{с1}}+b^{F_{\text{с1}}}_{\text{к.с1}}\delta F_{\text{с1}}=0, \tag{5.41}$$

where $a^{G_{\text{т.г}}}_{\text{к.с1}}=-1;\ b^{\bar{\tau}_{\text{с1}}}_{\text{к.с1}}=b^{F_{\text{с1}}}_{\text{к.с1}}=1;\ a^{p_{\text{к1}}}_{\text{к.с}}=1+\frac{1}{2n}\,\frac{(n+1)\bar{\pi}_{\text{с1}}^{2/n}-2\bar{\pi}_{\text{с1}}^{\frac{n+1}{n}}}{\bar{\pi}_{\text{с1}}^{\frac{n+1}{n}}-\bar{\pi}_{\text{с1}}^{2/n}};$

$$a^{p_{\text{к2}}}_{\text{к.с1}}=-\frac{1}{2n}-\frac{(n+1)\bar{\pi}_{\text{с1}}^{2/n}-2\bar{\pi}_{\text{с1}}^{\frac{n+1}{n}}}{\bar{\pi}_{\text{с1}}^{\frac{n+1}{n}}-\bar{\pi}_{\text{с1}}^{2/n}};$$

$$a^{G_{\text{т.т}}}_{\text{т.с}}\delta G_{\text{т.т}}+a^{p_{\text{к1}}}_{\text{т.т}}\delta p_{\text{к1}}+b^{\bar{\tau}_{\text{с.т}}}_{\text{т.т}}\delta\bar{\tau}_{\text{с.т}}+b^{F_{\text{кр.т}}}_{\text{т.т}}\delta F_{\text{кр.т}}=0, \tag{5.42}$$

where $a^{G_{\text{т.т}}}_{\text{т.т}}=-1;\ a^{p_{\text{к1}}}_{\text{т.т}}=b^{\bar{\tau}_{\text{с.т}}}_{\text{т.т}}=b^{F_{\text{кр.т}}}_{\text{т.т}}=1;$

$$a^{G_{\text{т1}}}_{G_{\text{т1}}}\delta G_{\text{т1}}+a^{G_{\text{т.г}}}_{G_{\text{т1}}}\delta G_{\text{т.г}}+a^{G_{\text{т.т}}}_{G_{\text{т1}}}\delta G_{\text{т.т}}=0, \tag{5.43}$$

where $a^{G_{\text{т1}}}_{G_{\text{т1}}}=-1;\ a^{G_{\text{т.г}}}_{G_{\text{т1}}}=\bar{\gamma};\ a^{G_{\text{т.т}}}_{G_{\text{т1}}}=1-\bar{\gamma};$

$$a^{G_{\text{т.т}}}_{\text{б.т2}}\delta G_{\text{т2}}+a^{G_{\text{т.г}}}_{\text{б.т2}}\delta G_{\text{т.г}}+a^{p_{\text{к2}}}_{\text{б.т2}}\delta p_{\text{к2}}+b^{d_{\text{в}}}_{\text{б.т2}}\delta d_{\text{в}}+b^{L_{\text{в}}}_{\text{б.т2}}\delta L_{\text{в}}+$$

$$+b^{u_{\text{в}}}_{\text{б.т2}}\delta u_{\text{в}}+b^{Q_{\text{т.т}}}_{\text{б.т2}}\delta Q_{\text{т2}}=0, \tag{5.44}$$

where $a^{G_{\text{т2}}}_{\text{б.т2}}=-1;\ a^{G_{\text{т.г}}}_{\text{б.т2}}=1-f(\bar{\varphi},\bar{K});\ a^{p_{\text{к2}}}_{\text{б.т2}}=\frac{\nu_2}{1-\beta}\,f(\bar{\varphi},\bar{K});$

$$b^{d_{\text{в}}}_{\text{б.т2}}=-\frac{2\beta-1}{1-\beta}\,f(\bar{\varphi},\bar{K});\ b^{L_{\text{в}}}_{\text{б.т2}}=b^{u_{\text{в}}}_{\text{б.т2}}=b^{Q_{\text{т2}}}_{\text{б.т2}}=\frac{1}{1-\beta}\,f(\bar{\varphi},\bar{K});$$

$$a^{G_{\text{в}}}_{\text{к.с2}}\delta G_{\text{в}}+a^{p_{\text{к2}}}_{\text{к.с2}}\delta p_{\text{к2}}+b^{F_{\text{кр2}}}_{\text{к.с2}}\delta F_{\text{кр2}}+b^{\bar{\tau}_{\text{с2}}}_{\text{к.с2}}\delta\bar{\tau}_{\text{с2}}=0, \tag{5.45}$$

where $a^{G_{\text{в}}}_{\text{к.с2}}=-1;\ a^{p_{\text{к2}}}_{\text{к.с2}}=b^{F_{\text{кр2}}}_{\text{к.с2}}=b^{\bar{\tau}_{\text{с2}}}_{\text{к.с2}}=1;$

$$a^{G_{\text{в}}}_{G_{\text{в}}}\delta G_{\text{в}}+a^{G_{\text{т1}}}_{G_{\text{в}}}\delta G_{\text{т1}}+a^{G_{\text{т2}}}_{G_{\text{в}}}\delta G_{\text{т2}}=0, \tag{5.46}$$

where $a^{G_{\text{в}}}_{G_{\text{в}}}=-1;\ a^{G_{\text{т1}}}_{G_{\text{в}}}=\frac{\bar{K}}{1+\bar{K}};\ a^{G_{\text{т2}}}_{G_{\text{в}}}=\frac{1}{1+\bar{K}};$

$$f(\bar{\varphi},\bar{K})=(1+\bar{\varphi}\bar{K})\left[1-\left(\frac{\bar{\varphi}\bar{K}}{1+\bar{\varphi}\bar{K}}\right)^{1-\beta}\right]. \tag{5.47}$$

By solving the system of linearized equations, let us find the coefficients of the effect (transfer) of the corresponding disturbances on the parameters of operation of the RDTT RS.

Table 5.3 gives expressions for determining these coefficients depending on the dimensionless relationships for the RDTT RS without the gas conductor of the bypass. Introduced into the coefficients of Table 5.3 are the following additional notations:

$$\lambda=\frac{\nu_1(1-\beta)(1+\bar{R})}{(1+\chi-\nu_1)[(1-\beta)(1+\bar{R})-\nu_2 f(\bar{R})]-\chi\nu_1(1-f(\bar{R})+\bar{R})}; \qquad (5.48)$$

$$\chi=\frac{1}{2n}\frac{(n+1)\bar{\pi}_{c1}^{2/n}-2\bar{\pi}_{c1}^{\frac{n+1}{n}}}{\bar{\pi}_{c1}^{\frac{n+1}{n}}-\bar{\pi}_{c1}^{2/n}};$$

$$f(\bar{R})=(1+\bar{R})\left[1-\left(\frac{\bar{R}}{1+\bar{R}}\right)^{1-\beta}\right].$$

Table 3

Parameters / Disturbances	δG_{v1}	δG_{v2}	δp_{*1}	δp_{*2}	δK
δF_{sp1} $\delta\varphi_{c1}$	$-\frac{\nu_1}{1-\nu_1}$	$-\frac{\nu_1}{1-\nu_1}(1-f(\bar{R}))$	$-\frac{1}{1-\nu_1}$	$-\frac{\nu_1}{1-\nu_1}\left(\frac{\bar{R}}{1+\bar{R}}\right)^{1-\beta}$	$-\frac{\nu_1}{1-\nu_1}f(\bar{R})$
δu_1 δs_1 δQ_{v1}	$\frac{1}{1-\nu_1}$	$\frac{1}{1-\nu_1}(1-f(\bar{R}))$	$\frac{1}{1-\nu_1}$	$-\frac{1}{1-\nu_1}\left(\frac{\bar{R}}{1+\bar{R}}\right)^{1-\beta}$	$\frac{1}{1-\nu_1}f(\bar{R})$
δF_{sp2} $\delta\varphi_{c2}$	0	0	0	-1	0
δL_2 δu_2 δQ_{v2}	0	$\frac{f(\bar{R})}{1-\beta}$	0	$-\frac{1}{1-\beta}\left[1-\left(\frac{\bar{R}}{1+\bar{R}}\right)^{1-\beta}\right]$	$\frac{f(\bar{R})}{1-\beta}$
δd_2	0	$\frac{2\beta-1}{1-\beta}f(\bar{R})$	0	$-\frac{2\beta-1}{1-\beta}\left[1-\left(\frac{\bar{R}}{1+\bar{R}}\right)^{1-\beta}\right]$	$\frac{2\beta-1}{1-\beta}f(\bar{R})$

The coefficients in Table 5.3 correspond to the subcritical case of the outflow of combustion products from the first chamber.

For the supercritical outflow when $\pi_{c1}=\frac{p_{*1}}{p_{*2}}=\left(\frac{n+1}{2}\right)^{\frac{n}{n-1}}$, the

coefficient χ vanishes and expressions for determining the coefficients are simplified.

Even simpler become expressions for determining the coefficients if the unit in the second chamber is non-self-burning, i.e., with $\nu_2=0$.

Table 5.4

Parameters / Disturbances	$\delta\sigma_{v1}$	$\delta\sigma_{v2}$	$\delta\rho_{s1}$	$\delta\rho_{s2}$	δK
δF_{cr1} $\delta\varphi_{c1}$	$-\lambda\left(1-\frac{\nu_2}{1-\beta}\frac{f(\bar K)}{1+\bar K}\right)$	$-\lambda\left(1+\frac{\nu_2}{1-\beta}\times\right.$ $\left.\times\frac{\bar K f(\bar K)}{1+\bar K}-f(\bar K)\right)$	$-\frac{\lambda}{\nu_1}\left(1-\frac{\nu_2}{1-\beta}\frac{f(\bar K)}{1+\bar K}\right)$	$-\lambda\left(1-\frac{f(\bar K)}{1+\bar K}\right)$	$-\lambda\left(1-\frac{\nu_2}{1-\beta}\right)f(\bar K)$
δm_1 δs_1 $\delta\sigma_{v1}$	$\lambda\frac{1+\chi}{\nu_1}\times$ $\times\left(1-\frac{\nu_2}{1-\beta}\frac{f(\bar K)}{1+\bar K}\right)$	$\lambda\frac{1+\chi}{\nu_1}\left(1+\frac{\nu_2}{1-\beta}\times\right.$ $\left.\times\frac{\bar K f(\bar K)}{1+\bar K}-f(\bar K)\right)$	$\frac{\lambda}{\nu_1}\frac{1+\chi}{\nu_1}\left(1-\frac{\nu_2}{1-\beta}\times\right.$ $\left.\times\frac{f(\bar K)}{1+\bar K}\right)-\frac{1}{\nu_1}$	$\lambda\frac{1+\chi}{\nu_1}\left(1-\frac{f(\bar K)}{1+\bar K}\right)$	$\lambda\frac{1+\chi}{\nu_1}\left(1-\frac{\nu_2}{1-\beta}\right)\times$ $\times f(\bar K)$
δF_{cr2} $\delta\varphi_{c2}$	$-\lambda\chi$	$-\lambda\left[\frac{1+\chi-\nu_1}{\nu_1(1-\beta)}\times\right.$ $\left.\times\nu_2 f(\bar K)+\chi(1-f(\bar K))\right]$	$-\frac{\lambda\chi}{\nu_1}$	$-\lambda\frac{1+\chi-\nu_1}{\nu_1}$	$\lambda\left[\frac{1+\chi-\nu_1}{\nu_1(1-\beta)}\nu_2-\chi\right]\times$ $\times f(\bar K)$
δL_2 δm_2 $\delta\sigma_{v2}$	$\frac{\lambda\chi}{1-\beta}\frac{f(\bar K)}{1+\bar K}$	$\lambda\left(\frac{1+\chi-\nu_1}{\nu_1}-\right.$ $\left.-\chi\frac{\bar K}{1+\bar K}\right)\frac{f(\bar K)}{1-\beta}$	$\frac{\lambda}{\nu_1}\frac{\chi}{1-\beta}\frac{f(\bar K)}{1+\bar K}$	$\lambda\frac{1+\chi-\nu_1}{\nu_1(1-\beta)}\frac{f(\bar K)}{1+\bar K}$	$-\frac{\lambda}{\nu_1}\times$ $\times\frac{(1+\chi)(1-\nu_1)}{1-\beta}f(\bar K)$
δd_2	$-\frac{\lambda\chi}{1-\beta}(2\beta-1)\frac{f(\bar K)}{1+\bar K}$	$-\lambda\left(\frac{1+\chi-\nu_1}{\nu_1}-\right.$ $\left.-\chi\frac{\bar K}{1+\bar K}\right)\frac{2\beta-1}{1-\beta}f(\bar K)$	$-\frac{\lambda\chi}{\nu_1}\frac{2\beta-1}{1-\beta}\frac{f(\bar K)}{1+\bar K}$	$-\lambda\frac{1+\chi-\nu_1}{\nu_1(1-\beta)}\times$ $\times(2\beta-1)\frac{f(\bar K)}{1+\bar K}$	$\frac{\lambda}{\nu_1}\frac{(1+\chi)(1-\nu_1)}{1-\beta}\times$ $\times(2\beta-1)\ f(\bar K)$

Table 5.4 gives expressions for determining these coefficients.

Given below is table 5.5 of results of the calculation of coefficients for the RDTT RS, which has the following dimensionless characteristics: $\nu_1=0,3$; $\bar\pi_{c1}=1,25$; $n=1,2$; $\bar K=3$; $\nu_2=0,2$; $\beta=0,67$.

For a comparison the calculations of coefficients of the supercritical outflow of combustion products from the gas generator ($\bar\pi_{c1}=2.5$).

According to results of the calculations given in table 5.5, in particular, it can be concluded that:

Table 5

Disturbances	Parameters							
	$\delta\sigma_{v1}$		$\delta\sigma_{v2}$		δp_{k2}		δK	
	$\bar{\pi}_{c1}=1,25$	$\bar{\pi}_{c1}=2,5$	$\bar{\pi}_{c1}=1,25$	$\bar{\pi}_{c1}=2,5$	$\bar{\pi}_{c1}=1,25$	$\bar{\pi}_{c1}=2,5$	$\bar{\pi}_{c1}=1,25$	$\bar{\pi}_{c1}=2,5$
δF_{kp1} $\delta\pi_{c1}$	−0,189	−0,434	−0,160	−0,368	−0,182	−0,417	−0,029	−0,066
δu_1 δs_1 δQ_{v1}	1,600	1,445	1,360	1,227	1,540	1,390	0,242	0,218
δF_{kp2} $\delta\pi_{c2}$	−0,308	0	−0,520	−0,231	−1,492	−1,070	0,212	0,231
δL_2 δu_2 δQ_{v2}	0,083	0	1,362	1,150	0,407	0,290	1,260	1,150
δd_2	−0,029	0	−0,463	−0,391	−0,138	−0,099	0,435	0,391

a) a change in the cross section of the nozzle (throttle installed in the pipeline which connects the chambers of the RDTT RS produces a change in the parameters in both chambers, whereupon in the second (thrust) engine chamber this change is somewhat weaker than that in the first; an increase in the cross section of the nozzle causes a drop in pressure and consumption of the propellant in both chambers;

b) deviations in dimensions of the charge of the gas generator or in the rate of its burning lead to a very considerable change in the parameters of the engine;

c) deviations in dimensions of the charge of the thrust chamber of area of its critical cross section produce changes in characteristics of this chamber, and with the subcritical outflow from the first chamber into the second (when the flow rate from the first chamber depends on the pressure in the second) - in characteristics of the first chamber. In this case a change in parameters of the first chamber is substantially less than the parameters of the second chamber;

d) in all the examined cases with a change in the factors which effect the operating conditions of the RDTT RS (i.e., in the presence of $\delta F_{кр1}$, δu_1, δs_1, $\delta F_{кр2}$, δu_2, etc), a change in the relationship of the flow rate of the components occurs. In certain cases (for example, under the effects of δu_2, δL_2, $\delta \rho_{т2}$, δd_2) this change can be very considerable;

e) an increase in the pressure differential in the pipeline which connects the chambers ($\bar{\pi}_{c1}$) affects the nature of the effect of different factors on parameters of the RDTT RS contradictorily: for example, the effects of $F_{кр2}$, L_2, u_2, $\rho_{т2}$ and $G_{т1}$ is weaked; however, the effect of $F_{кр}$ on these parameters is amplified;

f) the presence of the effect of the dimension of the cross section of the throttle installed in the pipeline which connects the chambers on engine characteristics makes it possible to realize both the adjustment and the regulation of the RDTT RS by a change in this cross section.

CHAPTER 6

THE CONTROL OF COMBINED ROCKET ENGINES

6.1. CONTROLLING PARAMETERS AND THE CONTROL SCHEMES OF COMBINED ROCKET ENGINES

6.1.1. Hybrid Rocket Engines With the Introduction of Liquid Only Into the Head of the Chamber

The problems and features of the control of the GRD [ГРД - hybrid rocket engine], just as for rocket engines of other types, can change to a considerable degree depending on the purpose and conditions of use of the engine.

Most typical is the control of a GRD based on thrust, i.e., the effect on the engine in the process of its operation for the purpose of a change in the thrust in the necessary manner. With constant fuel, geometry of the chamber and external pressure, the thrust is determined only by the pressure in the chamber and by the relationship of the propellant component flow:

$$P=P(p_к, K).$$

Consequently, as the controllable parameters of the engine in the case of the control of its thrust the pressure in the chamber and the relationship of flow rates of the components can be selected.

Let us note that the specific impulse depends on these parameters:

$$I = I(p_к, K).$$

For the purpose of providing for the maximum effect of the use of the engine, it is necessary to maintain value I in the process of control at as high a level as possible. At the same time it is known that the specific impulse usually depends on the relationship of the propellant component flow more greatly than on pressure (within the possible, with control, limits of the change in p and k). Furthermore, considerable changes in the relationship of the propellant component flow can lead to undesirable distinction in the times of burnout of the components. Therefore, in the majority of cases as a controlling parameter for an effect on the thrust of the GRD, it is advantageous to receive the pressure in the chamber. The relationship of the propellant component flow in the control process should be maintained as close to the optimum as possible.

As the controlling parameters, i.e., the values with the aid of which it is possible to change the pressure in the chamber, a number of the design and system parameters of the engine can be used. These parameters are established from an analysis of equations of the chamber of the GRD, the operating conditions of which determine the pressure in the chamber.

For the chamber of a GRD with the introduction of the liquid component only into the head, the equations will be such:

$$a^{p_к}_{к.с}\delta p_к + a^{G_ж}_{к.с}\delta G_ж + a^{G_т}_{к.с}\delta G_т + b^{F_{кр}}_{к.с}\delta F_{кр} + b^{\varepsilon}_{к.с}\delta\varepsilon_с + \\ + c^{T_ж}_{к.с}\delta T_ж + c^{T_т}_{к.с}\delta T_т = 0;$$

$$a^{G_т}_{б.т}\delta G_т + a^{G_ж}_{б.т}\delta G_ж + a^{p_к}_{б.т}\delta p_к + b^{u_1}_{б.т}\delta u_1 + b^{Q_т}_{б.т}\delta Q_т + \\ + b^{L}_{б.т}\delta L + b^{d}_{б.т}\delta d + c^{T_т}_{б.т}\delta T_т = 0.$$

By eliminating δG_T, from these equations we obtain

$$\delta p_к = f(\delta G_м, \delta F_{кр}, \delta u_1, \delta \varphi_c, \delta T_м, \delta T_т, \delta Q_т, \delta L, \delta d). \quad (6.1)$$

Any of the values which enter into the right side of equation (6.1) could in principle be used for an effect on pressure in the chamber. However, it is obviously impossible virtually to affect the pressure in the chamber in engine operation with a change in ϕ_c, $T_м$, $T_т$, and $\rho_т$. The dimensions of the charge of the solid component d and L in the process of the engine operation cannot be changed, and therefore these values can be used only as parameters for the programmed change in thrust, but not for its arbitrary control.

It can be concluded that for the control of thrust of the GRD with the introduction of a liquid component only into the head, the following changes can be used: the nozzle throat area of the chamber, the rate of gasification of the solid component and flow rate of the liquid component.

In turn, a change in the flow rate of the liquid component can be insured with several methods, for example, by a change in the tank pressure, by a change in the hydraulic friction of the main fuel lines, and so on.

Thus as the controlling parameters of the GRD it is possible to use the dimension of the critical cross section of the nozzle, tank pressure, hydraulic friction of the main lines, rate of gasification, and so on.

The selection of the controlling parameter is conducted by taking into account a number of criteria and values, according to which the quality of the work of the control system and the effect of its introduction on the characteristics of the entire engine are estimated. In the process of this selection the following is considered:

a) transit time;

b) value of the transfer constant;

c) the mass and overall dimensions of the controlling elements;

d) the reliability of the operation of the controlling elements;

e) the energy required for operation of the control system, etc.

It is not at present possible to estimate entirely the enumerated criteria and values in application to the control systems of the GRD, and also their effect on the engine performance in view of the absence of the necessary data on control systems of the hydrojet and elements. However, at the same time, with a high degree of reliability, being based on the experience of the development of methods and control systems of the RDTT [РДТТ - solid-propellant rocket engine] and the ZhRD [ЖРД - liquid-propellant rocket engine] it can be concluded that:

a) the control of the GRD by means of changing the nozzle throat area is possible. This control provides a high transfer constant; however, (according to the experience of the development of the RDTT) the creation of the variable-area nozzle is so complex a problem and produces such noticeable increases in the mass and reduction in the reliability of the engine that this method should be estimated as being virtually unsuitable;

b) the control of the GRD by a change in the tank pressure with the liquid propellant component (according to the experience of the development of the ZhRD) causes no design difficulties; however, by virtue the great inertia of the system, this control will be realized with such an insignificant transit time that this method of control should be rejected;

c) the control of the GRD by a change in the rate of gasification of the solid component in principle is possible, since, apparently, some methods of the effect on the rate of combustion of the solid fuel, established in the development of the RDTT, can also be used in the combined engines (for example, the effect on the rate of combustion of solid fuel by a change in the characteristics of ultrasonic oscillations of the gas column in the chamber). However, the obvious extreme complexity of this method and the noninvestigation of the corresponding processes make it possible to eliminate subsequently this method from the examination;

d) the control of the engine by a change in the hydraulic friction of the main lines of feed of the liquid component into the chamber is widely applied in a ZhRD. It is established (see [1]) that the controllable hydraulic friction in the ZhRD with pump fuel feed can be established both in the main lines which feed the components into the engine chamber and in main lines through which the component is guided into the gas generator. The use of the first version provides a short transit time and significant magnitude of the transfer constant. However, in the case of using a similar system in the ZhRD with high thrust (with a high flow rate of fuel), the control devices have a considerable mass and overall dimensions and consume much energy. In connection with this, the installation of controllable hydraulic resistances in the basic main fuel lines is recommended only for a ZhRD with low thrust; in a ZhRD with high thrust the feed of the propellant components into the gas generator is regulated.

In a ZhRD with the pressure propellant feed system, the controllable hydraulic resistances can be established, obviously, only in the main lines which feed the propellant components in the chamber.

These positions are also used for hybrid rocket engines. In connection with this, the designs of the controllable GRD's with

feed of the liquid component only into the head of the chamber, respectively, for cases of using pressure and pump feed systems can appear in the manner which is shown in figure 6.1a and 6.1b and c.

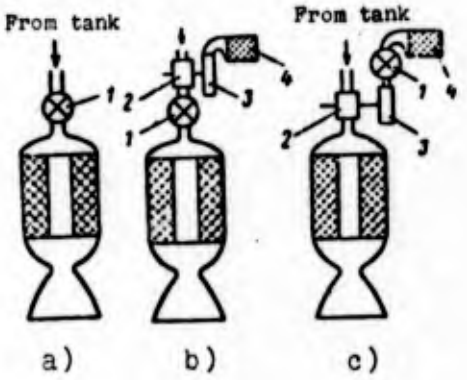

Figure 6.1. Diagrams of a GRD with the feed of the liquid component into the head of the chamber: 1 - regulator; 2 - pump; 3 - turbine; 4 - gas generator.

If it is necessary to increase thrust for engines of the first two designs (see figure 6.1a and b) the hydraulic friction created by the regulator in the main line of the feed of the liquid component is decreased; in the GRD of the third design (see figure 6.1c) the feed of the working medium into the turbine is increased. Each of these effects leads to an increase in the flow rate of the liquid component, which in turn produces an increase in the pressure and gas formation of the solid component; as a final result the thrust is increased.

Let us note that in the examined control schemes of the GRD the required change of only one parameter of the engine - thrust (pressure in the chamber) is provided, and this corresponds to the use of one controlling factor - the flow rate of the liquid component. The remaining parameters of the operating conditions are not controlled. In particular, the relationship of the flow rate of the component will be changed. In order to insure the simultaneous control of both the thrust and relationship of the propellant component flow, it would be required to use two controlling parameters, which, as was noted above, in the examined case is virtually impossible.

In the control loops of the GRD intended for a change in the flow rate of the liquid propellant component, regulators of the same design and design solutions as in the ZhRD can be used (see [43]).

6.1.2. GRD With Feed of the Liquid Component Into Head and Afterburner

For this type of GRD the operating process of the chamber is characterized by the following relations:

$$\left.\begin{aligned} &a^{p_к}_{к.с}\delta p_к + a^{G_ж}_{к.с}\delta G_ж + a^{G_т}_{к.с}\delta G_т + b^{F_{кр}}_{к.с}\delta F_{кр} + b^{r_с}_{к.с}\delta r_с + c^{T_ж}_{к.с}\delta T_ж = 0;\\ &a^{G_т}_{ф.т}\delta G_т + a^{G_{ж.г}}_{ф.т}\delta G_{ж.г} + a^{p_к}_{ф.т}\delta p_к + b^{u_1}_{ф.т}\delta u_1 + b^{G_т}_{ф.т}\delta G_т + b^{L}_{ф.т}\delta L +\\ &\quad + b^{d}_{ф.т}\delta d + c^{T_т}_{ф.т}\delta T_т = 0. \end{aligned}\right\} \qquad (6.2)$$

To those parameters which could be used as the controlling parameters for the GRD without feed into the afterburner ($G_ж$, $F_{кр}$, u_1) in this case one additional parameter is added - the flow rate of the liquid component into the head of the chamber. Since controlling the fluid flow rate into head is no more complicated than that of the general fluid flow rate into the engine, in the GRD of this design the possibility of using two controlling parameters proves to be real, and this means that it is possible to control immediately two parameters of the engine - for example, the thrust (pressure in the chamber) and relationship of the propellant component flow. A particular case can be the control of thrust in maintaining the relationship of flow rates of the components constant.

Let us note that since $G_ж = G_{ж.г} + G_{ж.г}$ and $\phi = G_{ж.г}/G_ж$, the controlling parameters can be selected as not only $G_ж$ and $G_{ж.г}$ but also generally any pair of the parameters from $G_{ж.г}$, $G_{ж.д}$ and ϕ.

The designs of the GRD for the examined case should include two regulators, which can be installed for example, in the same manner as it is shown in figure 6.2.

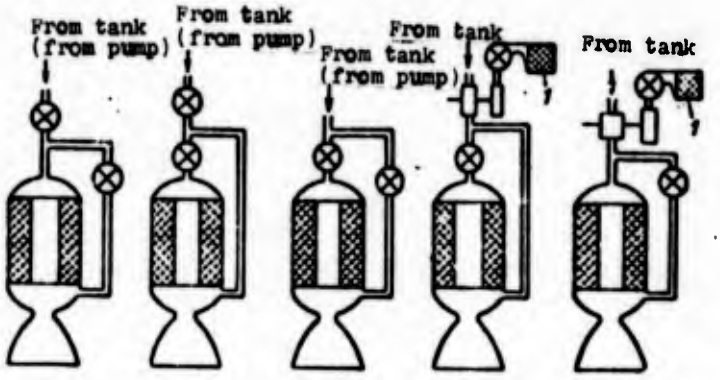

Figure 6.2. Diagrams of a GRD with feed of the component into the head and afterburner: 1 - gas generator.

In the control of a GRD of these designs one utilizes that fact that an *identical* change in the liquid feed into the engine chamber head and into the afterburner causes a *different* change in the rate of the gas formation of the solid component. A change in $G_{ж.д}$ affects the rate of gasification only in terms of a pressure change, while a change in $G_{ж.г}$ affects the rate in terms of a change in the rate of the flow of gases along the channel of the charge. Hence it follows that if $\beta=0$, then the control of the GRD by two parameters is impossible, and on the other hand the more β (the greater the effect of the speed of flow of the gases in the channel of the charge on the rate of gasification), the more effective the control can be.

In a hydrojet of the examined design it becomes fundamentally possible to carry out the simultaneity of the consumption of the propellant constituents. This control system can be fulfilled on the same principle as that in liquid-propellant rocket engines (see [43]). For this purpose installed in the body of the charge and in the tank with the liquid are systems of discrete measurement of levels of solid- and liquid-propellant components (figure 6.3). The maintaining of the proportional expenditure of the propellant components occurs by means of the redistribution of the liquid between the channel of the charge and the afterburner.

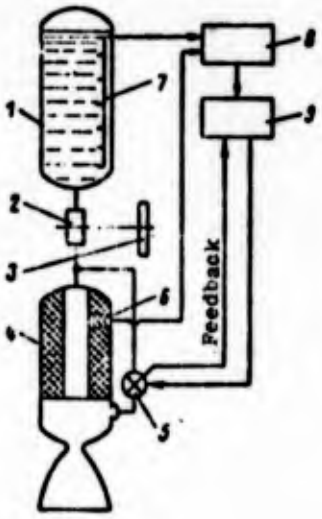

Figure 6.3. Diagram of a GRD with the system of proportional expenditure of the propellant components: 1 - tank; 2 - pump; 3 - turbine; 4 - chamber; 5 - controllable water resistance; 6 - sensor of burnout of the charge; 7 - sensor of the liquid level; 8 - amplifier-converter; 9 - computing device.

6.1.3. RDTT of Separate Loading

The work of the RDTT RS [PC - rocket missile] with a bypass of part of the gas in the afteburner is described by the following system of equations:

$$\left.\begin{aligned}
&\partial p_{к1} = f_1(\partial G_{т1}, \partial s_1, \partial u_1, \partial Q_{т1});\\
&\partial p_{к1} = f_2(\partial G_{т.г}, \partial \tau_{с1}, \partial p_{к2}, \partial F_{кр1});\\
&\partial p_{к1} = f_3(\partial G_{т.д}, \partial \tau_{с.д}, \partial F_{кр.д});\\
&\partial p_{к2} = f_4(\partial G_{т2}, \partial G_{т.г}, \partial d_2, \partial L_2, \partial u_2, \partial Q_{т2});\\
&\partial p_{к2} = f_5(\partial G_2, \partial F_{кр2}, \partial \tau_{с2}).
\end{aligned}\right\} \qquad (6.3)$$

where $p_{к1}$ and $p_{к2}$ are the pressure in the gas generator and in the thrust chamber, respectively; $G_{т1}$ and $G_{т2}$ - the gas formations of the charges; $G_{тг}$ and $G_{т.д}$ - components of $G_{т1}$ along two gas conductors;

$$G_2 = G_{т1} + G_{т2};\ G_{т1} = G_{т.г} + G_{т.д};$$

$F_{кр1}$, $F_{кр.д}$, $F_{кр2}$ - critical cross sections in the two gas conductors and of the main nozzle of the thrust chamber, respectively; s_1, d_1, d_2 - dimensions of the charges.

By the elimination from equations of the deviation of the propellant component flow, system (6.3) is reduced to the relations from which it follows that the pressures in the chambers can be affected by changing s_1, d_2, L_2, u_1, u_2, $\phi_{с1}$, $\phi_{с2}$, $\phi_{с.д}$, $F_{кр1}$, $F_{кр2}$, and $F_{кр.д}$.

The use as controlling parameters of deviations s_1, d_2, L_2, u_1, u_2, ϕ_{c1}, ϕ_{c2}, $\phi_{c.д}$, $F_{кр1}$, $F_{кр2}$, and $F_{кр.д}$ is virtually impossible. And only deviations of cross sections of throttles, installed in the pipelines, which connect the chambers of the RDTT RS, i.e., the values, $\delta F_{кр1}$ and $\delta F_{кр.д}$, can be examined as the possible controlling parameters for engines of this type. It should be noted that the temperature of the gases in the gas generator can be substantially lower than the temperature of the gases in the thrust chamber. This creates more favorable conditions for the reliable functioning of throttles with variable cross sections $F_{кр1}$ and $F_{кр.д}$.

In the same manner as for the GRD with the introduction of the liquid component into the head of the chamber and into its pre-nozzle space, in the RDTT RS of the examined design it is possible to realize control of the engine by two parameters - for example, according to thrust and according to the relationship of the flow rate of components. If it is necessary to increase the thrust while maintaining the relationship of the flow rates of the components constant (figure 6.4a), it follows to change both cross sections in the pipelines ($F_{кр1}$ and $F_{кр.д}$) in order that the flow rate of gases from the gas generator into the thrust chamber and the gas formation of the second charge would increase to an identical degree. With $\nu_1>0$, for an increase in the flow rate from the gas generator the total area ($F_{кр1}+F_{кр.д}$) should be decreased. In this case in order to insure the necessary increase in gas formation in the thrust chamber, this decrease should be realized mainly by a decrease in $F_{кр.д}$.

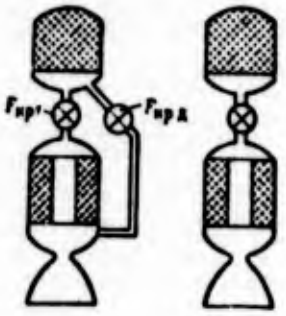

Figure 6.4. Diagrams of an RDTT of separate loading.

If the RDTT RS is made from the design without a bypass of part of the gases in the pre-nozzle volume (see figure 6.4b), then as the controlling effect a change of only one cross section $F_{кр1}$ can be used. In this case the engine can be controlled only by one parameter. The control of the thrust of such an RDTT RS in general will be accompanied by a change in the relationship of the propellant component flow.

6.2. FEATURES OF CONTROL OF A GRD

6.2.1. A GRD With Feed of the Liquid Component Only Into the Head of the Chamber

Let us examine some features of the control of the GRD in the case where a change in the feed of the liquid component is accepted as the controlling effect.

By examining the processes in the chamber of the GRD at the initial moment of time (parameters $p_{к0}$, $G_{ж0}$ etc.) and at a certain instantaneous time ($p_к$, $G_ж$ etc.), we find that

$$\frac{G_ж^{1-\beta}-G_{ж}^{1-\beta}}{G_{ж}^{1-\beta}-G_{ж0}^{1-\beta}}=\left(\frac{p_к}{p_{к0}}\right)^{\nu}\left(\frac{d}{d_0}\right)^{1-2\beta}.$$

Solving this equation in conjunction with the ratio

$$\frac{G_г}{G_{г0}}=\frac{p_к}{p_{к0}},$$

obtained from the equation of flow through the critical nozzle throat area, and assuming that $RT_к$=const, let us find the function of the relation between parameters of the chamber operation of the GRD:

$$\frac{G_ж}{G_{ж0}}=\frac{p_к}{p_{к0}}\left[\left(\frac{p_к}{p_{к0}}\right)^{\nu+\beta-1}\left(\frac{d}{d_0}\right)^{1-2\beta}+\right.$$
$$\left.+\left(\frac{1}{K_0}+1\right)^{1-\beta}\left[1-\left(\frac{p_к}{p_{к0}}\right)^{\nu+\beta-1}\left(\frac{d}{d_0}\right)^{1-2\beta}\right]\right]^{\frac{1}{1-\beta}}. \qquad (6.4)$$

Equation (6.4) is the equation of the control characteristic of the chamber of the GRD; it connects the pressure change in the chamber (thrust) with the change in flow rate of the liquid component.

An analysis of equation (6.4) makes it possible to make the following conclusions:

1) with $\nu+\beta=1$ a change in pressure in the chamber is proportional to a change in the flow rate of the liquid component, whereupon the proportionality factor of these values is changed with the heat erosion of the channel; at the initial moment ($d=d_0$) a relative change in the pressure is equal to a relative change in the fluid flow rate;

2) with $\beta=0.5$ a change in the diameter of the channel does not affect the parameters of the engine operation[1];

3) if $\beta=\nu=0.5$, then the direct proportionality between the consumption and pressure is retained during the entire operating time of the engine.

The control characteristic GRD for $d/d_0=1$ is given in figure 6.5.

Let us define the transfer constant of the chamber as a link of the automatic control system of the engine. A block diagram of the examined type of chamber is given in figure 6.6. The input signal for the chamber is the change in the fluid flow rate $\delta G_{ж}$, and the output signal is the change in pressure $\delta p_{к}$.

---

[1]The gas formation of the solid component is proportional to the product of the rate of the gas formation by the surface of gasification. When $\beta=0.5$ a decrease in the rate of the gas formation, with an increase in the diameter of the channel, is equal to an increase in the surface of gasification, and the gas formation of the solid component is not changed.

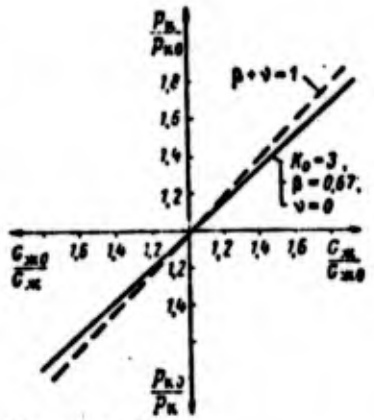

Figure 6.5

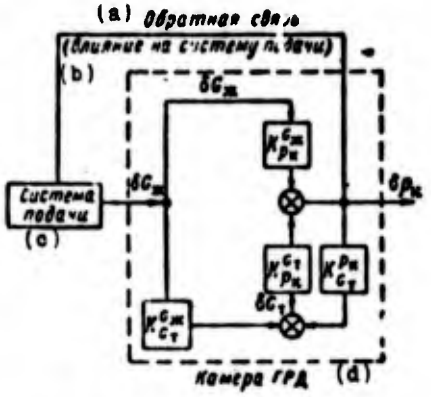

Figure 6.6

Figure 6.5. Control characteristic of the GRD.

Figure 6.6. Block diagram of the chamber of the GRD.
Key: (a) Feedback; (b) (Effect on the feed system); (c) Feed system; (d) Chamber of GRD.

The value of the transfer constant is established from an examination of equations of the chamber in small deviations, i.e., in the vicinity of the nominal system. In this case $d=d_0$ and the transfer constant should depend only on the parameters of the operating process.

The change in the flow rate of the liquid component affects pressure in the chamber in a complex way - directly in terms of a change in the gas formation of the solid component produced by a change in $G_ж$ and $p_н$. The corresponding transfer constants are designated as follows:

$$K^{G_ж}_{p_к}=\frac{(\delta p_к)^{G_ж}}{\delta G_ж};\quad K^{G_т}_{p_к}=\frac{(\delta p_к)^{G_т}}{\delta G_т}\ *).$$

*Quantities $(\delta p_н)^{G_ж}$ and $(\delta p_н)^{G_т}$ are deviations in $p_н$ caused, respectively, either only by the deviation in $\delta G_ж$ or only by the deviation in $\delta G_т$, i.e., determined without allowing for changes in the gas formation of the solid component or, correspondingly, without allowing for the effect of a change in the flow rate of the liquid component.

The transfer constant of the entire chamber, i.e., the ratio of the output signal to the input signal, is

$$K^{G_ж}_{p_к} = \frac{\partial p_к}{\partial G_ж} = \frac{a^{G_ж}_{к.с} - a^{G_т}_{к.с}\dfrac{a^{G_ж}_{бд}}{a^{G_т}_{бд}}}{a^{p_к}_{к.с} - a^{G_т}_{к.с}\dfrac{a^{p_к}_{бд}}{a^{G_т}_{бд}}},$$

where $a^{G_ж}_{к.с}$, ..., $a^{G_т}_{бд}$ - respectively the coefficients of equations (5.8) and (5.9), which depend on the relationship of the propellant component flow, exponents in the law of the rate of gas formation of a unit of solid component and the degree of the dependence of the efficiency of the gases in the chamber on the relationship of the consumption of components $\partial RT_к/\partial K$.

As was already mentioned above, in the process of control of the hydrojet it is profitable to maintain the value to close to the optimum. In this case the effect of K on $RT_к$ is unessential, and it can be disregarded.

Substituting the values of the coefficients and considering that $\partial RT_к/\partial K=0$, we find

$$K^{G_ж}_{p_к} = \frac{\left(\dfrac{\bar{K}}{1+\bar{K}}\right)^{1-\beta}}{1-\dfrac{\nu}{1-\beta}\left[1-\left(\dfrac{\bar{K}}{1+\bar{K}}\right)^{1-\beta}\right]}. \qquad (6.5)$$

Thus the transfer constant of the chamber as the link of the control system of the GRD complexly depends on the propellant properties and operating process.

Figure 6.7 gives results of the calculation of the transfer constants of the chamber at different values of quantities K, β and ν which determine this coefficient. According to results of the calculations given in figure 6.7, it can be concluded that

for the conditions taken (K=1-5; β=0.5-0.8; ν=0-0.2):

a) values of the transfer constant are 0.8-1, i.e., with the control of pressure (and thrust) of the GRD within limits of 10% it will be required to change the flow rate of the liquid component by approximately 10-13%;

b) the most noticeable effect on the transfer constant is exerted by the relationship of the propellant component flow;

c) the transfer constant can be increased by means of the use of a propellant with a high value of the relationship of flow rates of the components, and also when using a solid component the gasification rate of which is more sensitive to the pressure and mass flow rate of the gases.

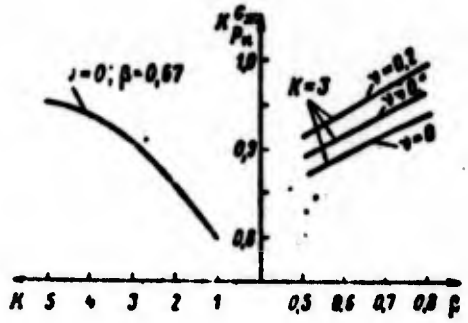

Figure 6.7. Dependence of the transfer constant of the chamber on β, K and ν.

Let us examine the features of the chamber operation of the GRD, one of the parameters of which is maintained constant. We use for an analysis the equation of the control characteristic (6.4).

The most probable and obvious cases of the control of this form can be:

1) the maintaining of the flow rate of the liquid propellant component in the chamber constant ($G_{ж}$=const);

2) the maintaining of the pressure in the chamber constant ($p_н$=const).

In the first case in equation (6.4) $G_ж/G_{ж0}$=1, i.e., the pressure change in the chamber is determined only by a change in the diameter of the channel. This fact characterizes one of the features of the operating process of the GRD, namely, the dependence of parameters of its operating process on the diameter of the channel of the charge of the solid component. Figure 6.8 depicts examples of such dependences. With an increase in the value of exponent β, in the law of the rate of gasification of the solid component, and with a decrease in the initial relationship of the propellant component flow K_0, the pressure in the chamber with heat erosion of the channel differs from the initial value more substantially.

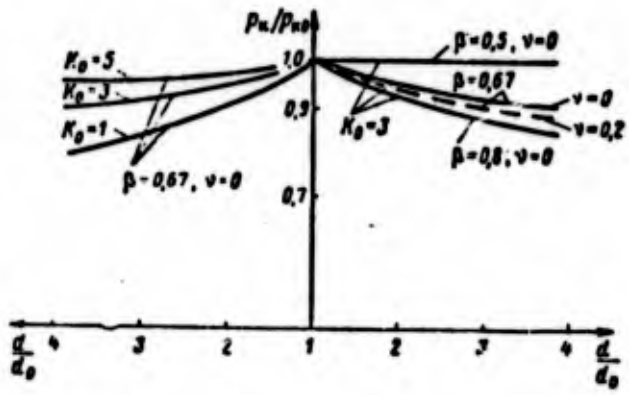

Figure 6.8. Dependence of $p_н/p_{н0}$ on d/d_0 with $G_ж$=const.

In the case of the control $p_н$=const in the equation of the control characteristic (6.4), $p_н/p_{н0}$=1 is accepted. This condition in the process of heat erosion of the channel is satisfied by means of the appropriate change (with β>0.5 - by means of an increase) in the flow rate of the liquid component (figure 6.9). In this case with an increase in β and with a decrease in K_0, the change in the parameters (required change in $G_ж$) increases.

Let us determine the transfer constants which characterize the features of control of the GRD while maintaining one of the parameters constant.

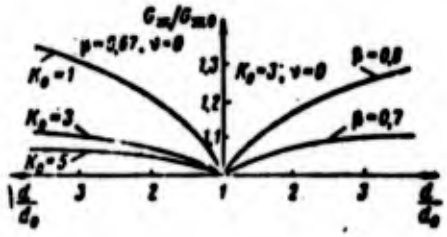

Figure 6.9. Dependence of $G_н/G_{нO}$ on d/d_0 with $p_н$=const.

For the case of control $G_н$=const the pressure change in the chamber, produced by a change in the diameter of the channel, can be estimated by using the coefficient $K^d_{p_н}$, which takes the following form:

$$K^d_{p_н} = \frac{\partial p_к}{\partial d} = \frac{1-2\beta}{1-\beta} \frac{1-\left(\frac{\bar{R}}{1+\bar{R}}\right)^{1-\beta}}{1-\frac{\nu}{1-\beta}\left[1-\left(\frac{\bar{R}}{1+\bar{R}}\right)^{1-\beta}\right]}. \qquad (6.6)$$

Results of calculations of coefficient $K^d_{p_н}$, which is the tangent to the angle of slope tangent to curves of $p_к/p_{кO}=f(d/d_0)$ at the point which corresponds to $p_к/p_{кO}=1$, $d/d_0=1$, and $K=K_0$, are given in figure 6.10. From an analysis of expression (6.6), it is possible to establish the condition already known to us under which the pressure in the chamber is not changed with an increase in the diameter of the channel. This case corresponds to $K^d_{p_н}=0$, which corresponds to $\beta=0.5$.

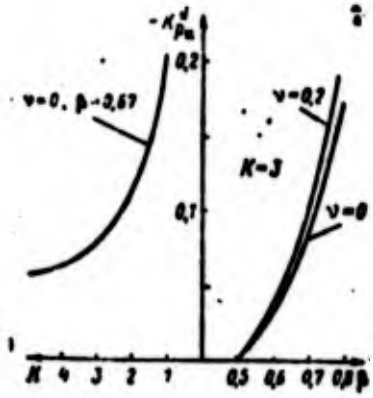

Figure 6.10. Dependence of the coefficient of $K^d_{p_н}$ on β, K and ν.

With $\beta \neq 0.5$ the pressure in the engine operation in general will be changed. The pressure change can be avoided by the appropriate change in the feed of the liquid component. This corresponds to the case of control $p_к$=const. From the equations of the chamber, assuming that $\delta p_к = 0$, we find the relation of changes in the flow rate of the liquid component and diameter corresponding to this condition:

$$K^{d}_{G_ж} = \frac{\delta G_ж}{\delta d} = \frac{2\beta - 1}{1 - \beta} \cdot \frac{1 - \left(\frac{\bar{R}}{1 + \bar{R}}\right)^{1-\vartheta}}{\left(\frac{\bar{R}}{1 + \bar{R}}\right)^{1-\vartheta}}. \qquad (6.7)$$

From given it can be concluded that in the process of the operation of a GRD having the chamber with the introduction of the liquid propellant component only through the head, as a result of a change in the diameter of the channel of the charge parameters of the operating process of the chamber will be changed. If we maintain the flow rate of the liquid component constant, then will be changed pressure and, together with it, the remaining parameters which depend on it, i.e., the flow rate of the solid component, the relationship of the flow rate of components and the mean-integral specific impulse. In order to maintain the pressure constant, it is necessary to change the flow rate of the liquid component, which will also cause a change in the relationship of the flow rate of the components and specific impulse.

Figure 6.11 depicts the dependences which characterize the change in the relationship of the flow rate of the components connected with a change in the diameter of the channel.

Other conditions being equal, the system with which the mean-integral specific impulse is changed less is more preferable. Let us examine in connection with this the ratio of the coefficients of transfer which connect the deviations of the relationship of the flow rates of the components depending on a change in

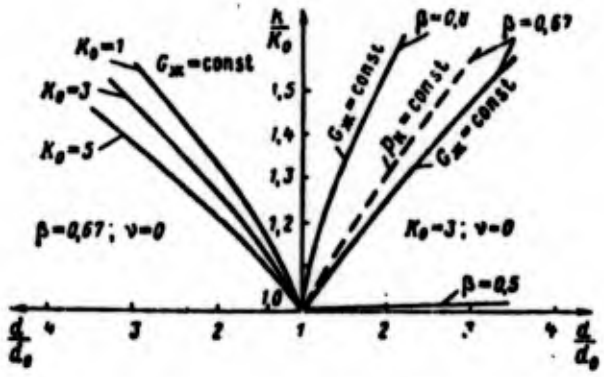

Figure 6.11. Dependence of K/K_0 on d/d_0.

the diameter of the channel with different methods of control: $G_{ж}$=const and $p_{к}$=const. From the system of equations (6.2), taking into account the fact that $\delta K=\delta G_{ж}-\delta G_{т}$, we obtain (under the assumption that $\delta RT_{к}/\delta K=0$):

for $G_{ж}$=const

$$(K_{к}^{d})_{G_{ж}}=\frac{2\beta-1}{1-\beta}\,\frac{(1+\bar{R})\left[1-\left(\frac{\bar{R}}{1+\bar{R}}\right)^{1-\beta}\right]}{1-\frac{\nu}{1-\beta}\left[1-\left(\frac{\bar{R}}{1+\bar{R}}\right)^{1-\beta}\right]}; \tag{6.8}$$

for $p_{к}$=const

$$(K_{к}^{d})_{p_{к}}=\frac{2\beta-1}{1-\beta}\,\frac{(1+\bar{R})\left[1-\left(\frac{\bar{R}}{1+\bar{R}}\right)^{1-\beta}\right]}{\left(\frac{\bar{R}}{1+\bar{R}}\right)^{1-\beta}}. \tag{6.9}$$

The ratio of the coefficients is equal to

$$\frac{(K_{к}^{d})_{p_{к}}}{(K_{к}^{d})_{G_{ж}}}=\frac{1-\frac{\nu}{1-\beta}\left[1-\left(\frac{\bar{R}}{1+\bar{R}}\right)^{1-\beta}\right]}{\left(\frac{\bar{R}}{1+\bar{R}}\right)^{1-\beta}}. \tag{6.10}$$

When $\nu=0$; $K=1-5$; $\beta=0.5-0.8$ this ratio takes values

$$\frac{(K_к^d)_{p_к}}{(K_к^d)_{G_ж}} = 1{,}03-1{,}43.$$

This means that the method of control by maintaining $G_ж$=const is connected with less changes in the relationship of the flow rates of the components than is the method calculated for maintaining $p_к$=const. Consequently, with $G_ж$=const a reduction in the specific impulse will be less noticeable.

Figure 6.12 gives for an example results of the calculation of the change in parameters in the chamber of the GRD which has the following characteristics: $\beta=0.65$; $\nu=0$; $K=1.9$. Shown here as a time function is the change (relative to the initial values) in the diameter of the channel of the charge, pressure in the chamber, flow rates of the solid and liquid propellant components and relationship of flow rates of components for two cases of control of the GRD - for the purpose of providing for a constant pressure in the chamber and for the purpose of maintaining the flow rate of the liquid component constant. Results of the calculations confirm that said above about features of the control of a GRD of this design.

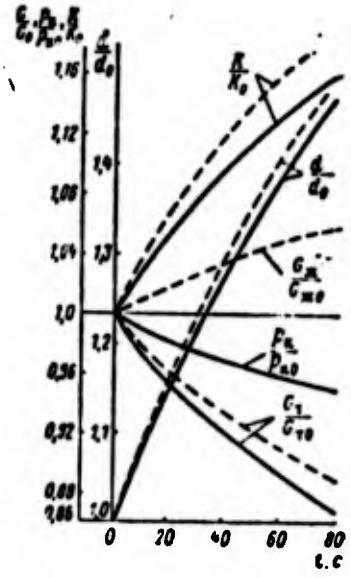

Figure 6.12. A change in parameters in the chamber of the GRD as a function of time: ——— - $G_ж$=const; --- - $p_к$=const

There is considerable interest in the analysis of the degree of the change in the relationship of the propellant component flow in the process of the control of pressure in the engine chamber:

$$K_{\text{к}}^{p_{\text{к}}} = \frac{\partial K}{\partial p_{\text{к}}} = \frac{1-\beta-\nu}{1-\beta}(1+\bar{K})\left[\left(\frac{1+\bar{K}}{\bar{K}}\right)^{1-\beta}-1\right]. \qquad (6.11)$$

Figure 6.13 gives results of the calculation of the transfer constant $K_{\text{н}}^{p_{\text{н}}}$ which shows the degree of the change in the relationship of the propellant component flow in the process of the control of pressure in the chamber.

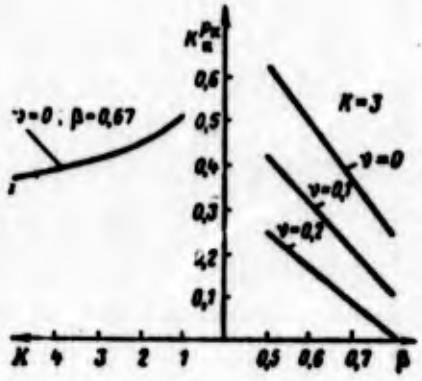

Figure 6.13. Dependence of the transfer constant $K_{\text{н}}^{p_{\text{н}}}$ on β, K and ν.

According to the calculations, it can be concluded that $K_{\text{н}}^{p_{\text{н}}}$ depends substantially both on the relationship of the flow rates of the components and on the exponents in the law of the rate of gasification of the solid component. An increase in K, just as an increase in the sum of the indices β+ν[when (β+ν)<1], leads to a decrease in the change in the relationship of the flow rates of the components in the process of the control of pressure in the chamber, i.e., favorably affects the characteristics of the GRD; $K_{\text{н}}^{p_{\text{н}}}=0$ with β+ν=1, which follows directly from equation (6.11).

In the examined example the value $K_{\text{н}}^{p_{\text{н}}}$ is found within limits of 0-0.6, i.e., with changes in pressure in the chamber of up to 10%, and the relationship of flow rates of the components will be changed by 0-6%.

Let us examine the possibility of maintaining the relationships of the propellant component flow constant in the process of operation of the GRD by a corresponding change in the flow rate of the liquid component. For this case, from the equation of the flow through the critical cross section of the nozzle, we will obtain

$$\frac{p_к}{G_ж} = \text{const.}$$

Utilizing equation (4.5), we find the condition of the provision of K=const in the form

$$\frac{G_ж}{G_{ж0}} = \frac{p_к}{p_{к0}} = \left(\frac{d}{d_0}\right)^{\frac{1-2\beta}{1-\beta-\nu}}. \qquad (6.12)$$

By analyzing this relation, it is possible to make, first of all, the conclusion already known to us that with $\beta=0.5$ the constancy of parameters of the operation of the GRD is retained. However, already with $\beta=0.67$, $\nu=0$ and $d/d_0=1.5$, for retention of the initial relationship of flow rates of the components it is necessary to decrease the flow rate of the liquid component by 1.5 times; the thrust of the engine is decreased 1.5 times, respectively. Thus in a GRD of this design the provision for a constant relationship of the propellant component flow is connected with the very noticeable changes in pressure in the chamber (thrust of the engine).

6.2.2. Hydrojets With a Bypass of the Liquid Component

As was already mentioned earlier, the presence of two controlling effects on the parameters of the chamber of the GRD with a bypass makes it possible to regulate simultaneously the two parameters of its operation.

Let us examine one of the most probable versions of control - the pressure change in the chamber (thrust of the engine) with

the simultaneous maintaining of the relationship of the propellant component flow (K=const) constant. As the controlling effects let us take the change in the total flow rate of the liquid component into the chamber $G_{ж}$ and the change in the coefficient of the bypass ϕ.

In this case the GRD will have two controlling characteristics - one for each of the controllable parameters.

The controlling characteristic according to pressure in the chamber is established directly from the equation of outflow (taking into account the fact that $G_{ж}/G_{т}$=const) in the form

$$\frac{p_к}{p_{к0}}=\frac{G_ж}{G_{ж0}}. \tag{6.13}$$

The controlling characteristic according to the relationship of the propellant component flow takes the form

$$\frac{(1+\varphi K_0)^{1-\beta}-(\varphi K)^{1-\beta}}{(1+\varphi_0 K_0)^{1-\beta}-(\varphi_0 K_0)^{1-\beta}}=\left(\frac{p_к}{p_{к0}}\right)^{\beta+\nu-1}\left(\frac{d}{d_0}\right)^{1-2\beta}. \tag{6.14}$$

From equation (6.14), it is possible to find the value of the coefficient of bypass ϕ, which must be had for the fulfillment of the stated condition (K=const) with the assigned initial characteristic (ϕ_0, K_0, β, ν) in cases of the change in the diameter of the channel of the charge (d/d_0) and pressure in the chamber ($p_к/p_{к0}$); from equation (6.13) it is possible to find here the required rate of discharge of the liquid $G_{ж}$.

It is necessary to keep in mind that the value of the coefficient of bypass is found within limits of $\phi_{min}\leq\phi\leq 1$, which is implied in the existence of boundaries of control with respect to pressure with the observance of K=const.

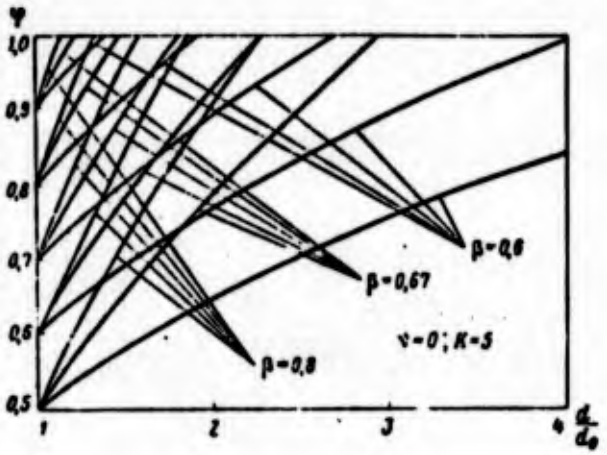

Figure 6.14. Change in the coefficient of bypass ϕ with heat erosion of the channel of the charge necessary for fulfillment of the condition K=const.

Figure 6.14 gives results of the calculation of the required change in the coefficient of bypass ϕ for maintaining K=const constant in the process of the engine operation at a constant pressure in the chamber (p=const). The value of ratio d/d_0, which corresponds $\phi=1$, is the maximum relative diameter of the channel up to which the fulfillment of the assigned condition (K=const) is possible.

Examples of the required change in the coefficient of bypass ϕ for the purpose of maintaining K=const, depending on the degree of boosting of the pressure in chamber $p_к/p_{к0}$ (with d=const), are represented in figure 6.15. The greatest effect on the value of the required change in the coefficient of bypass is exerted by the exponent with value $p_к/p_{к0}$. The more this exponent differs from zero, the greater the change in ϕ necessary with the given degree of boosting in order to maintain K=const. The value $p_к/p_{к0}$, which corresponds to $\phi=1$, is the upper limit of the boosting, up to which with the assigned initial characteristics the fulfillment of conditions K=const is possible by means of a change in ϕ.

A block diagram of the chamber of the hydrojet with bypass is given in figure 6.16.

For the case of K=const we will have $\delta p_к=\delta G_ж=\delta G_т$ and, therefore, coefficients $K^{G_ж}_{p_к}$ and $K^{G_т}_{p_к}$ are equal to unity, and the coefficient $K^{p_к}_{к}$ is equal to zero.

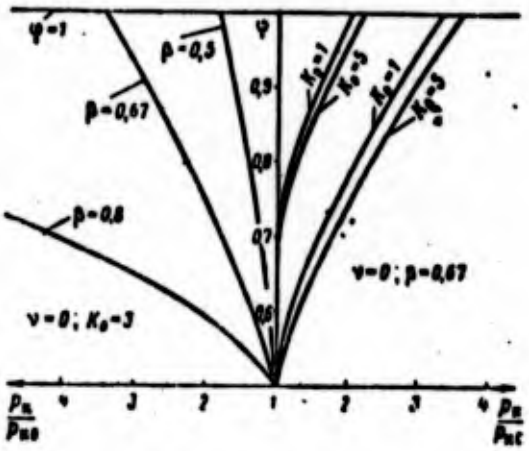

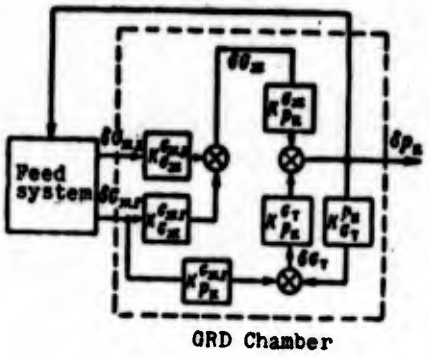

Figure 6.15 Figure 6.16

Figure 6.15. Dependence of the coefficient of bypass ϕ on the degree of the boosting of pressure in the chamber necessary for fulfillment of the conditions K=const.

Figure 6.16. Block diagram of the chamber of a GRD with a bypass.

The greatest interest is in the transfer constant, which connects the deviation of pressure in the chamber with the deviation of the coefficient of bypass:

$$K^{\varphi}_{p_к} = \frac{\delta p_к}{\delta \varphi}.$$

When d=const and K=const we obtain

$$K^{\varphi}_{p_к} = -\frac{a^{O}_{к.г}}{a^{p_к}_{б.г} + a^{O}_{к.г} + a^{O}_{т.г}}.$$

By substituting the values of coefficients and producing the appropriate conversions, we find

$$K^{\varphi}_{p_к} = \frac{1-\beta}{1-\beta-\nu} \frac{1-f(\bar{\varphi},\bar{R})}{f(\bar{\varphi},\bar{R})}. \qquad (6.15)$$

When $\beta+\nu=1$, $K^{\phi}_{p_к} = \infty$ is independent of values $\bar{\phi}$ and $\bar{K}$. An explanation of the physical reason for the existence of this value

of coefficient $K^{\phi}_{p_к}$ is possible in the following manner. It is known that when $\beta+\nu=1$ the correlation coefficient of the propellant component flow for a GRD with a feed of the liquid component only into the head of the chamber remains constant with a pressure change in the chamber.

In the chamber of the GRD with a bypass a similar phenomenon is observed if we examine the correlation coefficient of flow rates of the components at outlet from the channel. However, power engineering of the chamber is determined by the correlation coefficient of flow rates of the components at the nozzle entry of the chamber, i.e., when the part of the flow of the liquid component fed into afterburner is considered. Therefore, with the constant relationship of flow rates of components at the outlet from the channel, any change in the coefficient of bypass will involve a change in the relationship of flow rates of the components at the nozzle entry. Since the coefficient $K^{\phi}_{p_к}$ connects deviations in ϕ and $p_к$ with K=const, we will approach the fulfillment of the stated condition in such a case when flow rates of the components (and this means the pressure in the chamber) will approach infinity.

On the other hand, it can be concluded that under the condition of $\beta+\nu=1$ in the process of the throttling or boosting of the pressure in the chamber with a bypass, the maintaining of the relationship of flow rates of the components is realized by setting the coefficient of bypass ϕ constant.

For values of coefficients within limits of $\beta=0.5$-0.8; $K\phi=1$-5 and $\nu=0$-0.2, the indicated transfer constants, as follows from figure 6.17, is found within the limits

$$K^{\phi}_{p_к}=0{,}833\div\infty.$$

When evaluating the possibilities of control for the purpose of maintaining the relationship of the propellant component flow

constant in the process of heat erosion of the channel of the charge, it is interesting to analyze the transfer constant which connects the deviation of the coefficient of bypass ϕ with the deviation of the diameter of the channel d under the condition of K=const:

$$K_{\varphi}^{d}=\frac{\delta\varphi}{\delta d}=-\frac{b_{6d}^{d}}{a_{61}^{0_{\kappa.r}}}.$$

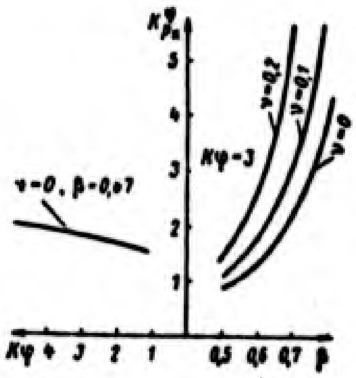

Figure 6.17. Dependence of the coefficient of $K_{p_H}^{\phi}$ on β, K and ν.

By substituting the values of coefficients, we find

$$K_{\varphi}^{d}=\frac{2\beta-1}{1-\beta}\,\frac{f(\bar{\varphi},R)}{1-f(\bar{\varphi},R)}. \tag{6.16}$$

With a change in the coefficients β, K and ν, in the aforementioned limits the examined transfer constant will be K_{ϕ}^{d}=0-0.865 (figure 6.18).

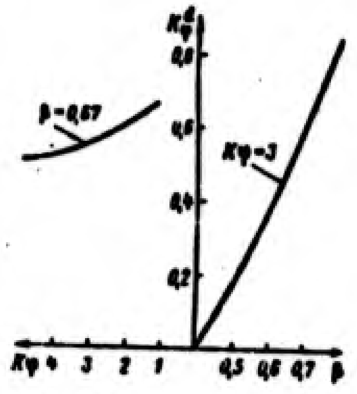

Figure 6.18. Dependence of the coefficient K_{ϕ}^{d} on β and K.

As follows from equation (6.16), with $\beta=0.5$ a change in the coefficient of bypass is not required for maintaining K=const in the process of the heat erosion of the channel.

6.3. EQUATION OF DYNAMICS OF THE CHAMBER OF A GRD

It has already been noted above that the established operating process of the chamber of the GRD is extremely complex. It is natural that even more complex are the transfer processes in such chambers. The change in the flow rate of the liquid component for the purpose of pressure control in the chamber causes the rearrangement of those fields of concentrations of the flow rate of components, temperatures and gas velocities within the channel of the charge on which the gas formation of the solid component depends. It is not represented possible to consider this in equations of the dynamics of the chamber. These equations are considerably complicated in the case of attempts of an account of the inconstancy of parameters of gas along the channel and a change in the shape of the channel. At the same time, these complications, by virtue of the insufficient study of processes in the chamber, thus far have not given a noticeable result.

In connection with that noted, let us examine the simplified equations of dynamics of the chamber of the GRD.

Let us introduce the following simplifying assumptions:

1) the propellant components burn instantly in a certain time interval $\tau_н$ after the injection of the liquid component into the chamber; by analogy with the appropriate characteristic for processes of fuel combustion in the ZhRD, we will call $\tau_н$ *the delay time* and assume that $\tau_н$=const;

2) the combustion products are an ideal gas which has a certain averaged work $(RT_к)_{пр}$, which will be called the *normalized*

efficiency; $(RT_к)_{пр}$ is equal to the efficiency of the equivalent gas, which in the free volume of the chamber creates the same pressure $p_к$ and which has the same mass $Y_к$ as the real combustion products;

3) the channel of solid unit has a cylindrical form; the diameter of the channel in those time intervals which are examined in the analysis of transfer processes is not changed.

Let us examine the chamber of a GRD without a bypass of the liquid component.

The equation of the balance of the mass of gaseous combustion products in the chamber is written in the form

$$\frac{d}{dt}Y_к = G_{пр} - G_Σ, \tag{6.17}$$

where $G_{пр}$ is the arrival of the combustion products; $G_Σ$ is flow rate of the combustion products through the nozzle.

The mass of the gaseous combustion products is determined by the equation of state:

$$Y_к = \frac{p_к W_{св}}{(RT_к)_{пр}},$$

where $W_{св}$ is the free volume of the chamber.

The normalized efficiency is connected with the operation of the gases in the pre-nozzle space. Let us assume for simplicity that these values are proportional to each other:

$$(RT_к)_{пр} = CRT_к,$$

where $C<1$; $C=\text{const}$.

The efficiency of the combustion products depends on the relationship of the propellant component flow and pressure. However, with the relationships of the flow rate of the components close to optimum, this dependence is weak, and it is possible to assume that $RT_к$ and, consequently, $(RT_к)_{пр}$ during the transfer processes are not changed.

In this case

$$\frac{d}{d\tau}Y_к = \frac{W_{св}}{(RT_к)_{пр}}\frac{d}{d\tau}p_к + \frac{p_к}{(RT_к)_{пр}}\frac{d}{d\tau}W_{св}.$$

Taking into account the adopted assumption about the instantaneous combustion of the propellant components, the per-second arrival of gases at the moment of time τ is determined by the quantity of the liquid component injected at the moment of time (τ is $\tau_к$):

$$G_{пр} = G_ж(\tau - \tau_к) + G_т[G_ж(\tau - \tau_к)].$$

The flow rate of the gas from the chamber is equal to

$$G_г = Ap_кF_{кр},$$

where

$$A = \varphi_c\sqrt{\frac{n\left(\frac{2}{n+1}\right)^{\frac{n+1}{n-1}}}{RT_к}}.$$

An increase in the free volume of the chamber occurs only as a result of the burnout of the solid component, and therefore

$$\frac{d}{d\tau}W_{св} = \frac{G_т}{\rho_т},$$

By substituting into equation (6.17) values $G_{пр}$, G_{Σ} and $-\frac{d}{d\tau}\gamma_к$, we find

$$\frac{W_{со}}{(RT_к)_{пр}}\frac{d}{d\tau}p_к + Ap_кF_{кр} = G_т\left[1 - \frac{p_к}{(RT_к)_{пр}\rho_т}\right] + G_{вп}. \qquad (6.18)$$

Let us estimate the value $p_к/(RT_к)_{пр}\rho_т$.

At the typical values of quantities $p_к$, $\rho_т$ and $(RT_к)_{пр}$ equal, respectively, to $p_к = 50\cdot10^5$ Pa, $\rho_т = 10^3$ kg/m^3 and $(RT_к)_{пр} = 5\cdot10^5$ J/kg, the value $p_к/(RT_к)_{пр\rho т} = 1/100$.

Let us disregard this value, which is equivalent to the neglect of the effect of a change in the free volume of the chamber on the pressure change. Then

$$\frac{W_{со}}{(RT_к)_{пр}}\frac{d}{d\tau}p_к + Ap_кF_{кр} = G_т + G_{вп}.$$

After introducing the expression which determines the arrival of the solid propellant component, we obtain the differential equation of the chamber of the GRD in the form

$$\theta_к\frac{d}{d\tau}p_к + p_к = Q\left[Bp_к^{\nu} + G_{вп}^{1-\nu}(\tau - \tau_к)\right]^{\frac{1}{1-\beta}}, \qquad (6.19)$$

where $\theta_к = \frac{\bar{p}_к W_{со}}{G_т(RT_к)_{пр}}$; $Q = \frac{1}{AF_{кр}}$;

$$B = 4^{\beta}\pi^{1-\beta}(1-\beta)u_т\rho_т L d^{1-2\beta}.$$

Equation (6.19) is very inconvenient to use. Let us write it in small relative deviations. After the conversion we obtain

$$T_к\frac{d}{d\tau}\delta p_к + \delta p_к = K_{p_к}^{G_{вп}}\delta G_{вп}(\tau - \tau_к), \qquad (6.20)$$

where $\delta p_к = \frac{\Delta p}{p_к} = \frac{p_к - \bar{p}_к}{\bar{p}_к}$;

$T_к = \frac{\theta_к}{1 - \frac{\nu}{1-\beta}\left[1 - \left(\frac{R}{1+R}\right)^{1-\beta}\right]}$ - time constant of the chamber;

$K^{G_м}_{p_к} = \frac{\left(\frac{R}{1+R}\right)^{1-\beta}}{1 - \frac{\nu}{1-\beta}\left[1 - \left(\frac{R}{1+R}\right)^{1-\beta}\right]}$ - amplification factor with respect to the consumption of the liquid propellant component.

As is evident from equation (6.20), the chamber of the GRD is the inertia link with the delay.

With a change in the flow rate of the liquid component in the form of a single step function $\delta G_м = 1(\tau)$, a change in pressure in the chamber is determined by the solution to equation (6.20):

$$\delta p_к(\tau) = 0 \text{ with } \tau < \tau_к;$$

$$\delta p_к(\tau) = K^{G_м}_{p_к}\left(1 - e^{-\frac{\tau}{T_к}}\right) \text{ with } \tau > \tau_к.$$

The chamber is a stable link, i.e., with a change in the flow rate of the liquid component the pressure in the chamber takes a constant value:

with $\tau = \infty$, $\delta p_к = K^{G_м}_{p_к}$ and $p_к = \bar{p}_к\left(1 + K^{G_м}_{p_к}\right)$.

The transfer characteristic of the chamber is given in figure 6.19.

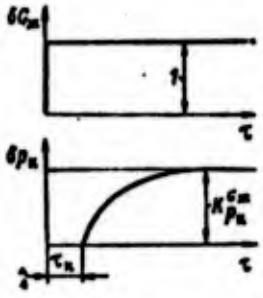

Figure 6.19. Transfer characteristic of the chamber of a GRD.

The time constant of the chamber $T_к$ depends mainly on the geometric dimensions of the chamber and characteristics of the operating process. With an increase in the free volume of the chamber, the time constant grows; and therefore the quality of the control of the GRD in the process of its operation deteriorates.

Thus, for instance, for a chamber with a single-channel charge with $\nu=0$ it is possible to consider approximately that the time constant increases in proportion to the square of the ratio of the current diameter of the channel of the charge to its initial value.

It is not difficult to see that the expression for an amplification factor $K_{p_к}^{G_ж}$, which enters into equation (6.20) of the dynamics of the chamber, coincides with equation (6.5) obtained previously (in section 6.2.1). As was already mentioned, the value $K_{p_к}^{G_ж}$ depends on the relationship of the propellant component flow and coefficients in the law of the rate of gasification of the solid fuel.

The equation of dynamics of the <u>chamber with a bypass</u> is written similar to equation (6.20). The time constant and amplification factor take the following form respectively:

$$T_к = \frac{\theta_к}{1-\frac{\nu}{1-\beta}\frac{1+\bar{\varphi}\bar{R}}{1+\bar{R}}\left[1-\left(\frac{\bar{\varphi}\bar{R}}{1+\bar{\varphi}\bar{R}}\right)^{1-\beta}\right]};$$

$$K_{p_к}^{G_ж} = \frac{1-\frac{1+\bar{\varphi}\bar{R}}{1+\bar{R}}\left[1-\left(\frac{\bar{\varphi}\bar{R}}{1+\bar{\varphi}\bar{R}}\right)^{1-\beta}\right]}{1-\frac{\nu}{1-\beta}\frac{1+\bar{\varphi}\bar{R}}{1+\bar{R}}\left[1-\left(\frac{\bar{\varphi}\bar{R}}{1+\bar{\varphi}\bar{R}}\right)^{1-\beta}\right]}.$$

With $\phi=1$ the expressions for $T_к$ and $K_{p_к}^{G_ж}$ take the form of the expressions for similar coefficients of the chamber without a bypass of the liquid component. The chamber of the GRD with a bypass is the general case, and $\phi=1$ is the particular case, which corresponds to the feed of the entire liquid only into the head.

6.4. FEATURES OF CONTROL OF AN RDTT OF SEPARATE LOADING

Let us examine some features of control of an RDTT RS in the case where gases from the gas generator are fed into the thrust chamber only through one gas conductor, i.e., only into the head of the chamber.

Used as a controlling effect is a change in the cross section $F_{кр1}$ of the throttle installed in this gas conductor. A change in $F_{кр1}$ produces a change in pressure $p_{к1}$ in the gas generator and gas formation of the charge in it, and there is a change in the flow rate of the gas into the thrust chamber, which leads as a final result to a change (control) of the pressure $p_{к2}$ in this chamber. If it is necessary to increase the pressure $p_{к2}$ (thrust of the engine) the cross section $F_{кр1}$ should be decreased.

If the outflow of the gases through $F_{кр1}$ is supercritical, then the relationship between the dimensionless pressure in the thrust chamber and the dimensionless throat area of the throttle is established (with a constant burning surface in the gas generator) by the relation

$$\frac{F_{кр1}}{F_{кр10}} = \left\{ \frac{\left(\frac{p_{к2}}{p_{к20}}\right)^{1-\beta} - \left(\frac{p_{к2}}{p_{к20}}\right)^{\nu_2} \left[1 - \left(\frac{K_0}{1+K_0}\right)^{1-\beta}\right]}{\left(\frac{K_0}{1+K_0}\right)^{1-\beta}} \right\}^{\frac{\nu_1 - 1}{\nu_2(1-\beta)}}. \qquad (6.21)$$

where $p_{к20}$, K_0, and $F_{кр10}$ refer to the initial (calculated) conditions.

Figure 6.20 depicts the dependence of $p_{к2}/p_{к20}$ on $F_{кр1}/F_{кр10}$, i.e., the controlling characteristic of the RDTT RS at defined values ν_1, ν_2, β and K_0. The possibilities of the control of the examined engine in the vicinity of the nominal mode can be established also by means of an analysis of the transfer constant, which connects the deviations of pressure in the thrust chamber

and the cross-sectional areas of the nozzle of the throttle:

$$K^{F_{кр1}}_{p_{к2}} = \frac{\delta p_{к2}}{\delta F_{кр1}} = -\lambda \left(\frac{\bar{K}}{1+\bar{K}} \right)^{1-\beta}, \qquad (6.22)$$

where λ is determined from the relation (5.48).

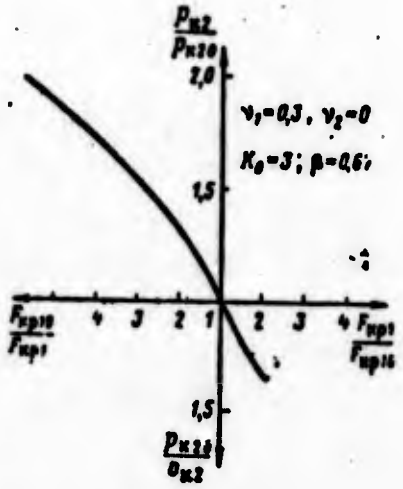

Figure 6.20

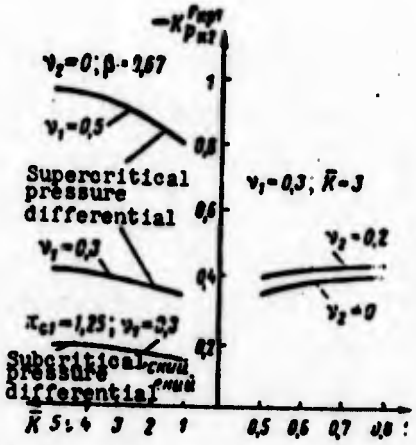

Figure 6.21

Figure 6.20. Controlling characteristic of the RDTT RS.

Figure 6.21. Dependence of the coefficient $K^{F_{кр}}_{p_{к2}}$ on ν_1, ν_2, β, and π_{c1}.

Figure 6.21 gives the dependences of $K^{F_{кр1}}_{p_{к2}}$ on the different dimensionless parameters. An analysis of these dependences and the controlling characteristic (see figure 6.20) shows that an increase in pressure in the thrust chamber is reached by a considerable decrease in the cross section $F_{кр1}$ of the intermediate rozzle. Thus, for instance, in order to increase the pressure in the thrust chamber by 10% for an engine which has the characteristics $\bar{K}=3$, $\beta=0.67$, $\nu_1=0.3$ and $\nu_2=0$ and a supercritical pressure differential on the intermediate nozzle, the throat area should be decreased by approximately 25%. If the pressure differential on the intermediate nozzle is subcritical, then the transfer constant $K^{F_{кр1}}_{p_{к2}}$ is decreased even more considerably. From

curve given in figure 6.21, it is also possible to conclude that for obtaining higher values of $K_{p_{к2}}^{F_{кр1}}$ most favorable is the use in the gas generator of a solid fuel with a larger index ν_1[1].

There is a definite interest when evaluating the possibilities of control in the analysis of the transfer constant, which connects the deviations of pressure in the gas generator and thrust chamber:

$$K_{p_{к1}}^{p_{к2}} = \frac{\delta p_{к2}}{\delta p_{к1}} = \frac{\nu_1 \left(\frac{\bar{K}}{1+\bar{K}}\right)^{1-\beta}}{1 - \frac{\nu_2}{1-\beta}\left[1 - \left(\frac{\bar{K}}{1+\bar{K}}\right)^{1-\beta}\right]}. \qquad (6.23)$$

Figure 6.22 depicts the graphic dependences of $K_{p_{к2}}^{p_{к1}}$ on the different dimensionless parameters. For an engine which has the characteristics ν_1=0.3, ν_2=0, β=0.67 and $\bar{K}$=3, an increase in pressure in the thrust chamber of 10% requires an increase in pressure in the gas generator of approximately 37%.

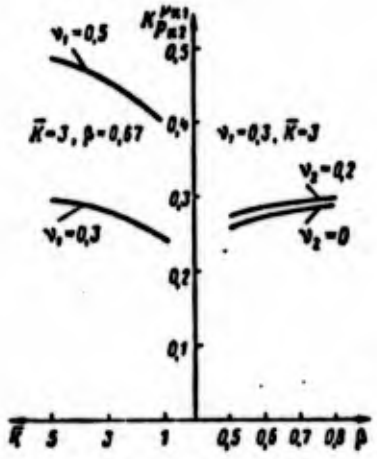

Figure 6.22. Dependence of coefficient $K_{p_{к2}}^{p_{к1}}$ on ν_1, ν_2, β and $\bar{K}$.

---

[1]The gas generator in this case is (with a supercritical outflow of gas from the nozzle) the standard RDTT. For such an engine, as is known, a change in the gas formation is proportional to $\delta F_{кр}\nu/(1-\nu)$, i.e., with an increase in ν_1, a change in the gas formation at the same value of $F_{кр1}$ increases.

With a pressure change there is a change in the relationship of the propellant component flow, which is characterized by the transfer constant $K_{н}^{p_{н}2}$:

$$K_{н}^{p_{н}2}=\frac{\partial K}{\partial p_{к2}}=\frac{1-\beta-\nu_2}{1-\beta}\cdot\frac{(1+\bar{K})\left[1-\left(\frac{\bar{K}}{1+\bar{K}}\right)^{1-\beta}\right]}{\left(\frac{\bar{K}}{1+\bar{K}}\right)^{1-\beta}}. \qquad (6.24)$$

Figure 6.23 gives the graphic dependences of this transfer constant on β and $\bar{K}$. Just as in the GRD, a deviation in the relationship of the flow rate of the components with a pressure change in the thrust chamber does not occur if $\beta+\nu_2=1$.

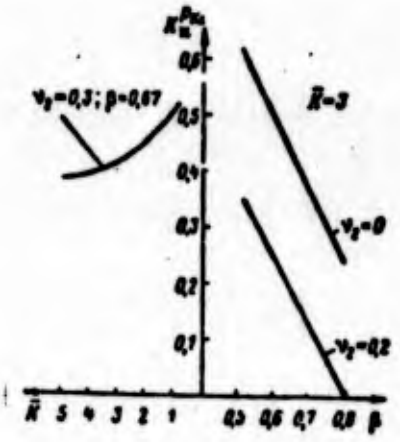

Figure 6.23. Dependences of coefficient $K_{н}^{p_{н}2}$ on $\bar{K}$, ν_2 and β.

The correlation coefficient of the propellant component flows is changed (with $\beta>0.5$ it is increased) in the process of the heat erosion of the channel of the charge in the thrust chamber. The value of the change in K can be characterized with $F_{нpl}=\text{const}$ by the transfer constant $K_{н}^{d_2}$:

$$K_{н}^{d_2}=\frac{\partial K}{\partial d_2}=\lambda\cdot\frac{1-\nu_1}{\nu_1}(1+\chi)\frac{2\beta-1}{1-\beta}f(\bar{K}). \qquad (6.25)$$

If in the RDTT RS it appears advisable to maintain the parameters of the engine operation constant (for example, $G_{т2}=\text{const}$ or $p_{н}=\text{const}$), then a change in the relationship of the propellant component flow will be similar to its change in the GRD in which the same controlling contours are used (see figure 6.11).

There can arise the need for maintaining constant the relationship of the propellant component flow by means of establishing the functional relation between changes in the burning surface in the gas generator and diameter of the channel of the charge of the thrust chamber. This relation establishes the geometry of the charge of the gas generator and is characterized by the transfer constant

$$(K_{s_1}^{d_2})_1=\left(\frac{\partial s_1}{\partial d_2}\right)_{K=\text{const}}=-\frac{(2\beta-1)(1-\nu_1)}{1-\beta-\nu_2}. \qquad (6.26)$$

An analysis of the equation for this coefficient shows that with $\beta=0.5$, just as in the GRD, any change in d_2 does not lead to a deviation of K. However, if $\beta+\nu_2=1$, then a change in d_2 cannot be compensated for by a change in s_1.

It is possible to establish a similar relation, having set the condition $p_{к2}=\text{const}$:

$$|K_{s_1}^{d_2}|_2=\left(\frac{\partial s_1}{\partial d_2}\right)_{p_к=\text{const}}=\frac{2\beta-1}{1-\beta}\,\frac{1+\chi-\nu_1}{1+\chi}\,\frac{f(\bar{K})}{1+\bar{K}-f(\bar{K})}. \qquad (6.27)$$

In this case it is interesting to estimate the change in the relationship of the propellant component flow, which is characterized by the coefficient $K_{к}^{d2}$ with $p_{к2}=\text{const}$:

$$K_{к}^{d_2}=\frac{\lambda}{\nu_1}(1+\chi)\frac{2\beta-1}{1-\beta}f(\bar{K})\left[1-\nu_1+\right.$$
$$\left.+\frac{1-\beta-\nu_2}{1-\beta}\,\frac{1+\chi-\nu_1}{1+\chi}\,\frac{1}{1+\bar{K}-f(\bar{K})}\right]. \qquad (6.28)$$

With $\chi=0$ the flow through $F_{кpl}$ is supercritical, $\nu_2=0$, and the equation for this coefficient is simplified:

$$K_{к}^{d_2}=\frac{\partial K}{\partial d_2}=\frac{2\beta-1}{1-\beta}f(\bar{K})\left[1+\frac{1}{(1+\bar{K})\left(\frac{\bar{K}}{1+\bar{K}}\right)^{1-\beta}}\right]. \qquad (6.29)$$

An analysis of the solution to equation (6.29), at different values of the quantities entering into it (figure 6.24), shows

that with the observance of condition $p_{к2}$=const the relationship of the flow rate of components can change substantially in the process of the heat erosion of the channel of the unit of the thrust chamber.

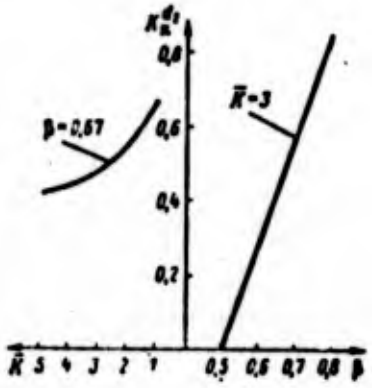

Figure 6.24. Dependence of the coefficient $K_к^{d_2}$ on $\bar{K}$ and β under the condition of $p_{к2}$= = const.

The control of the RDTT RS, in maintaining the relationship of the propellant component flow constant, is possible in such a case when the engine is made by a design with the bypass part of the gas from the gas generator in the pre-nozzle part of the thrust chamber.

The controlling characteristics of this engine for case of K=const take the following form:

$$\left(\frac{p_{к2}}{p_{к20}}\right)^{1-\beta-\varkappa_2}\left(\frac{d_2}{d_{20}}\right)^{1-2\beta}\left\{\left[\left(\frac{p_{к2}}{p_{к20}}\right)^{\frac{1-\varkappa_2}{\varkappa_1}}\varphi_0 K_0\left(\frac{F_{кр1}}{F_{кр10}}\right)+1\right]^{1-\beta}-\right.$$
$$\left.-\left[\left(\frac{p_{к2}}{p_{к20}}\right)^{\frac{1-\varkappa_2}{\varkappa_1}}\varphi_0 K_0\left(\frac{F_{кр1}}{F_{кр10}}\right)\right]^{1-\beta}\right\}=(\varphi_0 K_0+1)^{1-\beta}-(\varphi_0 K_0)^{1-\beta}; \quad (6.30)$$

$$\left(\frac{F_{кр.2}}{F_{кр.20}}\right)=\frac{\left(\frac{p_{к2}}{p_{к20}}\right)^{\frac{\varkappa_2-1}{\varkappa_2}}-\varphi_0\left(\frac{F_{кр1}}{F_{кр10}}\right)}{1-\varphi_0}. \quad (6.31)$$

Let us recall the notations in these equations: $p_{к20}$ and $p_{к2}$ - pressures in thrust chamber at the initial and instantaneous moments of time, respectively; d_{20} and d_2 - diameters of the channel of the charge of the thrust chamber; $F_{кр.д0}$, $F_{кр.д}$, $F_{кр10}$

and $F_{кр1}$ - critical cross sections of regulators in the pipelines which connect the gas generator and thrust chamber; ν_1, ν_2, β - coefficients in laws of the rate of gasification of the two components; ϕ_0 and K_0 - the coefficients of bypass and the relationship of the flow rate of components, respectively.

From equation (6.30) the change in $F_{кр1}$, which ensures the required change in pressure in the chamber (thrust of the engine), can be found. In order that in the process of control the relationship of the flow rate of the components would remain constant, simultaneously with this change $F_{кр1}$ there should be a change in $F_{кр.д}$; the magnitude of the new value $F_{кр.д}$ is found from equation (6.31).

The transfer constants with $\nu_2=0$ and $d_2=\text{const}$ take the following form:

$$K^{F_{кр1}}_{p_{к2}} = \frac{\delta p_{к2}}{\delta F_{кр1}} = \frac{[1-f(\bar{\varphi},\bar{K})]\nu_1}{\nu_1 - 1 + f(\bar{\varphi},\bar{K})}; \qquad (6.32)$$

$$K^{F_{кр.д}}_{p_{к2}} = \frac{\delta p_{к2}}{\delta F_{кр.д}} = \frac{\nu_1(1-\bar{\varphi})[1-f(\bar{\varphi},\bar{K})]}{(\nu_1-1)[1-f(\bar{\varphi},\bar{K})] - \bar{\varphi}[\nu_1 - 1 + f(\bar{\varphi},\bar{K})]}. \qquad (6.33)$$

where $f(\bar{\phi}, \bar{K})$ is the function determined by relation (5.47).

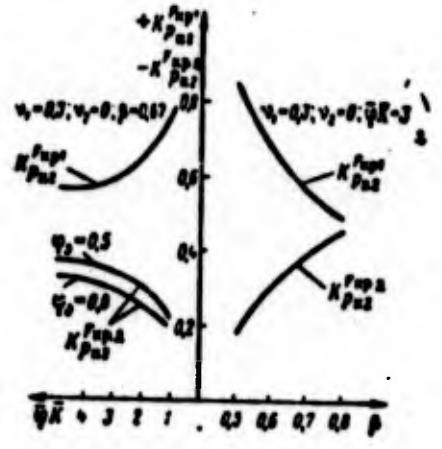

Figure 6.25. Dependence of coefficients $K^{F_{кр1}}_{p_{к2}}$ and $K^{F_{кр.д}}_{p_{к2}}$ on $\overline{\phi K}$, β and ϕ_0.

Results of the calculation of the transfer constants are given in figure 6.25. For an increase in pressure in the thrust chamber, it is necessary to decrease simultaneously the critical cross sections of both regulators, whereupon to a greater degree the cross section $F_{кр.д}$, i.e., the cross section of the regulator installed in the main line of the bypass should be decreased.

BIBLIOGRAPHY

1. Абрамович Г. Н. Прикладная газовая динамика. М., «Наука», 1969.
2. Алемасов В. Е., Дрегалин А. Ф. и Тишин А. П. Теория ракетных двигателей. М., «Машиностроение», 1969.
3. Бернар М. и др. Абляция твердого горючего под воздействием жидкой и физически гомогенной азотной кислоты. — «Ракетная техника и космонавтика», 1969, № 9.
4. Биль В. С. и Автократова Н. Д. Температурные зависимости теплопроводности и температуропроводности некоторых полимерных материалов. — «Пластические массы», 1965, № 10.
5. Волков Е. Б., Головков Л. Г. и Сырицын Т. А. Жидкостные ракетные двигатели. М., Воениздат, 1970.
6. Гибридные ракетные двигатели (обзор).—«Вопросы ракетной техники», 1965, № 10.
7. Григорьев А. И. Твердые ракетные топлива. М., «Химия», 1969.
8. Грин Л. Вводные замечания по вопросу горения топлива в гибридных ракетных двигателях. (Сб. «Гетерогенное горение»). М., «Мир», 1967.
9. Горман Ф. и Уайт Х. Исследование характеристик бериллийсодержащих твердых топлив. — «Вопросы ракетной техники», 1971, № 1.
10. Гухман А. А. и Илюхин Н. В. Основы учения о теплообмене при течении газа с большой скоростью. М., Машгиз, 1951.
11. Двигательные установки ракет на жидком топливе. М., «Мир», 1966.
12. Дементова А. А. и др. Таблицы газодинамических функций. М., «Машиностроение», 1966.
13. Добровольский М. В. Жидкостные ракетные двигатели. М., «Машиностроение», 1968.
14. Колмогоров А. Н. Доклады АН СССР, 1941, т. 30, № 4, стр. 299—303.
15. Коннагтон Дж. и др. Экспериментальное исследование процесса воспламенения и повторного запуска ГРД. — «Вопросы ракетной техники», 1966, № 7.
16. Коутс Р. Измерение скорости линейного пиролиза ТРТ. — «Ракетная техника и космонавтика», 1966, № 7.
17. Коэн Н. Горение топлива с избытком горючего. — «Ракетная техника и космонавтика», 1969, № 7.
18. Мадорский С. Термическое разложение органических полимеров. М., «Мир», 1967.
19. Мак-Алеви Р. и Су Ян Ли. Метод исследования процесса горения смесевых твердых ракетных топлив с помощью пористых зарядов и применение этого метода для гибридных ракетных двигателей. (Сб. «Гетерогенное горение»). М., «Мир», 1967.
20. Мак-Алеви Р., Су Ян Ли и Смит К. Линейный пиролиз полиметилметакрилата при наличии процесса горения. — «Ракетная техника и космонавтика», 1968, № 6.
21. Максмен Г., Вулдридж К. и Маззи Ф. Основы теории горения в пограничном слое твердого горючего гибридного топлива. (Сб. «Гетерогенное горение»), М., «Мир», 1967.

22. Махин В. А., Присняков В. Ф. и Белик Н. П. Динамика жидкостных ракетных двигателей. М., «Машиностроение», 1969.
23. Михеев М. А. Основы теплопередачи. М., Госэнергоиздат, 1956.
24. Мошкин Е. К. Нестационарные режимы работы ЖРД. М., «Машиностроение», 1970.
25. Орлов Б. В. и Мазинг Г. Ю. Термодинамические и баллистические основы проектирования ракетных двигателей на твердом топливе. М., «Машиностроение», 1968.
26. Осмон Р. Экспериментальное исследование ГРД, работающего на литийалюмогидриде и перекиси водорода, — «Вопросы ракетной техники», 1957, № 2.
27. Петухов Б. С. и Кириллов В. В. Теплообмен при турбулентном течении сжимаемого газа в трубах в области М до 4. — «Теплоэнергетика», 1960, № 5.
28. Саттон Г. Гидродинамика и теплообмен оплавляющейся поверхности. — «Вопросы ракетной техники», 1958, № 5.
29. Смут Л. и Прайс С. Скорости выгорания металлсодержащих горючих в гибридных топливах. — «Ракетная техника и космонавтика», 1966, № 5.
30. Смут Л. и Прайс С. Скорости горения неметаллизированных твердых компонентов гибридного топлива. — «Ракетная техника и космонавтика», 1965, № 8.
31. Соркин Р. Е. Газотермодинамика ракетных двигателей на твердом топливе. М., «Наука», 1967.
32. Спадаччини Л. и Чинниц В. Горение твердых горючих в сверхзвуковом потоке воздуха с высокой температурой. — «Ракетная техника и космонавтика», 1969, № 9.
33. Стоун М. Практический математический расчет конфигурации заряда. — «Вопросы ракетной техники», 1958, № 6.
34. Ткаченко Е. В., Улыбин В. Б. и Штейнберг А. С. Линейный пиролиз полиметилметакрилата. — «Физика горения и взрыва», 1969, т. 5, № 1.
35. Фарбар Л. и Дипью К. Теплообмен с потоком транспортируемых стеклянных частиц фиксированного размера. — «Теплопередача», 1963, т. 85, № 2, серия С.
36. Хансел Дж., Мак-Алеви Р. Тепловой баланс и химическая кинетика поверхностей деструкции полистирола в инертных и химически активных средах. — «Ракетная техника и космонавтика», 1966, № 5.
37. Харт Л. и Андерсон С. Гидродинамические факторы, влияющие на процесс горения в ТРД. — «Вопросы ракетной техники», 1967, № 8.
38. Хаузер Т. и Пек М. Исследование горения гибридной системы. (Сб. «Гетерогенное горение»). М., «Мир», 1967.
39. Хинце И. О. Турбулентность. М., Физматгиз, 1963.
40. Цукров М. и Грэхем А. Пленочное охлаждение ракетных двигателей. — «Вопросы ракетной техники», 1958, № 1.
41. Шапиро Я. М., Мазинг Г. Ю. и Прудников Н. Е. Теория ракетного двигателя на твердом топливе. М., Воениздат, 1966.
42. Шапиро Я. М., Мазинг Г. Ю. и Прудников Н. Е. Основы проектирования ракет на твердом топливе. М., Воениздат, 1968.
43. Шевяков А. А. Автоматика авиационных и ракетных силовых установок. М., «Машиностроение», 1970.
44. Штейнберг А. С. и Улыбин В. Б. О двух режимах линейного пиролиза конденсированных веществ. — «Физика горения и взрыва», 1969, т. 5, № 1.
45. Эккерт Э. Р. и Дрейк Р. М. Теория тепло- и массообмена. М., Госэнергоиздат, 1961.
46. Ankarswärd B. The Hybrid Rocket Engine. — «Interavia», 1964, vol. XIX, No. 12.
47. Bialla P. and Adams M. Analysis and Design of a Hybrid Terminal Stage. AIAA Paper, 1963, No. 656.
48. Barrére M. L'Allumage des Fusées Hybrides. — «La Recherche Aerospatiale», 1965, No 104.
49. Barrére M., Moutet A. La Propulsion par Fusées Hybrides. 14 Congr. Internat. Astronaut., Paris, 1963.
50. Chaiken R. and Anderson W. Kinetics of Surface Degradation of Polymethacrylate. — J. Chem. Phys., 1960, No. 32.
51. Dewey T. Entrance Region Heat Transfer Coefficients. — «Heat Transfer», 1963, No. 59.
52. Debize Fransis, Dussaut, Jean-Jacques Henri, Morin René, Théophile Albert. Générateur de Gaz Chauds a Ergol Hybride. Франц. пат. кл. F02 k, № 1595735 (Заявл. 25.11.68, опубл. 24.07.70). — Реферат. журнал ВИНИТИ «Авиационные и ракетные двигатели», 1971, № 7.

53. De Rieux E. Solid-Hybrid Propulsion. — «Astronautics», 1962, vol. 7. No. 3.
54. Hybrid Rocket Motor Tries out as Target-Missile Engine. — «Machinery Design», 1966, vol. 38, No. 30.
55. Judge J. Hybrid Concept Developing Rapidly Toward Goal of Tripropellant Engine. — «Missiles and Rockets», 1964, vol. 15, No. 19.
56. Judge J. Hybrid Engines First Flight is Successful. — «Aerospace Technology», 1968, vol. 21, No. 15.
57. Langemeier A. Betrachtungen zur Verbrennung in Lithergoltriebwerken, — «Raketentechnik und Raumfahrtforschung», 1962, Bd. VI, H. 4.
58. Materials of the 2-nd International Conference on Space Engineering. — Italy Paper, 1969.
59. Moutet Hélène, Pugibet Maurice. Utilisation dans les Systemes Hybrides de L'Eau Oxygenée comme Corburant. — «La Recherche Aérospatiale», 1969, No. 132.
60. Moutet A., Barrere M. Les Fusées a Lithergol on Fusées Hybrides. — «La Recherche Aeronautique», 1960, No. 75.
61. NASA Studying Large Cheap Rockets. — «Interavia Air Letter», 1969, No. 6671.
62. Ordahl D. Hybrid Propulsion. — «Space Aeronautics», 1964, vol. 41, No. 4.
63. Ordahl D. and Rains W. Recent Developments and Current Status of Hybrid Rocket Propulsion. — «Journ. of Spacecraft and Rockets», 1965, vol. 2, No. 6.
64. Parks E. G. Design, Test and Evaluation of a Hybrid Nozzle. NASA-CR-66566, 1967.
65. Robert H. and Schmucker R. Theoretische und Experimentelle Beiträge zum Hybridraketenantrieb. — «Raumfahrtforschung», 1970, Bd. 14, H. 5.
66. Roger L. O. Probleme Hochenergetischer Lithergoltrieb werke dargestellt am Beispiel der Entwicklung eines FLOX/Polyäthylen-Triebwerks. — «Raumfahrtforschung», 1969, Bd. 13, H. 5.
67. Stark Marvin W. Hybrid Rocket Motor. Патент США № 3423943, кл. 60-251. (Заявл. 27.02.67, опубл. 28.01.69). — Реферат, журнал ВИНИТИ «Авиационные и ракетные двигатели», 1970, № 5.
68. Taylor Robert L. Hybrid Fuel Grain Silver Reduction. Патент США № 3494286, кл. 102-99. (Заявл. 17.04.68, опубл. 10.02.70). — Реферат. журнал ВИНИТИ «Авиационные и ракетные двигатели», 1971, № 2.
69. UTC Hybrid Engine. — «Space Propulsion», 1970, vol. 7, No. 19.